UNIVERSITÉ DE STRASBOURG

ÉCOLE DOCTORALE DES SCIENCES DE LA VIE ET DE LA SANTÉ

CNRS UPR3212 – Institut des Neurosciences Cellulaires et Intégratives

THÈSE présentée par :

Tando Lerato MADUNA

soutenue le : **23 janvier 2017**

pour obtenir le grade de : **Docteur de l'université de Strasbourg**

Discipline / Spécialité : Neurosciences

Vasoactive intestinal peptide (VIP) controls the development of the nervous system and its functions through VPAC1 receptor signaling: Lessons from microcephaly and hyperalgesia in VIP-deficient mice.

THÈSE dirigée par :

M. LELIEVRE Vincent	PU, Université de Strasbourg, INCI, CNRS UPR 3212

RAPPORTEURS :

M. LANDRY Marc	PU, Université de Bordeaux, IINS, CNRS UMR 5297
M. MULLER Jean-Marc	PU, Université de Poitiers, 2RCT

AUTRE MEMBRE DU JURY :

M. CHELLY Jamel	PU, DR, INSERM-IGBMC Université de Strasbourg

---

INVITES :

M. GRESSENS Pierre	PU, DR INSERM-Paris Diderot (membre invité)
M. ANGLARD Patrick	DR, INSERM-LNCA, Université de Strasbourg (membre invité)

Remerciements

I would like to thank first and foremost Professor Vincent Lelièvre for directing my thesis, mentoring me from my MSc studies, welcoming me into his lab and supporting me through my whole PhD. I'd like to thank Professor Pierrick Poisbeau for taking me as part of his research team and allowing me to venture outside the comfort of developmental and molecular biology. Special thanks to all the members of the Determinants of Pain team who helped me through all these years.

I would like give a special mention to Dr. Yannick Goumon for his help and kindness: he is someone I could always count on in moments of doubt and has been in one way or other, like a father to us all.

Thank you to Dr. Michael Reber for his mentorship, for the long and honest professional discussions we've had and great advice.

Thank you to Dr Hervé Cadiou for all his professional advice, kindness, understanding and allowing me to dare to enjoy my work. And thank you for being the only person around during the weekends, feeding me and my mind with the best coffee and pâté.

I thank M. Adrien Lacaud, Dr. Pierre-Eric Juif and Mrs. Nathalie Petit-Demoulière for their teaching and technical assistance. I wish Ms. Marlene Salgado-Ferrer all the best in the continuation of my project with Professor Lelièvre.

I'd like to thank Dr Jim Sellmeijer for his unwavering friendship and support throughout my PhD.

I thank all the people I met and spent time with through these years at the INCI and who helped me in one way or another, with special thanks to M. Jérôme Wahis, Dr. EliseSavier, and M. Alvaro Sanz-Diez

Very special thanks to M. Ivan Weinsanto for his companionship and support, and filling my days with great humor and comfort. I greatly appreciate the amount of time and effort he has dedicated to me and making me feel at home.

Another special thanks to the JMN students who have filled my days with laughter, always kind and appreciative. I will miss your emails and texts in the middle of the night. I will be losing part of my extended family when I leave you.

I would like to give a special mention to Professors Jamel Chelly and Patrick Anglard whose comments and evaluations help to improve my project

Finally, I would like to thank Professors Marc Landry and Jean-Marc Muller for their patience and understanding and taking time to read and evaluate my work as part of my jury.

Table des matières

Résumé étendu en français

Action du peptide vasoactif intestinal (VIP) sur les récepteurs VPAC1 pour contrôler le développement du système nerveux et ses fonctions: Etudes des souris microcéphales et hyperalgiques par déficience en VIP

Le peptide vasoactif intestinal (VIP) appartient à la superfamille de peptides PACAP (pituitary adenylate cyclase activating polypeptide)/glucagon caractérisée par une signature N-terminale en histidyl-sérine. D'un point de vue phylogénétique, ces peptides ont été créés par duplication successive d'un gène ancestral. Ils partagent donc un processus de biosynthèse caractéristique : chez les mammifères, la traduction du gène VIP produit un prépropeptide dont la maturation donne naissance au peptide (accessoire) histidine-isoleucine/méthionine (PHI /PHM) et au VIP mature de 28 acides aminés.

Une évolution similaire a été proposée pour les récepteurs du VIP (nommés VPAC1 et VPAC2) liant le VIP et le PACAP avec des affinités similaires (pour revue: Harmar et al., 2012). Ils appartiennent à la famille des récepteurs couplés aux protéines G (GPCR) de classe II caractérisé par un grand domaine N-terminal extracellulaire de reconnaissance du ligand, ancré par un segment à 7 domaines transmembranaires lui-même entrecoupé de boucles extra- et intracellulaires impliquées respectivement dans la reconnaissance du ligand et la transduction du signal. Ce segment transmembranaire se termine par un domaine C-terminal intracellulaire crucial pour l'activation de protéines G hétérotrimériques spécifiques de couplage à l'adénylyl cyclase, à la phospholipase C et aux protéines kinases associées (PKA, PKC et MAPK).

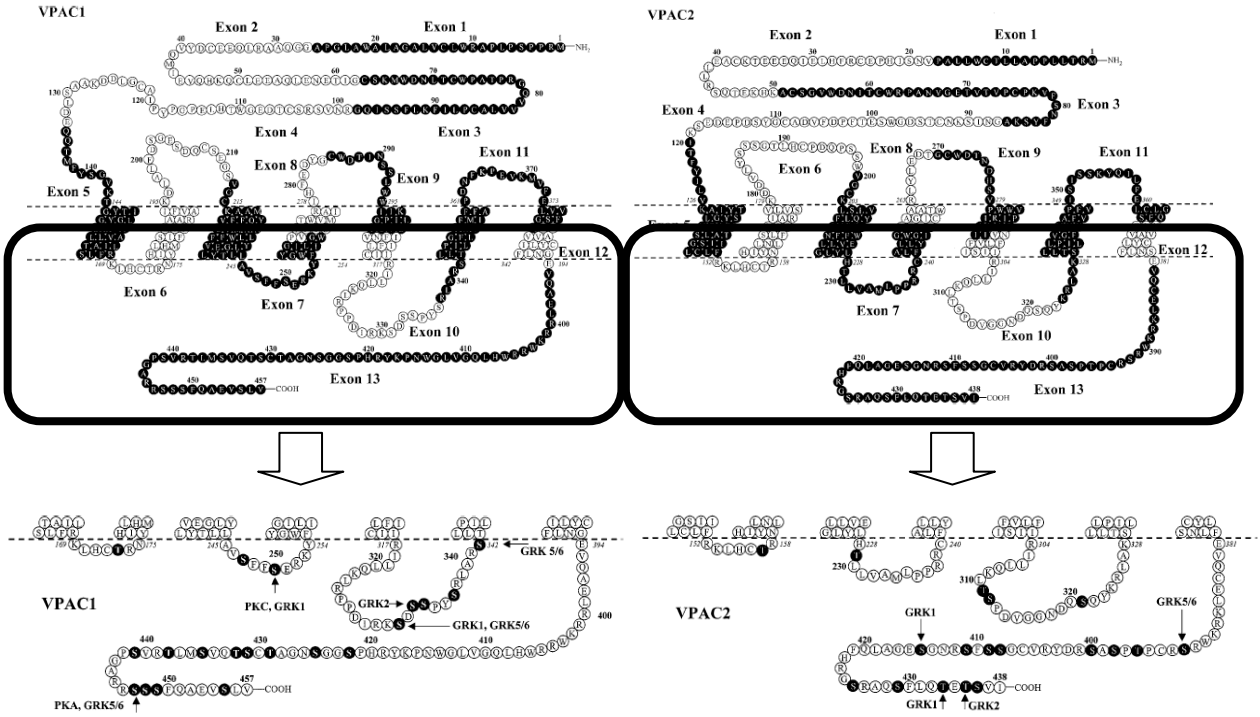

Représentation schématique en ruban des récepteurs VPAC1 and VPAC2 humains indiquant la séquence en acides aminés et son origine à partir des 13 exons codants. Gros plan sur les domaines intracellulaires des récepteurs et les acides aminés impliqués dans les séquences consensus de phosphorylation par les protéines kinases A (PKA), C (PKC) et les kinases spécifiques des récepteurs couples aux protéines G (GRK). Figure extraite de *Laburthe, Couvineau and Marie, Receptors and Channels, 8:137–153, 2002.*

Le choix de la voie de signalisation dépend du type cellulaire et peut varier en fonction des conditions biologiques en raison de l'existence de variants d'épissage et de l'interaction des récepteurs avec des protéines accessoires (RAMPs).

Au final, par l'intermédiaire de cascades de signalisation redondantes et complexes, le VIP et PACAP régulent de nombreuses fonctions biologiques. Ainsi le VIP agit de manière sélective sur le système nerveux central et périphérique, en conditions normales ou pathologiques (incluant tumeurs, lésions et maladies génétiques).

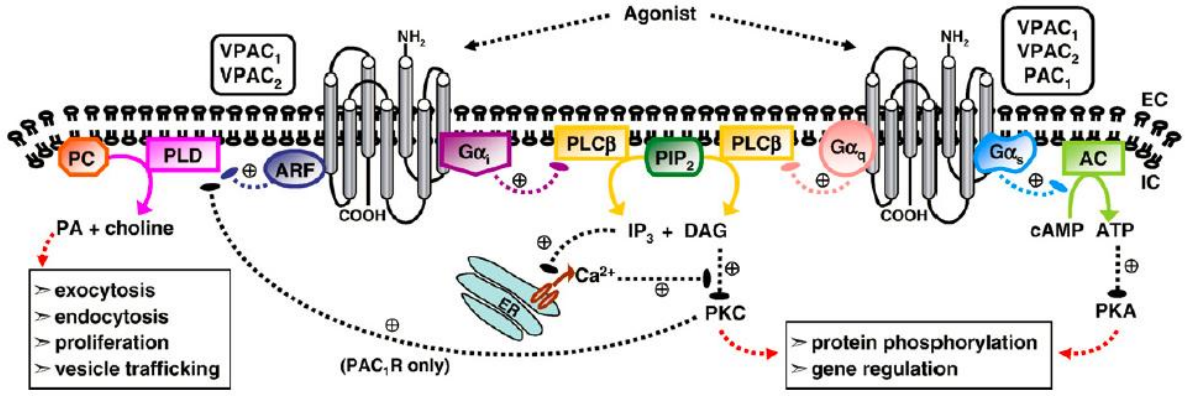

Représentation schématique des voies de signalisation intercellulaire stimulées par les récepteurs du VIP et du PACAP. Cette figure récapitule les principales voies de transduction couplées aux protéines G hétérotrimériques activées par les récepteurs VPAC1, VPAC2 and par la forme d'épissage de base (null) du récepteur PAC1. Apres activation, ces 3 récepteurs sont capables recruter la sous-unité Gαs conduisant à la production d'AMPc. De plus, ces récepteurs peuvent également activer les phospholipases C produisant une augmentation du calcium intracellulaire médiée via les sous-unités Gαq (commune) et Gαi (VPAC1 et VPAC2). L'activité phospholipase D peut être aussi stimulée par ces 3 récepteurs via des voies de transduction impliquant ARF (VPACs) et PKC (PAC1). Figure extraite de *Dickson & Finlayson, Pharmacology & Therapeutics 121 294–316, 2009*.

Ces études ont bénéficié des avancées technologiques, comme la production d'analogues pharmacologiques plus sélectifs et la création d'animaux présentant des pertes ou des gains de fonction. Ces animaux transgéniques ont permis de mieux comprendre les rôles spécifiques de ces neuropeptides sur la physiologie générale (y compris la reproduction et la digestion), mais aussi sur des fonctions particulières du système nerveux. En effet de nombreuses études ont démontré l'impact direct du VIP sur les noyaux suprachiasmatiques en relation avec les rythmes circadiens, sur l'hippocampe et la mémoire, sur l'axe hypothalamo-hypophysaire et la gestion du stress et de l'anxiété, mais aussi sur des structures comme l'amygdale connu pour contrôler les émotions et les comportements sociaux. Toutes ces activités sont considérablement impactées chez les animaux déficitaires en VIP qui développent progressivement des troubles autistiques et des comportements de type schizophrène. En effet le VIP et ses récepteurs sont normalement exprimés des les stades précoces du développement embryonnaires (pour revue; Maduna & Lelievre, 2016).

Dans ce contexte, les résultats antérieurs de notre équipe (Passemard et al., 2011) montrent que le blocage pharmacologique des récepteurs du VIP réduit de manière significative la taille du cerveau des souriceaux et son épaisseur corticale en inhibant le cycle cellulaire par l'intermédiaire de la voie Mcph1-Chk1. Ces données suggèrent que le VIP favorise la croissance corticale en régulant la prolifération des cellules progénitrices. Cette étape est cruciale au cours du développement normal du cerveau pour fournir un pool suffisant de cellules multipotentes permettant l'expansion du cerveau et du télencéphale. Les pathologies de croissance corticale sont communément appelées microcéphalies. Chez l'homme, ces microcéphalies provoquant des retards mentaux plus ou moins sévères peuvent émerger de conditions génétiques rares (microcéphalia vera ou microcéphalie primaire) mais ont souvent une origine accidentelle et ou environnementales liées à la grossesse. Chez l'enfant, ces pathologies sont souvent associées à des troubles neurologiques (hyperalgésie, dystonie musculaire) pour lesquels il n'existe pas de traitements.

Par conséquent mes études doctorales visent à:

1- Explorer le développement cérébral des souris déficientes en VIP pour savoir si ces animaux transgéniques sont un modèle approprié pour étudier les microcéphalies? Déterminer la ou les source(s) de VIP nécessaire au control de la taille du cerveau?

2- Rechercher si les troubles neurologiques tels que l'hyperalgésie sont également observés chez les mutants VIP?

OBJECTIF 1: Analyse du déficit de croissance corticale chez les souris déficientes en VIP.

Ce travail a été lancé dans le laboratoire du Dr Gressens à Paris et initié par Sandrine Passemard au cours de sa thèse de Sciences. Cette étude propose une exploration en profondeur du rôle de VIP au cours du développement cortical en utilisant des souris VIP sauvages (WT) ou porteuses de l'invalidation totale (KO) ou partielle (HZ) du gène VIP, à l'aide d'approches moléculaires (hybridation in situ, PCR quantitative, immunohistochimie) et morphométriques. Toutes ces techniques sont développées dans l'article de recherche en préparation, cependant des techniques plus pointues comme l'hybridation in situ sur embryon entier qui ont

nécessité une mise au point longue et fastidieuse sont détaillées dans la section METHODS du manuscrit.

a. Les souris KO VIP montrent un déficit de croissance corticale:

Chez les souris KO VIP, l'absence de VIP provoque une microcéphalie, avec réduction significative de l'épaisseur corticale démontrée par l'analyse morphométrique de l'épaisseur et de la surface corticale à partir de coupes sériées colorées au violet de Crésyl. Par comparaison avec nos études pharmacologiques initiales (Passemard et al., 2011) le déficit cortical est plus sévère et persiste jusqu'à l'âge adulte. En utilisant l'hybridation in situ sur des embryons entiers (âgés de 9 à 13 jours de vie embryonnaire, i.e. E9–E13) et la technique de RT-PCR quantitative, nous avons examiné le profil d'expression des gènes (Mcph) impliqués dans le développement des microcéphalies congénitales et retrouvé une réduction spectaculaire de l'expression de Mcph1 et ses gènes cibles Brca1 et Chk1. Ces résultats confortent les travaux initiaux basés sur l'utilisation de l'antagoniste des récepteurs VIP et démontre a l'aide des techniques d'hybridation in situ sur embryon entier que le cortex n'est pas la seule structure impactée puisque les patrons d'expression des gènes Mcph1 et Chk1 sont perturbés non seulement au niveau telencéphalique mais également dans les régions plus postérieures. Ainsi l'effet de l'absence de VIP qui se fait ressentir tout au long du neurodéveloppement engendre une réduction secondaire de la substance blanche. Cet effet est particulièrement visible au niveau du corps calleux des souriceaux âgés de 15 jours.

b. Le déficit cortical induit par l'absence de VIP est associé à une différenciation neuronale précoce:

En utilisant la technique d'hybridation in situ sur embryons entiers (prélevés aux stades E9 à E13) et de RT-PCR quantitative nous avons regardé d'un point de vue qualitatif et quantitatif les patrons d'expression des gènes-clés qui contrôlent la neurogenèse. Selon les spécialistes, la différenciation neuronale initiale repose sur l'activation séquentielle et transitoire des facteurs de transcription Dcx, Pax6, Tbr1/2. Dans les embryons KO, l'expression du gène Pax6 apparait prématurément et est significativement plus élevée à E9 et E10 comparativement aux embryons sauvages. L'expression des gènes et des protéines Tbr2 et Tbr1 est également prématurément exacerbée dans les vésicules télencéphaliques des embryons invalidés aux stades E12 et E13. D'autres marqueurs de maturation corticale, y compris Sox2, Emx2,

Cux1 et Dcx montrent des patrons d'expression altérés qui traduisent une accélération globale de la sortie de cycle cellulaire et de la spécification neuronale. A l'inverse, l'incubation en présence de VIP des cellules souches neurales (isolées à partir de cerveau antérieur au 10eme jour de vie embryonnaire (E10) provoque une augmentation significative de l'expression du gène STAT3 et la régulation négative des gènes Pax6 et Tbr1. De plus, en condition différenciante et en présence de VIP, ces cellules produisent plus de transcrits codant les gènes Otx, Ngn, Nurr1 et β3-tubuline. Ceci suggère que le VIP inhibe l'auto-renouvellement de ces cellules multipotentes au profit de la différenciation neuronale. Par ailleurs on observe des changements d'expressions des gènes de régulation épigénétique codant pour les enzymes de modification de la chromatine (HDAC, HAT) et de méthylation de l'ADN suggérant que les actions à long terme du VIP puissent être véhiculées par ce type de mécanisme:

c. La source principale de VIP pendant le pic de neurogenèse est maternelle:

Pendant la gestation, la concentration sanguine en VIP augmente de façon exponentielle partir du 8eme jour de gestation chez le rat pour atteindre un pic autour de E12 et retomber au niveau basal vers E16 (Voir figure ci-dessous). Ce surplus de VIP produit par les lymphocytes T placentaires atteint directement l'embryon par l'artère ombilicale. Au cours de l'embryogenèse le VIP maternel sera progressivement épaulé par une production locale de VIP par des cellules embryonnaires.

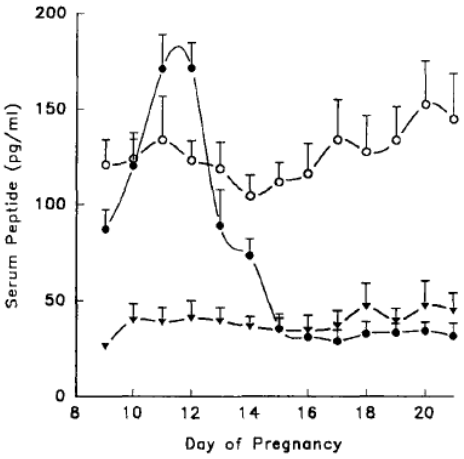

Variation de la concentration sanguine de VIP (●) pendant la gestation de la Ratte. Le pic de concentration sérique en VIP coïncide parfaitement avec la phase post-implantatoire et s'étend sur l'intégralité du pic de neurogenèse pour revenir au taux basal circulant. A l'inverse les concentrations de α-MSH (○) et de somatostatine (▼) ne sont pas affectées par la gestation. Les valeurs représentent la concentration moyenne (±SEM) exprimée en pg/mL déterminées par test radioimmunologique (RIA)**.** Figure extraite de *Hill et al. J Clin Invest 97(1):202-8 1996*

Pour savoir quelle est la source principale de VIP qui contrôle la croissance cérébrale, nous avons étudié la sévérité des symptômes, l'intensité de la répression de la voie Mcph1-Chk1 et l'expression précoce de marqueurs neuronaux chez les embryons sauvages (WT), ou invalidés partiellement (HZ) ou totalement (KO) nés de mères elles-mêmes WT, HZ ou KO. Ainsi il apparait une nette différence d'expression des gènes Mcph1 et Chk1 entre les embryons KO issus de mères KO ou hétérozygotes: Cette analyse transcriptomique nous révèle que l'expression de ces gènes est bien dictée principalement par le niveau de VIP maternel tandis que VIP embryonnaire ne contribue qu'à l'expression de marqueurs tardifs tel Tbr1. Ces résultats ont été confirmés par des expériences de sauvetage dans lesquelles les femelles gestantes ont été injectées quotidiennement avec des concentrations élevées de VIP (1 à 2 ug/g) de E9 à E11. Cet effet est clairement visible chez les embryons KO issus de mères KO pour lesquels les injections de VIP améliorent sensiblement le déficit morphométrique observé chez les embryons KO et rétablissent les niveaux d'expression des gènes Mcph1 et Chk1 au stade E12.

d. Modulation de la croissance cérébrale en condition de stress gestationnel:

Notre hypothèse est que les lymphocytes T placentaires peuvent réagir au stress en modulant leur production de VIP. En effet le promoteur du gène VIP contient de nombreux sites d'interaction avec des facteurs de transcription actives par les cytokines et le stress (voir schéma ci-contre).

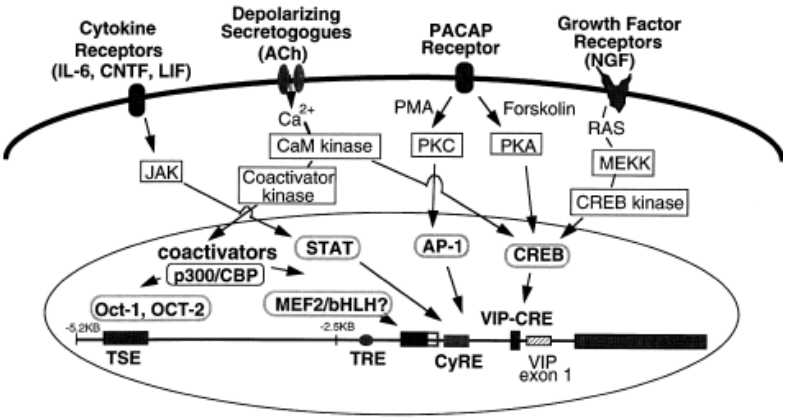

L'analyse du promoteur du gène VIP révèle la présence de sites de liaisons particuliers pour des facteurs de transcription impliqués dans la régulation de l'expression du VIP. De nombreux signaux primaires sont capables de stimuler, à titre individuel ou en combinaison, des voies de transduction multiples provoquant par phosphorylation ou déphosphorylation l'activation de facteurs de transcription tels que STAT-1 et -3, AP-1, CREB, et Oct-1 qui lient spécifiquement les séquences consensus des éléments régulateurs positionnés sur le gène VIP. On notera qu'au moins un des éléments régulateurs le site de liaison AP-1 ou TRE en position -2.3 kb sur le gène VIP a été démontré comme non-fonctionnel dans le contexte de transcription du gène VIP humain, et qu'un second élément, le site de liaison CRE du facteur CREB positionné à -.094 kb ne permet pas au PMA de stimuler la transcription même s'il induit l'expression du VIP en réponse aux esters de phorbol dans les cellules HeLa. Figure tirée de *Hahm & Eiden Ann N Y Acad Sci. 1998*.

Pour tester cette idée, des souris gestantes ont été soumis à une contention physique non douloureuse deux fois par jour pendant 45 min de E9 à E11. Ce stress affecte la production de VIP et réduit l'expression des gènes Mcph1 et Chk1 à E12 chez les embryons sauvages, suggérant que le stress maternel impacte le développement du cerveau par l'intermédiaire de fluctuation de la concentration de VIP circulante. Par ailleurs le stress n'a pas ces effets sur les embryons KO issus de femelles KO confortant l'idée que la production de VIP est un facteur clé dans la gestion du stress maternel. Enfin, chez les embryons obtenus à partir de femelles hétérozygotes, le stress abaisse l'expression de Mcph1 et de Chk1 aux niveaux atteints chez les embryons KO issus de mères KO. De même, l'expression exacerbée de PAX6 observée à E12 dans les embryons KO VIP issus de mères hétérozygotes atteint les niveaux observés chez les embryons KO générés à partir des femelles KO. Bien que préliminaires, ces résultats suggèrent qu'un stress léger (non-inflammatoire et non douloureux) comme la contention physique perpétrée

pendant une période critique (neurogenèse) a des effets délétères sur le développement du cerveau.

e. Effet global sur le développement périnatal du cerveau: preuve du rôle bénéfique du VIP sur la genèse des oligodendrocytes et la maturation de la substance blanche.

L'utilisation des colorations standards et au Bleu de Luxol montre que l'épaisseur du corps calleux est considérablement réduite chez les jeunes et les adultes KO par rapport aux souris sauvages de même âge. La RT-PCR quantitative confirme que l'expression de gènes de maturation des oligodendrocytes est réduite à P15. Ces déficits sont partiellement restaurés par les injections de VIP effectuées au stade embryonnaire E9-E11; suggérant que l'absence prolongée de VIP au delà de la période de prolifération des cellules souches et de la neurogenèse puisse également participer au défaut structural observé.

Conclusions de cette étude:

Prises dans leur ensemble, ces données confirment que les déficits initiaux de prolifération des progéniteurs affectent aussi l'ensemble du développement cérébral tardif, y compris la production des cellules progenitrices des oligodendrocytes responsables de la myélinisation des axones et de la formation de la substance blanche. Ces expériences révèlent également que la production de VIP par les lymphocytes T maternels qui colonisent le placenta dès le stade E7.5 de la gestation joue un rôle prépondérant dans le contrôle humoral de la croissance corticale. Ce résultat est particulièrement important car il confirme que le stress subit par la mère au cours des périodes embryonnaires affecte bien directement la neurogenèse et le programme génétique de formation du cerveau. Ce résultat sous-entendant également qu'une supplémentation de la mère en VIP administrée de façon directe par injection intrapéritonéale ou indirecte en stimulant sa libération lymphocytaire pourrait améliorer le pronostic de développement cortical.

Il reste cependant beaucoup de question en suspens. Mon travail est déjà repris par une nouvelle étudiante en thèse dont le projet permettra de mieux appréhender :

-1 le rôle de BRCA1 dans le phénotype microcéphalie et les processus de développement cérébral . Brca1 (breast cancer 1) bien connu comme marqueur de prédisposition au cancer du sein est une cible moléculaire directe de Mcph1. La protéine Brca1 est impliquée dans la réparation de l'ADN endommagé par le stress et les rayonnements ionisants mais également dans le processus de transcription en facilitant la décondensation de l'hétérochromatine. De ce fait l'expression réduite de BRCA1 dans les souris invalidée pour le gène VIP pourrait participer au phénotype global et contribuer de façon plus franche a la sensibilité exacerbée de ces souris mutantes au stress gestationel.

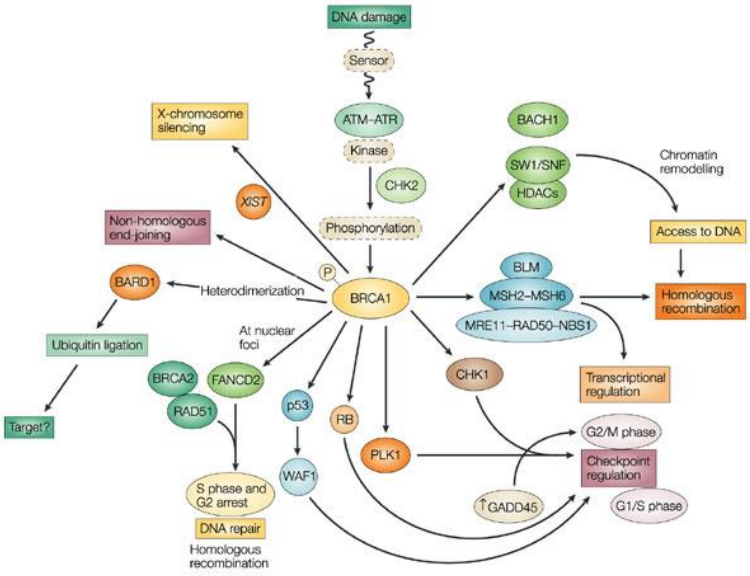

Voies de signalisation et fonctions biologiques de la protéine BRCA1. Si l'interaction de la protéine BRCA1 avec protéine CHK1 pour contrôler la transition G1/S -G2/M est en lien direct avec nos études précédentes. Le rôle de BRCA1 dans le remodelage de la chromatine en relation avec des protéines HDAC reste intégralement à explorer. Il en va

2- l'impact de la nature du stress sur le déficit cortical et les fonctions cognitives :

Dans la littérature de nombreux protocoles de stress anténatal ou gestationnel ont été décrits comme étant capables de produire des défauts de développement cérébral. En parallèle, l'hypothèse du ***Double Hit*** initialement élaborée pour caractériser le développement tumoral a été étendue aux pathologies du développement cérébral (IMC) et à d'autres maladies psychiatriques comme la schizophrénie et l'autisme. Cette hypothèse propose qu'une anomalie fonctionnelle d'un gène important du développement cérébral constitue une première atteinte, qui rend le sujet sensible à des facteurs environnementaux responsables d'une seconde atteinte entraînant la maladie. Dans notre cas, l'absence totale ou partielle de VIP rend le cerveau en développement vulnérable aux effets délétères d'un stress environnemental potentiellement anodin dans le cas d'un individu sain.

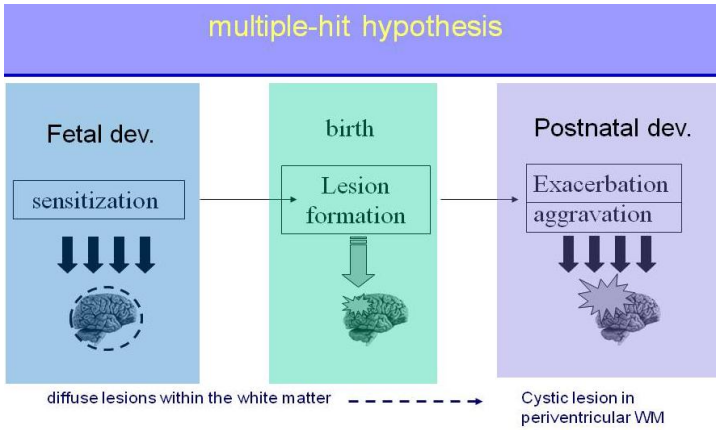

Représentation schématique de l'hypothèse des chocs doubles (double hit) ou répétés (multiple hit) dans les leucomalacies péri-ventriculaires. Pendant la période embryonnaire ou fœtale, le cerveau en développement subit des agressions ponctuelles ou chroniques qui sensibilisent la structure immature. L'accouchement à terme ou prématuré représente alors une épreuve traumatique qui provoque des lésions kystiques ou diffuses dans la substance blanche imputables à la fragilité intrinsèque des oligodendrocytes immatures à ce stade du développement. Plus tard, pendant l'enfance ou l'adolescence des événements délétères d'origines diverses (stress, infection ou inflammation etc...) peuvent exacerber la taille des lésions et les troubles neurologiques, cognitifs ou psychiatriques associés. Figure extraite de *Leviton & Gilles, Am J Pathol 1971.*

Si nos résultats indiquent que le programme génétique de développement du cerveau de souris HZ est impacté plus durement par le stress de contention administré à la mère gestante confirme l'hypothèse du double hit dans notre modèle animal, il reste cependant de nombreuses interrogations.

Tout d'abord il convient de spécifier la nature, l'intensité et la fenêtre d'application du stress. Ainsi nous proposons de poursuivre ces études en comparant les effets du stress de contention avec ceux deux autres stress de nature différente. Nous étudierons l'impact du stress inflammatoire (en utilisant le protocole d'injection du LPS ou de ses composants pro-inflammatoires diffusibles (Il-6 et TNF-alpha) ou non (IL-1beta) à travers la barrière placentaire et du stress toxique (alcoolisation fœtale). Si le premier modèle est très intéressant car il mime les conditions de stress psychique léger connu pour activer de façon chronique ou aigue l'axe HPA et la libération de cortisol, le stress inflammatoire reproduit de façon simple les symptômes des pathologies infectieuses ou inflammatoires de la grossesse et des inflammations secondaires de l'embryons (FIRS) telle la funisite. De plus des travaux antérieurs du laboratoire ont pu établir un rôle neuroprotecteur du VIP sur la maturation de la substance blanche. Le dernier modèle de stress proposé dans les perspectives de mes travaux de thèse est l'alcoolisation fœtale. Ce projet me tient particulièrement à cœur car l'alcoolisation fœtale représente un fléau dans mon pays d'origine, De plus il est connu que cette intoxication induit des microcéphalies et que la mort cellulaire (neuronale) induite par l'alcool dans le cerveau embryonnaire et dans le cervelet de souris adulte peut être réprimée par administration de VIP.

3- Régulation épigénétique induite VIP au cours du neurodéveloppement

Dans les cellules souches neuronales en condition de différenciation le traitement par le VIP induit une spécification accrue de la différenciation cellulaire et des changements drastiques d'expression des gènes codant certains enzymes impliqués dans la condensation/décondensation de la chromatine et des modifications des cytosines au niveau des ilots CpG dans les régions promotrices des gènes en relation avec leur transcription. En considérant les intervalles de temps qui séparent le stress et ou les injections de VIP (E9-E11) et les symptômes anatomiques ou fonctionnels visibles encore à l'âge adulte ou initiés après la naissance (substance blanche), il apparait légitime d'explorer cet aspect plus en détails.

OBJECTIF 2: Evaluation de l'hypersensibilité chez les souris adultes déficientes en VIP.

Ce travail est le fruit d'une collaboration avec le Pr Poisbeau. L'hypothèse d'une hypersensibilité douloureuse chez la souris déficiente en VIP est étayée par deux observations importantes et indépendantes: 1- Les nourrissons souffrant de déficits neurologiques (y compris un retard mental ou une paralysie cérébrale) développent souvent des symptômes d'hyperalgie et des troubles digestifs douloureux. 2- les souris KO VIP ont une faiblesse musculaire ou une fatigue à l'effort qui pourraient provenir de douleurs chroniques. Par ailleurs il a été démontre dans de nombreux modèles murins de lésions de nerfs une élévation des transcrits du VIP sous 24h qui persiste plusieurs semaines . Par exemple facial moteur et sciatique (voir figure ci-dessous) l'élévation de la production de VIP dans les DRG pourrait participer à la régénération fonctionnelle mais également aux douleurs chroniques.

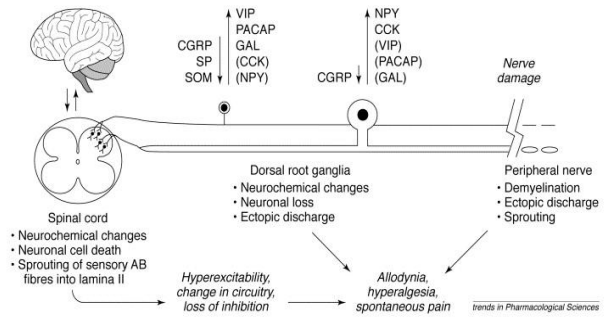

Représentation schématique de la plasticité des voies médullaire sensorielles et motrices après lésion du nerf sciatique. Les neurones sensoriels de petits et gros diamètres localisés dans le ganglion de la racine dorsale (DRG) subissent de nombreuses altérations neurochimiques. Dans les gros neurones des DRG on observe une élévation des niveaux de NPY, de CCK et de VIP, alors que la production de CGRP diminue. Dans les neurones de petit diamètre la production de SP, de CGRP et de somatostatine s'effondre, au profit de la galanine, du VIP et du PACAP. En parallèle dans la moelle et le nerf lésé, on observe des variations importantes dans l'expression de leurs récepteurs. Figure extraite de *Dickinson & Fleetwood-Walker, Trends Pharmacol Sci. 20(8):324-9 1999*.

Dans ce contexte nous avons entrepris de creuser cette hypothèse et nous avons pu démontrer que :

a. Les souris KO VIP présentent des hypersensibilités au froid (mais pas au chaud) et aux stimuli mécaniques:

En utilisant les tests standards de mesure de seuil nociceptif en réponse à des stimuli électriques ou mécaniques (filaments calibrés de Von Frey), et thermiques (plaques à température fixe ou variable), nous avons déterminé que les souris KO VIP adultes sont très sensibles aux stimuli froids et mécaniques alors que leur seuil

de réponse au chaud reste normal. L'enregistrement électrophysiologique des neurones des couches profondes de la corne dorsale de la moelle épinière, en réponse à des stimuli mécaniques ou électriques périphériques confirment que les fibres nociceptives de type C sont activées chez les animaux KO pour des tensions nettement inférieures aux seuils nociceptifs des animaux sauvages. Ces résultats suggèrent un phénotype allodynique des souris KO VIP.

b. L'injection de VIP chez les animaux KO rétablit des niveaux normaux de sensibilité:

L'injection intrapéritonéale de VIP chez les souris KO restaure les seuils sans affecter les autres fonctions animales. Une injection IP unique est suffisante pour normaliser en 3 heures les seuils de douleur et qui reste complètement normaux pendant 3 jours. L'action bénéfique du VIP est entièrement mimée par l'agoniste VPAC1 et pleinement bloquée par l'antagoniste VPAC1 soutenant l'idée que l'action du VIP sur les seuils de douleur est principalement médiée par les récepteurs VPAC1. L'activation de ces récepteurs engendre la translocation nucléaire rapide des facteurs cFos/ΔFosB et pCREB pour affecter la transcription en général et en particulier celle des gènes liés à la douleur.

c. La perte du gène VIP induit une régulation spécifique et réversible de la transcription de gènes de la douleur.

Sur la base des résultats précédents, nous avons lancé à partir d'échantillons de moelle épinière et de DRG, un tri sélectif parmi les ARNm codant pour des protéines et des peptides connus pour affecter la perception et l'intégration des signaux douloureux, Pour identifier ceux qui participaient directement au phénotype, la stratégie consistait à ne considérer que les gènes dont l'expression était significativement modifiée dans les échantillons KO mais rétablie après l'injection de VIP. L'analyse quantitative a révélé que parmi les gènes de peptides sécrétés, seuls le CNTF et deux membres de la famille du GDNF (artémine et perséphine) répondaient aux critères d'inclusion. Parmi les gènes codant les canaux et les récepteurs membranaires, seuls ASIC3, Cav3.2 et TRPM8 présentent des variations d'expression compatibles avec le phénotype. Ces candidats sont très intéressants car ils sont impliqués dans la détection des douleurs mécaniques et au froid. Des études récentes ont lié le processus de chronicisation de la douleur à des modifications épigénétiques. Sur la base de ces observations, nous avons supposé

qu'en l'absence de VIP la régulation épigénétique de l'expression des gènes Asic3, Cav3.2 et Trpm8 pourrait expliquer la mise en place d'un tel phénotype. Cette hypothèse a été testée en utilisant un test MeDIP (methylated DNA Immunoprecipitation). Cette expérience a révélé que la séquence de ces 3 gènes est hypométhylée chez les animaux KO. En outre, les tissus KO présentent des variations significatives des niveaux de transcrits codant pour des enzymes de compaction de la chromatine (Hdac1 et Kat2b) et de méthylation de l'ADN (Dnmt1) ou des protéines de liaison de l'ADN méthylé (Mecp2). On retrouve également des variations énormes des niveaux d'expression des ARN non codant impliqués dans chronicisation des douleurs neuropathiques (miRNA7 et miRNA21). Enfin des travaux préliminaires suggèrent que l'action bénéfique du VIP sur les seuils nociceptifs est bloquée par l'injection de SAHA un inhibiteur non sélectif des enzymes HDAC.

CONCLUSIONS ET PERSPECTIVES GENERALES:

Les études réalisées au cours mon doctorat ont permis de démontrer que les souris déficientes en VIP présentent une microcéphalie ayant principalement une origine maternelle qui affecte secondairement le développement de la substance blanche. De plus, cette production placentaire par une population particulière de lymphocytes T pourrait être affectée dans des pathologies du système immunitaire. Si l'idée de présenter le VIP comme un régulateur neuro-immun n'est pas nouvelle; elle n'a jamais été clairement explorée au cours du développement embryonnaire (voir figure ci-dessous).

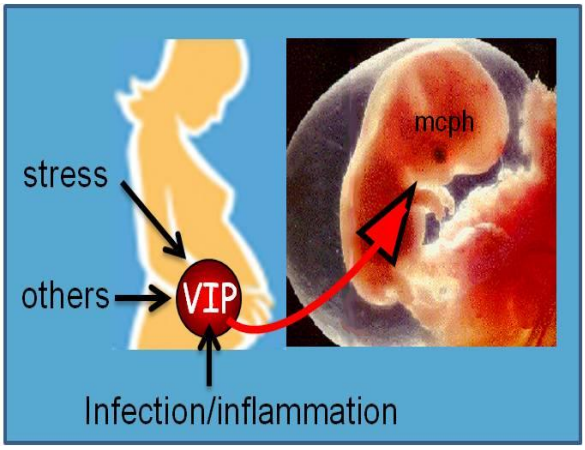

Représentation synthétique de notre hypothèse de travail. Les lymphocytes T placentaires produits par le système immun maternel adaptent leur production de VIP en réponse à différents stimuli environnementaux. Le VIP produit est libéré dans la circulation ombilicale et diffuse dans le tube neural pour retrouver ses récepteurs de type VPAC1 localisés à la surface des cellules souches neurales, de la glie radiaire et des progéniteurs télencéphaliques. L'activation de ces récepteurs initie une cascade de signalisation dépendante de l'AMPc et des facteurs de transcription en aval conduisant à la modulation de l'expression du gène Mcph1 et des fonctions de la protéine microcéphaline. (figure originale)

La suite de mes travaux se propose de tester différent paradigmes de stress sur ce modèle animal.

De plus nos données indiquent que le manque de production VIP prédispose à l'apparition de troubles sensoriels dont la nociception fait partie intégrante. Il existe donc une possibilité que les déficits précoces de développement du cerveau murin et l'apparition de l'hypersensibilité cutanée mécanique et thermique froide soient en fait deux facettes d'une même pathologie. Cette hypothèse a également été conforté par les données préliminaires obtenues en mesurant l'activité de décharges spontanées des neurones dans du thalamus sensoriel chez des mâles adultes préalablement anesthésiés. Les neurones des animaux KO sont naturellement hyperexcités, ce qui suggère qu'ils reçoivent probablement plus d'informations douloureuses en provenance de la moelle épinière ou que l'activité inhibitrice des interneurones des réseaux locaux est réduite.

Liste des abréviations

ASPM……..Abnormal spindle-like microcephaly associated protein
BRCA1……Breast cancer 1
CHK1……Checkpoint kinase 1
(p)CREB..... (phosphorylated) cAMP response element-binding protein
DIG..... Digoxigenin
DRG..... Dorsal root ganglion
E……Embryonic day
GIP……Glucose-dependent insulinotropic polypeptide
GLP-1/2……Glucagon-like peptide-1
GPCR……...G-protein coupled receptors
GRF/GHRH…….Growth hormone releasing hormone
Hz……Heterozygous (heterozygote)
IPC……Intermediate progenitor cell
KO……Knockout
LDDM.....Laterodorsal dorsomedial thalamus
M1.....Primary motor cortex
MCPH1……Microcephalin1
MS.....Maternal stress
NSC……..Neural stem cell
P……Postnatal day
PACAP……..Pituitary adenylate cyclase-activating polypeptide
Pax 6……Paired box transcription factor 6
PHI/M……Peptide histidine isoleucine/methionine
PMC.....Postmitotic cell
PP……Preplate
RGC……..Radial glial cell
RT-PCR..... Reverse transcription polymerase chain reaction
RT-qPCR..... Quantitative real-time RT-PCR
SC.....Spinal cord (spine)

S1.....Primary somatosensory cortex

SVZ.....Subventricular zone

Tbr2 and 1.....T-box domain transcription factor 2 and 1

VIP..... Vasoactive intestinal peptide

VPAC1 and 2..... VIP/PACAP receptors

VA.....VIP/PACAP receptor antagonist (neurotensin hybrid)

VL.....Ventral lateral nucleus

VZ.....Ventricular zone

WISH..... Whole-mount *in situ* hybridization

WT..... Wildtype

Introduction

1. Background

1.1. Vasoactive intestinal peptide (VIP) belongs to the Pituitary adenylate cyclase-activating polypeptide (PACAP) family of peptides

VIP has been characterised as a member of the pituitary adenylate cyclase-activating polypeptide (PACAP)/glucagon superfamily of bioactive peptides that include glucagon-like peptide-1 (GLP-1), GLP-2, glucose-dependent insulinotropic polypeptide (GIP), GH-releasing hormone (GRF/GHRH), secretin, glucagon, helodermin, peptide histidine isoleucine/methionine (PHI/M) and PACAP, due to their high similarity in amino acid structure at the N-terminus that contains the characteristic histidyl-seryl residue (Mutt and Said 1974; Sherwood et al. 2000). VIP shares 68% structural homology with PACAP-27, which through further amidation at the C-terminus, results in PACAP-38 (Miyata et al. 1990). This family of peptides is suggested to have evolved from duplications of an ancestral exon (see Figure 1), whereby VIP is suggested to originate from gene duplication of the PACAP gene (Sherwood et al. 2000), resulting in a VIP gene sequence that is highly conserved within mammalian species (Giladi et al. 1990; Lamperti et al. 1991). The VIP gene is also highly conserved in function within lower and higher vertebrates (Mathieu et al. 2001; Thwaites et al. 1989).

VIP is a 28 amino acid octacosapeptide that received its name after displaying strong vasodilatory actions in the mammalian small intestine. VIP became a candidate gastrointestinal peptide exerting secretin-like stimulation of pancreatic secretion, though with weaker effect than secretin, and regulating blood glucose levels which is the main function of glucagon (Said and Mutt 1972). In addition VIP displayed a wide variety of biological actions including the regulation of arterial blood flow and pressure, increase of cardiac output, stimulation of chemoreceptors causing hyperventilation and blood glucose regulation (Said and Mutt 1970), actions that are redundant with the peptides of the glucagon family. In addition, VIP is also

characterized as a neuropeptide, showing high immunoreactivity in the nerves of the gut and different regions of the brain including the hypothalamus (Larsson et al. 1976), and as a neurotransmitter due to spatio-temporal localization of VIP within large-dense core vesicles at the axon terminals and in the synaptic compartments of rat brains (Besson et al. 1979; Pelletier et al. 1981). In accordance, VIP release is calcium-mediated (Waschek et al. 1987) and may result from K+ administration (Emson et al. 1978). Taken together, these studies and more (Said 1984; Said 1986) have provided experimental evidence for VIP as more than a gastrointestinal peptide but as a key neuropeptide with pleiotropic functions in the brain and periphery.

1.1.1. VIP gene and biosynthesis

1.1.1.1 VIP gene

The human VIP gene is ~9kb in size consisting of 7 exons (Linder et al. 1987) which are highly conserved in the human, rat and mouse (Giladi et al. 1990; Lamperti et al. 1991; Yamagami et al. 1988) . Interestingly, VIP is the only peptide within its family whereby the gene encodes two bioactive peptides, VIP and PHI/M (in which the methionine residue in human is replaced by isoleucine in non-human species). Similarly, the PACAP gene also encodes two peptides, PACAP-27/38 and PACAP related peptide (PRP) although its bioactivity has yet to be demonstrated (Tam et al. 2007).

Exon 1 encodes a 5' untranslated leader sequence whereas exon 2 encodes the signal peptide which is important during peptide synthesis to allow entry of the newly forming peptide into the endoplasmic reticulum. Exon 3 encodes for the spacer protein sequence which is only synonymous with VIP and PACAP, and has been determined to be important for elongating neuropeptides during synthesis to allow their entry into the membranes of the endoplasmic reticulum (Holmgren and Jensen 2001). PHI/M and VIP are found on the VIP gene at exons 4 and 5, respectively (Bodner et al. 1985; Itoh et al. 1983). Exon 6 directs the synthesis of the remainder of the protein coding sequence, whereas exon 7 consists of the 3' untranslated region (Linder et al. 1987).

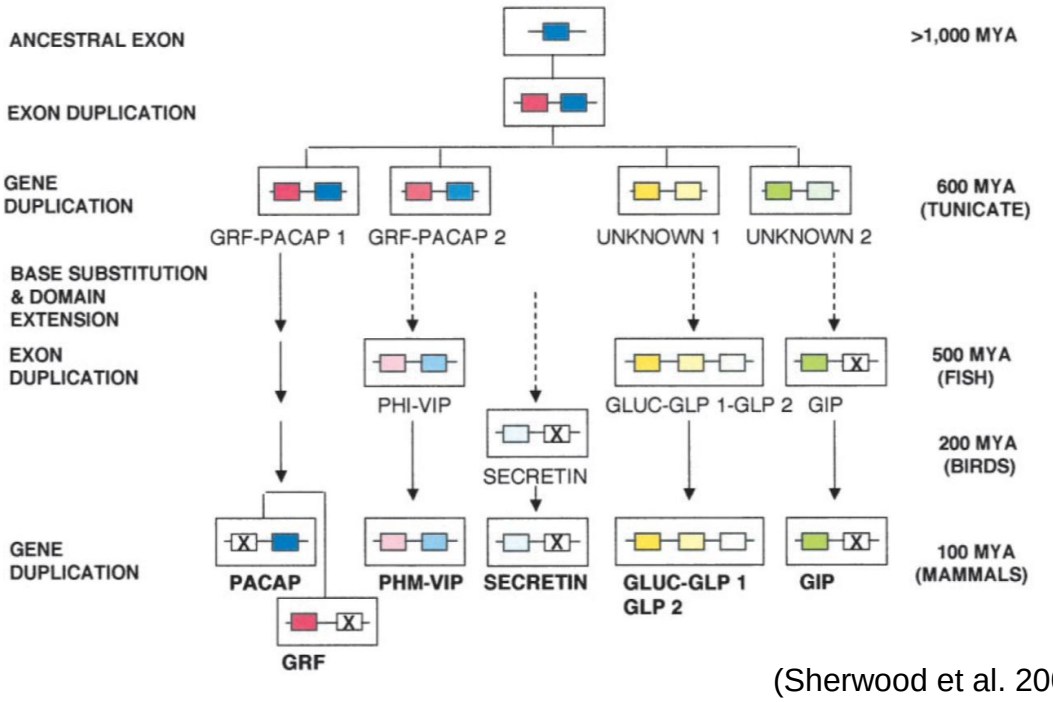

(Sherwood et al. 2000)

Figure 1A: The VIP gene evolved from ancestral PACAP gene duplication

```
                                  10        20        30        40
PACAP                             |         |         |         |
human/sheep/rat/mouse             HSDGIFTDSYSRYRKQMAVKKYLAAVLGKRYKQRVKNK
chicken                           HIDGIFTDSYSRYRKQMAVKKYLAAVLGKRYKQRVKNK
lizard                            HSDGIFTDSYSRYRKQMAVKKYLAAVLGKRYKQ.....
green frog                        HSDGIFTDSYSRYRKQMAVKKYLAAVLGKRYKQRIKNK
salmon                            HSDGIFTDSYSRYRKQMAVKKYLAAVLGKRYRQRYRNK
catfish                           HSDGIFTDSYSRYRKQMAVKKYLAAVLGRRYRQRFRNK
stargazer                         HSDGIFTDSYSRYRKQMAVQKYLAAVLGRRYRQRVRNK
stingray                          HSDGIFTDSYSRYRKQMAVKKYLAAVLGKRYKPKVKNS/GRRVFY
tunicate-I                        HSDGIFTDSYSRYRNQMAVKKYLAAVL
tunicate-II                       HSDGIFTDSYSRYRNQMAVKKYINALL

VIP*
human/monkey/pig/cattle/
sheep/goat/dog/rabbit/
rat/mouse                         HSDAVFTDNYTRLRKQMAVKKYLNSILN
guinea pig                        HSDALFTDTYTRLRKQMAMKKYLNSVLN
oppossum                          HSDAVFTDSYTRLLKQMAMRKYLDSILN
chick/turk/allig/frog             HSDAVFTDNYSRFRKQMAVKKYLNSVLT
cod                               HSDAVFTDNYSRFRKQMAAKKYLNSVLA
trout/bowfin                      HSDAIFTDNYSRFRKQMAVKKYLNSVLT
dogfish                           HSDAVFTDNYSRIRKQMAVKKYINSLLA
```

(Sherwood et al. 2000)

Figure 1B: VIP and PACAP protein sequences are highly conserved amongst species

1.1.1.2. From gene to peptide

VIP and PHM/I are encoded in the same preprohormone (Itoh et al. 1983) of molecular weight 20 000 (Obata et al. 1981) and exhibit high similarity at the C-terminus of their peptide sequences important for their biological functions (Bodner et al. 1985; Fahrenkrug et al. 1985). Indeed these two peptides exert the same biological functions as they do colocalize in equal ratio, in human (Bloom et al. 1983; Tatemoto and Mutt 1980). However, they may also be differentially expressed due to alternative splicing (Bodner et al. 1985), although very little evidence exists in this regard. Previous studies suggest VIP and PHI post-transcriptional processing at specific cleavage sites results in the loss of one exon while the other retains its functionality. Separate neuropeptides could result from alternative splicing, allowing one unit to be removed to satisfy tissue-specific expression of the other (Lamperti et al. 1991; Talbot et al. 1995). A tissue specifier element in the VIP gene drives cell-specific regulation of VIP gene transcription (Hahm and Eiden 1999). VIP and PHI are expressed according to physiological requirement, as shown in fowl in which the VIP prepropeptide regulates prolactin secretion in the absence of PHI expression. Nesting behaviour was also correlated with differential expression and tissue-specific distribution of PHI and VIP (Talbot et al. 1995; You et al. 1995).

The VIP prepropeptide(hormone) is 17 500 Dalton (Obata et al. 1981) and undergoes post-translational processing, although very little evidence exists (Fahrenkrug 1985). Although VIP and PHI/M colocalize, they are not secreted in the same ratios in all tissues, contrary to previous findings (Bloom et al. 1983). Human prepro-VIP is preceded by two basic amino acids, Lysine and Arginine, whereas PHM only by Arginine, resulting in differential post-translational processing of the two peptides. In addition , although VIP and PHI may colocalize in neurons, they may be expressed in variable concentrations (Fahrenkrug et al. 1985). Post-translationally VIP is polyadenylated at the N-terminus and amidated at the C-terminus, which was also elucidated for PHI (Lamperti et al. 1991). As such, understanding VIP function has relied immensely on the loss of function construct, the full VIP knockout mouse model (Figure 2), through the insertion of a neomycine cassette at the PHI exon (Colwell et al. 2003) . In this model, both the PHI and VIP gene expression are disrupted such that overlapping PHI expression and function should not be accountable for the knockout phenotype. The main drawback being that obliterated

functions cannot exclusively be attributed to only VIP loss of function, but also PHI. Thus, the use of VIP administration has been explored in my project, to deduce VIP-specific actions during embryogenesis and in adulthood.

1.1.1.3. Induction of VIP gene expression

As demonstrated in spinal cord cultures (Agoston et al. 1991), following upregulation of intracellular cAMP, VIP gene transcription is driven by a cAMP response element (CRE) upstream from the promoter sequences (Giladi et al. 1990; Tsukada et al. 1987). Protein kinase C upregulation by diacyl glycerol also upregulates VIP synthesis (Agoston et al. 1991; Davidson et al. 1996), highlighting the important role of second messengers in VIP gene regulation. Characteristic to neurotransmitters, VIP synthesis can be stimulated through depolarisations and significantly reduced by tetrodotoxin (TTX) application. In addition VIP can also stimulate its own expression as demonstrated in embryonic spinal cord cultures (Agoston et al. 1991). Other factors have also been shown to stimulate VIP gene transcription in human cell lines and *in vivo* (Beinfeld et al. 1988). This is of interest and suggests the potential regulation of endogenous VIP function by stimulating its secretion through the introduction of an exogenous source of VIP or other factors. VIP expression is also upregulated in spinal cord injury (Waschek 2013).

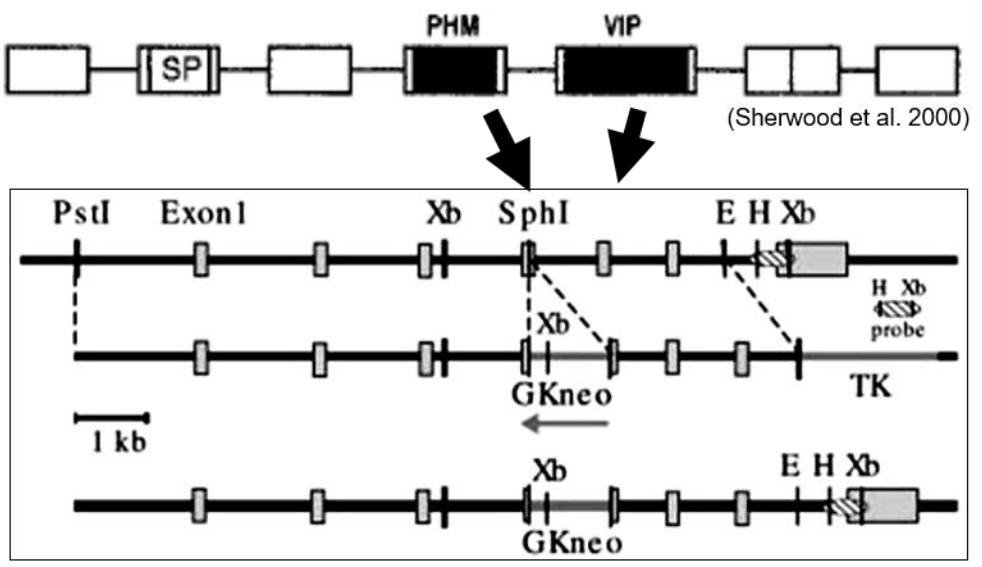

1. **Figure 2: VIP knockout construct was achieved through the insertion of a neomycin cassette disrupting both PHI and VIP expression**

1.1.2. VIP expression

Upon discovery the VIP polypeptide was characterized with a molecular weight of 3500 Dalton (Mutt and Said 1974). Indeed, VIP is stored in and secreted by large dense core vesicles localized at the axon terminals (Besson et al. 1979; Pelletier et al. 1981) and ultimately degraded by chymases and tryptases according to biological requirement (Caughey et al. 1988) with a half-life of about 3 minutes, as reported by Said and colleagues (1986). VIP neurons have pleiotropic central and peripheral effectors, more especially in the brain, spine, respiratory tract and the digestive system (Said 1986).

In the CNS, the so-called VIPergic neurons can be detected throughout the cerebral cortex and limbic structures, projecting either locally or distally to other structures throughout the mammalian brain and spine. In the cerebral cortex, cell bodies are enriched mainly along cortical layers II-IV, with axons terminating at the deeper layers V-VI (Loren et al. 1979; Sims et al. 1980), and are arranged either perpendicularly or parallel to the pial surface (Hajós et al. 1988; Morrison et al. 1984). Neurons that express VIP are mainly GABAergic interneurons (Rogers, 1992) exhibiting either bipolar, bitufted or multipolar morphologies each associated with distinct firing patterns (Loren et al. 1979; Rudy et al. 2011). Thus, VIPergic interneurons are further subdivided into either calretinin positive (CR+) or negative (CR-) and display irregular-spiking and fast-adapting firing patterns, respectively (Miyoshi et al. 2010; Rossignol 2011). Indeed, the distribution of VIPergic interneurons throughout the cortex implicates VIP function on the development and regulation of cognitive behaviour, which may be impaired in VIP-related pathology such as neurodevelopmental disorders (Rossignol 2011) and motor impairments (Lee et al. 2013). In addition to the cortex, VIP immunoreactivity is ubiquitous throughout the murine brain (Loren et al. 1979) as schematically summarized on Figure 3. VIP distribution within the hypothalamus suggests a role for VIP in the maintenance of the hypothalamic–pituitary–adrenal axis as previously demonstrated through local administration of VIP in the paraventricular nucleus (Alexander and Sander 1994). However, limited evidence exists, demonstrating the direct action of VIPergic transmission and circuitry in this region with data only reporting that VIP stimulates

growth hormone and prolactin release and is involved in circadian rhythms (Tohei 2004), functions overlapping with PACAP (Murakami et al. 2001). In addition, in sub-cortical regions, VIP is implicated in cerebral blood flow maintenance and vasodilation (Cauli et al. 2004).

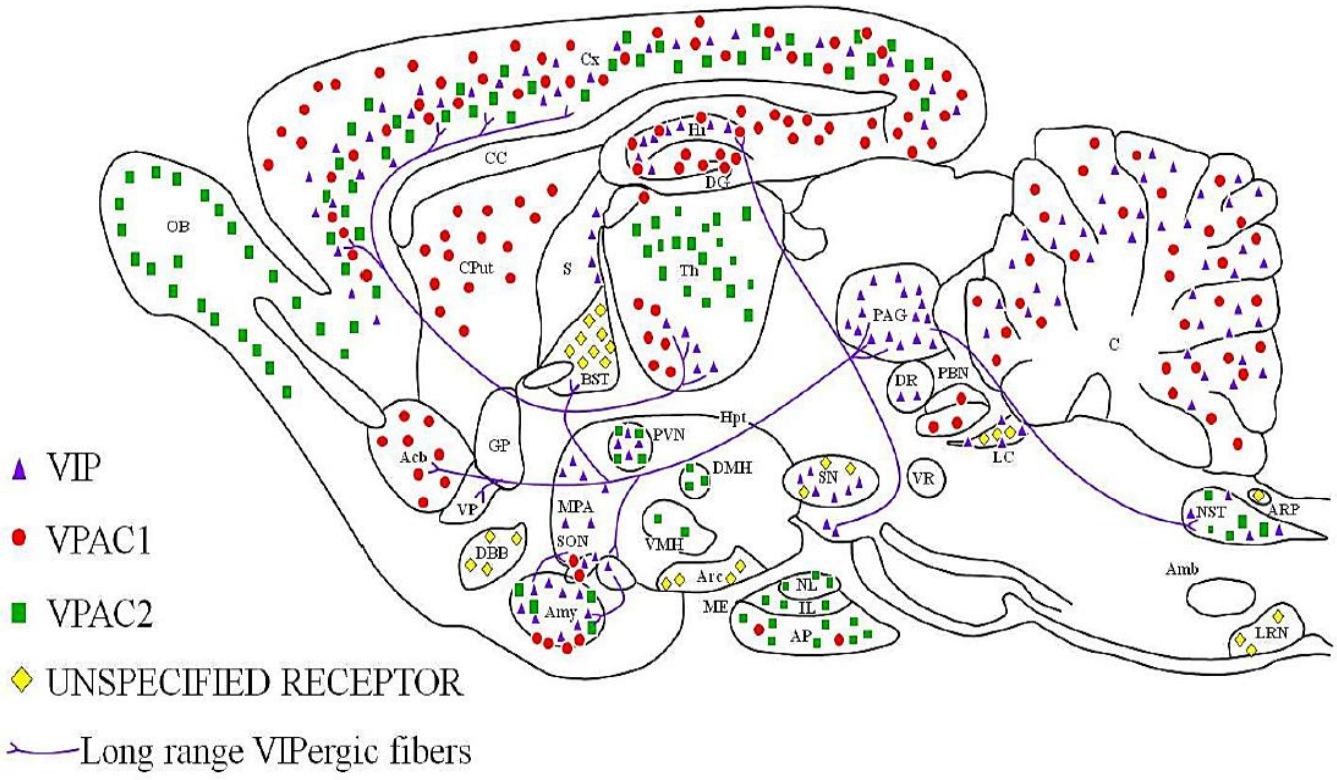

Figure 3: Schematic representation of VIP and VPAC distribution in the adult murine brain

Abbreviations:Acb,nucleusaccumbens;Amb,nucleusambiguus;Amy,amygdala;AP,anteriorpituitary;Arc,arcuatenucleusofhypothalamus;ARP,areapostrema;BST,bednucleusofstriaterminalis;C,cerebellum;CC,corpuscallosum;CPut,caudateputamen;Cx,cerebralcortex;DBB,diagonalbandofBroca;DG,dentategyrus;DMH,dorsomedialnucleusofhypothalamus;DR,dorsalraphenucleus;GP,globuspalidus;Hi,hippocampus;Hpt,hypothalamus;IL,intermediatelobeofpituitary;LC,locuscoeruleus;LRN,lateralreticularnucleus;ME,medianeminence;MPA,medialpreopticarea;NL,neurallobeofpituitary;NST,nucleusofsolitaryract;OB,olfactorybulb;PAG,periaqueductalgray;PBN,parabrachialnucleus;PVN,paraventricularnucleusofhypothalamus;S,septum;SN,substantianigra;SON,supraopticnucleus;Th,thalamus;VMH,ventromedialnucleusofhypothalamus;VP,ventralpallidum;VR,ventralraphenuclei

Indeed, VIP and PACAP are both expressed in the spine and dorsal root ganglia, with levels markedly increased during nerve damage (Dickinson and Fleetwood-Walker 1999). In humans, VIP has long been identified in the lumbar and sacral spinal cords of healthy post-mortem samples, dorsal regions showing significantly higher levels compared to the ventral spine (Anand et al. 1983) as also shown in animals. VIP is expressed in the cat and rat spinal cords, with secretion more pronounced in the dorsal horn compared to the ventral (Yaksh et al. 1982). In various mammalian species VIP-positive axons were found in the white matter, increasing from thoracic to sacral length of the spine. VIP-immunoreactivity has been documented all along the spine, from the cervical to sacral regions, terminating at Layers I to III of the dorsal horn (LaMotte and de Lanerolle 1986). Just as in the brain, VIP innervation in the spine is due to long-range projection fibers connecting the spine to supraspinal structures, and short-range locally projecting fibers (Fuji et al. 1983). The fact that VIPergic axon terminals are enriched at the superficial layers of the dorsal horn (increasing caudally) and that VIP-positive cell bodies are localized and upregulated in nerve damage at the level of the dorsal root ganglion (Dickinson and Fleetwood-Walker 1999) suggests the involvement of VIP in the relay of pain-induced information. In addition, VIP secretion was blocked ipsilaterally in rhizotomy (Yaksh et al. 1982), VIP-positive terminals are found throughout the length of the spine and fibers extend between the brain and the spine (Fuji et al. 1983; Loren et al. 1979): together, these data suggest the involvement of a supraspinal component in the relay and processing of nociceptive information. Thus, it is of interest to study any possible functional changes that may arise in the presence of VIP, either focusing on pain processing or the relay and transmission of sensory information within sensory supraspinal structures such as the brainstem and thalamus.

That VIP is highly expressed in the periphery has been documented historically and a large body of evidence has proven that VIP is one of the main neurotransmitters and neuromodulators in the enteric system (Giachetti et al. 1977; Larsson et al. 1976). Indeed in the digestive tract VIP-expressing interneurons form part of the non-adrenergic, non-cholinergic (NANC) circuitry that mediates gut motility (Furness 2000).

Clinically, VIP is implicated in gut function and immunity due to its oversecretion in what were characterized as VIPomas due to very high levels of

circulating VIP in patients (Bloom et al. 1988). The bronchodilatory actions of VIP have also been demonstrated to treat asthmatic patients (Morice et al. 1984), whereas elevated circulating VIP concentrations in heart failure cases have raised interest in clinical research to investigate the mechanisms of VIP signalling in systemic functions with the use of loss of function models such as the VIP knockout mouse (Szema et al. 2015).

1.1.3. Lessons from VIP knockout mouse studies

As expected from high VIP immunoreactivity in the suprachiasmatic nucleus and the hypothalamo-pituitary axis (Gozes and Brenneman 1989), adult VIP knockout mice exhibit altered circadian rhythm (Colwell et al. 2003) corresponding to their hyperactivity in the open field arena (Girard et al. 2006) which, in addition to disarrayed locomotor activity, may be indicative of anxiety-like phenotype. On the other hand, the absence of VIP in the spinal cord (see *§1.1.2. VIP expression*), especially the lumbar column, may infer a sensory hyperactivity as VIP expression may be the missing link in the relay of information from the spine to the supraspinal compartments.

VIP knockout mice have respiratory dysfunctions in the form of airway hyper-responsiveness indicative of asthma (Hamidi et al. 2006), which may be partially alleviated by exogenous VIP administration (Szema et al. 2006), as well as impairments in large and small intestinal morphology and motility (Lelievre et al. 2007). In addition, impairments of muscular strength further implicate VIP in skeletal muscle control (Girard et al. 2006).

Thus, complete absence VIP may have predisposed adult mice to developmental deficits resulting in the impairment of these well-catalogued VIP regulated systemic functions in the mouse as well as to behavioural defects due to disruptions in the developing brain, as observed in many human cognitive and psychiatric disorders (Girard et al. 2006)

The influence of VIP deficiency on development was demonstrated when wildtype, heterozygous or knockout offspring, originating from partially or completely VIP-deficient mothers, displayed delays in developmental milestones and disruptions

in social behaviour. In addition, offspring of VIP-deficient mothers exhibited severe weight gain reduction, which was more pronounced in knockout offspring (Lim et al. 2008). These studies delineated the contribution of exogenous VIP to rescue and protect the developing embryo (please see Publication 1 for a more in-depth discussion).

1.1.4. VIP and PACAP receptors

Herein is a brief introduction of the VIP and PACAP receptors in general. A more detailed summary of PAC1 structure is given in Publication 1 (see page 1473).

VIP receptors belong to the Class II (Group B) family of G-protein coupled receptors (Laburthe et al. 2007) and also to the Type II receptors in the case of PACAP. PACAP binds to another receptor, PAC1, which also binds VIP but with less affinity (Gottschall et al. 1990; Shivers et al. 1991). Both VPACs bind the other peptides belonging to the VIP family in the following order of decreasing affinity, VIP=PACAP>GHRF>PHI=PHM>GRF>secretin, as summarized from various studies (Harmar et al. 1998; Laburthe and Couvineau 2002; Ulrich et al. 1998). This report will focus on VPAC1 and VPAC2 protein structure and function.

1.1.4.1. VPAC1 vs. VPAC2

These G-protein coupled receptors exhibit structural similarity with the secretin and calcitonin receptor, containing an extracellular N-terminal domain that is typically large in this family of GPCRs, 7-transmembrane domains associated with extracellular loops and an intracellular C-terminal tail (Ishihara et al. ; Lutz et al. 1993).

The selectivity of ligand binding and recognition by the VPACs is determined by the N-terminal domain extracellularly positioned for this purpose (Vilardaga et al. 1995). Here the first 27 amino acids contain the signal peptide, also characteristic of the class II family of GPCRs, and implicated in recruitment of VPAC1 onto the cell surface for optimum exposure and interaction with the ligand (Couvineau et al. 2004). This may be due to the general function of the signal peptide to signal its entry into

the endoplasmic reticulum for processing and cleavage. Thus the signal peptide may fulfill the same role for VPAC2, although studies on this receptor are still lacking. The N-terminus also contains 3 N-glycosylation sites important for receptor expression on the cell membrane (Couvineau et al. 1996). Various residues have been identified and determined crucial for the recognition and binding of VIP to VPAC1. These include a tryptophan residue on amino acid position 67 (Trp67 or W67), which is conserved in VPAC1 and VPAC2 and has been shown to play a crucial role in the binding of VIP to human VPAC1 (Nicole et al. 2000). Six conserved cysteine residues have been identified that maintain the tertiary structure of the extracellular ligand-binding domain in the VPACs, PAC1, secretin receptor and the GHRH receptor (Laburthe and Couvineau 2002; Lutz et al. 1993).

The transmembrane domains are highly conserved within the Group B GPCR family in different species, as was shown in rat, mouse and human studies (Svoboda et al. 1994). However, a significant degree of divergence exists for the N- and C-termini (Lutz et al. 1993) possibly allowing for ligand specificity and to selectively discriminate between signaling cascades. Two conserved residues at the first extracellular loop, Lys195 and Asp196, are associated with the transmembrane domain and play an important role in VIP binding and receptor activation, as well as in cAMP production in VPAC1 (Du et al. 1997; Langer et al. 2003). On the second extracellular loop, Thr274 is important for VIP binding with VPAC2 (Laburthe et al. 2002).

The intracellular C-terminus of VPACs is crucial for intracellular signaling, mainly through activation of G-proteins. Indeed VPACs couple to almost all identified G-proteins, encompassing both GTP- sensitive and insensitive characteristics depending on brain region as shown in the rat (Hill et al. 1992). Mainly VPACs couple to Gs and Gq type of G∝-proteins (Laburthe and Couvineau 1988; Sreedharan et al. 1991) involved in 2nd messenger pathways and calcium mobilization in the cell, respectively. In addition, recent studies report accessory proteins that form a link between the C-terminus and G-proteins to further regulate the interaction of the receptor with intracellular signaling cascades. GPCR-interacting proteins (GIPs) are involved in the regulation of the receptors' pharmacological properties, intracellular signaling and also in the regulation of receptor trafficking and desensitization. The amino acid sequence, SLV (serine, lysine, valine) at the C-terminal tail of VPAC1 interacts with PDZ (post synaptic density protein (PSD95), Drosophila disc large

tumor suppressor (DlgA), and zonula occludens-1 protein (zo-1)) domains. PDZ domains consist of 80-90 amino acids and bind proteins containing PDZ-binding motifs (such as the SLV sequence) with the consensus sequence E(S/T)X(V/I) for type I and ΦXΦ for type II motifs whereby X represents any amino acid and Φ is any hydrophobic amino acid (Hirbec et al. 2002).

VPAC2 contains the SVI (serine, valine, isoleucine) consensus sequence although further studies are necessary to elucidate whether an interaction occurs between VPAC2 and PDZ domains, as well as the functional significance of this possible interaction. PDZ domains form protein-protein interactions with PDZ motifs of membrane proteins and form scaffolding networks that anchor target proteins such as receptor tyrosine kinases (RTKs), glutamate receptors and GPCRs, as well as signaling molecules within a subcellular domain to regulate their function. This mechanism of interaction also involves receptor transactivation. This is of importance as VPAC-mediated signaling is responsible for the trophic actions of VIP, which may result from mitogen-activated protein kinase (MAPK) signaling via receptor tyrosine kinases. Thus, PDZ domains that interact with VPACs may activate RTKs to control the cell cycle and cell growth processes or most likely direct the switch between up- and down-regulation of 2nd messengers and the preference of proliferation and differentiation of neural precursors. Although VIP indirectly activates RTK/MAPK signaling of distal neurons (Gressens et al. 1998) it is yet to be determined whether VIP can locally transactivate RTKs in the same cell.

However, the interaction of VPACs with PDZ domains has been suggested (Laburthe et al. 2002) and shown in endothelial cells (Yung Gee et al. 2009). S-SCAM, a PDZ-based adaptor protein that is a synaptic scaffolding molecule, was able to inhibit VPAC1 internalization and intracellular increase of cAMP. This implicated S-SCAM in the regulation of VPAC1 activation as aberrant VPAC1 activation was suggested in the causation of the watery diarrhea syndrome in VIPoma. This was rendered essential in normal epithelial VIP-mediated fluid and electrolyte secretion as inhibition of cAMP signaling was implicated in inducing electrolyte and fluid flux through transmembrane channels. Three types of receptor activity modifying proteins (RAMPS), RAMP1, RAMP2 and RAMP3, have been identified so far. RAMPs are known to heterodimerize with the calcitonin receptor-like receptor (CRLR) or with the calcitonin receptor (CTR), resulting in a structural

modification and ultimately changing the expression and pharmacological profile of receptors related to the calcitonin family of peptides (McLatchie et al. 1998). Of interest RAMPs were shown to heterodimerize with VPAC1 as well as other receptors from the VIP/PACAP family of receptors. Heterodimerization of VPAC1 with, exclusively, RAMP2 resulted in an increase in phospho-inositide hydrolysis in COS-7 cells, although there were no effects in intracellular cAMP regulation. This suggests a role for RAMP2 in the regulation of cAMP-independent signaling pathways that are activated by VIP through VPAC1 (Christopoulos et al. 2003). This may have implications for intracellular calcium signaling in VIPergic neurons and may 'hint' to the important roles of RAMP2 in the excitability as well as cytoskeleton organization (and possibly receptor trafficking and positioning) in these neurons although any role of this interaction is still to be elucidated. Recently VPAC2 was found to interact with all three RAMPs, especially 1 and 2 which enhanced receptor coupling with Gi/o/t/z (Wootten et al. 2013), also increasing the scope of G-proteins that can couple with VPACs. The third intracellular loop of VPAC1 has been identified as crucial in discriminating between signaling cascades activated by VIP binding through binding directly to specific Gα subtypes (comprehensive review on Langer (2012)).

1.1.4.2. Intracellular signalling and functions of VIP receptors

As already mentioned, VPACs associate with the Gs subtype of Gα proteins that activate adenylyl cyclase and upregulate intracellular cAMP levels. cAMP activates PKA which further phosphorylates other proteins in signalling cascades that mediate the trophic actions of VIP (Purves et al. 2004). Kinases that are phosphorylated by PKA include ERK (extracellular-signal-regulated kinase), which mediates cell growth and differentiation. In addition, cAMP upregulation results in the phosphorylation and translocation of CREB (cAMP response element binding protein), a transcription factor that is involved in the regulation of neural development and growth (Drahushuk et al. 2002). In addition, PKA also activates the mitogen-associated protein kinase (MAPK), (Purves et al. 2004) which has been implicated in VIP-stimulated neuroprotection of developing brains (Gressens et al. 1997). cAMP signalling is also implicated in VIP-mediated trophic actions through regulation of the

cell cycle. This has been demonstrated in immune cells (Anderson and Gonzalez-Rey 2010). In this study, VIP inhibited the synthesis of the cyclins D3 and E which control the progression of cells within the cycle from G1 to the S phase, and cAMP and PKA activation was found to stabilize the cyclin dependent kinase (CDK) inhibitor, p27. This is of interest as inhibition of G1/S phase progression may result in increased cell growth as the cells are kept longer in the cell cycle. Previously this VIP action has been demonstrated in neural precursors as VIP shortened the G1/S phase transition, leading to increased mitosis and embryonic growth (Gressens et al. 1998). PKA also phosphorylates ligand-gated ion channels to increase calcium influx into the cell (Purves et al. 2004). This was suggested in a previous study in which cAMP upregulation was associated with increases in intracellular calcium concentrations, which were determined to be of extracellular origin, thus supporting the notion of intracellularly-activated calcium channels (Jang et al. 1998). Jang and colleagues (1998) then demonstrated that calcium influxes through membrane-bound L-type channels were important for the induction of the transcription factor cFos, which is implicated the regulation of cell growth and differentiation.

VIP also exerts its biological actions through the activation of other signalling cascades by coupling with Gq and Gs proteins to activate phospholipase C (PLC) and subsequently, to generate DAG and inositol-1,4,5-triphosphate (IP3) (Purves et al. 2004).

VIP was shown to stimulate intracellular calcium through activation of inositol phosphates (IPs), including IP3 in CHO cells (Van Rampelbergh et al. 1997). IP3 is known to stimulate the release of calcium from intracellular stores, such as the endoplasmic reticulum, following the activation of Gq-type of G-proteins (Purves et al. 2004). This had already been shown in lymphoblasts as IP3 was suggested to increase calcium concentrations in VIP-stimulated cells through Gq and PLC signalling (Anton et al. 1993). In contrast, Van Rampelbergh and colleagues (1997) reported that VPAC1-mediated PLC activation resulted from Gi/o G-proteins, although Gi/o proteins are generally accepted to inhibit intracellular signalling by inhibiting cAMP. However, it may be considered that Gq signalling was activated following/coinciding with Gs and cAMP signalling inhibition. This can be supported by the results of Jang and colleagues (1998) as they also demonstrated that cAMP

signalling becomes inhibited when calcium is released from intracellular stores. In addition the intracellular calcium increase was correlated with a high VPAC1 density which suggests that although VIP may have inhibited receptors coupled to Gα proteins, there was a high availability of VPAC1 coupled to Gq receptors which was not quantitatively determined. Thus, VIP activates intracellular signalling via activation of either Gαs, Gαq or Gi/o proteins.

VIP decreased cell proliferation in colonic adenocarcinoma cell lines though increasing cAMP levels in these cells (Lelievre et al. 1998). Here the authors suggested the presence of another pathway that could be activated by VIP which is involved in regulating cell growth.

VIP has been shown to exert trophic action on neurons indirectly through astrocytic release of other factors such as interleukin (IL)-1, IL-6, IGF and activity-dependent neurotrophic factor (Brenneman et al. 1995; Gottschall et al. 1994; Servoss et al. 2001). The mechanism of the modulatory action of VIP involves PKC and the MAPK pathway. VIP receptors are also located on astrocytes and their activation results in intracellular PKC activation (Gressens et al. 1998). Subsequent downstream events result in the release of trophic factors, such as mentioned above, which then bind their respective receptors on neighbouring neurons. It can be assumed that these receptors include the RTKs, which activate the MAPK pathway. This was shown in newborn mice as VIP upregulated astrocytic PKC activity followed by downstream activation of neuronal PKC and MAPK and therefore, neuroprotection and axonal repair (Gressens et al. 1998). Involvement of the MAPK pathway suggests that VIP plays a role in cell cycle progression and mitosis. This has been shown in neural precursors, in which VIP stimulated growth and mitosis in sympathetic neuroblasts (Pincus et al. 1994).

VIP was also suggested to regulate phosphatidylinositol 3-kinase (PI3K)-Akt signalling which is involved in cell survival (Anderson and Gonzalez-Rey 2010). VIP promoted cell survival in prostate cancer cells through phosphorylation of the PI3K/Akt target, the proapoptotic protein, BAD (Sastry et al. 2006). BAD phosphorylation was mediated through PKA activation and resulted in inactivation of BAD and inhibition of apoptosis in these cells.

1.1.4.3. Receptor inactivation/desensitization and trafficking

VPACs had long been suggested to contain phosphorylation sites at the C-terminal tail (Sreedharan et al. 1991). GPCR kinases (GRKs) phosphorylate GPCRs at the C-terminus and initiate receptor desensitization after excessive ligand binding to prevent the prolongation of cellular responses. Phosphorylated GPCRs bind arrestins, a family of cytosolic adaptor proteins, preventing further interaction of GPCRs with G-proteins. Other adaptor proteins are then recruited that target the GPCRs to endocytotic pathways whereby the receptor is internalized within a lysosome. Herein the receptor may undergo degradation or be recycled and trafficked back to the membrane surface (Bünemann and Hosey 1999). In addition, two GRK phosphorylation sites are reported by Laburthe and colleagues (2002) for VPAC1 and VPAC2, exhibiting large diversity in distribution. Although GRK sites are found exclusively on the C-terminal tail of VPAC2, they also appear on the intracellular loops 2 and 3 of the transmembrane domain. GRK1 and GRK5/6 coincide with PKA (GRK5/6) and PKC (GRK1) phosphorylation sites on VPAC1. Although the importance of this co-localization is yet to be determined, PKA has also been implicated as a candidate kinase that may phosphorylate VPACs for desensitization. This was shown in COS7 and HEK293 cells that both expressed VPAC2. Excessive administration of VIP to these cells resulted in phosphorylation of human VPAC2. In addition, receptor-independent activation of PKA with forskolin induced phosphorylation of VPAC2 in these cells, though at a lesser degree than VIP alone. These results suggested the involvement of a specific GPCR kinase as well as PKA in receptor phosphorylation (McDonald et al. 1998). GRK2, 3, 5 and 6 have also been demonstrated to phosphorylate VPAC1. In this study the involvement of β-arrestins in internalization of phosphorylated endogenously expressed VPAC1 was demonstrated in HEK293 cells (Shetzline et al. 2002). An additional phosphorylation site was reported for VPAC1, whereby substitution of Thr429 reduced receptor phosphorylation. This study presented Thr429 phosphorylation as a putative early event in receptor downregulation as internalization could be achieved in the absence of phosphorylation of the other GRK sites (Langlet et al. 2006). Although PKA phosphorylation sites were not shown for VPAC2, a redundancy may exist for the roles of protein kinases and GRKs in receptor phosphorylation.

1.1.4.4. VIP functions elucidated from pharmacological models

Functions of VIP receptors signalling have been elucidated with the use of agonists and antagonists, including the highly selective VIP antagonist (VA) that has been previously described (Figure 4). This hybrid peptide consists of a replacement of amino acids 1-6 of the VIP sequence by neurotensin (Gressens et al. 1997) and inhibits VIP binding with higher affinity than VIP in neuronal and glial cells. VA binding attenuated cAMP accumulation and induced neuronal cell death in tissue culture. In vivo, VA inhibited VIP-stimulated sexual behaviour and penile erection, destabilized diurnal rhythm and produced learning deficits in adult rodents (Gozes et al. 1991).

Of interest are the VA-induced developmental perturbations reported in rodents. Neonatal administration of VA in rats delayed motor-related developmental milestones, including limb righting and grasping (Hill et al. 1991). In mice, additional developmental milestones were impaired severely following prenatal administration of VA during the previously identified critical period of VIP control of neurogenesis (Gressens et al. 1997; Wu et al. 1997). Follow-up studies confirmed the neurodevelopmental relationship between prenatal blockade of VIP signalling (with VA) and neurobehavioral perturbations in postnates (and adults). These include lack of social recognition, male-specific cognitive defects and anxiety-like behaviour which is neither increased nor decreased in the presence of a stranger, reminiscent of an apathetic response and the associated autism-like phenotype (Hill et al. 2007a; Hill et al. 2007b). In addition, VIP gene and peptide expression are significantly elevated in VA offspring similarly as in the Ts65Dn mouse model of Down syndrome (Hill et al. 2003; Hill et al. 2007b; Sahir et al. 2006).

VA-induced impairments exhibit similar developmental deficits as VIP deficient mice, such as delays in developmental milestone acquisition, more severe social deficits including apathy to maternal affiliation and in play behaviour (Lim et al. 2008) as well as lack of social interest (in the social approach task and sociability test), where males were more afflicted, just as the VA pups. VIP-deficient mice also exhibited weakened motor and strength abilities in the open field and rotarod tests (Stack et al. 2008). Overall, these studies delineate the contribution of maternal contribution on the developing embryo, whether as a consequence of prenatal disturbance during a critical period or that of the chronic absence of VIP. VIP has

been implicated in prenatal development in the rodent due to its significant release from the placenta which was detected in embryonic tissues as early as E6 in the mouse embryo, with VIP binding sites detected at E9 (Hill et al. 1996; Spong et al. 1999). Therefore, VIP effects on embryonic growth and development may depend more on the maternal VIP than that of embryonic origin. Indeed administration of VA to pregnant females resulted in abnormal brain growth in mouse embryos and neurobehavioral development in mouse neonates (Gressens et al. 1994; Wu et al. 1997). Thus, VIP deficiency and time-dependent blockade of VIP-signaling on development may recapitulate the cognitive and neurobehavioral deficits observed in human patients with abnormal brain growth and development. Thus, we undertook an exploration of the spatio-temporal functions of VIP and PACAP in brain development, in a review describing peptidergic control of regionalized neural development as well as glial specification. This review is reproduced below (Publication 1).

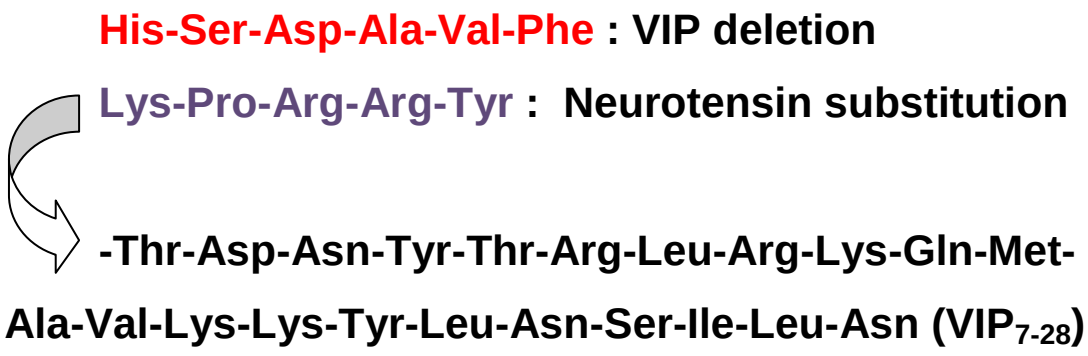

Figure 4: The VIP antagonist chimera prevents VIP signaling due to the substitution of the first 6 amino acids of the VIP peptide crucial for receptor–ligand recognition and selective binding, with a neurotensin sequence.

2. Publication 1: Neuropeptides shaping the central nervous system development: Spatiotemporal actions of VIP and PACAP through complementary signaling pathways.

Journal of Neuroscience Research 00:00–00 (2016)

Review

Developmental Neuroscience and Developmental Disorders

Neuropeptides Shaping the Central Nervous System Development: Spatiotemporal Actions of VIP and PACAP Through Complementary Signaling Pathways

Tando Maduna and Vincent Lelievre*

Institut des Neurosciences Cellulaires et Intégratives, Centre National de la Recherche Scientifique UPR3212, Université de Strasbourg, Strasbourg, France

Pituitary adenylate cyclase–activating polypeptide (PACAP) and vasoactive intestinal peptide (VIP) are neuropeptides with wide, complementary, and overlapping distributions in the central and peripheral nervous systems, where they exert important regulatory roles in many physiological processes. VIP and PACAP display a large range of biological cellular targets and functions in the adult nervous system including regulation of neurotransmission and neuroendocrine secretion and neuroprotective and neuroimmune responses. As the main focus of the present review, VIP and PACAP also have been long implicated in nervous system development and maturation through their interaction with the seven transmembrane domain G protein–coupled receptors, PAC1, VPAC1, and VPAC2, initiating multiple signaling pathways. Compared with PAC1, which solely binds PACAP with very high affinity, VPACs exhibit high affinities for both VIP and PACAP but differ from each other because of their pharmacological profile for both natural accessory peptides and synthetic or chimeric molecules, with agonistic and antagonistic properties. Complementary to initial pharmacological studies, transgenic animals lacking these neuropeptides or their receptors have been used to further characterize the neuroanatomical, electrophysiological, and behavioral roles of PACAP and VIP in the developing central nervous system. In this review, we recapitulate the critical steps and processes guiding/driving neurodevelopment in vertebrates and superimposing the potential contribution of PACAP and VIP receptors on the given timeline. We also describe how alterations in VIP/PACAP signaling may contribute to both (neuro)developmental and adult pathologies and suggest that tuning of VIP/PACAP signaling in a spatiotemporal manner may represent a novel avenue for preventive therapies of neurological and psychiatric disorders.

Key words: neuropeptide receptor signaling; organizer; patterning; proliferation; differentiation; neurodevelopment

FOREWORD

As incredible as it can be, the whole mammalian nervous system is derived from a unique cell that initiates formation of the primordial neuroepithelium. This

SIGNIFICANCE

Pituitary adenylate cyclase–activating polypeptide (PACAP) and vasoactive intestinal peptide (VIP) are neuropeptides widely distributed in the nervous system, where they exert important regulation of neuronal activity, hormonal secretion, and immune system functions but also protect against injuries and pathologies. In the present review, we recapitulate the potential regulatory contribution of these neuropeptides on the critical developmental steps shaping up the nervous system in vertebrates. We also describe how alterations in VIP/PACAP signaling may contribute to pathologies and suggest that tuning of VIP/PACAP signaling in a spatiotemporal manner may offer novel preventive strategies against neurological and psychiatric disorders.

*Correspondence to: Pr Vincent Lelievre, CNRS UPR-3212, Institut des Neurosciences Cellulaires et Intégratives (INCI), 5 rue Blaise Pascal, 67084 Strasbourg, France. E-mail: lelievre@inci-cnrs.unistra.fr

Received 2 June 2016; Revised 4 August 2016; Accepted 15 August 2016

Published online 00 Month 2016 in Wiley Online Library (wileyonlinelibrary.com). DOI: 10.1002/jnr.23915

structure progressively subdivides into distinct regions in a spatiotemporal patterning process governed by small groups of cells called organizers known to release multiple neutralizing factors (for review, see Kiecker and Lumsden, 2012). Indeed, the dorsal blastopore lip, also known as the Spemann organizer, provides the crucial neural plate patterning along its anteroposterior and mediolateral axes. A fully oriented neural tube is obtained with the appearance of secondary and antagonizing organizers that release diffusible morphogenic and/or trophic signaling factors controlling dorsoventral patterning. These phenomena initiate the generation of multiple cell types at the right place and the right time. Those organizer-derived secreted factors have long been identified, with their respective roles and mechanisms of action studied in great detail. However, tight regulation of these and subsequent events that generate the different neural cell types and incorporate into functional neural networks has been also proposed based on the observed detrimental effects induced by pharmacological treatments and genetic ablation. The present review aims at recapitulating the differential roles of vasoactive intestinal peptide (VIP) and pituitary adenylate cyclase–activating peptide (PACAP) along the progressive development of the central nervous system, with special emphasis on potential therapeutic actions of these molecules in diagnosis, prevention, and treatment of pathologies with neurodevelopmental origins.

These two peptides belong to the PACAP/glucagon superfamily of neuropeptides and share very high similarity in both nucleotidic and amino acid sequences. They all present the characteristic signature of the histidyl-seryl residues at the N-terminus (Sherwood et al., 2000). Originating from gene duplications occurring early in evolution, this family shares a very conserved biosynthesis process whereby inactive prepropeptides are cleaved and secreted into one or two bioactive molecules. In the case of mammalian VIP and PACAP genes, the whole processing gives rise to peptide histidine isoleucine (PHI)/methionine (PHM), which only differ by the single substitution of isoleucine into PHM in human, and VIP or PACAP-related peptide and PACAP-38 (the 38-amino-acid-long peptide that can be further shortened to PACAP-27), respectively.

A similar evolution has been proposed for their receptors (Ng et al., 2012), together providing a satisfactory explanation for the equal binding affinities of the two neuropeptides for their so-called VIP-PACAP receptors. In addition, VIP and PACAP display partial redundancy in their distribution patterns and exert complementary functions from embryonic stages to adulthood (Nishizawa et al., 1985; Linder et al., 1987; Sherwood et al., 2000).

Indeed, VIP and PACAP bind the polyvalent VIP-PACAP receptors, VPAC1 and VPAC2, which display similar nanomolar affinity for PACAP and VIP (Harmar et al., 2012). VPACs belong to the class II family of G protein–coupled receptors (GPCRs) bearing the characteristically large extracellular N-terminal domain important for ligand recognition and binding (Laburthe et al., 2007), anchored by a seven-transmembrane domain intersected by intra- and extracellular loops involved in signal transduction and ligand recognition, respectively. The seven-transmembrane domain extends further to the intracellular C-terminal domain crucial for activating G protein–dependent signaling that is mainly coupled to adenylate cyclase and phospholipase C (Laburthe et al., 2007).

VPAC structure is highly conserved within the species (Couvineau and Laburthe, 2012) and shares almost 50% homology with PAC1 in rats (Vaudry et al., 2009). Indeed, VPACs are also characterized as type II receptors for PACAP. However, PACAP binds another receptor (the type I PACAP receptor), PAC1, which may also bind maxadilan (an unrelated peptide identified in sand fly) and VIP but with less affinity (Gottschal et al., 1990; Moro and Lerner, 1997). Binding selectivity can be modulated in PAC1 receptors through the presence of specific splice variants, in particular the "short" and "very short" variants harboring deletions in the N-terminus (Dickson and Finlayson, 2009). In addition, both VPACs bind other members of the PACAP/glucagon family exhibiting a pharmacological profile that differs in various cell types and species (Harmar et al., 2012).

PAC1 and VPACs activate the same signaling pathways including the canonical 3′,5′-cyclic adenosine monophosphate/adenylate cyclase and the inositol 1,4,5-trisphosphate/phospholipase C cascades necessary to activate other downstream protein kinases including protein kinase A (PKA), protein kinase C (PKC), and mitogen-activated protein kinase (MAPK). Signaling pathway preference may be cell-type or tissue dependent and also vary according to biological conditions due to splicing variants affecting the third intracellular loop of PAC1 (Holighaus et al., 2011) and the interaction of VPACs with some specific receptor-interacting proteins such as receptor activity–modifying proteins (Christopoulos et al., 2003). A few variants of the VPACs have been also identified with differential signaling. Of special interest for the review, one of them displaying a very low affinity for PACAP (Teng et al., 2001; Zhou et al., 2006) supports the idea initially proposed by Gressens that a selective VIP receptor was responsible for mediating the neuroprotective effects of VIP against ibotenate-induced brain lesions in newborn mice (Gressens, 1999; Rangon et al., 2006).

Ultimately, acting through these redundant, though overlapping and complex, signaling cascades, VIP and PACAP have been shown to regulate many biological functions in normal and pathological tissues of the peripheral and nervous systems, resulting from tumors, injuries, and genetic diseases (Moody et al., 2011). As articulated below in greater detail, their functions and mechanisms of action evolve along the neurodevelopmental timeline.

INITIAL NEURULATION

In amniotes, gastrulation that allows the mesoderm to be formed takes place in the primitive streak (equivalent to

the blastopore in lower vertebrates) and requires signals that induce nonneural tissues such as bone morphogenic proteins (BMPs) and Wnts. Starting around embryonic day (E) 6.5, initiation of neural plate formation requires inhibition of BMP signaling produced by the gastrula organizers and mesoderm factors such as noggin and chordin. Generated at E7.5, the Hensen node, acting as the Spemann organizer in upper vertebrates, initiates neuroectodermal formation and elongation. Neural induction is mostly completed by E8.5 as the neural plate begins to form a tube of neural tissue with anteroposterior patterning and segmentation of forebrain, midbrain, hindbrain, and spinal cord (for review, see Kiecker and Lumsden, 2012). Coincidental to this critical neural period, expression of PAC1 receptors has been investigated using in situ hybridization in the developing primitive streak of rat embryos at E9, revealing intense labeling in the neuroepithelium and underlying mesoderm subajacent to the headfold. In addition, PAC1 mRNA expression has been shown, corresponding to null and hop1 splicing forms (Zhou et al., 1999). The latter information is critical because hop variants differ from the null (normal size) form of PAC1 by a short cassette insertion in the third intracellular loop that activates different intracellular cascades. In vitro studies performed on mouse embryonic stem cells undergoing neural differentiation confirm the presence of VPAC2 and PAC1 receptors, whilst embryoid body–derived cells only express functional PAC1 receptor. Embryonic stem cell incubation with PACAP or VIP for a week enhanced the neuronal specification in embryoid bodies (Cazillis et al., 2004), demonstrating that activation of PAC1 and VPAC2 promotes embryonic stem cells towards neuronal cell fate.

AXIS FORMATION AND PATTERNING

As mentioned above, the brain/axis specification relies on anteroposterior patterning. In the future head, vesicle formation is made possible by several discrete local organizers that include the midbrain–hindbrain boundary that plays a role in cerebellar development and the anterior neural boundary/commissural plate that regulates forebrain development. In addition, the zona limitans intrathalamica appears as a narrow strip of sonic hedgehog (Shh)-expressing cells in the alar plate of the diencephalon, involved in isolating the prethalamus from the thalamus. In the posterior brain, retinoic acid–dependent hindbrain development leads to rhombomere formation and segmentation using rhombomere boundaries (Kiecker and Lumsden, 2012).

Although the fine tuning of anteroposterior patterning in mice has been extensively characterized, there is limited evidence of direct participation of PACAP or VIP signaling in this process. The first suggestion came from studies performed in neuroblastoma cells showing that retinoic acid affects VIP/PACAP receptor expression (Waschek et al., 1997); the second came from zebrafish embryos showing a potential negative interaction between PKA and Shh signaling (Hammerschmidt et al., 1996). Together, this suggests that according to retinoic acid levels, adenylate cyclase–coupled VIP/PACAP receptors could be differentially expressed and modulate Shh-induced patterning (Waschek et al., 2006). Indeed, PACAP expression has been identified as early as E10.5 in the subventricular zone of the developing neural tube, while its receptor PAC1 is differentially expressed in the midbrain and spinal cord with a higher level in the hindbrain (Waschek et al., 1998). In line with this, follow-up studies by Huang and colleagues (2002) demonstrated that the loss of function of PKA in transgenic mice causes dorsal expansion of Shh signaling as early as E9.5 in the thoracic to sacral regions correlating with neural tube defects including spina bifida, whilst upper regions of the neural tube appear normal. This strongly suggests a crucial role of PACAP/PAC1/PKA signaling along the anteroposterior axis to control neural tube patterning and development, an idea that was further demonstrated in transgenic mice exhibiting neural tube defects due to the presence of multiple copies of the human PACAP receptor gene (*ADCYAP1R1*) to generate gain of function of PAC1 signaling (Lang et al., 2006). In contrast, maternal VIP precedes embryonic VIP, which is expressed in the developing neural tube as early as E10 and strongly underlies the brain vesicles by E12 (Fig. 1A), and may be signaling through VPAC1 receptors that are expressed specifically in the forebrain as early as E9 with a peak of expression in the forebrain and midbrain at E10 (Fig. 1B).

In tight cooperation with anteroposterior development of the neural axis, dorsoventral patterning controls cell fate through many signaling pathways that antagonize or synergize with each other (Hebert and Fishell, 2008). The dorsal phenotype is established at the neural tube under induction signals of mainly the transforming growth factor beta family of transcription factors. Mainly BMPs have been identified to be highly concentrated at the roof plate and promote dorsal identity (Wilson and Rubenstein, 2000). This establishes a dorsoventral gradient that induces neural crest stem cells and specific dorsal interneurons (ID1–6) to be formed at the alar plate. In the opposite position, Shh is transiently expressed and secreted by the notochord to induce its own expression in the floor plate of the developing neural tube. Because of its concentration gradient in the ventral half of the tube, it affects the generation of motor neurons (MN1–2) and diverse ventral interneuron (V1–3) subtypes but also astrocytes and oligodendrocytes (see dedicated "Glial Development" sections) in a temporal and dose-dependent manner. Ventralizing Shh signaling is mainly antagonized through crosstalks between transcription factors Gli-3 and paired box factor (Pax)6 and fibroblast growth factor (FGF) signaling and is modulated by the dorsalizing effects of other morphogens and transcription factors, mainly BMPs and Wnts. Although dorsoventral patterning occurs throughout the developing neural tube, its implication in the adult central nervous system is particularly well understood in spinal cord, hindbrain, and telencephalon (Ulloa and Briscoe, 2007). Altogether, when initiated, dorsoventral patterning may greatly affect

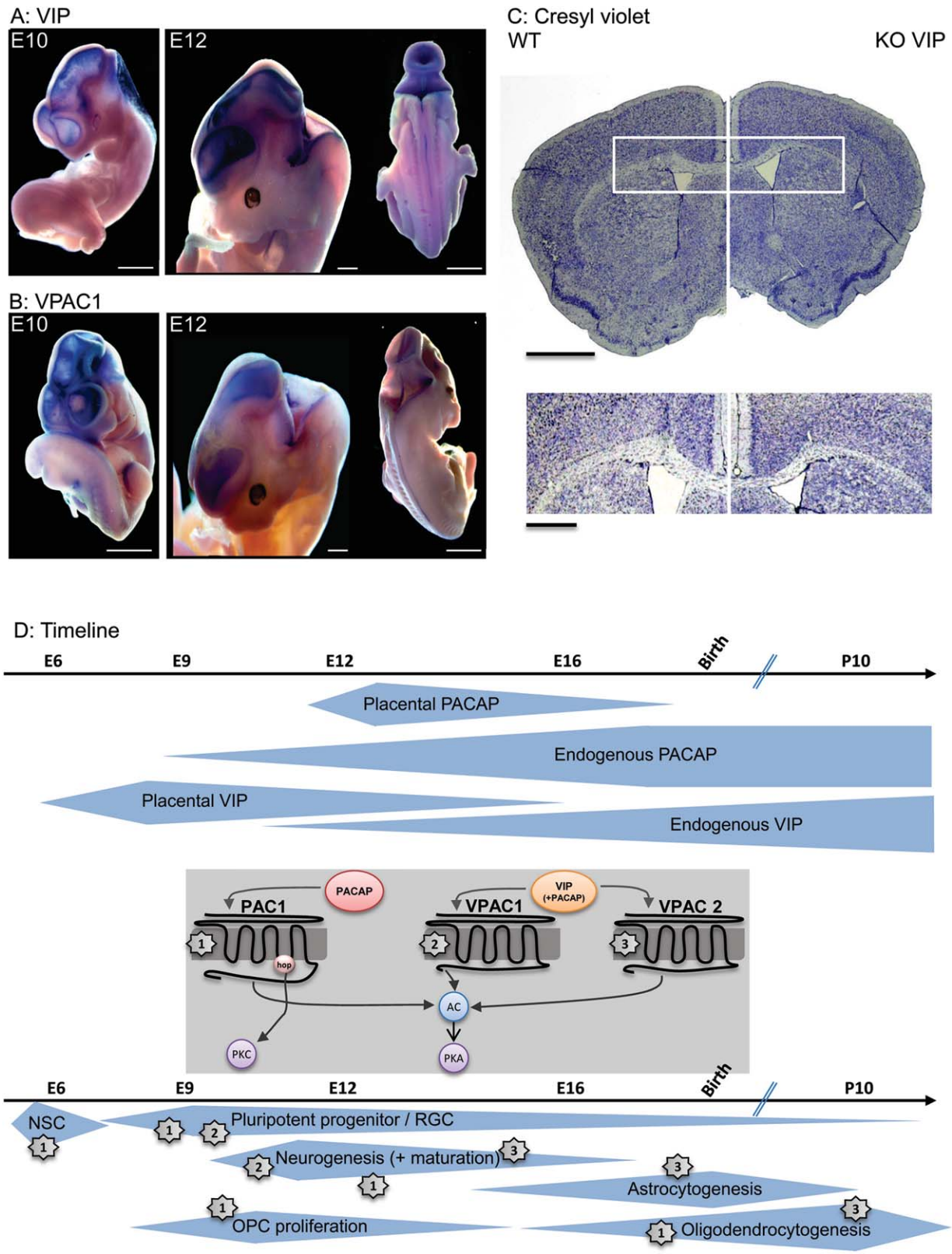
A: VIP
E10
E12
B: VPAC1
E10
E12
C: Cresyl violet
WT
KO VIP
D: Timeline
E6
E9
E12
E16
Birth
P10
Placental PACAP
Endogenous PACAP
Placental VIP
Endogenous VIP
PACAP
PAC1
VIP
(+PACAP)
VPAC1
VPAC 2
hop
AC
PKC
PKA
NSC
Pluripotent progenitor / RGC
Neurogenesis (+ maturation)
Astrocytogenesis
OPC proliferation
Oligodendrocytogenesis

Fig. 1.

the following steps of neurodevelopment and cell specification starting with neurogenesis. As already mentioned, Shh-induced ventral patterning is greatly controlled by PACAP-PAC1 signaling through PKA-dependent signaling pathways in hindbrain-derived structures (Waschek et al., 1998; Nicot et al., 2002). In addition, the ventral midbrain gives rise to dopaminergic neurons in a Shh-dependent manner (Gazea et al., 2016). Gene transactivation by the orphan nuclear receptor Nurr1 is required for the development of the ventral mesencephalic dopaminergic neurons. Among the potential downstream target genes of Nurr1, differential display revealed that VIP transcripts were overexpressed upon activation of Nurr1-responsive cis elements. As a feedback loop, dopaminergic cells release and use VIP to mediate their own survival (Luo et al., 2007). In addition, neural progenitors isolated from mouse embryonic stem cells (Cazillis et al., 2004) or directly from the neural tube of E10 mouse embryos (unpublished data) overexpressed tyrosine hydroxylase, a key enzyme of the dopamine biosynthesis, when cultured in the presence of PACAP or VIP. These findings are of special interest because these dopaminergic neurons are invariantly lost in patients with Parkinson disease.

Special Role in Hindbrain Neurogenesis

In adult vertebrates, the hindbrain hosts numerous structures and nuclei that are essential for motor function, postural positioning, and balance, but also autonomic functions such as control centers for breathing, rhythms, and sleep patterns. Therefore, it is worth noting that PACAP and PAC1 expression have been identified in the central cardiorespiratory center (Farnham and Pilowsky, 2010). This provides a biological explanation for the observation of sudden death in neonatal PACAP knockout mice (Cummings et al., 2004) and the detection of specific PAC1 variants in Caucasian and African American infants dying of sudden infant death syndrome (Barrett et al., 2013).

In addition to what was mentioned above, the precise expression patterns of PACAP and PAC1 have been mapped in mouse from E10.5 until E12 (Sheward et al., 1998) and rats from E11 until adulthood (Zhou et al., 1999) but also in lower vertebrates such as xenopus (Hu et al., 2001) and zebrafish (Wu et al., 2006). In good agreement with these ontogenic studies, PACAP (expressed mainly in subventricular zone) acting on PAC1 receptors (expressed in ventricular zone) may modulate hindbrain development by inhibiting Shh-induced ventral patterning and neurogenesis (Waschek et al., 1998). Overexpression of the human PAC1 gene in mice that resulted in strong receptor signals in hindbrain, midbrain, and diencephalon, as well as in the dorsal root ganglia as early as E10.5, triggered neural tube defects including hydrocephalus-related phenotypes (Lang et al., 2006). Such a phenotype may be in part related to abnormal cilia in ependymocytes, whose development and function rely on GPCR-controlled Shh signaling (Pal and Mukhopadhyay, 2015).

Early hindbrain delineation depends on the hox-dependent rhombomere compartmentalization for its future functions. Of greater interest to us, the cerebellar primordium arises from the dorsal part of the first rhombomere (for review, see Tong et al., 2015) before separating into the ventricular zone and the anterior rhombic lip. In mice, Shh signaling induces the ventricular zone to first generate prospective deep cerebellar nuclei before E10.5, then the production of Lhx1/5-positive Purkinje progenitors. In parallel, under BMP-7 stimulation, anterior rhombic lip generates T-box domain transcription factor (Tbr1/2)-positive precursors around E10.5 to E11.5 that will first become deep cerebellar nuclei and then the granule progenitor cells. After E13.5, the ventricular zone starts to produce Pax2-positive GABAergic interneuron precursors, and ventricular zone–derived Calbindin-positive Purkinje cells undergo radial migration towards pial surface. In the meantime, granule progenitor cells in the external granular layer proliferate to expand its cell population. Later, around E16.5, the ventricular zone and anterior rhombic lip switch to generate glial cells and unipolar brush cells, respectively, while Shh-secreting Purkinje cells adopt their final position between the external granular layer and the prospective white matter. Just before birth, cerebellar foliation starts to allocate cells into different compartments (future lobules) whilst cell migration achieves fine tuning of the position of cells within the cerebellum. Finally, granule progenitor cells stop proliferating and undergo centripetal migration to generate the internal granule cell layer (Tong et al., 2015). As already mentioned, PACAP/PAC1 expression levels are very high in the mouse hindbrain as early as E10.5, suggesting that they participate in cerebellum development (Waschek et al., 1998). Follow-up studies by Skoglösa et al. (1999) and Nicot et al. (2002) have investigated in

Fig. 1. **A and B**: Whole mount in situ hybridization performed on C57bl/6 mouse embryos at E10 and E12 using PCR-generated antisense digoxigenin-labeled riboprobes spanning, respectively, 754 and 628 nucleotides of the mouse VIP (**A**) and VPAC1 (**B**) coding sequences. Time course studies confirmed that VIP expression starts in the telencephalon around E10, whilst its receptor VPAC1 is already expressed at E9 (not shown), solely in the forebrain. By E12 its expression is also abundant in dorsal mid- and hindbrain. Corresponding sense probes were tested in similar conditions and show no specific signal (not shown). Digoxigenin labeling and NBT/BCIP chromogenic revelation were performed according to manufacturer instructions (Roche). Scale bar: E10 = 500 μm; E12: left inset = 2 mm; right inset = 500 μm. **C**: Cresyl violet–stained (14-μm thick) coronal sections of brain from 3-month-old wildtype C57bl/6 and VIP null males revealed that VIP deficiency induced a strong microcephaly associated with reduced cortical thickness and surface without obvious lamination impairment (top). High magnification of the corpus callosum shows a reduced thickness in the knockout structure (bottom). Scale bar: top = 2 mm; bottom = 500 μm. **D**: Schematic representation of the major but differential actions and timing of endogenous vs. maternal VIP and PACAP, and associated signaling during the major steps of brain development.

great detail the expression pattern of PACAP and its receptor in the developing cerebellum. PACAP is expressed in the developing cerebellum as early as E13, with higher expression in specialized structures such as deep cerebellar nuclei and inferior olive at P1, whilst its expression in Purkinje cells slowly increases toward adulthood. In parallel, PAC1 mRNA is present in the anterior rhombic lip but absent in the ventricular zone at E12.5, suggesting that its signaling may affect Shh-dependent anterior rhombic lip-derived cells such as granule progenitor cells. This hypothesis is strongly reinforced by the observation that PAC1 transcripts corresponding to null and hop1 variants colocalize with those encoding transcripts for Shh receptor, Patched1, and target gene Gli1 in the external germinal layer. In rats, granule progenitor migration toward their final internal destination was transiently inhibited in a layer-specific manner when PACAP was administrated in vivo in the early postnatal mouse cerebellum (Cameron et al., 2007). Finally, primary cultures of mouse and rat granule progenitor cells isolated at postnatal day (P) 6 that keep proliferating under Shh exposure were markedly inhibited when costimulated with PACAP. These findings are of special interest in the physiopathology of granule progenitor cell–derived medulloblastoma (Wang and Wechsler-Reya, 2014). Indeed, heterozygous mice lacking one allele of both Ptch1 and PACAP genes exhibit prolonged EGL proliferation coupled with a threefold increase of medulloblastoma incidence compared with the Patched1 heterozygous mutants, suggesting that endogenous crosstalk between PACAP and Shh signaling is necessary to pilot the in vivo granule progenitor cell proliferation rate and duration (Lelievre et al., 2008). This crosstalk involves not only activation of PKA but also inhibition of the translocation of the Shh-dependent transcription factor Gli2 (Niewiadomski et al., 2013).

NEUROGENESIS IN DEVELOPING NEOCORTEX

Just as in hindbrain, telencephalic vesicles rely on ventral and dorsal patterning to generate their complete pool of cells. Neocortical development begins with extensive symmetrical cell division and proliferation of neuroepithelial progenitors forming the ventricular zone of the dorsal forebrain. Initially, neural stem cells (NSCs) undergo solely proliferation to generate a progenitor pool in the ventricular zone (Dehay and Kennedy, 2007). Studies have identified temporal waves of notch signaling as one of the major determinants of neural stem identity and subsequent differentiation (Shimojo and Kageyama, 2016). Thus, activation of notch signaling at the apical end of the dorsal neural tube maintains the neuroepithelial progenitor identity and proliferation to generate a sufficient progenitor pool by promoting cell cycle progression at earlier stages. During later stages the notch downstream effector, the basic helix-loop-helix transcription factor, Hes1, has been implicated in regulating the switch between symmetrical and asymmetrical division to generate one identical and one differentiated daughter cell. The latter migrates out (radially) towards the basal end of the neural tube. Thus, attenuation of Notch signaling, either due to the consequential basal localization of progenitors (Del Bene et al., 2011) or auto(down)regulation of Hes1 expression, may result in temporary proneural gene expression initiating asymmetrical cell division and thus neural differentiation (Shimojo et al., 2008). During this stage, the dorsal neural tube is highly populated by neurogenic radial glial cells (RGCs) spanning the apical to basal extension of the current ventricular zone. RGCs are generated through interkinetic nuclear migration, following notch "apical-basal" gradients during G1/G2 of the neuroepithelial progenitor cell cycle (Dong et al., 2012). These cells preferentially express Pax6, which was shown to promote symmetrical division by preventing cell cycle exit and further increasing the progenitor pool in the ventricular zone (Quinn et al., 2007). Indeed, Pax6 maintains the proliferative and neurogenic identity of these RGCs, which around E12 begin asymmetrical division to generate one identical and one differentiated daughter cell that migrates radially along the mature RGCs to form the subventricular zone. Indeed, starting at E11 in mice and E12 in rats, neuronal progenitors from the ventricular zone migrate towards the apical surface of the developing cortex (Dehay and Kennedy, 2007). In more detail, the ventricular zone serves as the initial site for excitatory glutamatergic neuron generation and development whereby RGCs divide symmetrically to produce more RGCs. They may also undergo asymmetric division to produce intermediate progenitor cells that migrate to the subventricular zone and additional RGCs to maintain an adequate pool of ventricular cells. Intermediate progenitor cells may also undergo differentiative symmetrical division and remain within the subventricular zone. The crucial aspects of symmetrical/asymmetrical division and cell cycle duration control of telencephalic progenitors are highlighted in human primary microcephaly. In patients, 12 loci have been identified encoding 12 mutated genes as directly responsible for the loss of neurons, reduced (>2 SD) occipital-frontal circumference, and mental retardation. Those 12 genes have been characterized for their direct role in the centrosome to control mitotic spindle organization and the symmetric/asymmetric division switch (i.e., *MCPH5, aspm*) or cell cycle dynamics (i.e., *MCPH1, microcephalin*) (Morris-Rosendahl and Kaindl, 2015). VIP action seems to specifically target telencephalic development and seems crucial for the concerted expression of markers for cortical outgrowth. Blocking this pathway with the VPAC antagonist (VIP-neurotensin hybrid) during E9–11 results in reduced cortical thickness independent of cell death but still maintaining normal lamination of the six-layered cortex (Gressens et al., 1994). In the same experimental model, further studies demonstrated that this antagonist specifically interferes with cAMP-coupled VPAC1 signaling, resulting in a reduction in cortical thickness through an inhibition in MCPH1 expression and its target gene, the checkpoint kinase 1. Cell cycle dynamics are therefore altered in the

ventricular zone through doubling of cell cycle duration (Passemard et al., 2011a). Similar or even greater cortical deficit is expected in VIP knockout, as our unpublished data reveal (Fig. 1C, top).

Normal action of VIP on telencephalic development appears to be maternally driven with VIP source as placental T lymphocytes (Spong et al., 1999) until E12 in mice, when significant VIP expression arises from telencephalic vesicles, as unpublished whole-mount in situ hybridization microphotographs revealed (Fig. 1A). Based on these findings we can easily assume that cortical development also should be impaired in VIP null embryos and neonates in a graded manner based on the genotype (null or heterozygous) of the mothers. Such a hypothesis is somewhat sustained by the observation that VIP-deficient offspring exhibit delays in developmental milestone acquisition predisposing them to cognitive and behavioral deficits whose severity is directly linked to maternal status (Lim et al., 2008; Stack et al., 2008).

PACAP acting independently of VIP through PAC1 receptors also has been cited as a potential regulator of cortical development. In an early study by Suh et al. (2001), the authors showed PACAP and PAC1 expression in E14.5–E15.5 developing rat cortex. Transuterine intracerebroventricular injection of PACAP at E15.5 triggers a rapid but transient nuclear translocation of phosphorylated CREB followed by a reduction of cell proliferation, as tritiated thymidine and 5-bromo-2-deoxyuridine (BrdU) injections revealed. Conversely, injection of PAC1 antagonist (M65, derived from maxadilan) triggers an opposite action on developing neurons and neuronal progenitors. However, the action of PACAP on the developing cortex appears more complex since recent findings suggested that PACAP-deficient mice exhibit a decrease in telencephalic BrdU incorporation at E9.5, when the NSCs highly expressed the short form of the receptor (Yan et al., 2013). Altogether, this suggests that the action of PACAP highly depends on the stage of development and the specific PAC1 receptor variants expressed.

At a later stage, postmitotic cells are generated to form the upper layers and ultimately the marginal zone of the putative telencephalon and cerebral cortex (Dehay and Kennedy, 2007). Tbr2 is highly expressed by intermediate progenitor cells at the subventricular zone, serving as a marker for progenitor cell cycle exit and differentiation. Thus, Pax6, Tbr2, and Tbr1 are sequentially expressed as Pax6-positive RGCs proliferate in the ventricular zone, differentiate into intermediate Tbr2-positive progenitor cells of the subventricular zone, and further migrate and differentiate into postmitotic Tbr1-positive projection neurons of the upper layers (Englund et al., 2005). Regulation of cell division/differentiation turnover that directs this Pax6-Tbr2-Tbr1 sequence involves regulation at the G1/S checkpoint whereby the cells can either enter G0 and exit the cell cycle to further differentiate into Tbr2/Tbr1-positive cells or reenter the cycle for further mitotic events and growth as Pax6-positive progenitors.

In vivo administration of PACAP to lateral ventricles of E13.5 mouse embryos has been successfully performed by Ohtsuka et al (2008). Immunohistochemical analyses on P1 cortical sections of the position and the nature of the BrdU-positive, postmitotic neurons born at E13.5 revealed that PACAP treatment not only impaired the migration of the cells, with many of the cells migrating into layers V and VI instead of layers III and IV, but also led to their adopting the phenotype of neurons of the layer they stopped in. Based on these findings and on our own published and unpublished data (Passemard et al., 2011a), one can speculate that VIP that can slow down proliferation by increasing cell cycle duration may enhance G1/G0 exit and neuronal differentiation. Keeping in mind that (1) during early pregnancy, the main source of VIP is found in maternal decidual cells and placental T lymphocytes, and (2) during the peak of telencephalic neurogenesis (E9–E11) in mice, a high amount of VIP can cross the barrier to infuse the whole embryo (Hill et al., 1996), we also speculate that detrimental conditions including infection, inflammation, stress, and others may alter maternal neuropeptide delivery to developing brain. This hypothesis is also plausible for PACAP because it has been found as early as gestational week 7 in human stromal cells surrounding the blood vessels within stem villi (Koh et al., 2005) and released in umbilical arteries (Reglodi et al., 2010).

At the ventral telencephalon (in mice), cortical interneurons arise first from the medial (MGE) around E11, the lateral (LGE) at E12, and finally the caudal (CGE) ganglionic eminence at E13 in the mouse embryo (Hernández-Miranda et al., 2010; Miyoshi et al., 2010). Indeed, this concerted process is maintained through Pax6 expression, which initially inhibits the expression of LGE and MGE markers during the peak of radial migration at the dorsal end (Quinn et al., 2007). Indeed, under Gli regulation, Pax6 is implicated in establishing the dorsoventral border. Subsequent downregulation of Pax6 at the ventral end may be the initial trigger for MGE and LGE neuron specification (Quinn et al., 2007; Hebert and Fishell, 2008). VIP is found to play a crucial role in neuronal (tangential) migration reported around E16–E17 in mice and rats. In addition, VIP displayed autocrine and brain-derived neurotrophic factor (BDNF)-dependent stimulation of somatostatin secretion in the developing MGE-derived cortical interneurons (De los Frailes et al., 1991; Villuendas et al., 2001), therefore suggesting a role for VIP in facilitating tangential migration and interneuron development. In addition, 30% of the ionotropic serotonin receptor (5HT3aR)-expressing cortical interneurons are actually VIP-positive interneurons, which are key elements in neurovascular coupling (Cauli et al., 2004), the regulation of neuronal energy metabolism (Magistretti et al., 1998), and also cortical activity facilitation since they mainly synapse on other interneurons (Jackson et al., 2016). This disinhibitory microcircuit onto somatostatin-positive interneurons has been functionally characterized in the visual, the auditory, and the primary somatosensory (barrel) cortex. In the latter, VIP-positive neurons are mainly located in layer II/III, where they inhibit somatostatin-positive interneurons, which

themselves inhibit pyramidal cells (Rudy et al., 2011). The whole microcircuit should trigger a gain of function in sensory information processing in the cortex that could be lost in VIP-deficient mice (Lee et al., 2013). Considering the growing evidence reporting interneuron dysfunctions in schizophrenia, and the genetic association between microduplications of chromosome 7q36.3 spanning VPAC2 gene and schizophrenia in humans (Vacic et al., 2011), there is need for further studies looking at interneuron impairment in VIP-deficient mice.

GLIAL DEVELOPMENT

VIP and PACAP play various roles in regulating glial cell formation and function, as well as acting as a secretagogue stimulating the release of trophic and neuroprotective factors by glial cells (Brenneman et al., 1997; Shioda and Nakamachi, 2015). Numerous lines of evidence have documented the actions of VIP and PACAP in astrocytes, oligodendrocytes, and activated resident macrophages (microglia) to promote normal brain development, but also neuronal and glial survival in both normal and pathological situations. Interestingly, prenatal blockade of VIP function with intraperitoneal injections of the VIP-neurotensin hybrid generates pups displaying neuronal and behavioral phenotypes somewhat resembling patients with autism, Down syndrome, and/or mental retardation (Hill et al., 2007). This animal model also highlighted the importance of the maternal contribution on normal brain development and function, a support that is lost in preterm infants, implicating VIP and other maternal factors with neuroprotective action as potential preventing treatments against white matter disorders (WMDs)/injury (Passemard et al., 2011b).

In Astrocytes . . .

Following neural migration from the ventricular zone to form the multilayered neocortex, astrocytes develop from RGCs starting around E17/E18 and continuing during the first postnatal days in mice (Mission et al., 1991; Pinto and Götz, 2007). Notch signaling promotes glial fibrillary acidic protein (GFAP) expression only at the termination of neural differentiation and migration (Wakamatsu, 2004). The transition NSC-RGC has been extensively studied in both developing spinal cord and forebrain, and RGCs are known to generate different types of astrocytes based on their dorsoventral position and the final destination of their progenies (Rowitch, 2004). Indeed, protoplasmic astrocytes in the gray matter are morphologically distinct from those fibrous in the white matter (Miller and Raff, 1984). NSC-RGC switch relies on two independent phenomena. One is the epigenetic derepression of astrocytic gene transcription; the second requires the cytokine-dependent activation of the janus kinase/signal transducers and activator of transcription (gp130/JAK/STAT3) pathway to induce astrocytic gene transcription. These events may occur in a sequential manner starting with cytokine-insensitive epigenetic mechanisms described in early-gestational and mid-gestational-stage NSCs capable of targeting the promoters of astrocytic genes such as GFAP (which are highly methylated at these stages), then continuing with the early activation of the gp130/JAK/STAT3 pathway by cytokines of the interleukin (IL)-6 family to induce the astrocyte differentiation of RGCs (for review, see Namihira and Nakashima, 2013). Altogether, RGCs lose their neurogenic potential coincidental to the time when they dissociate/lose contact with the apical surface of the ventricular zone, suggesting that local neurogenic factors maintain their pluripotency and prevent early differentiation and progenitor depletion (Götz et al., 2002; Kanski et al., 2014). The apical surface acts as an extracellular matrix or basement membrane enriched with growth factors promoting self-renewal of NSCs instead of gliogenesis (Pinto and Götz, 2007). Therefore, dissociating them from the apical surface may decrease sensitivity of RGCs to growth factors, such as FGF and neurogenin1 (Rowitch and Kriegstein, 2010), allowing them to undergo by default gliogenesis and/or to become more susceptible to gliogenic factors including cytokines, a scenario observed in vitro when culturing NSCs. In line with this theory, ciliary neurotrophic factor (CNTF), as many gliogenic factors, has been shown to promote astrocytogenesis by upregulating the canonical JAK-STAT pathway (Bonni, 1997). In parallel, BMPs, mainly acting through serine/threonine kinase receptors, can recruit Smad-1, -5, or -8 transcription factors known to generate active complex with Smad4, which in turn shuttles to the nucleus and activates its specific target genes. However, Smads can also induce astrocytic gene expression when creating a complex with STAT3 in the presence of p300/CBP (Kanski et al., 2014). More intriguingly, initial studies show that transient exposure of cortical precursor cells to PACAP, but not VIP, induces astrocyte differentiation from initially nestin-positive cortical progenitors isolated from E17 rat fetuses (Vallejo and Vallejo, 2002). This astroglial differentiation was blocked by Rp-cAMPS, consistent with a cAMP-dependent signaling cascade initiated by PACAP interaction with the short (null) isoform of PAC1 receptor expressed by the cells. Later, PACAP was found to stimulate expression of GFAP and astroglial differentiation of mouse E14.5 NSCs (Ohno et al., 2005) through intracellular PKC and PLC upregulation (Watanabe et al., 2006). This suggests that PACAP may differentially affect precursor cells depending on the developmental stage of cortical progenitors and the nature and concentration of selective PAC1 splice variants. Another hypothesis is that PACAP may be acting initially in a cAMP-independent mechanism to initiate the cascade of NSC differentiation during neurogenesis, eventually stimulating cAMP signaling for GFAP transcription. In greater detail, the PACAP-induced PAC1 receptor may recruit small GTPases Rap1 and Ras and elicit a cAMP-dependent calcium influx. Elevation of intracellular calcium stimulates the transcription factor downstream regulatory element antagonist modulator, known to recognize specific sites of the promoter of the GFAP gene, to promote its expression during astrocyte differentiation

(Vallejo, 2009). Although most evidence points to PACAP/PAC1 signaling as one crucial mechanism to control proliferation and differentiation of NSCs, polyvalent VIP/PACAP binding sites have previously been identified in the neocortical germinative zone as neuronal proliferation ceases (Hill et al., 1999). More interestingly, VIP receptors present in glial cells (at significantly lower levels than PAC1) belong almost exclusively to VPAC2 subtype (Grimaldi and Cavallaro, 1999; Vallejo and Vallejo, 2002). Downstream signaling cascades may induce the translocation of PKC from the cytoplasm to the nucleus instead of elevating intracellular cAMP levels, as treatment with subnanomolar concentrations of VIP revealed in neonatal cortical astrocytes (Olah et al., 1994). Consistent with the pattern of receptors, VIP appears to play differential roles during gliogenesis from PACAP, acting as an astroglial mitogen in culture (Brenneman et al., 1990) and promoting astrocyte maturation, as deduced from the observation of reduced astrogliogenesis in mouse neonates prenatally treated with the VIP antagonist (Lamboley et al., 1999). This effect was more likely mediated through VPAC2 (Zupan et al., 1998) since the antagonist-induced inhibition of astrocytogenesis was also reversed by Ro 25-1553, a long-acting cyclic VIP agonist selective for VPAC2 receptor. The long-term consequences of the transient blockade of astrocytogenesis were very impressive since VIP antagonist-treated neonates also display impairments in neurite differentiation and synapse formation (Zupan et al., 2000). One possible explanation for such dramatic effects is that VIP stimulates secretion of trophic factors by astrocytes, which promotes neural survival and network formation (Gottschall et al., 1990; Brenneman et al., 1997; Giladi et al., 2007). This paracrine trophic loop seems to be highly relevant in cases of perinatal brain damage. As proposed by Gressens (1999), intracerebral administration of ibotenate to newborn mice induces excitotoxic white matter lesions. In this model of human periventricular leukomalacia, coinjection of VIP (but not PACAP) protects against the white matter lesions. As a matter of fact, VIP did not prevent the initial appearance of white matter lesions but, instead, efficiently promoted a secondary repair with axonal regrowth. Pharmacological studies using signal transduction inhibitors showed that both PKC and MAPK pathways were critical for neuroprotection and suggested the following model: VPAC2 activates PKC in astrocytes, which releases soluble factors; these released factors activate neuronal MAPK and PKC to promote axonal regrowth (Gressens, 1999). Another potent VIP-induced trophic factor released by astrocytes is the activity-dependent neurotrophic peptide (ADNP) (Brenneman et al., 1990; Brenneman and Gozes, 1996). This peptide has a similar effect to VIP on VIP antagonist–induced inhibition of astrocytogenesis and is crucial for brain formation (Gozes et al., 1999). In addition to growth factors, VIP- or PACAP-stimulated astrocytes secrete a wide array of cytokines (Brenneman et al., 2003) that also display trophic functions in the developing brain (Bauer et al., 2007). For instance, at subnanomolar concentrations, VIP stimulated astrocytic release of tumor necrosis factor (TNFα) and macrophage- or granulocyte-colony–stimulating factors, possibly via mobilization of intracellular calcium and PKC activity (Brenneman et al., 2003), whilst acting at nanomolar concentrations on cAMP-dependent release of astrocytic IL-1α (Brenneman et al., 1990), IL-3 (Brenneman et al., 2003), and IL1β, which then potentiates the release of IL-6 (Gottschall et al., 1990). The latter was even stronger in the presence of PACAP-38 than VIP.

Developmental disorders include a whole family of psychiatric diseases characterized by dysregulated astroglial function. These include Down syndrome and autism spectrum disorder. Evidence for abnormal circulating VIP levels has been documented in these developmental pathologies (Nelson et al., 2006), which further strengthens the idea that VIP may play a crucial endogenous role in glial functions, especially during the end of gestation and early postnatal life. Consistent with this hypothesis, Ts65Dn mice, which exhibit many characteristics of Down syndrome including small size, developmental delays, and accelerated cognitive decline, also exhibit abnormal resistance to VIP stimulation (Sahir et al., 2006). More interestingly, transient injection of VIP or ADNP improves cognitive function in Ts65Dn mice (Incerti et al., 2012). Compared with Down syndrome, autism spectrum disorder is a prominent neurodevelopmental disorder in which patients develop social deficits, impaired communication skills, and stereotyped and repetitive behaviors during the first three years of life. Although no definitive cause for autism spectrum disorder has been stated, both genetic and environmental origins have been pointed out. In addition to abnormal levels of neuropeptides, such as VIP, calcitonin gene-related peptide, and related neurotrophic factors (BDNF and neurotrophin4/5) (Miyazaki et al., 2004), it is quite striking that patients with autism spectrum disorder may also suffer from inflammatory bowel disorders and that polymorphisms in the upstream region of the VPAC2 receptor gene have been genetically linked to autism spectrum disorder patients with gastrointestinal and stereotypical behaviors (Asano et al., 2001). In VIP-deficient mice, deficits in social behavior and cognitive function have also been observed, suggesting that targeting VIP signaling may offer therapeutic opportunities (Girard et al., 2006; Stack et al., 2008).

. . . Oligodendrocytes

During embryogenesis, initial oligodendrocytogenesis happens as early as E12.5 and E14 in developing spinal cord of mice and rats, respectively. Initial studies revealed that a restricted group of neural cells expressing the platelet-derived growth factor (PDGF) receptor appears in the ventral ventricular zone of the neural tube. Because oligodendrocyte precursors (OPCs) are known to proliferate in response to PDGF, these highly proliferating cells have been proposed to represent the founders of the spinal cord oligodendrocyte lineage (Miller, 1996). These progenitors actually arise from a common pool of neural

progenitors including the so-called pMN domain in the ventral area of the neural tube where Shh is known to control and orient local progenitor cell fate (Orentas et al., 1999). The motor-neuron-to-oligodendrocyte fate switch seems to rely on the secreted sulfatase 1 that locally acts as an enhancer of Shh signaling (Touahri et al., 2012). The basic helix-loop-helix protein Olig2 interacts in a time-dependent manner with successive regulatory partners, first neurogenin1/2 and Pax6 (to generate motoneurons and V3 interneurons), and then Nkx2.2 to specify OPCs. A second wave of OPCs arises from dorsal neural tube around E15.5 in mice. The specification of these cells occurs in an Shh-independent manner but requires a reduced BMP signaling. Taken together, ventral and dorsal OPCs participate to the white matter in an 80/20 ratio, respectively (Cai et al., 2005). In a similar manner, a group of cells expressing PDGFα receptor mRNA were detected in the ventricular and mantle zone of the ventral diencephalon of the E13 rat. Those progenitors were proposed to represent the founders of the forebrain oligodendrocyte lineage. OPC production actually occurs in the forebrain and follows a similar pattern to that in the spinal cord. In the ventral part of the subventricular zone of the forebrain, Shh drives glial progenitor production in three distinct waves. The first wave of Nkx2.1-positive OPCs arise in the MGE at E12.5 and migrate tangentially and dorsally to colonize the entire forebrain. Three days later, a second wave of OPCs emerge from Gsh2-expressing OPCs in the LGE of the developing medial forebrain and migrate throughout the forebrain in a preferentially dorsally manner. A third and final wave of Emx1-positive OPCs occurs right before birth. These dorsally originating OPCs migrate locally to populate the corpus callosum and greatly contribute to the white matter of the overlying cortex that matures around P10 in mice. Although most of them exit the cell cycle to differentiate into myelinating oligodendrocytes at their final destination, about 5% persist as stably resident OPCs in mice, providing a reliable source of cells to achieve normal myelin turnover (Goldman and Kuypers, 2015). OPC differentiation into mature myelin-producing cells has been extensively studied in vitro and in vivo and follows a tightly controlled sequential program. Besides the trophic actions of Shh, FGF, PDGF, neurotrophin3, and other endogenous secreted molecules, oligodendrocytes can also be regulated by PACAP (Masmoudi-Kouki et al., 2007), but small evidence exists for VIP action on oligodendrocyte progenitor differentiation. According to the timeline of in vitro oligodendrocyte production (McCarthy and de Vellis, 1980), PACAP stimulates oligodendrocyte proliferation but delays maturation of oligodendrocyte progenitors, with high expression of PAC1 in the subventricular zone and optical chiasma that are rich in OPCs in the developing brain of newborn mice (Lee et al., 2001). In line with these findings, PACAP-deficient mice exhibit neither myelination deficits nor abnormal patterning but, instead, an earlier initiation of the myelination process in the cortex, resulting in higher density of myelinated fibers in all examined brain areas (Vincze et al., 2011).

Interestingly, there appears to be a switch between VIP and PACAP actions in oligodendrocyte development from proliferation to differentiation. This may rely on an interaction between the two peptides, switching OPC signaling from proliferation to differentiation. When VIP and VPACs were expressed in differentiating OPCs, this was paralleled by PACAP suppressing mitogenic factors that promote cell growth in the progenitors, such as Shh and PDGF signaling. VPAC2 expression was pronounced in differentiating OPCs and downregulated the PACAP-activated cAMP expression that had been previously shown to promote OPC proliferation (Lelievre et al., 2006). Thus, although differential actions are displayed by these two peptides in developing neural and glial cells, there appears to be a strong regulatory interaction that directs the proper timing of growth and maturation of progenitors to fulfill the ontogenic requirements of the developing brain. Considering that VIP null mice exhibit a myelination deficit clearly visible at the level of the corpus callosum (Fig. 1C, bottom), we can propose that VIP enhances myelination in vivo. In the absence of PACAP such as in PACAP null mice, one can hypothesize that loss of PACAP-induced OPC self-renewal further enhances VIP differentiating effects, a phenomenon that is responsible for early oligodendrocyte differentiation. In animal models suffering from injuries or insults occurring during the perinatal period before corticocortical and thalamocortical projections are myelinated, reduction of OPC and/or myelinating oligodendrocytes in key structures such as commissural (including corpus callosum) and associated fibers has been observed with intense local inflammation (Volpe et al., 2011). Therefore, it is no surprise to observe that lipopolysaccharide or exogenous or glia-derived proinflammatory molecules (such as IL-1β) acting through toll-like receptor signaling can solely trigger or exacerbate central hypomyelination when released or injected during the postnatal critical period of OPC maturation (Wang et al., 2009; Favrais et al., 2011; Deng et al., 2014). In these models mimicking perinatal WMDs in humans (Dean et al., 2014), direct injections or viral delivery of neurotrophic factors (such as CNTF, neurotrophin3, and BDNF), hormones (thyroid hormone and progesterone), and others proved efficient to counteract deleterious effects of cuprizone diet, hypoxia, or excitotoxic injection (for review, see Chew and DeBoy, 2015). In line with these findings, VIP or PACAP induces robust protection of the differentiating oligodendrocyte through cAMP-dependent VPAC1 signaling (Favrais et al., 2007).

Later, in adults exposed to experimental pathological conditions, VIP is implicated in axon repair and growth as well as remyelination (Zhang et al., 2002), events relying on adult OPC reactivation. VIP and VIP mRNA are upregulated in the DRG and spinal cord following peripheral axotomy (Waschek, 1996) where VIP plays a reparative role in nerve injury (Zhang et al., 2002). This is VPAC1 mediated, resulting in upregulation of intracellular PKA signaling (Delgado et al., 2004).

Finally, as observed in a mouse model of perinatal white matter damage, ibotenate-induced white matter lesions and cognitive deficits were remarkably reversed by NSC therapy to a greater extent when NSCs were preincubated with PACAP (Titomanlio et al., 2011). This result strongly supports the potential role for VIP and PACAP as boosters in experimental cell therapy of nervous system injuries and degenerative diseases.

. . . And Microglia

Microglia act as resident macrophages of the CNS and represent about 5% of the total adult CNS cell population. Recent findings reveal that microglia are actually directly involved in many developmental processes, including regulation of cell number and spatial patterning at early stages, as well as myelination and formation and refinement of neural networks (Frost and Schafer, 2016). Microglia arise from erythromyeloid precursor cells generated in the embryonic yolk sac, which then migrate throughout the whole embryo and populate the developing brain as early as E9.5 in mice. After invading the developing neural tube, these amoeboid precursor cells evolve into ramified microglia and spread everywhere in the mature CNS, a critical step made possible by very intense proliferation between E10.5 and P0 (for review, see Tay et al., 2016). During this early step, microglia release trophic cytokines/factors such as insulin-like growth factor 1, IL-1β, IL-6, TNFα, and interferon γ that stimulate neurogenesis and oligodendrogenesis. Activated microglia acting as macrophages were found to proliferate and accumulate in highly apoptotic areas to clear the aftermath of neuronal death. In addition, the function of microglial phagocytosis also restricts the number of neural precursor cells in proliferative niches of the developing telencephalon in perinatal rats and macaques (Cunningham et al., 2013). Adult neurogenesis occurs in restricted brain areas including the dentate gyrus of the hippocampus to support lifelong efficient learning and memory. Recent studies reveal that depleting microglia from cultures reduces NSC survival and proliferation, whereas infusing microglia or their conditioned culture medium stimulates it (Walton et al., 2006). VIP produced and released by dentate gyrus GABAergic interneurons interacts with microglial VPAC1 receptors to enhance the release of IL-4, which directly targets neural stem/progenitor cells and stimulates their proliferation (Nunan et al., 2014). This indirect/microglial-driven neurotrophic action of VIP on dentate gyrus neurogenesis is associated with a direct action of VIP release by GABAergic neurons on VPAC1/2-expressing, nestin-positive dentate progenitors (Zaben et al., 2009). Differential interaction of VIP on VPAC1 and VPAC2 drives nestin-positive NSCs toward granular cell phenotype with or without progenitor pool expansion. Thus, VPAC2 null neonates showed a high mortality rate and dentate neurogenesis in adults, whilst VIP deficient mice exhibited normal learning and memory recall of the fear-conditioned behavior 24 hr after training, which quickly disappeared within the next 24 hr (Chaudhury et al., 2008). This demonstrates a pivotal role of VIP in the neuro-immuno-neurogenic pathway and suggests that any interference with normal actions of VIP or PACAP (PACAP acting on microglial VPACs) can affect normal microglial actions on embryonic or adult neurogenesis. Mature microglia are known to oscillate between M1 and M2 states in which activated microglia secrete various proinflammatory cytokines and neurotoxic mediators (M1), or instead promote tissue reconstruction by releasing anti-inflammatory cytokines (M2) (for review, see Franco and Fernández-Suárez, 2015). Keeping in mind that VIP and PACAP inhibit the release of proinflammatory chemokines by lipopolysaccharide-activated microglia through VPAC1 and cAMP signaling (Delgado et al., 2002), one can speculate that these neuropeptides favor M2 activation. Therefore, in pathological conditions where combined cognitive impairments, interneuron loss, and immune system activation occur, such as traumatic brain injuries, temporal lobe epilepsy, and Alzheimer disease, therapeutic strategies exacerbating PACAP/VIP signaling pathways and M2 microglial state could provide interesting alternatives. Indeed, a recent report showed successful neuroprotection by PACAP-producing stem cells after brain ischemia due to their capabilities of redirecting the microglial response toward a neuroprotective M2 phenotype (Brifault et al., 2015).

CONCLUSION

VIP and PACAP produced by maternal and embryonic tissues interact with their natural receptors expressed differentially in various developing structures of the central nervous system. Because of positioning and timing constraints of their receptors, but also plasticity of their signaling cascades, they offer a wide range of actions during the whole process of making a functional nervous system, starting with cell generation (as depicted on Fig. 1D), but also during cell migration, maturation, synaptogenesis, and myelination as well as during programmed cell death since these neuropeptides are known to be neuroprotective. As described in great detail in the present review, VIP and PACAP gene patterning correlates to the precise spatiotemporal genetic program driving nervous system formation, suggesting their direct involvement in neural development. These studies have benefited largely from pharmacological as well as loss-and-gain-of-function studies using transgenic animal models. The very same transgenic animals provided better understanding of the specific roles of these neuropeptides in adult brain. Indeed, many studies have demonstrated the direct impact of VIP and/or PACAP on retina and suprachiasmatic nuclei in relation to circadian rhythms (Hannibal et al., 2001; Colwell et al., 2004; Aton et al., 2005), on hippocampus and memory formation and consolidation (Matsuyama et al., 2003; Chaudhury et al., 2008), on the hypothalamic–pituitary–adrenal axis in regard to stress management anxiety and posttraumatic stress disorder (Nowak et al., 1994; Ressler et al., 2011; Tsukiyama

et al., 2011; Mustafa et al., 2015), and also on specific structures such as the amygdala, the hypothalamus, the locus coeruleus, and the periaqueductal gray known to cope with emotions and control social behavior (Ago et al., 2015), activities that are dramatically impacted in animals lacking PACAP or VIP, exhibiting schizophrenia-like and/or autism-like phenotypes (Hashimoto et al., 2007; Nijmeijer et al., 2010; Vacic et al., 2011). The role of PACAP in schizophrenia seems to be even more complex based on studies showing that patients exhibiting a gain of function in chromosomal areas where PACAP and PAC1 genes are localized suffered from hydrocephalus and mental retardation highly associated with schizophrenia (Miller et al., 1979; Faraone et al., 2005). The next challenge is now to figure how to merge these different sides of the very same story and elucidate how much developmental VIP and PACAP participate in adult brain function and, therefore, whether targeting VIP and PACAP signaling at specific neurodevelopmental stages or providing VIP or PACAP supplementation may alleviate specific symptoms of adult neurological conditions. Future investigation of selective nonpeptide analogues (with extended half-life) and of validated antibodies against receptor variants is warranted.

ACKNOWLEDGMENT

This publication has been supported by the Centre National pour la Recherche Scientifique (CNRS) and the University of Strasbourg. TM is a doctoral fellow of the National Research Foundation (NRF) of South Africa.

CONFLICT OF INTEREST STATEMENT AND ROLE OF THE AUTHORS

The authors have no conflicting financial interests. All authors had full access to all the data in the study and take responsibility for the integrity of the data and the accuracy of the data analysis. Study concept and design: VL. Acquisition of data: TM. Analysis and interpretation of data: VL and TM. Drafting of the manuscript: TM. Critical revision of the manuscript for important intellectual content: VL. Statistical analysis: not applicable. Obtained funding: VL. Administrative, technical, and material support: VL. Study supervision: VL.

REFERENCES

Ago Y, Condro MC, Tan Y-V, Ghiani C, Colwell CS, Cushman JD, Fanselow MS, Hashimoto H, Waschek JA. 2015. Reductions in synaptic proteins and selective alteration of prepulse inhibition in male C57BL/6 mice after postnatal administration of a VIP receptor (VIPR2) agonist. Psychopharmacology 232:2181–2189.

Aton S, Colwell CS, Hamar AJ, Waschek JA, Herzog ED. 2005. Vasoactive intestinal polypeptide mediates circadian rhythmicity and synchrony in mammalian clock neurons. Nat Neurosci 8:476–483.

Asano E, Kuivaniemi H, Mahbubul Huq AHM, Tromp G, Behen M, Rothermel R, Herron J, Chugani DC. 2001. A study of novel polymorphisms in the upstream region of vasoactive intestinal peptide receptor type 2 gene in autism. J Child Neurol 16:357–363.

Barrett KT, Rodikova E, Weese-Mayer DE, Rand CM, Marazita ML, Cooper ME, Berry-Kravis EM, Bech-Hansen NT, Wilson RJA. 2013. Analysis of PAC1 receptor gene variants in Caucasian and African American infants dying of sudden infant death syndrome. Acta Paediatr 102:e546–e552.

Bauer S, Kerr BJ, Patterson PH. 2007. The neuropoietic cytokine family in development, plasticity, disease and injury. Nat Rev Neurosci 8: 221–232.

Bonni A. 1997. Regulation of gliogenesis in the central nervous system by the JAK-STAT signaling pathway. Science 278:477–483.

Brenneman DE, Nicol T, Warren D, Bowers LM. 1990. Vasoactive intestinal peptide: a neurotrophic releasing agent and an astroglial mitogen. J Neurosci Res 25:386–394.

Brenneman DE, Gozes I. 1996. A femtomolar-acting neuroprotective peptide. J Clin Invest 97:2299–2307.

Brenneman DE, Phillips TM, Festoff BW, Gozes I. 1997. Identity of neurotrophic molecules released from astroglia by vasoactive intestinal peptide. Ann N Y Acad Sci 814:167–173.

Brenneman DE, Phillips TM, Hauser J, Hill JM, Spong CY, Gozes I. 2003. Complex array of cytokines released by vasoactive intestinal peptide. Neuropeptides 37:111–119.

Brifault C, Gras M, Liot D, May V, Vaudry D, Wurtz O. 2015. Delayed pituitary adenylate cyclase-activating polypeptide delivery after brain stroke improves functional recovery by inducing m2 microglia/macrophage polarization. Stroke. 46:520–528.

Cai J, Qi Y, Hu X, Tan M, Liu Z, Zhang J, Li Q, Sander M, Qiu M. 2005. Generation of oligodendrocyte precursor cells from mouse dorsal spinal cord independent of Nkx6 regulation and Shh signaling. Neuron 45:41–53.

Cameron DB, Galas L, Jiang Y, Raoult E, Vaudry D, Komuro H. 2007. Cerebellar cortical-layer-specific control of neuronal migration by pituitary adenylate cyclase-activating polypeptide. Neuroscience 146:697–712.

Cauli B, Tong XK, Rancillac A, Serluca N, Lambolez B, Rossier J, Hamel E. 2004. Cortical GABA interneurons in neurovascular coupling: relays for subcortical vasoactive pathways. J Neurosci 24:8940–8949.

Cazillis M, Gonzalez BJ, Billardon C, Lombet A, Fraichard A, Samarut J, Gressens P, Vaudry H, Rostène W. 2004. VIP and PACAP induce selective neuronal differentiation of mouse embryonic stem cells. Eur J Neurosci 19:708–808.

Chaudhury D, Loh DH, Dragich JM, Hagopian A, Colwell CS. 2008. Select cognitive deficits in vasoactive intestinal peptide deficient mice. BMC Neurosci 9:63.

Chew LJ, DeBoy CA. 2015. Pharmacological approaches to intervention in hypomyelinating and demyelinating white matter pathology. Neuropharmacology (in press).

Christopoulos A, Christopoulos G, Morfis M, Udawela M, Laburthe M, Couvineau A, Kuwasako K, Tilakaratne N, Sexton PM. 2003. Novel receptor partners and function of receptor activity-modifying proteins. ?J Biol Chem 278:3293–3297.

Colwell CS, Michel S, Itri J, Rodriguez W, Tam J, Lelièvre V, Hu Z, Waschek JA. 2004. Selective deficits in the circadian light response in mice lacking PACAP. Am J Physiol Regul Integr Comp Physiol 287: R1194–R1201.

Couvineau A, Laburthe M. 2012. VPAC receptors: structure, molecular pharmacology and interaction with accessory proteins. Br J Pharmacol 166:42–50.

Cummings KJ, Pendlebury JD, Sherwood NM, Wilson RJA. 2004. Sudden neonatal death in PACAP-deficient mice is associated with reduced respiratory chemoresponse and susceptibility to apnoea. J Physiol 555: 15–26.

Cunningham CL, Martínez-Cerdeño V, Noctor SC. 2013. Diversity of neural precursor cell types in the prenatal macaque cerebral cortex exists largely within the astroglial cell lineage. PLoS ONE 8:e63848.

De los Frailes MT, Sanchez Franco F, Lorenzo MJ, Tolon RM, Lara JI, Cacicedo L. 1991. Endogenous vasoactive intestinal peptide (VIP) regulates somatostatin secretion by cultured fetal rat cerebral cortical and hypothalamic cells. Regul Pept 34:261–274.

Dean JM, Bennet L, Back SA, McClendon E, Riddle A, Gunn AJ. 2014. What brakes the preterm brain? An arresting story. Pediatr Res 75:227–233.

Dehay C, Kennedy H. 2007. Cell-cycle control and cortical development. Nat Rev Neurosci 8:438–450.

Del Bene F, Wehman AM, Link BA, Baier H. 2011. Regulation of neurogenesis by interkinetic nuclear migration through an apical-basal notch gradient. Cell 134:1055–1065.

Delgado M, Gonzalez-Rey E, Ganea D. 2004. VIP/PACAP preferentially attract Th2 effectors through differential regulation of chemokine production by dendritic cells. FASEB J 18:1453–1455.

Delgado M, Jonakait GM, Ganea D. 2002. Vasoactive intestinal peptide and pituitary adenylate cyclase-activating polypeptide inhibit chemokine production in activated microglia. Glia 39:148–161.

Deng Y, Xie D, Fang M, Zhu G, Chen C, Zeng H, Lu J, Charanjit K. 2014. Astrocyte-derived proinflammatory cytokines induce hypomyelination in the periventricular white matter in the hypoxic neonatal brain. PLoS One 9:e87420.

Dickson L, Finlayson K. 2009. VPAC and PAC receptors: from ligands to function. Pharmacol Ther 121:294–316.

Dong Z, Yang N, Yeo SY, Chitnis A, Guo S. 2012. Intralineage directional Notch signaling regulates self-renewal and differentiation of asymmetrically dividing radial glia. Neuron 74:65–78.

Englund C, Fink A, Lau C, Pham D, Daza RA, Bulfone A, Kowalczyk T, Hevner RF. 2005. Pax6, Tbr2, and Tbr1 are expressed sequentially by radial glia, intermediate progenitor cells, and postmitotic neurons in developing neocortex. J Neurosci 25:247–251.

Faraone SV, Skol AD, Tsuang DW, Young KA, Haverstock SL, Prabhudesai S, Mena F, Menon AS, Leong L, Sautter F, Baldwin C, Bingham S, Weiss D, Collins J, Keith T, vanden Eng JL, Boehnke M, Tsuang MT, Schellenberg GD. 2005. Genome scan of schizophrenia families in a large Veterans Affairs Cooperative Study sample: evidence for linkage to 18p11.32 and for racial heterogeneity on chromosomes 6 and 14. Am J Med Genet B Neuropsychiatr Genet 139B:91–100.

Farnham MMJ, Pilowsky PM. 2010. The role of PACAP in central cardiorespiratory regulation. Respir Physiol Neurobiol 174:65–75

Favrais G, Couvineau A, Laburthe M, Gressens P, Lelievre V. 2007. Involvement of VIP and PACAP in neonatal brain lesions generated by a combined excitotoxic/inflammatory challenge. Peptides 28:1727–1737.

Favrais G, van de Looij Y, Fleiss B, Ramanantsoa N, Bonnin P, Stoltenburg-Didinger G, Lacaud A, Saliba E, Dammann O, Gallego J, Sizonenko S, Hagberg H, Lelievre V, Gressens P. 2011. Systemic inflammation disrupts the developmental program of white matter. Ann Neurol 70:550–565.

Franco R, Fernández-Suárez D. 2015. Alternatively activated microglia and macrophages in the central nervous system. Prog Neurobiol. 131: 65–86.

Frost JL, Schafer DP. 2016. Microglia: architects of the developing nervous system. Trends Cell Biol 8:587–597.

Gazea M, Tasouri E, Tolve M, Bosch V, Kabanova A, Gojak C, Kurtulmus B, Novikov O, Spatz J, Pereira G. 2016. Primary cilia are critical for Sonic hedgehog-mediated dopaminergic neurogenesis in the embryonic midbrain. Dev Biol 409:55–71.

Giladi E, Hill JM, Dresner E, Stack CM, Gozes I. 2007. Vasoactive intestinal peptide (VIP) regulates activity-dependent neuroprotective protein (ADNP) expression in vivo. J Mol Neurosci 33:278–283.

Girard BA, Lelievre V, Braas KM, Razinia T, Vizzard MA, Ioffe Y, El Meskini R, Ronnett GV, Waschek JA, May V. 2006. Noncompensation in peptide/receptor gene expression and distinct behavioral phenotypes in VIP- and PACAP-deficient mice. J Neurochem 99:499–513.

Goldman SA, Kuypers NJ. 2015. How to make an oligodendrocyte. Development 142:3983–3995.

Gottschall PE, Tatsuno I, Miyata A, Arimura A. 1990. Characterization and distribution of binding sites for the hypothalamic peptide, pituitary adenylate cyclase-activating polypeptide. Endocrinology 127:272–277.

Götz M, Hartfuss E, Malatesta P. 2002. Radial glial cells as neuronal precursors: a new perspective on the correlation of morphology and lineage restriction in the developing cerebral cortex of mice1. Brain Res Bull 57:777–788.

Gozes I, Bassan M, Zamostiano R, Pinhasov A, Davidson A, Giladi E, Perl O, Glazner GW, Brenneman DE. 1999. A novel signaling molecule for neuropeptide action: activity-dependent neuroprotective protein. Ann N Y Acad Sci 897:125–135.

Gressens P, Hill JM, Paindaveine B, Gozes I, Fridkin M, Brenneman DE. 1994. Severe microcephaly induced by blockade of vasoactive intestinal peptide function in the primitive neuroepithelium of the mouse. J Clin Invest 94:2020–2027.

Gressens P. 1999. VIP neuroprotection against excitotoxic lesions of the developing mouse brain. Ann N Y Acad Sci 897:109–124.

Grimaldi M, Cavallaro S. 1999. Functional and molecular diversity of PACAP/VIP receptors in cortical neurons and type I astrocytes. Eur J Neurosci 11:2767–2772.

Hammerschmidt M, Bitgood MJ, McMahon AP. 1996. Protein kinase A is a common negative regulator of Hedgehog signaling in the vertebrate embryo. Dev Biol 10:647–658.

Hannibal J, Jamen F, Nielsen HS, Journot L, Brabet P, Fahrenkrug J. 2001. Dissociation between light-induced phase shift of the circadian rhythm and clock gene expression in mice lacking the pituitary adenylate cyclase activating polypeptide type 1 receptor. J. Neurosci 21: 4883–4890.

Harmar AJ, Fahrenkrug J, Gozes I, Laburthe M, May V, Pisegna JR, Vaudry D, Vaudry H, Waschek JA, Said SI. 2012. Pharmacology and functions of receptors for vasoactive intestinal peptide and pituitary adenylate cyclase-activating polypeptide: IUPHAR review 1. Br J Pharmacol 166:4–17.

Hashimoto R, Hashimoto H, Shintani N, Chiba S, Hattori S, Okada T, Nakajima M, Tanaka K, Kawagishi N, Nemoto K. 2007. Pituitary adenylate cyclase-activating polypeptide is associated with schizophrenia. Mol Psychiatry 12:1026–1032.

Hebert JM, Fishell G. 2008. The genetics of early telencephalon patterning: some assembly required. Nat Rev Neurosci 9:678–685.

Hernández-Miranda LR, Parnavelas JG, Chiara F. 2010. Molecules and mechanisms involved in the generation and migration of cortical interneurons. ASN Neuro 2:e00031.

Hill JM, McCune SK, Alvero RJ, Glazner GW, Henins KA, Stanziale SF, Keimowitz JR, Brenneman DE. 1996. Maternal vasoactive intestinal peptide and the regulation of embryonic growth in the rodent. J Clin Invest 97:202–208.

Hill JM, Lee SJ, Dibbern DA Jr, Fridkin M, Gozes I, Brenneman DE. 1999. Pharmacologically distinct vasoactive intestinal peptide binding sites: CNS localization and role in embryonic growth. Neuroscience 93:783–791.

Hill JM, Hauser JM, Sheppard LM, Abebe D, Spivak-Pohis I, Kushnir M, Deitch I, Gozes I. 2007. Blockage of VIP during mouse embryogenesis modifies adult behavior and results in permanent changes in brain chemistry. J Mol Neurosci 31:183–200.

Holighaus Y, Mustafa T, Eiden LE. 2011. PAC1hop, null and hip receptors mediate differential signaling through cyclic AMP and calcium leading to splice variant-specific gene induction in neural cells. Peptides 32:1647–1655.

Huang Y, Roelink H, McKnight GS. 2002. Protein kinase A deficiency causes axially localized neural tube defects in mice. J Biol Chem 277: 19889–19896.

Hu Z, Lelievre V, Rodriguez WI, Tam J, Cheng JW, Cohen-Cory S, Waschek JA. 2001. Embryonic expression of pituitary adenylyl cyclase-activating polypeptide and its selective type I receptor gene in the frog Xenopus laevis neural tube. J Comp Neurol 441:266–275.

Incerti M, Horowitz K, Roberson R, Abebe D, Toso L, Caballero M, Spong CY. 2012. Prenatal treatment prevents learning deficit in Down syndrome model. PLoS One 7:e50724.

Jackson J, Ayzenshtat I, Karnani MM, Yuste R. 2016. VIP + interneurons control neocortical activity across brain states. J Neurophysiol 115:3008–3017.

Kanski R, van Strien ME, van Tijn P, Hol EM. 2014. A star is born: new insights into the mechanism of astrogenesis. Cell Mol Life Sci 71: 433–447.

Kiecker C, Lumsden A. 2012. The role of organizers in patterning the nervous system. Annu Rev Neurosci 35:347–367.

Koh P-O, Won C-K, Noh H-S, Cho G-J, Choi W-S. 2005. Expression of pituitary adenylate cyclase activating polypeptide and its type I receptor mRNAs in human placenta. J Vet Sci 6:1–5.

Laburthe M, Couvineau A, Tan V. 2007. Class II G protein-coupled receptors for VIP and PACAP: structure, models of activation and pharmacology. Peptides 28:1631–1639.

Lamboley G, Evrard P, Gressens P. 1999. Prenatal inhibition of intestinal vasoactive peptide and cerebral excitatory lesions in the newborn mouse. Arch Pediatr 6:67–74.

Lang B, Song B, Davidson W, MacKenzie A, Smith N, McCaig CD, Harmar AJ, Shen S. 2006. Expression of the human PAC1 receptor leads to dose-dependent hydrocephalus-related abnormalities in mice. J Clin Invest 116:1924–1934.

Lee M, Lelievre V, Zhao P, Torres M, Rodriguez W, Byun JY, Doshi S, Ioffe Y, Gupta G, de los Monteros AE, de Vellis J, Waschek J. 2001. Pituitary adenylyl cyclase-activating polypeptide stimulates DNA synthesis but delays maturation of oligodendrocyte progenitors. J Neurosci 21:3849–3859.

Lee S, Kruglikov I, Huang ZJ, Fishell G, Rudy B. 2013. A disinhibitory circuit mediates motor integration in the somatosensory cortex. Nat Neurosci 16:1662–1670.

Lelievre V, Ghiani CA, Seksenyan A, Gressens P, de Vellis J, Waschek JA. 2006. Growth factor-dependent actions of PACAP on oligodendrocyte progenitor proliferation. Regul Pept 137:58–66.

Lelievre V, Seksenyan A, Nobuta H, Yong WH, Chhith S, Niewiadomski P, Cohen JR, Dong H, Flores A, Liau LM, Kornblum HI, Scott MP, Waschek JA. 2008. Disruption of the PACAP gene promotes medulloblastoma in ptc1 mutant mice. Dev Biol 313:359–370.

Lim MA, Stack CM, Cuasay K, Stone MM, McFarlane HG, Waschek JA, Hill JM. 2008. Regardless of genotype, offspring of VIP-deficient female mice exhibit developmental delays and deficits in social behavior. Int J Dev Neurosci 26:423–434.

Linder S, Barkhem T, Norberg A, Persson H, Schalling M, Hökfelt T, Magnusson G. 1987. Structure and expression of the gene encoding the vasoactive intestinal peptide precursor. Proc Natl Acad Sci U S A 84: 605–609.

Luo Y, Henricksen LA, Giuliano RE, Prifti L, Callahan LM, Federoff HJ. 2007. VIP is a transcriptional target of Nurr1 in dopaminergic cells. Exp Neurol 203:221–232.

Magistretti PJ, Cardinaux JR, Martin JL. 1998. VIP and PACAP in the CNS: regulators of glial energy metabolism and modulators of glutamatergic signaling. Ann N Y Acad Sci 865:213–225.

Masmoudi-Kouki O, Gandolfo P, Castel H, Leprince J, Fournier A, Dejda A, Vaudry H, Tonon MC. 2007. Role of PACAP and VIP in astroglial functions. Peptides 28:1753–1760.

Matsuyama S, Matsumoto A, Hashimoto H, Shintani N, Baba A. 2003. Impaired long-term potentiation in vivo in the dentate gyrus of pituitary adenylate cyclase-activating polypeptide (PACAP) or PACAP type 1 receptor-mutant mice. Neuroreport 14:2095–2098.

McCarthy KD, de Vellis J. 1980. Preparation of separate astroglial and oligodendroglial cell cultures from rat cerebral tissue. J Cell Biol 85:890–902.

Miller M, Kaufman G, Reed G, Bilenker R, Schinzel A. 1979. Familial, balanced insertional translocation of chromosome 7 leading to offspring with deletion and duplication of the inserted segment, 7p15 leads to 7p21. Am J Med Genet 4:323–332.

Miller R, Raff M. 1984. Fibrous and protoplasmic astrocytes are biochemically and developmentally distinct. J Neurosci 4:585–592.

Miller RH. 1996. Oligodendrocyte origins. Trends Neurosci 19:92–96.

Mission JP, Takahashi T, Caviness VS Jr. 1991. Ontogeny of radial and other astroglial cells in murine cerebral cortex. Glia 4:138–148.

Miyazaki K, Narita N, Sakuta R, Miyahara T, Naruse H, Okado N, Narita M. 2004. Serum neurotrophin concentrations in autism and mental retardation: a pilot study. Brain Dev 26:292–295.

Miyoshi G, Hjerling-Leffler J, Karayannis T, Sousa VH, Butt SJ, Battiste J, Johnson JE, Machold RP, Fishell G. 2010. Genetic fate mapping reveals that the caudal ganglionic eminence produces a large and diverse population of superficial cortical interneurons. J Neurosci 30:1582–1594.

Moody TW, Ito T, Osefo N, Jensen RT. 2011. VIP and PACAP. Recent insights into their functions/roles in physiology and disease from molecular and genetic studies. Curr Opin Endocrinol Diabetes Obes 18:61.

Moro O, Lerner EA. 1997. Maxadilan, the vasodilator from sand flies, is a specific pituitary adenylate cyclase activating peptide type I receptor agonist. J Biol Chem 272:966–970.

Morris-Rosendahl DJ, Kaindl AM. 2015. What next-generation sequencing (NGS) technology has enabled us to learn about primary autosomal recessive microcephaly (MCPH). Mol Cell Probes 29:271–281.

Mustafa T, Jiang SZ, Eiden AM, Weihe E, Thistlethwaite I, Eiden LE. 2015. Impact of PACAP and PAC1 receptor deficiency on the neurochemical and behavioral effects of acute and chronic restraint stress in male C57BL/6 mice. Stress 18:408–418.

Namihira M, Nakashima K. 2013. Mechanisms of astrocytogenesis in the mammalian brain. Curr Opin Neurobiol 23:921–927.

Nelson PG, Kuddo T, Song EY, Dambrosia JM, Kohler S, Satyanarayana G, Vandunk C, Grether JK, Nelson KB. 2006. Selected neurotrophins, neuropeptides, and cytokines: developmental trajectory and concentrations in neonatal blood of children with autism or Down syndrome. Int J Dev Neurosci 24:73–80.

Ng SY, Chow BK, Kasamatsu J, Kasahara M, Lee LT. 2012. Agnathan VIP, PACAP and their receptors: ancestral origins of today's highly diversified forms. PloS One 7:e44691.

Nicot A, Lelievre V, Tam J, Waschek JA, DiCicco-Bloom E. 2002. Pituitary adenylate cyclase-activating polypeptide and sonic hedgehog interact to control cerebellar granule precursor cell proliferation. J Neurosci 22:9244–9254.

Niewiadomski P, Zhujiang A, Youssef M, Waschek JA. 2013. Interaction of PACAP with Sonic hedgehog reveals complex regulation of the hedgehog pathway by PKA. Cell Signal 25:2222–2230.

Nijmeijer JS, Arias-Vásquez A, Rommelse NNJ, Altink ME, Anney RJL, Asherson P, Banaschewski T, Buschgens CJM, Fliers EA, Gill M. 2010. Identifying loci for the overlap between attention-deficit/hyperactivity disorder and autism spectrum disorder using a genome-wide QTL linkage approach. J Am Acad Child Adolesc Psychiatry 49:675–685.

Nishizawa M, Hayakawa Y, Yanaihara N, Okamoto H. 1985. Nucleotide sequence divergence and functional constraint in VIP precursor mRNA evolution between human and rat. FEBS Lett 183:55–59.

Nowak M, Markowska A, Nussdorfer GG, Tortorella C, Malendowicz LK. 1994. Evidence that endogenous vasoactive intestinal peptide (VIP) is involved in the regulation of rat pituitary-adrenocortical function: in vivo studies with a VIP antagonist. Neuropeptides 27:297–303.

Nunan R, Sivasathiaseelan H, Khan D, Zaben M, Gray W. 2014. Microglial VPAC1R mediates a novel mechanism of neuroimmune-

modulation of hippocampal precursor cells via IL-4 release. Glia 62: 1313–1327.

Ohno F, Watanabe J, Sekihara H, Hirabayashi T, Arata S, Kikuyama S, Shioda S, Nakaya K, Nakajo S. 2005. Pituitary adenylate cyclase-activating polypeptide promotes differentiation of mouse neural stem cells into astrocytes. Regul Pept 126:115–122.

Ohtsuka M, Fukumitsu H, Furukawa S. 2008. PACAP decides neuronal laminar fate via PKA signaling in the developing cerebral cortex. Biochem Biophys Res Commun 369:1144–1149.

Olah Z, Lehel C, Anderson WB, Brenneman DE, van Agoston D. 1994. Subnanomolar concentration of VIP induces the nuclear translocation of protein kinase C in neonatal rat cortical astrocytes. J Neurosci Res 39:355–363.

Orentas DM, Hayes JE, Dyer KL, Miller RH. 1999. Sonic hedgehog signaling is required during the appearance of spinal cord oligodendrocyte precursors. Development 126:2419–2429.

Pal K, Mukhopadhyay S. 2015. Primary cilium and sonic hedgehog signaling during neural tube patterning: role of GPCRs and second messengers. Dev Neurobiol 75:337–348.

Passemard S, El Ghouzzi V, Nasser H, Verney C, Vodjdani G, Lacaud A, Lebon S, Laburthe M, Robberecht P, Nardelli J, Mani S, Verloes A, Gressens P, Lelievre V. 2011a. VIP blockade leads to microcephaly in mice via disruption of Mcph1-Chk1 signaling. J Clin Invest 121:3071–3087.

Passemard S, Sokolowska P, Schwendimann L, Gressens P. 2011b. VIP-induced neuroprotection of the developing brain. Curr Pharm Des 17: 1036–1039.

Pinto L, Götz M. 2007. Radial glial cell heterogeneity—the source of diverse progeny in the CNS. Prog Neurobiol 83:2–23.

Quinn JC, Molinek M, Martynoga BS, Zaki PA, Faedo A, Bulfone A, Hevner RF, West JD, Price DJ. 2007. Pax6 controls cerebral cortical cell number by regulating exit from the cell cycle and specifies cortical cell identity by a cell autonomous mechanism. Dev Biol 302:50–65.

Rangon CM, Dicou E, Goursaud S, Mounien L, Jégou S, Janet T, Muller JM, Lelièvre V, Gressens P. 2006. Mechanisms of VIP-induced neuroprotection against neonatal excitotoxicity. Ann N Y Acad Sci 1070:512–517.

Reglodi D, Gyarmati J, Ertl T, Borzsei R, Bodis J, Tamas A, Kiss P, Csanaky K, Banki E, Bay C, Nemeth J, Helyes Z. 2010. Alterations of pituitary adenylate cyclase-activating polypeptide-like immunoreactivity in the human plasma during pregnancy and after birth. J Endocrinol Invest 33:443–445.

Ressler KJ, Mercer KB, Bradley B, Jovanovic T, Mahan A, Kerley K, Norrholm SD, Kilaru V, Smith AK, Myers AJ. 2011. Post-traumatic stress disorder is associated with PACAP and the PAC1 receptor. Nature 470:492–497.

Rowitch DH. 2004. Glial specification in the vertebrate neural tube. Nat Rev Neurosci 5:409–419.

Rowitch DH, Kriegstein AR. 2010. Developmental genetics of vertebrate glial-cell specification. Nature 468:214–222.

Rudy B, Fishell G, Lee S, Hjerling-Leffler J. 2011. Three groups of interneurons account for nearly 100% of neocortical GABAergic neurons. Dev Neurobiol 71:45–61.

Sahir N, Brenneman DE, Hill JM. 2006. Neonatal mice of the Down syndrome model, Ts65Dn, exhibit upregulated VIP measures and reduced responsiveness of cortical astrocytes to VIP stimulation. J Mol Neurosci 30:329–340.

Sherwood NM, Krueckl SL, McRory JE. 2000. The origin and function of the pituitary adenylate cyclase-activating polypeptide (PACAP)/glucagon superfamily. Endocr Rev 21:619–670.

Sheward WJ, Lutz EM, Copp AJ, Harmar AJ. 1998. Expression of PACAP, and PACAP type 1 (PAC1) receptor mRNA during development of the mouse embryo. Brain Res Dev Brain Res 109:245–253.

Shimojo H, Ohtsuka T, Kageyama R. 2008. Oscillations in notch signaling regulate maintenance of neural progenitors. Neuron 58:52–64.

Shimojo H, Kageyama R. 2016. Oscillatory control of Delta-like1 in somitogenesis and neurogenesis: a unified model for different oscillatory dynamics. Semin Cell Dev Biol. 49:76–82.

Shioda S, Nakamachi T. 2015. PACAP as a neuroprotective factor in ischemic neuronal injuries. Peptides. 72:202–207.

Skoglösa Y, Takei N, Lindholm D. 1999. Distribution of pituitary adenylate cyclase activating polypeptide mRNA in the developing rat brain. Brain Res Mol Brain Res 65:1–13.

Spong CY, Lee SJ, McCune SK, Gibney G, Abebe DT, Alvero R, Brenneman DE, Hill JM. 1999. Maternal regulation of embryonic growth: the role of vasoactive intestinal peptide. Endocrinology 140:917–924.

Stack CM, Lim MA, Cuasay K, Stone MM, Seibert KM, Spivak-Pohis I, Crawley JN, Waschek JA, Hill JM. 2008. Deficits in social behavior and reversal learning are more prevalent in male offspring of VIP deficient female mice. Exp Neurol 211:67–84.

Suh J, Lu N, Nicot A, Tatsuno I, DiCicco-Bloom E. 2001. PACAP is an anti-mitogenic signal in developing cerebral cortex. Nat Neurosci 4: 123–124.

Tay TL, Hagemeyer N, Prinz M. 2016. The force awakens: insights into the origin and formation of microglia. Curr Opin Neurobiol 39:30–37.

Teng BQ, Grider JR, Murthy KS. 2001. Identification of a VIP-specific receptor in guinea pig tenia coli. Am J Physiol Gastrointest Liver Physiol 281:G718–G725.

Titomanlio L, Bouslama M, Le Verche V, Dalous J, Kaindl AM, Tsenkina Y, Lacaud A, Peineau S, El Ghouzzi V, Lelièvre V, Gressens P. 2011. Implanted neurosphere-derived precursors promote recovery after neonatal excitotoxic brain injury. Stem Cells Dev 20:865–879.

Tong KK, Ma TC, Kwan KM. 2015. BMP/Smad signaling and embryonic cerebellum development: stem cell specification and heterogeneity of anterior rhombic lip. Dev Growth Differ 57:121–134.

Touahri Y, Escalas N, Benazeraf B, Cochard P, Danesin C, Soula C. 2012. Sulfatase 1 promotes the motor neuron-to-oligodendrocyte fate switch by activating Shh signaling in Olig2 progenitors of the embryonic ventral spinal cord. J Neurosci 32:18018–18034.

Tsukiyama N, Saida Y, Kakuda M, Shintani N, Hayata A, Morita Y, Tanida M, Tajiri M, Hazama K, Ogata K. 2011. PACAP centrally mediates emotional stress-induced corticosterone responses in mice. Stress 14:368–375.

Ulloa F, Briscoe J. 2007. Morphogens and the control of cell proliferation and patterning in the spinal cord. Cell Cycle 6:2640–2649.

Vacic V, McCarthy S, Malhotra D, Murray F, Chou H-H, Peoples A, Makarov V, Yoon S, Bhandari A, Corominas R. 2011. Duplications of the neuropeptide receptor gene VIPR2 confer significant risk for schizophrenia. Nature 471:499–503.

Vallejo I, Vallejo M. 2002. Pituitary adenylate cyclase-activating polypeptide induces astrocyte differentiation of precursor cells from developing cerebral cortex. Mol Cell Neurosci 21:671–683.

Vallejo M. 2009. PACAP signaling to DREAM: a cAMP-dependent pathway that regulates cortical astrogliogenesis. Mol Neurobiol 39:90–100.

Vaudry D, Falluel-Morel A, Bourgault S, Basille M, Burel D, Wurtz O, Fournier A, Chow BK, Hashimoto H, Galas L, Vaudry H. 2009. Pituitary adenylate cyclase-activating polypeptide and its receptors: 20 years after the discovery. Pharmacol Rev 61:283–357.

Villuendas G, Sanchez-Franco F, Palacios N, Fernandez M, Cacicedo L. 2001. Involvement of VIP on BDNF-induced somatostatin gene expression in cultured fetal rat cerebral cortical cells. Brain Res Mol Brain Res 94:59–66.

Vincze A, Reglodi D, Helyes Z, Hashimoto H, Shintani N, Abraham H. 2011. Role of endogenous pituitary adenylate cyclase activating polypeptide (PACAP) in myelination of the rodent brain: lessons from PACAP-deficient mice. Int J Dev Neurosci 29:923–935.

Volpe JJ, Kinney HC, Jensen FE, Rosenberg PA. 2011. Reprint of "The developing oligodendrocyte: key cellular target in brain injury in the premature infant." Int J Dev Neurosci 29:565–582.

Wakamatsu Y. 2004. Understanding glial differentiation in vertebrate nervous system development. Tohoku J Exp Med 203:233–240.

Walton NM, Sutter BM, Laywell ED, Levkoff LH, Kearns SM, Marshall GP, Scheffler B, Steindler DA. 2006. Microglia instruct subventricular zone neurogenesis. Glia 54:815–825.

Wang X, Hellgren G, Lofqvist C, Li W, Hellstrom A, Hagberg H, Mallard C. 2009. White matter damage after chronic subclinical inflammation in newborn mice. J Child Neurol 24:1171–1178.

Wang J, Wechsler-Reya RJ. 2014. The role of stem cells and progenitors in the genesis of medulloblastoma. Exp Neurol 260:69–73.

Waschek JA. 1996. VIP and PACAP receptor-mediated actions on cell proliferation and survival. Ann N Y Acad Sci 805:290–300.

Waschek JA, Lelievre V, Bravo DT, Nguyen T, Muller JM. 1997. Retinoic acid regulation of the VIP and PACAP autocrine ligand and receptor system in human neuroblastoma cell lines. Peptides 18(6):835–841.

Waschek JA, Casillas RA, Nguyen TB, Dicicco-Bloom E, Carpenter EM, Rodriguez WI. 1998. Neural tube expression of pituitary adenylate cyclase-activating peptide (PACAP) and receptor: potential role in patterning and neurogenesis. Proc Natl Acad Sci USA 95:9602–9607.

Waschek JA, Dicicco-Bloom E, Nicot A, Lelievre V. 2006. Hedgehog signaling: new targets for GPCRs coupled to cAMP and protein kinase A. Ann N Y Acad Sci 1070:120–128.

Watanabe J, Ohba M, Ohno F, Kikuyama S, Nakamura M, Nakaya K, Arimura A, Shioda S, Nakajo S. 2006. Pituitary adenylate cyclase-activating polypeptide-induced differentiation of embryonic neural stem cells into astrocytes is mediated via the beta isoform of protein kinase C. J Neurosci Res 84:1645–1655.

Wilson SW, Rubenstein JL. 2000. Induction and dorsoventral patterning of the telencephalon. Neuron 28:641–651.

Wu S, Adams BA, Fradinger EA, Sherwood NM. 2006. Role of two genes encoding PACAP in early brain development in zebrafish. Ann N Y Acad Sci 1070:602–621.

Yan Y, Zhou X, Pan Z, Ma J, Waschek J, DiCicco-Bloom E. 2013. Pro- and anti-mitogenic actions of PACAP in developing cerebral cortex: potential mediation by developmental switch of PAC1 receptor mRNA isoforms. J Neurosci 33:3865–3878.

Zaben M, Sheward WJ, Shtaya A, Abbosh C, Harmar AJ, Pringle AK, Gray WP. 2009. The neurotransmitter VIP expands the pool of symmetrically dividing postnatal dentate gyrus precursors via VPAC2 receptors or directs them toward a neuronal fate via VPAC1 receptors. Stem Cells 27:2539–2551.

Zhang QL, Liu J, Lin PX, Webster H. 2002. Local administration of vasoactive intestinal peptide after nerve transection accelerates early myelination and growth of regenerating axons. J Peripher Nerv Syst 7: 118–127.

Zhou CJ, Shioda S, Shibanuma M, Nakajo S, Funahashi H, Nakai Y, Arimura A, Kikuyama S. 1999. Pituitary adenylate cyclase-activating polypeptide receptors during development: expression in the rat embryo at primitive streak stage. Neuroscience 93:375–391.

Zhou H, Huang J, Murthy KS. 2006. Molecular cloning and functional expression of a VIP-specific receptor. Am J Physiol Gastrointest Liver Physiol 291:G728–G734.

Zupan V, Hill JM, Brenneman DE, Gozes I, Fridkin M, Robberecht P, Evrard P, Gressens P. 1998. Involvement of pituitary adenylate cyclase-activating polypeptide II vasoactive intestinal peptide 2 receptor in mouse neocortical astrocytogenesis. J Neurochem 70:2165–2173.

Zupan V, Nehlig A, Evrard P, Gressens P. 2000. Prenatal blockade of vasoactive intestinal peptide alters cell death and synaptic equipment in the murine neocortex. Pediatr Res 47:53–53.

3. VIP: a very important peptide in cortical development

Studies have reported high levels of VIP in embryonic tissues shown to be of maternal origin, with a peak of expression between E10 and E12 in rat maternal serum (Hill et al. 1996). In addition VIP and VPAC gene expression were reported between E6 and E12 in rodents (Spong et al. 1999) coinciding with the peak of neurogenesis and early corticogenesis (Dehay and Kennedy 2007) Interestingly, embryonic VIP was reported only after E12 with almost undetectable levels prior to that age, implicating maternal VIP in the regulation of embryonic growth, especially during corticogenesis (Hill et al. 1996; Maduna and Lelievre 2016). VIP blockade in VA treated mothers, between E9 and E11, altered brain development resulting in severe microcephaly in the developing mouse (Gressens et al. 1994) that mimicked the prominent clinical feature of human autosomal recessive primary microcephaly (MCPH), also referred to as primary microcephaly or *microcephaly vera* and characterized by gross reduction in brain size. This study provided strong emphasis of VIP's impact on brain growth as this crucial time of VIP action coincides with neurogenesis and the start of corticogenesis in rodents (Dehay and Kennedy 2007). Therefore VIP may play a crucial role in brain development, especially at the onset of brain growth, with special emphasis on progenitor proliferation and migration from the neuroepithelium to the newly forming cortical layers laminating the dorsal telencephalon, as demonstrated by Gressens and colleagues (1997).

MCPH is a rare genetic disorder that presents with mild to moderate mental retardation and is characterized by a reduced cerebral cortex size and occipital frontal circumference of -2SD from the normal range (Kaindl et al. 2010; Passemard et al. 2009) without altering normal cortical lamination. MCPH patients may also present with mild to severe mental retardation at birth, delay in motor milestones and short stature in some cases (Mahmood et al. 2011), (Figure 5A). The impact of VIP deficiency in rodents is reminiscent of the aforementioned manifestations as offspring of deficient mothers also presented behavioural and physiological developmental deficits. Additionally, a reduction in somite number in embryos of VA treated mothers (Gressens et al. 1997) also

suggests a link between VIP and neuronal development in general.

MCPH cortical defects were shown to result from a dysregulation of cell proliferation/differentiation turnover, without any impact on or of cell death in the developing brain (Passemard et al. 2011). To date, 12 MCPH loci (Figure 5B) have been identified in MCPH patients which are also involved in the cell cycle and in the regulation of mitotic spindle organization (Figure 5C), which is implicated as a crucial mechanism with which neural stem cell self-renewal and progenitor radial migration occur, which govern cortical lamination in the developing brain (Thornton and Woods 2009). The *Mcph1* gene encodes microcephalin and is expressed along the telencephalic neuroepithelium in mice (Jackson et al. 2002). It has been recently identified, *in vitro* and *in vivo,* to play a crucial role in cortical development (corticogenesis) with special emphasis on its role in cell cycle checkpoint regulation and progenitor proliferation in the developing brain (Gruber et al. 2011; Passemard et al. 2011). MCPH5, also known as abnormal spindle-like microcephaly associated homolog (ASPM) has also been suggested to increase the self-renewal capacity of pluripotent precursors during this process and its deficiency is the most prevalent factor in MCPH cases (Bond et al. 2002; Thornton and Woods 2009). Corticogenesis is governed through a tight regulation of progenitor proliferation/differentiation events, whereby a sufficient progenitor pool is generated to further provide cells that differentiate and laminate different layers of the cerebral cortex. In addition, the length and duration of the cell cycle of these is crucial as progenitors may either remain in the cell cycle for continued proliferation or may exit the cycle and undergo differentiation. Dysregulation of proliferation/dysregulation at this time may result in depletion of progenitors and reduction of the number of cells that may differentiate into the different layers of the cortex (Dehay and Kennedy 2007). This dysregulation has recently been implicated in the etiology of MCPH with VIP signaling identified as a mechanism through which progenitor cell cycle and microcephaly genes are regulated in the developing brain (Passemard et al. 2011).

A Clinical manifestation of MCPH

-Rare autosomal recessive pathology

-12 identified MCPH loci

-Small OFC < -2SD

-Small stature in some cases

-Mild to severe mental retardation

(Kaindl et al. 2010; Mahmood et al. 2011)

B Microcephaly genes encode centrosomal proteins

Cell cycle regulation	
MCPH1(microcephalin)	: BRIT1
MCPH4	: CEP152
MCPH6	: CENJP
MCPH8	: CEP135
MCPH10	: ZNF335
MCPH11	: PHC1
MCPH12	: CDK6

Mitotic spindle organization	
MCPH2	: WDR62
MCPH3	: CDK5RAP5
MCPH5	: ASPM
MCPH7	: STIL
MCPH9	: CEP152

(Hussain et al. 2013)

C Localization of the main microcephaly genes in metaphase

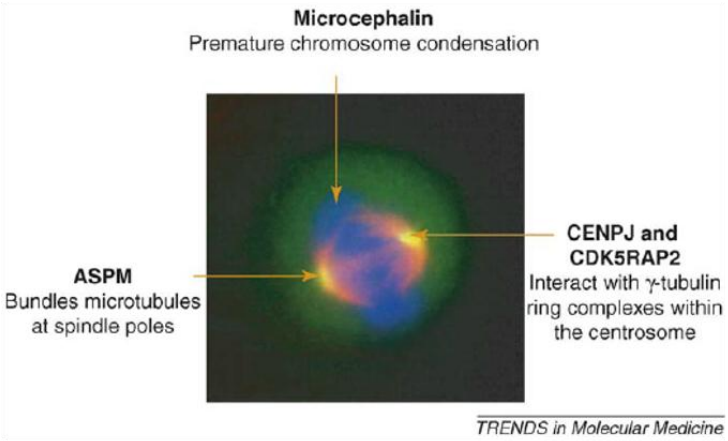

(Cox et al. 2006)

Figure 5: Human microcephaly results from a null mutation in one of 12 identified genes which have been characterized to encode centrosomal proteins

In general, corticogenesis commences around E10 and continues postnatally in rodents and between the 12^{th} and 24^{th} weeks of gestation in primates. Neural stem cells (NSCs) migrate outward from the innermost neuroepithelium of the neural tube to the apical surface to form the cerebral cortex. During corticogenesis symmetric and asymmetrical divisions generate the neural pool that makes up the cortical layers. While symmetric division gives rise to either identical neural or differentiating neuroblasts, asymmetrical division results in the generation of an identical daughter cell and another that loses its multipotency and migrates outwards to form the upper layers of the cerebral cortex. In the ventricular zone (VZ), radial glial cells (RGCs), bipotent progenitors that originate from NSCs, divide symmetrically to produce either more RGCs or short neural precursor (SNPs) cells, or undergo asymmetric division to produce intermediate progenitor cells (IPCs) that migrate to the subventricular zone (SVZ) and additional RGCs to maintain an adequate pool of cells in the VZ. Such IPCs may also undergo differentiative symmetrical division (Dehay and Kennedy 2007). Paired box domain transcription factor 6 (Pax6), a transcription factor crucial for the determination of cortical RGC count and function which is also implicated in the regulation of their cell cycle (Quinn et al. 2007), and T-box domain transcription factor (Tbr2) that serves as a marker for the transition of RGCs into IPCs have been identified in normal brain development . In addition to Tbr1, these factors are sequentially expressed as RGCs proliferate in the VZ (Pax6) then ultimately differentiate into IPCs (Tbr2) of the SVZ (Arnold et al. 2008). Tbr1 is expressed later as precursors further migrate and differentiate into postmitotic projection neurons of the upper layers (Englund et al. 2005). Regulation of cell division/differentiation turnover that accompanies/directs this Pax6-Tbr2-Tbr1 sequence involves regulation at the G_1/S checkpoint whereby the cells can enter G_0 and either exit to further differentiate (Tbr2-Tbr1) or re-enter the cycle for further mitotic events and growth (Pax6) (Asami et al. 2011).

4. Research proposal

In recent studies (Passemard et al. 2011), VIP blockade with VA resulted in reduced brain weight and cortical thickness, in which VIP signaling was implicated in cell cycle regulation and MCPH1 signaling modulation. This results from downregulation in the crosstalk between VIP signaling and MCPH1-CHK1 signaling, mediated via VPAC1-cAMP/PKA signaling which is crucial in cell cycle regulation and proliferation of progenitors. MCPH1 regulates CHK1 expression during DNA damage (Xu et al. 2004), a major checkpoint kinase that phosphorylates the protein phosphatase Cdc25 at the G_2/M checkpoint resulting in the nuclear translocation and sequestration of Cdc25 and blockade of the G_2/M transition. This has been implicated in the inhibition of cell cycle progression (Xiao et al. 2003). Indeed trophic factors have been previously implicated in cell cycle regulation and duration through p27 inhibition (Boehm et al. 2002). VA increased the amount of p27kip1 expressing cells in the telencephalon of E11.5 mice demonstrating an early exit of these cells from the cell cycle towards a differentiated state. In the VA model, early cell cycle exit by cortical progenitors is demonstrated to result from lengthening of the cell cycle duration. This coincides with premature upregulation of the differentiation marker, Dcx, in the embryonic telencephalon.

In addition to the aforementioned brain defects, a large body of evidence has implicated VIP (and PACAP) in other central functions (Waschek 2013) which we aimed to explore. As previously mentioned, VIP and PACAP are upregulated in spinal injury (Dickinson and Fleetwood-Walker 1999) although no direct link has been made to demonstrate the specific function of VIP in sensory processing, and specifically in pain (Figure 6). Therefore, the following aims set to characterize VIP function in brain development, to explore the function of VIP in adult sensory physiology and to ultimately find a link between the developmental deficits due to VIP deficiency that could explain deficits in VIP deficient adult mice. This is of utmost interest as circulating VIP is implicated in the etiology of autism and cerebral palsy, with affected individuals reporting gastrointestinal symptoms such as bowel distention and sleep disturbances (Nelson 2001; Nelson et al. 2006)

reminiscent of the VIP knockout phenotype. Thus, the ultimate goal of the work presented herein investigates and introduces VIP as an exogenous (or rather maternal) factor linking neurodevelopment and adult neurophysiology.

Thus, as pups and adult mice prenatally treated with VA exhibit most of the developmental and behavioural deficits reported in VIP knockout mice, we posed the following questions:

1. Can we propose the VIP knockout mouse as a mouse model for human microcephaly? If so, to what extent does the VIP knockout mimic human microcephaly, and is the phenotype more severe than what is reported in the VA model?
   This aim was explored and reported in Publication 2 (in preparation)

2. What are the behavioural and molecular implications of VIP deficiency in pain processing, in adult mice?

3. What is the link between neurodevelopmental deficits and abnormal pain processing as observed in adults VIP-knockout mice?

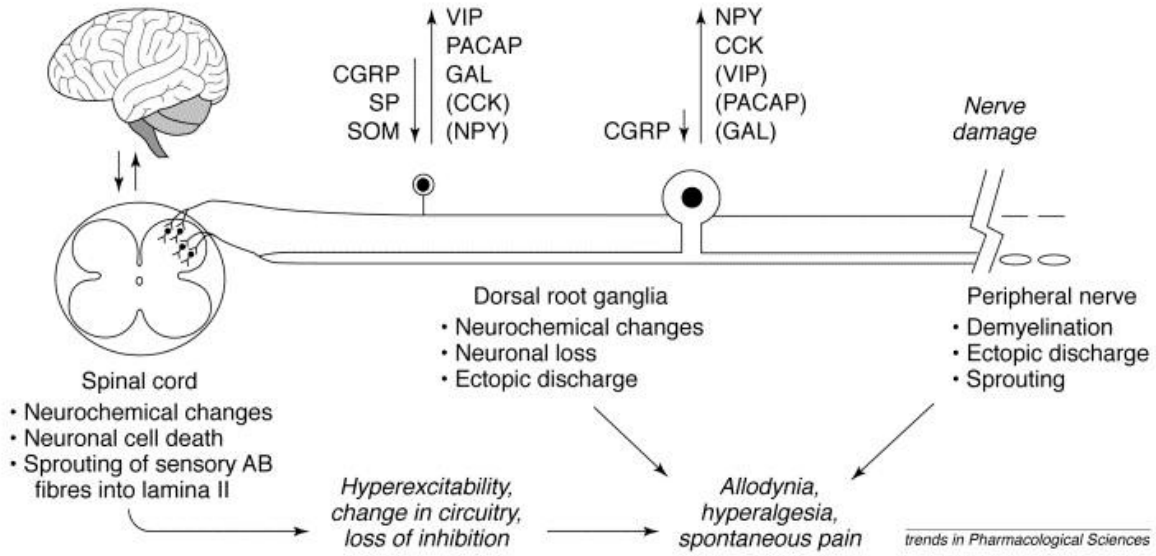

(Dickinson and Fleetwood-Walker 1999)

Figure 6: VIP and PACAP are upregulated in the dorsal root ganglia following peripheral nerve damage.

Materials and methods

1. Animal breeding and genotyping

VIP KO mice received from Professor JA Waschek (David Geffen School of Medicine, UCLA) and all of the C57BL/6 strain mice used in this study were housed at Chronobiotron IFR Neurosciences animal facility (University of Strasbourg, France) where breeding and mating are continuously carried out for all experiments undertaken during this project. Mice are housed under a 12 hour light/dark cycle and food pellets administered ad libitum. Breeding is done every second day and carried out during the last hour of the dark cycle, where females are introduced into the male cage and left for an additional hour (at the beginning of the light cycle), then immediately returned to their home cage of no more than 3 females per cage. Females are introduced into the male cage to avoid hierarchical conflict that may arise should a male be introduced into a new environment. Thus, this strategy serves to facilitate male interest and copulation. Vaginal plug is considered as E0. The VIP knockout colony is maintained by ongoing backcrossing, whereby VIP heterozygous males are housed in the same cage with one or two heterozygous females. Pups are genotyped after postnatal day (P) 7, to avoid maternal cannibalization, and no later than P12 while the nociceptive system is not fully developed yet, as maturation is reached at P21 in mice (Fitzgerald 2005), and the pups are still easier to handle. Tailsnips are collected and mice tattooed then genotyped (KAPA mouse genotyping kit, KAPA Biosystems) using specific sense and antisense primers for VIP (for wildtypes), and the specific ONEO10 primer sequence for the larger VIP knockout sequence to genotype full knockouts and heterozygotes (EUROGENTEC), (Figure 7).

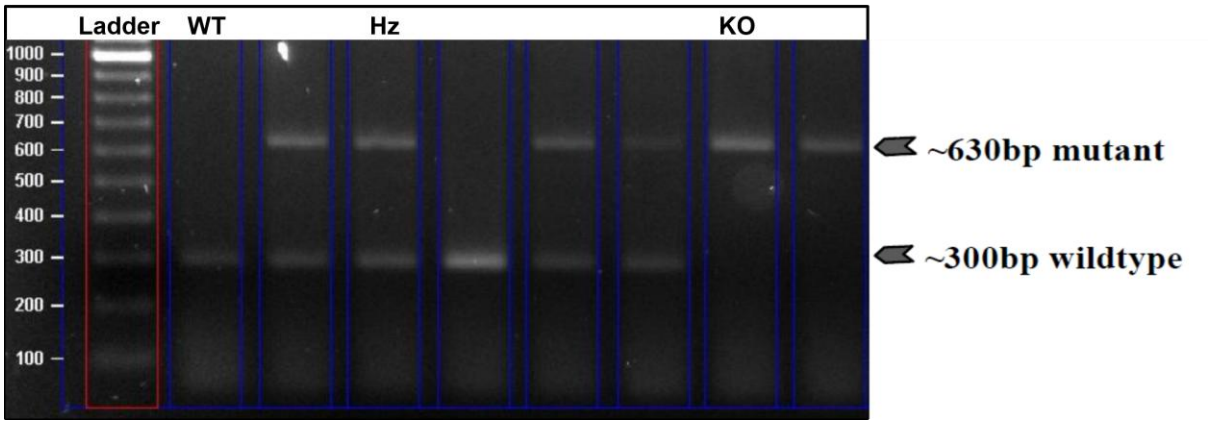

Figure 7: Highly specific primers for VIP are used to genotype animals, following tailsnip, or embryonic paws where necessary. The VIP sequence is of 350bp whereas the larger knockout sequence spans 630bp due to the neomycine cassette insertion

2. Technical approaches

In the next section, specific technical approaches used during this project are described in detail: Additional tools are described in detail as part of specific publications amended to the Results sections:

1. Whole mount *in situ* hybridization and main troubleshooting points
2. Von frey assessment of mechanical sensation of pain and dynamic cold plate test for the assessment of sensitivity to cold temperature
3. *In vivo* electrophysiology on anaesthetized animals for the recording of single cell firing patterns in adult brain

2.1. Whole-mount *in situ* hybridization:

To characterize the ontogeny of target genes that we hypothesize should be dysregulated in VIP knockouts, I performed whole-mount *in situ* hybridization on embryos extracted from E9 until E13, where necessary. The advantage of this approach is the ability to perform time-lapse localization, on a multi-dimensional platform, of specific genes of interest, *Mcph1, Chk1 and Vpac1* to confirm their expression in suitable compatibility with their regulatory crosstalk and to also visualize spatiotemporal and sequential expression of *Pax6, Tbr2 and Tbr1* early differentiation markers.

The 5-day protocol is attached as Annexe1, and is summarized on Figure 8A (excerpt taken from “In situ Hybridization: Seeing RNA expression at the right place. Maduna T and Lelievre V. Neurotech Seminar Series”, available for download on http://www.slideshare.net/NeurotechSeminars/in-situ-hybridization)

Some examples of sense and antisense probe comparisons are shown on Figure 8B.

Apart from the advantages of this technical approach, some limitations still remain which should be taken into account:

Probe penetrance: due to the compound structure of a full embryo, this is a parameter that is difficult to ensure. Thus after revelation, embryos could be dissected to verify probe labelling of internal structures (Figure 8, Panel C). Dark arrows show specific digoxigenin labelling which could penetrate within the embryos and show *Mcph1* antisense labelling in the dorsal telencephalon (left panel) and along the developing spinal column (right panel).

Protein kinase treatment for probe permeability: this presents a limitation that tissue becomes easily susceptible to damage depending on the duration of treatment (Figure 8, Panel D, left), thus causing probe leakage and preventing optimum probe hybridization to the region of interest if the treatment was too long. The red border shows a damaged forebrain. This embryo lost some tissue along the dorsal surface of the head, along with any possible probe labelling. This confounding issue made it impossible to compare this wildtype embryo with the corresponding knockout. However if treatment is too short, that also prevents optimum probe penetration resulting in very low staining (Figure8, Panel D, right)

Probe concentration: due the high specificity of the probes we were able to generate, the revelation duration became too quick resulting in very high background. Thus probe concentration was decreased to half dose for certain probes as shown (Figure 8, Panel E). Here I show the differences between 1µg/mL vs 0.5µg/mL final concentration of the Mcph1-dig probe

Clearing for optimal visualization: very few clearing methods have been explored for whole mount *in situ* hybridization. Thus incorporating the bleaching step with 6% hydrogen peroxide introduced by Komatsu and colleagues (2014) has improved the background and allow visualization as deep within the embryo as possible (Figure 8, Panel F)

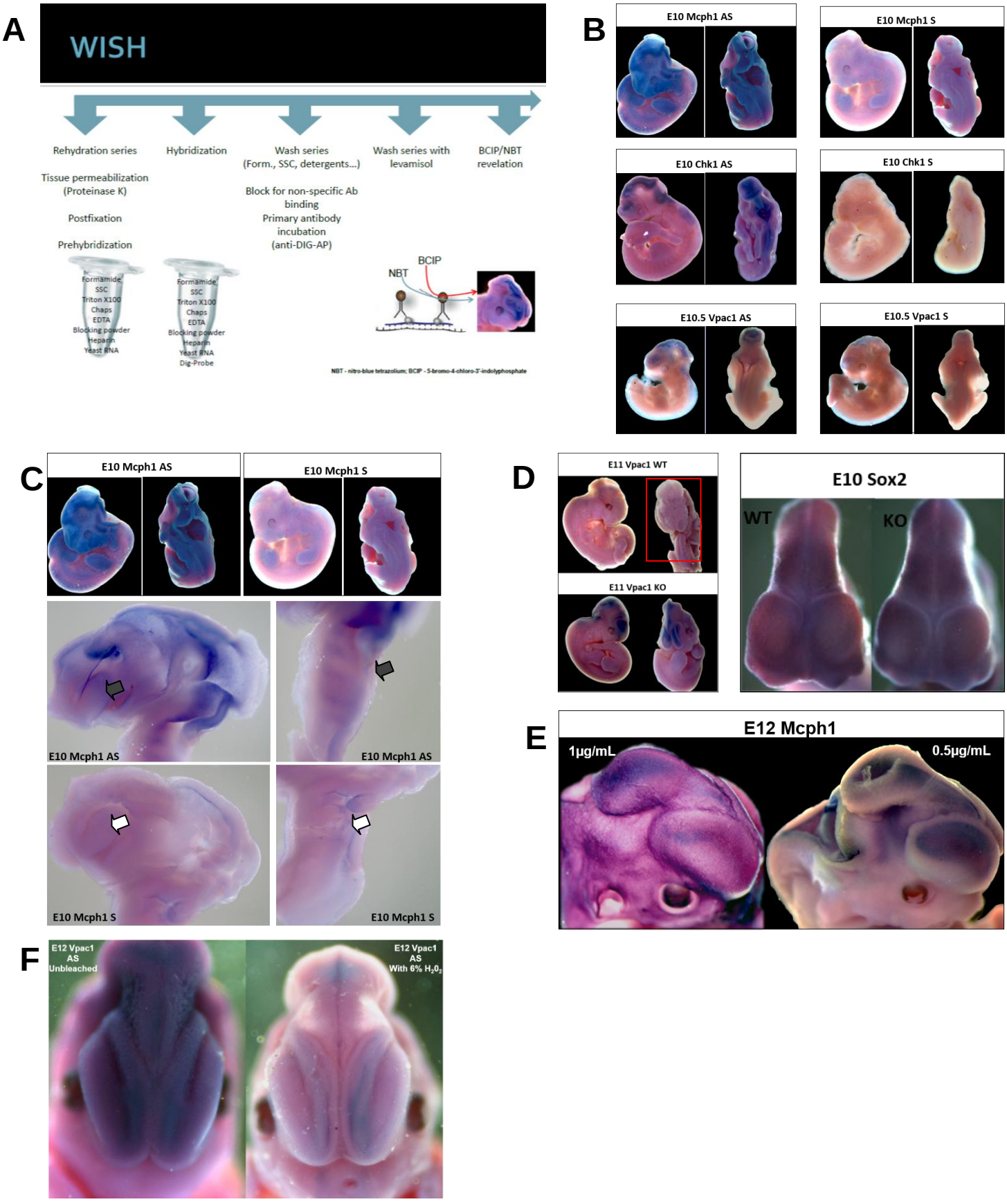

Figure 8: Reference images for troubleshooting methods

2.2 Pain assessment on pregnant mice

In order to investigate the impact of VIP on the sensory system, we performed Von Frey and Dynamic cold plate tests to measure the threshold of pain perception on pregnant females subjected to restraint stress from E9 to E11. With Von Frey tests we measured the threshold to mechanical stimulation. Dynamic cold plate tests were performed to investigate the threshold of sensitivity to cold temperatures. These are standardized and certified tests for nociception that are routinely employed in rodents, and have been reviewed extensively (Barrot 2012; Yalcin et al. 2009).

2.2.1. Animals

At vaginal plug pregnant wildtype, heterozygous and knockout females were placed into 2 groups: maternal tress (MS) and controls (no stress = NS). MS females were subjected to restraint stress, also referred to as maternal stress or forced restraint, during E9, E10 and E11. Restraint stress was delivered twice a day, once in the morning and once in the evening, according to the schematic representation and timeline shown on Figure 9B.

2.2.2. Restraint stress

The protocol for restraint stress is also described in Publication 2. Historically, restraint stress was performed very early during post implantation and dramatically decreased the pregnancy success rate in mice (Liu et al. 2014). Therefore, a different timing was adapted to promote sampling and to target the peak of neurogenesis, thus stress was carried out at E9 to E11. The duration of stress was also decreased from 4 hours per day, to 45 minutes per session and 2 sessions per day to lessen the severity of the stress.

Conventionally, for pain assessments, the investigator should first measure the baseline response in control animals, i.e. untreated wildtype mice. However, as pain response was assessed in pregnant mice, in which the embryos are developing and growing daily (Figure 9), it was not possible to measure the baseline response for these mice. In addition, daily assessment was avoided in order to prevent additional stress which could have teratogenic implications. Thus, Von Frey and Dynamic cold

plate tests were performed at E8 and E9 before the introduction of stress and at E12 before cervical dislocation (Figure 9). 3 month old wildtype female mice were subjected to Von Frey and dynamic cold plate testing to measure the control baseline threshold in non-pregnant females that also did not receive restraint stress.

2.2.3. Von Frey assessment of mechanical pain

Materials

- Von Frey metal table
- Clear plexiglas individual chambers with lids to prevent escape
- Blue absorbing paper
- Set of 20 Von Frey monofilaments ranging from 0.008g to 100g (#Bio-VF-M; BioSeb)

Preparation

- The clear plexiglas individual chambers are set up on top of the Von Frey metal table. Our setup can only accommodate up to 10 mice maximum per experiment (1 animal per chamber)
- Blue absorbing paper is placed on the bottom part of the table for hygiene purposes

Procedure

1) Each mouse is placed in the individual chamber which is then covered with the heavy lid for 20 min during which the mouse is allowed habituation to the chamber and the context
2) After habituation, each mouse is tested for paw withdrawal reflex by pressing the tip of the filaments against the surface of the hind paws. The tip of the filament of a given weight (force) and diameter is pressed against the skin of the middle part of the plantar surface of each hind paw until the fiber bends. The conventions followed are the following:

- Test right paw first, left paw second
- Each filament is tested 5 times on each paw. A positive response is considered as at least 3 out of 5 paw withdrawals to a given filament.

- The first two consecutive positive responses for each individual paw are recorded as the threshold of mechanical perception, after which the test is stopped
- Left and right paws are tested and recorded to be averaged as 1 paw for statistical analysis since there should be no contralateral differences

3) After all the mice have been tested, they are returned to their home cages

2.2.4. Dynamic cold plate

The following protocol was adapted from Yalcin and colleagues (2009) to test pregnant females without imposing stress due to extreme conditions. The dynamic cold pate differs from the conventional cold plate as, instead of subjecting the mouse to a single and constant cold temperature to measure the time it takes to respond to the cold temperature, a descending temperature ramp is used in this case to measure the highest temperature that the animal responds to as aversive and will attempt to escape (jumps). Instead of 0°C, the minimum temperature set for pregnant mice was 4°C. This was a confounding factor as the majority of mice tend to respond starting from 4°C (Yalcin et al. 2009). However, this issue was resolved in this case as most mice had a lower threshold and responded before 4°C were reached.

Materials

- Cold/hot plate instrument (#BIO-CHP, BioSeb)
- Computer with HotCold Single Program (BioSeb)
- Cleaning materials

Procedure

1) The mouse is placed on the cold plate chamber for 20 min at 20° C for habituation
2) After habituation, animals are subjected to the following ramp
   Ramp: 2°C/min
   Final temperature: 4 °C
3) The temperature at which the mouse jumps, and the time it takes before the first jump, are recorded as the threshold which can either be recorded as

temperature or latency to respond (seconds). The cut-off point is taken as 4°C + 2minutes.

4) Mice are then returned to their home cage

A

B

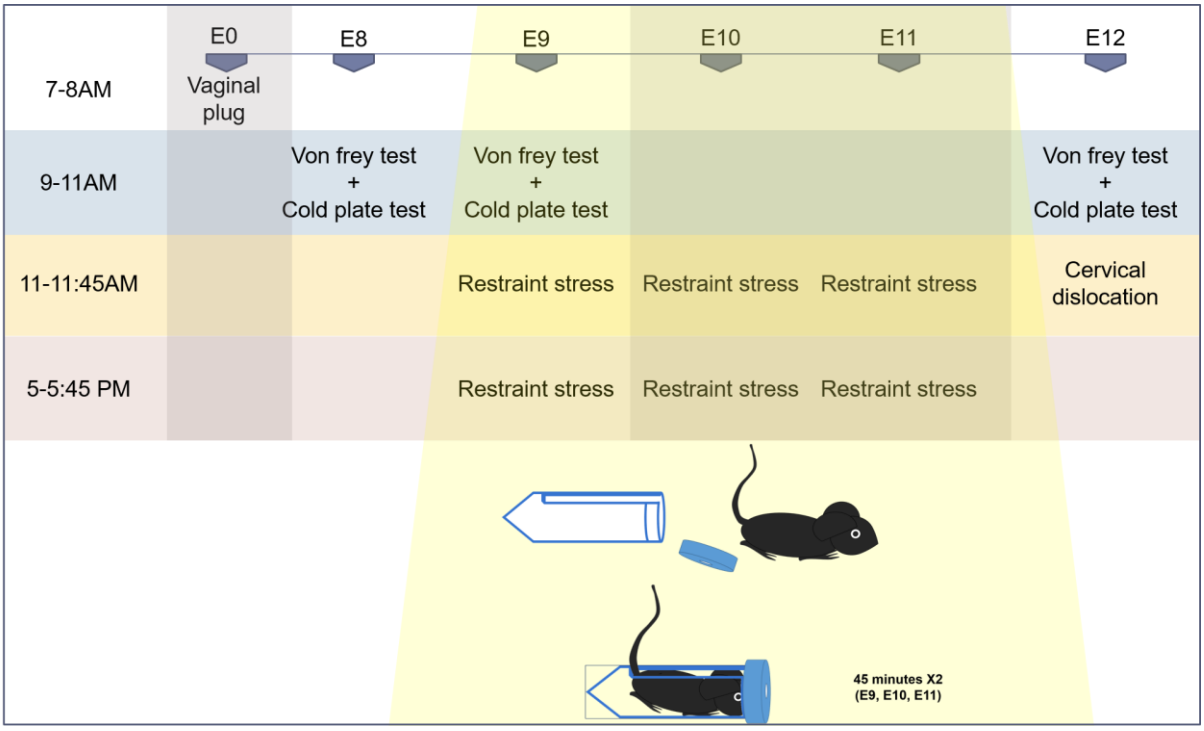

Figure 9A: Mouse embryonic growth increases rapidly, daily, possibly causing daily maternal physiological and behavioural changes as well.

Figure 9B: Timeline for forced restraint and pain assessments in pregnant females. Mice were tested at E8 and E9 before restraint, then again at E12 after undergoing restraint at E9, E10 and E11. To induce prenatal stress, pregnant females are forced into a plastic centrifuge tube for 45 minutes, once in the morning and once in the early evening.

2.3. *In vivo* electrophysiology

In order to characterize the functional properties of VIP knockout mice in sensory processing, we measure single cell firing activity in anesthetized adult male mice, aged 3 to 4 months. Single-cell recordings were performed in the sensory thalamus, specifically the lateral thalamus, to investigate the neural activity in the intermediary pathways between the spine and the supraspinal, and cortical structures. Recordings were made in the primary sensory cortex (S1) and the laterodorsal thalamic nucleus, dorsomedial part (LDDM) and laterodorsal thalamic nucleus, ventrolateral part (LDVL), as well as the ventrolateral thalamic nucleus (VL), (black dots on the coronal sections of Figure 10B).

In this study the dorsomedial part of the thalamic nucleus served as the negative control as this region is involved in emotional processing as opposed to sensory processing. An additional negative control was the primary sensory cortex, which was expected to show very limited activity in anesthetized animals and also exhibit no differences in sensory processing, being a higher cortical structure.

Protocol

The following protocol was provided by Dr Jim Sellmeijer (INCI, CNRS UPR3212), who also generously implemented the training for the surgical procedures and *in vivo* electrophysiological recordings, and analysed the firing rates recorded from the lateral thalamus and the cortex with Matlab programming software (Matlab 2015a).

Animals were anesthetized in an induction box with a 2% isoflurane/air mixture (Vetflurane, Virbac) after which they were placed in a Kopf stereotaxic frame (KOPF 1730) equipped with a nose mask to continuously deliver the anaesthetic (Figure 10 A). A cranial window spanning the midline was prepared for the recording of cells with the Bregma range of -0.94 to -1.58mm for the dorsoventral access of the S1, LDDM, LDVL and VL. The dura was opened to allow access for lowering the glass electrode into the brain.

Recordings of spontaneous activity were performed using sharp electrodes pulled from borosilicate micropipettes (1.2 mm outer and 0.69 mm inner diameters, Harvard Apparatus, 30-0044), with a Narashige pipette puller (tip diameter < 1 µm, resistance ±25 MΩ). The glass electrodes were filled with 0.5 M potassium acetate solution. The electrode signal was recorded through a silver wire, amplified with an operational amplifier (Neurodata IR-183A, Cygnus Technology inc.; gain x10), and then amplified further and filtered using a differential amplifier (Model 440, Brownlee Precision; gain x100; band pass filter 0.1-10kHz). The signal was then digitized with a CED digitizer (sampling rate: 20.8 KHz) and recorded with Spike2 software (Version 7.12b, Cambridge Electronic Design, Cambridge, UK). Raw data files were exported into Matlab and analysed with custom Matlab scripts (Matlab 2015a).

During the recording procedure, isoflurane anaesthesia was lowered to 0.5-0.75% and was monitored by paw pinching. The glass pipette was slowly lowered using a Scientifica one dimensional micromanipulator and recordings were done as described above.

Neurons were recorded from the brain surface until 4000 µm deep. Once stable cell activity was detected, a 5-minute segment of spontaneous activity was recorded.

Recording sites were marked by iontophoretically injecting a 4% Pontamine Sky blue dye (Sigma) in 0.5 M sodium-acetate solution (Sigma). The position of the recorded cells was registered using microdrive reference point with respect to the Pontamine Sky blue dye deposit.

At end of the recording, mouse brains were dissected for brain weight measurements and upcoming histological assessments.

Single-unit analysis (performed by Dr Jim Sellmeijer)

Spike detection and spike sorting were done using Spike2. Further single-unit analysis was performed using custom Matlab scripts (Version 2014a, Matworks inc.). Firing rate and bursting activity were calculated. Bursts were defined as 3 or more spikes within a 50 msec time window. Bursting activity was analysed by calculating the total number of bursting events within a 90 second data segment. The average number of spikes within a bursting event were also calculated.

The following parameters are reported:

fire_freq = firing frequency in Hz;

fire_freq_rep_burst = firing frequency in Hz for when the burst events are replaced by single action potentials

number_of_bursts = number of bursting events in a recording

APs_per_ burst = number of action potentials (AP) per burst

proportion_of_aps_in_burst = the number of APs in a burst divided by the total number of APs.

Those parameters were analysed for statistical significance using GraphPad Prism 6. Because cell firing patterns are not normally distributed, non-parametric tests were performed to compare wildtype from knockout firing and bursting activities.

A

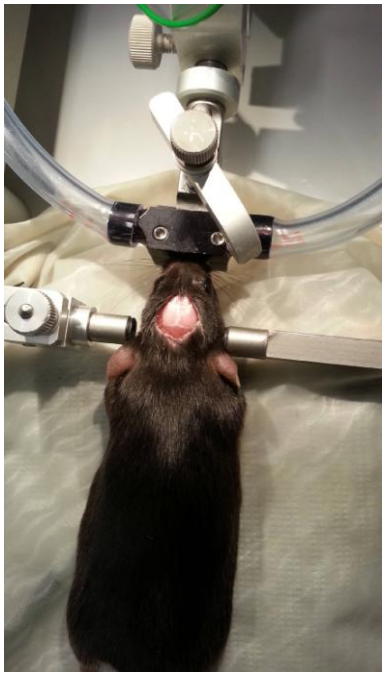

Figure 10A: Adult male mice were fixed on the stereotaxic frame, tightly aligned to measure and calculate the appropriate theoretical and actual coordinates for single units recorded in the primary somatosensory cortex and the thalamus.

B

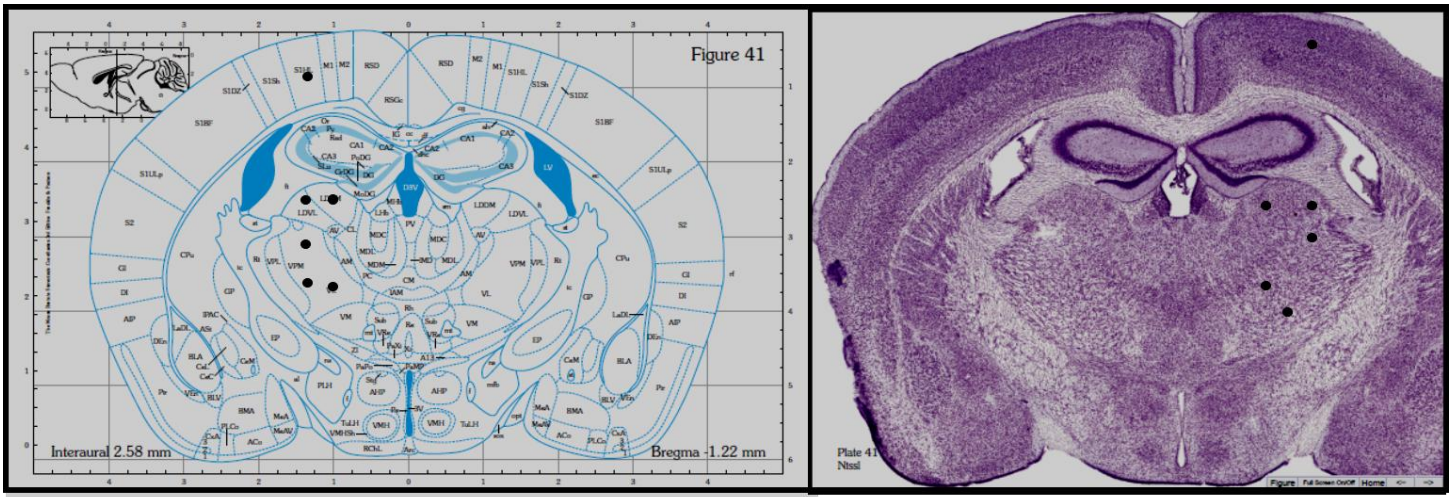

Figure 10B: Black dots indicate theoretical coordinates where single cell activity was measured in the primary somatosensory cortex (S1) and the thalamus (LDDM, LDVL and VL). Representations are shown on the mouse brain map and on Nissl-stained coronal sections (Franklin and Paxinos, 3rd edition).

Results

Results will be presented in the following format:

1. Publication 2 (in preparation): Loss of VIP causes microcephaly with sustained cortical defect due to localized downregulation of Mcph1-Chk1 crosstalk and premature neuronal differentiation.

2. Publication 3 (in submission): Hyperalgesic VIP-deficient mice exhibit VIP-reversible alterations in molecular and epigenetic determinants of cold and mechanical nociception

3. VIP knockout mice exhibit spontaneous hyperactivity in the thalamus

Supplementary Results

VIP deficiency predisposes pregnant mice to mechanical but not cold allodynia

Result 1. Publication 2 (in preparation): VIP-deficient offspring display impaired cortical development due to lack of maternal VIP

VIP-deficient offspring display impaired cortical development due to lack of maternal VIP

Tando Maduna[1], Sandrine Passemard[2], Shaveta Walia[1,2], Marlene Salgado-Ferrer[1], Adrien Lacaud[1], Pierre Gressens[2] and Vincent Lelievre[1],

1 Strasbourg University and CNRS UPR312, cellular and integrative neuroscience Institute (INCI), 67084 Strasbourg, France. 2 Paris Diderot University and INSERM, U1141, Robert Debre Hospital, 75019 Paris, France

Abstract:

VIP knockout mice exhibit neurodevelopmental and cognitive deficits due to the pleiotropic functions of this neuropeptide, including autism-like manifestations. Our current research suggests a microcephaly-like phenotype in early postnatal VIP knockout mice. VIP mutants exhibit brain size deficits with long-term morphometric impairments. As expected VIP deficiency triggers the downregulation of MCHP1-CHK1 signaling, shownwith quantitative RT-PCR, without drastic change in gene patterning as demonstrated by whole mount *in situ* hybridization. Furthermore, mutants exhibit early neuronal differentiation as Pax6 and Tbr1/2 markers revealed. Injection of VIP during the peak of neurogenesis restores the main deficits in brain size and normal gene expression. Using different combinations of breeding sets to generate wildtype, heretozygous or knockout offspring we confirm the key maternal origin of the VIP during early embryogenesis that is later replaced by embryonic production. Finally, we apply mild forced restraint stress to pregnant females to modulate VIP production and subsequently affect brain outgrowth. We demonstrate that prenatal stress significantly downregulates Mcph1-Chk1 crosstalk in wildtype and knockout embryos, and reduces expression in embryos obtained from hereterozygous females.

Introduction

Primary microcephaly is a rare developmental pathology characterized by gross reduction in brain size. Clinically, this rare genetic disorder is diagnosed when patients present with a gross reduction in cerebral cortex size and occipital frontal circumference of -2SD from the normal range without any severe motor defects and very mild to severe mental retardation at birth (Kaindl et al. 2010; Mahmood et al. 2011). This disorder results from a mutation in one of the 12 MCPH genes that have been identified so far (Hussain et al. 2013), which encode centrosomal proteins subdivided into two groups and either involved in cell cycle regulation or mitotic spindle organization in the etiology of primary microcephaly (Bond and Woods 2006). The vast majority of microcephalies that exist are syndromic and result from both pre- and postnatal detrimental interactions with environmental factors such as drugs of abuse, alcohol and intra-uterine infection (Evrard et al. 1997; Hosseini et al. 2012). Interfering with VIP signaling during a specific time-window, the peak of neurogenesis specifically identified at embryonic day 9 to 11 in mice (Gressens et al. 1997) triggers microcephaly in pups (Gressens et al. 1994; Passemard et al. 2011). Coincidentally, maternal plasma and placental VIP reach a peak of expression slightly earlier and during this time-point, paralleled by a peak in VIP receptor upregulation in decidual tissues (Hill et al. 1996; Spong et al. 1999). Thus, VIP produced by the placenta is delivered to and bathes the developing embryo within the intra-uterine compartment, where it acts on specific VIP receptors to exert its growth factor actions on brain development (Hill et al. 1999). Recent findings from our colleagues demonstrated the link between prenatal blockade of specific VIP signaling and downregulation of microcephaly-related genes. Blocking VPAC1-cAMP signaling in pregnant mice during E9-11, with the use of the VPAC antagonist (VA), preferentially downregulates Mcph1 gene expression and function, and downregulates the expression and function of the MCPH1 downstream target, Chk1. Disrupting the VPAC1-MCPH1 crosstalk also resulted in cell cycle lengthening and early neural progenitor differentiation in the telencephalic neuroepithelium and ultimately, postnatal microcephaly with gross reduction in cortical thickness in mice (Passemard et al. 2011).

In the present study, we aim at gaining novel insights on the origin of this pathology as well as on the molecular mechanisms through which VIP can control brain development using a genetic mouse model achieved through complete disruption of

the VIP gene. VIP knockout mice exhibit numerous phenotypes due to the pleiotropic actions of this neuropeptide. During early postnatal stages the absence of VIP delays developmental milestones including motor-related behaviours and sociability such that knockout pups display an autism like phenotype (Lim et al. 2008; Stack et al. 2008). Adult knockout mice exhibit dysregulation of their circadian rhythm, anxiety-like behaviour and gastrointestinal dysfunction and bowel distention to name a few (Colwell et al. 2003; Girard et al. 2006; Lelievre et al. 2007). The neurodevelopment alterations caused by loss of VIP in mice mimic the clinical presentation of developmental disorders such as autism and cerebral palsy that present with gastrointestinal and sleep disturbances in addition (Nelson 2001; Nelson et al. 2006). Thus we investigated whether VIP mutants exhibit brain size deficits, and the implications on Mcph1-Chk1 signaling using localization approaches to study gene patterning in whole embryos, as well as quantitative approaches. We've also studied the implication of the absence of VIP on early neuronal differentiation, Pax6 and Tbr1/2 and follow their ontogeny throughout the mouse neural tube. Furthermore, using combination of breeding sets to generate wildtype, heretozygous or knockout offspring we've investigated the maternal versus the embryonic contribution of VIP during early embryogenesis and their involvement in the regulation of Mcph1 expression. Finally, keeping in mind that maternal production of VIP originates from maternal T lymphocytes that populate the developing placenta, we applied a mild stress to pregnant females to modulate VIP production and subsequently affect brain outgrowth. We investigated whether prenatal forced restraint would affect MCPH1 signaling in VIP-deficient embryos born from wildtype and heretozygous females. Thus we explore this approach as a putative murine model for syndromic microcephaly.

Methods

Animals

VIP KO mice received from Professor JA Waschek (David Geffen School of Medicine, UCLA) and all of the C57BL/6 strain mice used in this study are housed at Chronobiotron IFR Neurosciences animal facility (University of Strasbourg, France) where breeding and mating are continuously carried out. Mice were housed at a 12 hour light/dark cycle with water and food pellets administered *ad libitum*.

Adult C57BL/6 mice (2-9 months old) were assigned to breeding groups to generate either wildtype, knockout or heterozygous embryos and pups from either homozygous or heterozygous breeding setsWildtype, knockout or heterozygous offspring were obtained from heterozygous females bred with wildtype, heterozygous or knockout males. Breeding was during the last hour of the dark cycle, and females were introduced into the male cage and left for an additional hour at the beginning of the light cycle, then immediately returned to their home cage of no more than 3 females per cage. Vaginal plug was considered as E0.

For embryo collection, females were sacrificed by cervical dislocation at E9 to E16.5, along the whole neurogenesis timeline.

Pups werecollected at birth, postnatal day (P) 0, and every 5 days afterwards at P5, P10 and P15 in order to measure morphometric and gene expression changes at key time-points of astrocyto- and synaptogenesis, as well as oligodendrocytogenesis and myelination. Pups and adult males were either aneasthetized with pentobarbital (Ceva Sante Animale) or ketamine (Imalgene 1000, Merial) respectively, then intracardially perfused with phosphate buffered solution (PBS), followed by 4% paraformaldehyde (PFA), for morphometric analyses. Samples were then postfixed overnight in 4% PFA at 4°C. For gene expression assays, pups were decapitated and adults sacrificed by cervical dislocation. Whole brains were dissected out and immediately immersed in cold Diethylpyrocarbonate-treated PBS, then weighed separately. Whole cortices were then dissected from each sample for subsequent RNA extraction. Body weights were measured before tissue collection. Tails were collected from anesthetized animals or fresh cadavers for genotyping, where necessary.

All animal experiments were performed according to protocols approved by the institutional local review committee that meet the CNRS-INCI guidelines for care and use of laboratory animals.

VIP injections

VIP knockout females, pregnant at E9, E10 and E11 were injected intra-peritoneally with either phosphate buffered saline (PBS), the vehicle, or VIP (Bachem) according to initial studies by Gressens (1993). Pregnant wildtype females received only PBS injections. All females were injected twice a day (9-10AM and 5-6PM) with 8µL of PBS or VIP each session, for a daily final VIP concentration of 2µg/g body weight.

Maternal restraint stress

At E9, E10 and E11 pregnant females were subjected to restraint stress, previously described to disrupt embryonic development (Wiebold et al. 1986). Each pregnant mouse was forced into a ventilated plastic centrifuge tube (see Supplementary Figure 1) as described by Liu and colleagues (2014). However the protocol was adapted in order to avoid or limit mortality in utero, thus ensuring embryo survival such that sufficient sampling may be possible. Therefore, in an attempt to lessen stress severity, two separate sessions were performed, one in the morning (10AM) and another in the early evening (5PM). In addition, stress duration was reduced from 4 hours to 45 minutes per session. At E12.5 females were sacrificed by cervical dislocation and embryos, blood and placenta collected (see “Tissue collection").

Tissue collection

Placenta

Placenta was collected immediately after cervical dislocation, and then washed in PBS at room temperature to remove, thoroughly, all excess blood. Following embryo extraction, placenta were collected into 1.5mL eppendorf tubes and stored at -80°C for future assays.

Blood plasma

Blood was extracted intracardially, with a heparin-coated syringe, into lithium heparin collection tubes (GreinerBioOne, VACUETTE, Ref# 454008) that were immediately inverted 10 times then placed on ice. To extract plasma, blood was centrifuged at

1500rpm for 20 minutes, at 4°C. Plasma was then transferred into 1.5mL eppendorf tubes, then stored at -80°C for future use.

Embryos

Embryos were harvested immediately into cold PBS, followed by two washes in fresh PBS at room temperature, after which a single paw was extracted from each sample for genotyping when necessary. From a single female, embryos were designated into 2 groups whereby half of the embryos were immediately placed in 4% PFA and postfixed overnight at 4°C, and the other half was placed in fresh cold PBS for neural tube dissections.

Enzyme immune assay to measure peptide concentrations in frozen tissue

VIP (peptide) in the placenta of females subjected to forced restraint was extracted by precipitation in hydrochloric acid:ethanol (1:7) solution. Each sample was homogenized using the Ultraturex instrument and incubated at room temperature for 30 minutes. Each homogenate was centrifuged at 3,000 x g for 30 min at 4°C. Supernatants were transferred into new tubes and evaporated using the Speedvac apparatus for 3 hours. Plasma VIP was assayed directly from blood plasma without additional peptide extraction procedures. The enzyme immune assay was carried according to manufacturer instructions and the full protocol is available on Supplementary Methods.

In vitro cell culture for neurosphere generation

Neurospheres were generated, under sterile conditions, from E10.5 wildtype and knockout embryos as previously described (Passemard et al. 2011). To study the effect of exogenous VIP on cell fate, cells were stimulated towards differentiation by culturing on plastic-coated plates for optimal cell adhesion and in culture medium containing a decreased final concentration of Fibroblast Growth Factor-Basic heparin from 20ng/mL to 2ng/mL (Sigma Ltd, USA) and incubated at 37°C (5% CO2). After 3 days VIP was administered at a final concentration of 10^{-8}M after which the cells were further incubated as described, then harvested after either 12, 24 or 48 hours of treatment. Cells were harvested rapidly and RNA extracted as mentioned below.

RNA extraction and relative quantification of gene expression by Real-time PCR

Total RNA was isolated from neural stem cell cultures, from neural tubes dissected from whole embryos at E9 to E16 of gestation (whereby the putative fore-, mid- and hindbrains are dissected and separated for region-specific analysis) and from cortices dissected from mice at different postnatal stages, using the extraction protocol previously described (Lelievre et al. 2002), initially adapted from Chomczynski and Sacchi (1987). RNA samples were then stored at -80C for further use including real-time RT-PCR. Gene amplification was performed as previously described (Passemard et al. 2011) using highly selective primers (see Table1 for details) designed using the open source bioinformatic tool, mfold3.1 (Zuker, 2003) to optimize PCR amplification, and Oligo6 Primer design software. RNA quality and concentration were assessed using a Nanodrop spectrophotometer and capillary electrophoresis on biochips loaded on a 2100 Bioanalyzer (Agilent). Total RNA (600 ng) was subjected to reverse transcription using the Iscript™ kit (Biorad). Negative controls (samples in which reverse transcriptase was omitted) were individually amplified by PCR using the different primer sets used in the present study to ensure the absence of genomic DNA contamination. To specifically amplify mRNA encoding various mouse proteins, we designed the specific primer sets (sense and antisense respectively) using Oligo6.0 and mfold3.1 for amplifying the different genes of interest whose sequences are given in Table 1. To standardize the experiments, 3 classic housekeeping genes were tested; i.e. beta2-microglobulin, glyceraldehyde-3-phosphate dehydrogenase (*Gapdh*), and hypoxanthine guanine phosphoribosyl transferase (*Hprt*) as well as *18S* ribosomal RNA. Preliminary experiments showed that *Hprt* levels remained highly stable among the different samples and treatment conditions. This housekeeping gene was therefore chosen to standardize all the quantitative experiments presented here. Realtime PCR was set up using SYBR green-containing supermix™ (Biorad) for 45 cycles of a three-step procedure including a 20-second denaturation step at 96°C, a 20-second annealing step at 60°C, followed by a 20-second extension step at 72°C. All PCR quantification were performed using specific standard curves performed for all the genes of interest.

Whole mount *in situ* hybridization

Probes

Specific primers (Table 2) were designed as mentioned above. The protocols for probe template generation and in vitro transcription of the digoxigenin-labeled probes were adapted from Schaeren-Wiemers and Gerfin-Moser (1993). cDNA was amplified from mouse embryonic (E10-E16) forebrain total RNA extracted as previously mentioned. After verification of amplicon specificity, PCR products were ligated into plasmid vector (pCR®II-TOPO® 4.0 kb, Invitrogen) for transformation in bacterial cells (DH5α or TOP10 cells, Invitrogen). Plasmids were then extracted with a miniprep extraction kit (Quantum Prep®Plasmid Miniprep Kit, Bio-Rad). The PCR product insertion and size were determined with EcoRI restriction enzyme digestion at restriction sites flanking the sequence of interest. Restriction maps were generated (NEBcutterv2.0, New England Biolabs; restrictionmapper.org) to determine the orientation of the inserts within the vector and optimize the in vitro transcription using the Sp6 or T7 promoter. Linearized plasmids were loaded onto agarose gel for electrophoresis separation then excised out and purified (NucleoSpin®ExtractII, Macherey-Nagel). cDNA template (~1µg/µL) obtained from linearized plasmid was then added to digoxigenin-containing RNA labeling mix (Riboprobe Gemini System II Buffer, Promega), containing T7 or Sp6 promoter, depending on orientation to generate either the sense (negative control) or antisense (positive control) probes. Digoxigenin-labelled probe mixture was then incubated for 2 hours at 37°C, followed by 15 minutes DNase digestion at 37°C (Boehringer). Each probe was precipitated with TE 1X buffer (Tris+EDTA, pH9), 3M sodium acetate and 100% ethanol for overnight storage (-20°C). Supernatant was discarded following 30 minutes of centrifugation and washed with 70% ethanol at 4°C. The pellets were finally resuspended in TE 1X buffer and kept at -20°C for 30 minutes. The probe yield and quality was verified on 1.2% agarose gel (Gel DOC™ EZ Imager, Bio-Rad).

in situ Hybridization

To maintain the integrity of the embryos and keep the tissue intact for whole-mount in situ hybridization, postfixed embryos at E9.5 to E13.5 were dehydrated in increasing concentrations of 25%; 50%; 75% methanol in PBT (PBS in Triton X100) and then twice in 100% methanol to maintain the integrity of the tissue. Embryos were then stored in 100% methanol at -20°C for future use. Whole-mount *in situ* hybridization

was performed following a 5 day protocol adapted and optimized from Correira and Conlon (2001) and the Cepko/Tabin Lab Core protocols (Harvard Medical School). All washing steps were under agitation, while the embryos were completely submerged to ensure optimal exposure to wash solutions.

Fixed embryos are rehydrated in a descending methanol series (75%, 50%, 25%). E12.5 and E13.5 embryos were bleached in 6% hydrogen peroxidase dissolved in sterilized distilled water (Komatsu et al. 2014) to clear the embryos for background optimization. Embryos were permeabilized with Proteinase K treatment during 1 minute for each embryonic day dated from 0.5, thus embryos at E9.5 were washed in Proteinase K for 9 minutes, etc. Proteinase K digests the surrounding tissue, while maintaining full structural integrity, for easy penetration of the probe into the embryonic tissue. Embryos were prehybridized overnight at 60°C, then hybridized with the specific digoxygenin-labelled cRNA probe (Roche Applied Systems) at a final concentration ranging between 0.5-1µg/mL. Anti-dig, coupled to alkaline phosphatase oxidizes BCIP (5-bromo-4-chloro-3'-indolyphosphate) to produce an indigo colour and reduces NBT (nitro-blue tetrazolium) in a redox reaction that produces blue coloration on the regions where anti-dig-AP binds digoxygenin. Alkaline phosphate activity was revealed in a colorimetric reaction containing 3.5µL BCIP and 4.5µL NBT per 1mL of buffer, which was changed and replaced with fresh medium every 2 hours while awaiting coloration of labelled regions. Revelation was stopped with PBT at 4°C then embryos postfixed overnight in formaldehyde at 4°C.

For stereomicroscopy, embryos were embedded in viscous solution (OCT, Sakura Finetek, USA), images captured with AxioCam MRc (Carl Zeiss Vision, 2008) and analyzed with AxioVision Rel4.7.1 software (Carl Zeiss Imaging Solutions, 2008). Magnification, exposure time and light incidence were adjusted on control samples for optimal picture quality then fixed and used for all the samples used in the same experiments.

Immunohistochemistry

Postfixed VIP wildtype and knockout embryos at gestational stage E12.5 were cryoprotected with 30% sucrose (PBS) then cryosectioned at 10 µm. For immunohistochemistry, slides were rinsed twice with PBS and once with PBS-gelatin -Triton X100 (PBS/Gel/Tx) for 10 min each at room temperature. Tissues were blocked with 10% goat or donkey serum in PBS/Gel/Tx for one hour at room

temperature, then incubated at 4°C overnight with specific monoclonal, i.e. anti-Pax6 (1/1000) and anti-Tuj1 (1/500), and polyclonal, i.e. anti-Tbr2 (1/500) and Tbr1 (1/500) primary antibodies from Covance Research Products Inc. and Abcam, respectively. Slides were then gently washed twice with PBS and once with PBS/Gel/Tx (10 min each). Tissue was incubated with either goat anti-mouse Alexa488 (1/1000) from Invitrogen or goat anti-rabbit Cy3 (1/500) from Jackson. Secondary antibody mix contained 5% serum and PBS/Gel/Tx and samples were incubated for 90 min in the dark at room temperature. After PBS washes, samples were stained with Dapi (1/1000) for 2 min.

Image acquisition and processing were performed with confocal microscopy (Zeiss Ltd., Germany) or optic microscopy and processed using Axiovision Rel4.7.1 software (Carl Zeiss Imaging Solutions, 2008) or Photoshop software. Cell counting was performed in a 5 cm^2 fields. For cell counting, the nucleus was considered as the small countable object.

Morphometry

Following postfixation (see “Animals”) pup and adult brains were fully submerged for cryoprotion in 30% sucrose (PBS) at 4°C until descent. Brain weights were measured after cryopreservation, for safety issues since PFA is poisonous. Images were captured from the dorsal surface for overall brain perimeter comparison between wildtype and knockout mice using fixed magnification adjusted on control brains. Brains were then embedded in O.C.T. (Sakura Finetek, USA) and stored at -20°C until cryosectioning into coronal sections of 14µm thickness and stained with 0.5% Cresyl Violet (Sigma). The following parameters were measured; cortical surface, cortical thickness, cortical lamination and corpus callosum thickness.

For all cortical measurements, the left and right hemispheres were measured to account for section asymmetry and both values were averaged per measurement and per brain. In addition, the polygonal selector tool was used for all measurements, and data presented as area of a polygon, where applicable. Morphometry was measured along the rostral brain based on a previous study (Passemard et al, 2009) and such that the primary motor cortex, the primary somatosensory cortex the corpus callossum could be measured simultaneously and along the same plane and axis. Measurements were taken at Bregma 1.10 to 0.74 in adults (The mouse brain in stereotaxic coordinates, G. Paxinos and KBJ Franklin, 2007, 3rd edition, Elsevier).

Cortical surface, cortical thickness and lamination region selection and measurements were based on previous research (Passemard et al, 2009), with the inclusion of the primary motor cortex and corpus callossum. Positions relative to adult coordinates were selected for pup brains, along with the use of the Allen Developing Mouse Brain Reference Atlas (Allan Institute for Brain Science, USA). All parameters were measured and analyzed with ImageJ software (NIH, USA).

Statistical Analyses

All statistical analyses were performed on GraphPad Prism 6.01 (GraphPad Software). All data are presented as mean ± SEM and results compared using a 2-tailed Student's t-test or the non-parametric Mann-Whitney test for behavior and other non-normally distributed datasets. ANOVA with Bonferroni's multiple comparisons tests were performed for grouped data, with the alternative Kruskall-Wallis test and Dunn's multiple comparisons test for non-normally distributed datasets. $p < 0.05$ was considered as significant.

Results

Lack of VIP causes microcephaly with long-term severe reduction in cortical thickness, preferentially at the primary motor cortex, in VIP knockout pups and adult males

VIP blockade during neurogenesis results in microcephaly during early postnatal stages, as previously shown (Passemard et al. 2011) and we investigated whether this could be mimicked in the overall absence of VIP, in VIP knockout pups and adults. Morphometric analyses were performed in P15 as well as 4 month old male wildtype and knockout brains. The rostral brain was selected as the region of interest to measure the primary motor cortex, the primary somatosensory cortex as well as the corpus callosum simultaneously as alterations in one or more of these structures provides morphological evidence of VIP knockout mice displaying autism-like characteristics. From Cresyl violet stained coronal sections, we report a significant reduction of brain perimeter at P15, which was not observed and seems to be rescued in adults (Figure 1A). However, more in depth analyses revealed a significant gross reduction of cortical surface in knockout pups as well as adults (Figure 1B), corresponding to gross reduction of cortical thickness specifically at the primary motor cortex (Figure 1C) but not the primary somatosensory cortex. At the primary somatosensory cortex, Layer II-IV was significantly thinner in P15 knockouts but rescued in adults, compared to wildtypes. However, in the adult primary somatosensory cortex, Layer V-VI was significantly thinner than age-matched wildtypes (Figure 1D). All measures were taken Bregma 1.10 to 0.74 in adults (The mouse brain in stereotaxic coordinates, G. Paxinos and KBJ Franklin, 2007, 3rd edition, Elsevier) and relative regions in P15 brains. The corpus callossum was significantly thinner, specifically at Bregma 0.98 in knockout adult and P15 brains, compared to wildtypes (Figure 2).

During neurogenesis, absence of VIP downregulates Mcph1 gene expression throughout the neural tube of VIP knockout embryos

To investigate whether brain malformations observed in VIP knockout embryos were due to dysregulation in microcephaly-related genes, we studied the ontogeny of *Mcph1*, which was investigated and localized with whole-mount *in situ* hybridization throughout neurogenesis. In developing wildtype embryos, *Mcph1* was localized at

the fore-, mid- and hindbrains E10 to E13.5. Here we show a strong and more diffuse digoxigenin-labelling of *Mcph1* at E10.5 which decreases and becomes more specifically localized in the whole neural tube of E12.5 embryos (Figure 3A, upperpanel). Knockout age-matched embryos exhibit a similar distribution and pattern for *Mcph1* although showing decreased labelling, especially at the dorsal regions of the telencephalic vesicles and diencephalon. In knockout E12.5 embryos, *Mcph1* labelling is restricted at the periphery of the telencephalic vesicle and minimal at the mesencephalic and rhomboncephalic vesicles, suggesting reduced level of gene expression throughout the knockout neural tube. Indeed, gene expression in these embryos is mainly detected at the dorsal surface. Thus, we quantified overall gene expression in isolated forebrains with quantitative RT-PCR. *Mcph1* was significantly downregulated from E9 to E16 in the forebrains of age-matched knockout embryos (Figure 3A). The trend of *Mcph1* expression corresponds to that of *Brca1*, which was downregulated in forebrains of E10 to E16 embryos. We measured the ontogeny of other microcephaly genes (data not shown) and found no effect of VIP loss. These included *Aspm* (Figure 3B), whose expression remained unchanged in VIP knockouts. *Stil* and *Pcnt* were significantly downregulated only in E12 forebrains, with no significant differences in their expression in early and later stages (Figure 3B).

During neurogenesis, absence of VIP downregulates Chk1 gene expression throughout the neural tube of VIP knockout embryos

Chk1 was localized solely in the neural tube of wildtype embryos from E10.5 to E13.5. Here we show robust *Chk1* riboprobe hydridization and alkaline phosphatase-dependent staining throughout the telencephalic vesicles in wildtype E10.5 embryos, with a more focal representation at the rostral region in older E12.5 embryos (Figure 4, upper panel). *Chk1* labelling is also reduced in E10.5 knockout midbrain, however even more severely in older embryos. No definite hindbrain expression could be detected in both wildtype and knockout embryos. Quantitative RT-qPCR revealed that although wildtype forebrain *Chk1* expression increases during the peak of neurogenesis (E9-11), and is doubled between E9 and E12, this is significantly reduced back to E9 levels at E14 and continues to decrease with age. However, knockout forebrain expression of *Chk1* is significantly lower compared to age-matched wildtypes, and remains at the E9 baseline throughout the timeline of E9 to E12, and decreases from E14. Therefore, during the peak of neurogenesis *Chk1*

expression is at a half dose compared to wildtypes, specifically in the developing forebrain (Figure 4).

Vpac1 gene is expressed throughout the neural tube of mouse embryos during the peak of neurogenesis, but is specifically downregulated in the forebrains of VIP knockout embryos

Because it is well known that VIP and its related neuropeptide PACAP can crossreact with their different receptors VPAC1, VPAC2 and PAC1 we also looked at their expression profile to exclude compensatory changes. We localized Vpac1 gene expression in the developing embryo with whole-mount *in situ* hybridization for an overall multi-dimensional overview (Figure 5A, photomicrographs on top panel) and quantified forebrain expression patterns with quantitative RT-PCR (Lower panel). In wildtype embryos, *Vpac1* localized solely in the primitive forebrain at E9. By E10 (data not shown) and E10.5 we report distinct and restricted *Vpac1* distribution in the fore-, mid- and hindbrains of wildtype embryos. However, we found minimal *Vpac1* labelling at E9, with no distinguishable distribution by E10.5 in VIP knockout embryos. A closer and quantitative examination (Figure 5A, Lower panel) revealed a significant downregulation of *Vpac1* gene expression in isolated knockout forebrains at E9 and E10, compared to wildtypes. There were no significant differences in forebrain expression of between wildtype and knockout embryos at E12, although whole mount *in situ* hybridization suggests a higher labelling in the fore-, mid- and hindbrains of knockouts compared to wildtypes starting at E12.5 (Figure 5A, photomicrographs on top panel). There were no significant differences in forebrain *Vpac2* and *Pacap* gene expression (Figure 5B), as expected.

Pax6 gene expression is prematurely upregulated in the neural tube and specifically upregulated as early as E9 in knockout forebrains

To verify whether microcephaly in VIP knockout mice is due to low cortical progenitor turnover, we investigated the distribution and expression of *Pax6* throughout the timeline of neurogenesis (Figure 6, top panel). Thus, we localized *Pax6* in the forebrain, the rostral midbrain, the hindbrain and spine of E10.5 wildtype embryos. However, we also found marked *Pax6* labelling in the fore- and midbrains of E9.5 knockout embryos, which increases by E10.5 and is much higher than age-matched wildtypes (Figure 6, Photomicrographs on top panel). There was a similar pattern

surrounding the optic vesicle. Indeed quantitative analyses (RT-qPCR) revealed more than a double increase of *Pax6* gene expression from E9 to E10 in knockout forebrains, which in addition to being a more striking increase than what is observed in wildtypes, was also significantly higher than in wildtypes (Figure 6, Lower panel). With whole mount *in situ* hybridization, we also found that at E12.5 *Pax6* labelling is distributed throughout the neural tube, in the eye (as expected) as well as the primordial paws and caudal tail. No distinct labelling can be detected in the E12.5 spine. Interestingly, at this stage, there is a visible increase in *Pax6* labelling not only throughout the dorsal surface, but also along the ventral surface as can be observed rostrally (see Photomicrographs on top panel). There were no significant differences observed at later stages.

Tbr2 gene expression is prematurely upregulated in the neural tube and specifically upregulated as early as E12.5 in knockout forebrains

To further support the idea of significant decline in early progenitor turnover and early neuronal differentiation, we investigated the distribution and expression of the early progenitor differentiation marker, Tbr2 (Figure 7). Whole mount *in situ* hybridization localized *Tbr2,* with a distribution that is markedly increased in E12.5 knockout embryos, throughout the neural tube but with no distinct labelling of the spine. At E13.5, no differences could be distinguished between wildtype and knockout embryos as observed along the dorsal surface (Figure 7, Photomicrographs on top panel). Quantitative analyses confirmed these results and reported a significant increase in forebrain *Tbr2* gene expression, already starting at E10 in knockouts whereby it is almost absent in wildtypes. At E12, there is twice the amount of *Tbr2* expressed in knockout forebrains compared to wildtypes. There were no significant differences quantifiable at E13.

Tbr1 gene expression is prematurely upregulated in the neural tube and specifically upregulated as early as E12.5 in knockout forebrains

We also localized and measured the expression of another differentiation marker, Tbr1, to investigate whether it would also be upregulated premature in the absence of VIP. Indeed, compared to wildtype, we found a marked increase in *Tbr1* labelling throughout the E12.5 neural tube, including the whole spinal column. In contrast,

wildtype labelling is restricted along the dorsal surface of the fore-, mid- and hind-brain, with specific and restricted staining along the spine. A total of 3 separate experiments performed on different days and under different ambient conditions, with embryos extracted from 3 different pregnancies, revealed a strikingly high staining surrounding the fore- and midbrain, which was maintained even after revelation duration was adjusted. These results suggest that *Tbr1* is markedly increased throughout the dorsal, as well the ventral telencephalon. At E13, a similarly robust increase in *Tbr1* labelling can be observed encompassing the entire area of the neural tube (Figure 8, Photomicrographs on top panel). Indeed, quantitatively, *Tbr1* expression is doubled in knockout forebrains, compared to wildtypes, already at E11 and continues to increase along the timeline (Figure 8, Lower panel).

Reduced cortical thickness in VIP knockout mice is due to prenatal reduction in proliferation of cortical neurogenic progenitors

We analyzed the in vivo phenotype of VIP knockout embryos by immunohistochemical staining with specific antibodies targeted towards Pax6 (for ventricular zone (VZ) progenitors) and Tbr2 (for subventricular zone (SVZ) progenitors). Although *Pax6* gene expression is higher in knockout forebrains at E12.5, we report a downregulation of Pax6 functional expression specifically at the lateral telencephalic vesicles (Figure 9A), which is not the case at the dorsal level. As expected, Tbr2 was highly expressed in both VZ and SVZ regions of knockout embryos at E12.5, especially along the lateral telencephalic vesicles, when compared with wildtypes. However, no differences were observed in immunolabelling at the dorsal region. In addition, we counted more Tbr2-positive cells localized diffusely throughout the ventricular and subventricular zones of knockout lateral telencephalic vesicles. We also report an early increase in Tbr1 immunolabelling at the lateral telencephalic vesicles of E12.5 knockout embryos (Figure 9B). Here Tbr1-positive cells were densely distributed throughout the cortical plate showing a significantly higher cell count than wildtypes.

Tuj1 functional expression was also investigated to show the distribution of immature neurons in the proliferative VZ and SVZ of developing telencephalon in the absence of VIP. Although Tuj1 immunolabelling was detected mainly at the preplate (PP) of both wildtype and knockout lateral telencephalic vesicles (Figure 9C), we found some

TuJ1 positive cells, in lower numbers at the VZ, whilst a higher cell count was found along the border between the VZ and SVZ in the knockout lateral telencephalic vesicles. The marginal zone and the sub plate zone are also very heavily labeled suggesting early differentiation of progenitors and their extension into SVZ (Figure 9C).

Exogenous VIP administration, specifically during the peak of neurogenesis (E9-11) is an intra-uterine factor regulating Mcph1 and Chk1 gene expression

To investigate whether exogenous VIP could be implemented to rescue the expression of microcephaly genes and early neural differentiation markers, we injected pregnant VIP wildtype and knockout females with VIP at E9, E10 and E11. As expected, knockout embryos showed decreased *Mcph1* and *Chk1* distribution throughout the neural tube. However, embryos from VIP-treated females exhibited very similar levels of *Mcph1* and *Chk1* staining, as seen in wildtypes. *Mcph1* rescue seemed more robust, including the mid- and hind-brain. In contrast to *Chk1* where the rescue is mainly observed at the forebrain. In addition *Chk1* rescue was more marked along the caudal telencephalic vesicles and hindbrain. *Tbr1* staining seemed slightly decreased in VIP-treated E12 embryos (Figure 10, Photomicrographs on top panel). This was quantified with RT-qPCR (Figure 10, Lower panel), demonstrating that, indeed in isolated knockout forebrains. *Tbr1* gene expression is rescued following earlier VIP-treatment. We also report that VIP-treatment rescued *Brca1* gene expression as a downstream target of MCPH1. *Pax6* and *Tbr2* gene expression were also returned to wildtype levels in isolated forebrains extracted from VIP-treated knockout embryos.

Maternal VIP genotype determines *Mcph1* and *Chk1* gene expression in E12 embryos

Aforementioned results suggest that maternal expression of VIP directs gene expression patterns of *Mcph1* and *Chk1* genes. Thus, we bred heterozygous females with knockout males to investigate whether knockout embryos would display previously demonstrated decreases in *Mcph1* and *Chk1* gene expression. With whole-mount *in situ* hybridization (Figure 11, Photomicrographs on top panel), we found that the VIP knockout *Mcph1* expression profile mimicked that observed in wildtypes, showing identical distribution in the telencephalic vesicles as well as along

the spine. Quantitative RT-PCR from isolated forebrains demonstrate that at E10 and E12, compared to wildtypes, *Mcph1* and *Chk1* gene expression are downregulated in knockout embryos obtained from heterozygous females. Surprisingly, these knockouts exhibit a higher relative gene expression compared to heterozygous and knockout embryos obtained from knockout females (Figure 11, Lower panel).

Maternal VIP genotype rescues Pax6 gene expression in E12 embryos

We also bred knockout females with heterozygous males to generate heterozygous embryos. However, in this case, the difference from the aforementioned experiment (Figure11) being that these heterozygous embryos would not have been supplemented with daily intra-peritoneal VIP injections. Indeed at E12, relative gene expression of wildtype (from wildtype females) and heterozygous (from heterozygous females) were almost similar (Figure 12, Lower panel) as observed with RT-qPCR performed from isolated forebrains. However, heterozygous and knockout embryos displayed similar levels of *Pax6 gene* expression in E12 forebrains, though significantly different. In addition, whole mount *in situ* hybridization (Figure 12, Photomicrographs on top panel) reveals an intermediate distribution of *Pax6* labelling in E12 embryos, where *Pax6* expression seemed higher at the caudal telencephalic vesicles and was almost diminished along the rostral end. There were no distinguishable differences in the mid- and hind-brain.

Maternal VIP genotype determines timing of oligodendrocyte maturation in postnates

In this study, we generated the following:

$VIP^{+/+}$ offspring - from wildtype and heterozygote females to investigate whether gene expression would be influenced by VIP deficiency in otherwise wildtype offspring.

$VIP^{+/-}$ offspring – from wildtype females to assess whether gene expression in these heterozygotes would reflect that of wildtype offspring due to full maternal supplementation of prenatal (maternal) VIP

$VIP^{+/-}$ offspring – from knockout females to assess whether gene expression would be driven by the presence of endogenous VIP or would reflect that of full knockout offspring

$VIP^{-/-}$ offspring – from knockout females to assess whether gene expression would be affected in the complete absence of VIP

Thus, at P15, although *Olig2* expression was already downregulated in wildtype cortices (from homozygous wildtype parentage), the expression was three times higher in all other offspring from VIP-expressing mothers. Indeed, wildtype offspring from wildtype female crossed with a heterozygous male displayed the same expression of *Olig2* as heterozygous pups from the same breeding set. They also displayed the same high expression as heterorygotes from heterozygous females crossed with knockout males. Knockouts from the homozygous breeding sets also showed a marked decrease of *Olig2*, similar to controls. This suggests the importance of VIP dosage in the onset and repression of oligodendrocyte precursor differentiation. Markers for oligodendrocyte maturation were unaffected in all wildtype pups. However, *Plp* and *Mbp* were equally downregulated in all heterozygote offspring, and dramatically reduced, equally in all progeny of knockout mothers. Thus, the maternal genotype regulates axon myelination as severity of maternal VIP deficiency determined the extent of downregulation of *Plp* and *Mbp* with knockouts showing the lowest expression profile regardless of the genotype of the offspring. *Cnpase* expression was not affected in the cortex of wildtypes and heterozygotes. However, this was significantly reduced in heterozygotes and knockouts from knockout females. This suggests VIP as a crucial activator of myelination in the cortex. Thus, maternal VIP emerges a crucial exogenous factor involved in oligodendrocytogenesis as well the onset of myelination as heterozygous pups from knockout females also showed a marked decrease in relative expression of *Cnpase.*

When implemented during the crucial period of neurogenesis (E9-E11) forced restraint stress of pregnant females significantly reduces *Mcph1* and *Chk1* expression in the forebrain of E12.5 embryos

We investigated whether environmental factors would mimick malformations observed in the microcephalic VIP knockout mice, and whether the same molecular mechanism would be involved. Thus mice at gestational stage E9 to E11 were subjected to forced restraint as this protocol has been shown to have various implications during early pregnancy in mice, including a decreased T-lymphocyte density, proliferation and secretion. Thus, we hypothesized that forced restraint would attenuate VIP secretion due to the loss of T-lymphocyte activity in the uterus. In this pilot study, E12 embryos from stressed wildtype, heterozygous and knockout females

were assayed for changes in gene expression with whole mount *in situ* hybridization and quantitative RT-qPCR. We were mainly interested in the impact of stress on heterozygous females and whether the stress would definitely impact VIP intra-uterine expression, either lowering or completely inhibiting VIP secretion (Research still ongoing) and whether microcephaly-related gene expression would be affected at a higher or lower severity in knockout and heterozygous embryos obtained from heterozygous females. Whole mount *in situ* hybridization demonstrated a significant decrease in *Mcph1* labelling in embryos obtained from stressed females, with the highest severity amongst embryos from VIP-deficient females (Figure 14, Photomicrograph A). In genotype-matched deficient embryos *Mcph1* was restricted along the lateral borders of the telencephalic vesicles, and was almost absent throughout the medial surface. Knockout embryos from heterozygous females exhibited an *Mcph1* distribution similar to that of knockouts from knockout females, whereby labelling is faint along the rostro-caudal axis of the telencephalic vesicle (Figure 14, Photomicrograph A2). *Chk1* followed the same distribution exhibiting even less localization along the rostro-caudal axis of the telencephalic vesicle in knockout embryos from stressed heterozygous females (Figure 14, Photomicrograph B2). In accordance, this result was verified at the quantitative level (Figure 14 C). *Mcph1*, and in addition, *Brca1* and *Chk1* relative expression in E12 forebrains were significantly reduced by prenatal stress. As suggested by the localization study, knockout embryos from stressed heterozygotes not only exhibited the same reduction of gene expression as knockouts from both stressed and unstressed females, but they were also expressed at the same level as these knockouts. Knockouts from unstressed females exhibited *Mcph1*, *Brca1 and Chk1* expression that was unchanged compared to heterozygotes from unstressed females. However heterozygous embryos (from heterozygous females) showed significant downregulation of gene expression compared non-stressed heterozygotes. Maternal stress had no significant effect on wildtype nor knockout embryos from homozygous pairings, thus suggesting that VIP-deficient females are the ones mainly affected, further suggesting that our implementation of the maternal stress protocol may affect the immune conditions within the intra-uterine environment during early pregnancy. Indeed circulating and placental concentrations of VIP were measured with an enzyme immune assay. VIP immunoreactivity was decreased both in wildtype and heterozygous females that underwent forced restraint (Figure 15). This proved further

evidence of the maternal contribution of VIP and its direct action on gene expression changes and the cortical development.

VIP administration promotes neural stem differentiation and cell specification *in vitro*

In neural stem cells cultured from E10 forebrains, we investigated the impact of VIP supplementation in wildtype conditions on different cellular mechanisms. After 24 hours of VIP administration, *Stat3* gene expression was significantly decreased which lasted even after 48 hours of treatment. Conversely, while *Pax6* and *Tbr2* genes were not expressed in control cells, treatment with VIP upregulated their expression after 24 hours, and increasing when treatment was longer (48 hours). In addition, the neuronal differentiation markers *Otx2, Ngn2, Nurr1* and *Tuj1* were significantly upregulated from 24 to 48 hours of treatment. Taken together, these results suggest that in wildtype conditions, VIP inhibits self renewal of neural progenitors (*Stats3*) while promoting neuronal differentiation (*Pax6, Tbr2*). Furthermore VIP action upregulated the monoaninergic *Aadc* and *Th* gene expression further implicating VIP in cell lineage determination and specification (Figure 16A).

Furthermore, VIP downregulate the astroglial differentiation markers *Gfap* and *S100b* (Figure 16B). In contrast after 24 hours of VIP treatment, we report a significant upregulation of oligodendrocyte precursor differentiation marker, *Pdgfrα.* Oligodendrocyte maturation markers were also markedly increased after 24 hours of treatment.

To further elucidate how VIP can induce neural stem cell differentiation and specification, we investigated whether the same treatment of VIP *in vitro* would change the expression of specific enzymes involved in transduction control through epigenetic modulation (Figure 16C). VIP treatment result in very early upregulation of most of the markers assayed, just 12 hours post-treatment. *Hdac1*, *Hdac2* and *Kat2b* were significantly upregulated 12 hours after incubation, suggesting early impact of VIP on histone modifications and subsequent repression of gene expression. The DNA methylation markers, *Mecp2 and Mbd3* were also immediately upregulated following 12 hours of VIP administration. *Mbd1* expression was also upregulated however after longer incubation (48 hours), suggesting that VIP regulates gene transcription in a time-dependent manner. DNMTs are implicated in maintenance of DNA methylation and in neural function. In this assay, VIP

upregulated *Dnmt1* and *Dnmt3a* expression, while also upregulating *miRNA23*, which is involved in regulating gene expression.

Thus, in culture, VIP promotes progenitor differentiation and directs cell fate by its regulation of gene expression in an epigenetic manner. This action remains to demonstrate in vivo.

Discussion

VIP knockout as a mouse model for human microcephaly

This current study aimed to introduce the VIP knockout as a novel model for human primary microcephaly, investigating whether the phenotypes presented by VIP null mice would correspond to changes in molecular cues and framework which are dysregulated in affected individuals. Indeed, the peak of neurogenesis, and the crucial time of VIP-mediated cortical growth was previously identified by blocking specific VIP signaling with prenatal injections of the VIP antagonist to pregnant mice at E9 to 11 resulting in microcephaly in neonates and postnatal mice (Gressens et al. 1994; Passemard et al. 2011). Thus, we investigated whether animals completely devoid of VIP would exhibit the same phenotype, and whether the severity of the defect would mimic that of the VA model or be exacerbated. VIP knockout pups displayed a gross reduction in brain perimeter observed at P15, which was accompanied by a significant reduction in cortical surface, in comparison with wildtypes. Although adult brain perimeter was normal, the cortical size defect was maintained suggesting the long-term effects of VIP loss as opposed to local and time-dependent blockade of VIP signaling. Although cortical thickness was normal at the primary somatosensory cortex, the primary motor cortex was severely affected in pups and adults. Further analysis identified a novel structure affected by the loss of VIP as we found the corpus callosum to be significantly thinner in knockout pups and adults. VIP knockouts have long been suggested to present an autism-like phenotype due to the converging evidence of behavioural and cognitive deficits they display, including delayed development of motor milestones as well as other weakened cognitive and motor abilities (Stack et al. 2008) but also hyperactivity and anxiety-like activity in the open field at adulthood (Girard et al. 2006), Thus, our current data demonstrates early morphological data that may explain the behavioural deficits observed in these mice to draw a link between the VIP knockout phenotype and diagnostic picture of human primary microcephaly.

Our previous work demonstrated that VPAC1 target VA-induced microcephaly was due exclusively to prenatal downregulation of the expression and activity of the microcephaly gene, *Mcph1*, resulting in the subsequent downregulation of its downstream target, *Chk1.* Here we've localized Mcph1 and Chk1 gene expression patterns within the putative cortex and found them to be downregulated significantly

throughout the timeline of neurogenesis. We've also localized and quantified *Vpac1* gene patterns and found the receptor expression to be downregulated in the same manner as *Mcph1* and *Chk1.* Thus, our knockout model recapitulates the previously reported molecular changes and provides direct evidence of localized gene expression defects in the etiology of microcephaly due to the loss of VIP and VPAC1 signaling. We could also conclude that the developmental control of cortical growth was specifically VIP-VPAC1-MCHP1 mediated as we found no impact on other microcephaly genes nor on Vpac2 expression. In support of previous findings showing that VIP and PACAP and their receptors show differences in their spatio-temporal distribution and functions during development (Girard et al. 2006), we have also found that in knockout embryos *Pacap* was increased only at later stages (E12) of mouse neurogenesis and was not altered in the developing cortex. This further proves that in the absence of VIP, PACAP does not compensate for VIP actions on brain development, as previously shown by Girard and colleagues (2006). Recently, Brca1 has emerged as a downstream target of Mcph1 not only in DNA damage repair but also in regulating the G2/M checkpoints, similarly as Chk1 (Lin et al. 2005). We report that *Brca1* was similarly downregulated in the developing cortex, following the same ontogeny as Mcph1 and Chk1 gene, spanning the whole timeline for neurogenesis. This provided an additional, though indirect, marker that proves VIP regulates cortical size through lengthening of the cell cycle by specifically increasing length of the S-phase as demonstrated by our colleagues (Gressens et al. 1994; Passemard et al. 2011). The gene encoding the centrosomal protein, PCNT, functions in concert with MCPH1 in the recruitment of CHK1 in cell cycle control of the cell cycle (Thornton and Woods 2009) therefore, it was no surprise that in our model Pcn*t* gene expression was downregulated in the VIP knockout forebrain.

Normal corticogenesis is spatio-temporally controlled through radial/tangential migration of neural progenitors from the neuroepithelium, however tightly regulated to generate a sufficient progenitor pool in the ventricular and subventricular zones, and through concerted symmetrical/asymmetrical divisions (Dehay and Kennedy 2007). Thus, depletion of cortical progenitors during early neurogenesis results in cortical thinning. Prenatal VA treatment resulted in significant reduction of ventricular zone thickness (Passemard et al. 2011). We report that although the sequential expression of the radial migration markers, Pax6, Tbr2 and Tbr1 was maintained in knockouts, they were upregulated prematurely than in knockouts. Thus microcephaly, due to

loss of VIP, is due to consequential early differentiation of ventricular zone progenitors as well as early maturation of progenitors that should populate the subventricular zone. Indeed, this was further demonstrated by early neuronal identity (Tuj1) of VZ and SVZ layers as early as E12.

However the critical issue regarding the generation and fate of the cortical VIPergic interneurons is yet to be elucidated. Indeed dysfunctional interneurons in VIP deficient mice may trigger unbalanced inhibition of excitatory pyramidal neurons known to play a role in autism (Zikopoulos and Barbas 2010). From previous data (Passemard et al. 2011) we know that expression of calretinin marker in lateral ganglionic eminence-migrating cells also occurs earlier than expected in VA-treated embryos. However their GABAergic activity in the absence of VIP production may be impaired leading to cortical deficit in the excitatory-inhibitory balance of the cortical circuits. This excitation/inhibition imbalance may have dramatic consequences on cognitive functions and behavior. Indeed elevation, but not reduction, of cellular excitation/inhibition balance within the mouse medial prefrontal cortex was found to elicit a profound impairment in cellular information processing, associated with social deficits observed in many neuropsychiatric disease such as schizophrenia (Yizhar et al. 2011). This speculation is further supported by evidence of deficits in social behavior in male offspring of VIP deficient female mice (Stack et al. 2008)

Maternal VIP provides a link between environmental factors and intrinsic molecular machinery within the intra-uterine compartment

After establishing this mouse strain as a model of human primary microcephaly due its specific impact on MCPH1, we then investigated therapeutic potential to overcome the severe phenotype demonstrated with clinical implications. In two sets of studies, we found that intra-peritoneal injection of VIP prenatally, as well as prenatal contribution of VIP by the mother could rescue the Mcph1-related signaling. In addition, this extra-embryonic supplementation with VIP could also rescue the normal expression of early differentiation markers, and presumably their spatio-temporal expression, although the latter is yet to be demonstrated.

To further investigate the clinical significance of maternal VIP and its contribution to normal brain growth, we implemented the forced restraint stress method in an effort to perturb prenatal VIP secretion. VIP is secreted by placental T-lymphocytes, during

the postimplantation period in rodents (Hill et al. 1996; Spong et al. 1999), that are resident and are activated in the interphase between placenta and the developing embryo (Heyborne et al. 1992). We specifically targeted this model at E9 to E11 to investigate whether this mimics the microcephaly phenotype displayed in knockouts. Indeed, stressing heterozygous females resulted in the same gene expression profile as reported in knockout embryos. Restraint stress is known to decrease T-lymphocyte secretions in mice (Liu et al. 2014) and we have demonstrated a significant reduction in VIP expression in the placenta of restrained females with the more severe implications on deficient (heterozygotes) females. Therefore now we are currently investigating whether offspring from stressed pregnancies display the morphological defects in accordance with the observed gene expression deficits, and whether exogenous VIP can rescue gene expression and brain morphology.

VIP supplementation exerts early epigenetic modifications favouring neural differentiation and oligodendrocyte maturation and axon myelination: Clues from *in vitro* studies

Administration of exogenous VIP in culture inhibited neural stem cell self renewal and promoted neural differentiation and specification. In addition, early upregulation of HDACs corresponded to that of oligodendrocyte differentiation and maturation and myelination markers. Thus, time-dependent supplementation with VIP *in vivo* could present therapeutic potential to curb and rescue developmental deficits. However, a complete exploration of epigenetic change in VIP-deficient mice compared to wild type remains to be performed.

Table 1: List of primer sequences used to amplify genes of interest by quantitative RT-PCR

Mcph1	5’-GCACAGGCCTTGTCAGACCTC-OH3’
	5’-GCTTCTCAGATGGCATGCTTG-OH3’
Aspm	5’-TCCACTTTACAGCAGCTGCCT-OH3’
	5’-CCATGTGCTTCTTAGCGTTCC-OH3’
Stil	5'-CAGGCAGCTGAGACTACTTCA-OH3'
	5'-ACGGTCGCTACTGTCTTATG-OH3'
Pcnt	5'-GCGGTGTCATCCTTAATGC-OH3'
	5'-GAGCTGGACCTGGAGTTCTGC-OH3'
Brca1	5’-CTTGTGCCCTGGGAAGACCTG-OH3’
	5’-GCGCTCTTCAAATTTTGGCTT-OH3’
Chk1	5’-AAGCACATTCATTCCAATTTG-OH3’
	5’-TGGCTGGGAACTAGAGAACTT-OH3’
Vpac1	5'-TCACTATGTCATGTTTGCCTT-OH3'
	5'-GAAAGACCCTACGACGAGTT-OH3'
Vpac2	5’-TCTACAGCAGACCAGGAAACA-OH3’
	5’-GTAGCCACACGCATCTATGAA-OH3’
Pacap	5'-TGGTGTATGGGATAATAATGC-OH3’
	5'-GTCGTAAGCCTCGTCTTCT-OH3’
Pax6	5'-TGCCCGGGAAAGACTAGCAG-OH3’
	5'-CTCCATTTGGCCCTTCGATTA-OH3’
Tbr2	5'-CGCCTGTCCAGCAACCTGTG-OH3’
	5'-TCTGCAGGGGCAAGGACTTA-OH3’
Tbr1	5'-TGGATCGAGACGCCCTCCTC-OH3’
	5'-AGATCCGCCTCCGCTTGG-OH3’
Sox2	5'-GCAGACCTACATGAACGGCT-OH3’
	5'-ACTTGACCACAGAGCCCATG-OH3’
Cux1	5'-CACAGGACTCTACCAAGCCC-OH3’
	5'-AGGTCACTGTTGGAGATGCG-OH3’
Cux2	5'-AATCCGCACACCTGAGACAG-OH3’
	5'-GCTGGGGAGTTCTTGGACTC-OH3’
Emx1	5'-TGGAGCGAGCCTTTGAGAAG-OH3’

	5'-TGGAACCACACCTTCACCTG-OH3’
Emx2	5'-CCGTCCCAGCTTTTAAGGCT-OH3’
	5'-AAGACTGAGACTGTGAGCCA-OH3’
Stat3	5'-TGATCGTGACTGAGGAGCTG-OH3’
	5'-CGAAGGAGTGGGTCTCTAGGT-OH3’
Otx2	5'-TTTACTAGGGCACAGCTCGAC-OH3’
	5'-TGGATTCTGGCAAGTTGATTT-OH3’
Ngn2	5'-TCATCCTCCAACTCCACGTCC-OH3’
	5'-GGCTGCCAGTAGTCCACGTCT-OH3’
Nurr1	5'-CGCCGAAATCGTTGTCAGTAC-OH3'
	5'-CTCCGGCCTTTTAAACTGTCC-OH3'
βIII-tubulin	5'-CTACAACGCCACCCTGTCC-OH3'
	5'-GCAGATGTCGTAGAGGGCTTC-OH3'
Aadc	5'-GGCGCATTCCTCTGTAGAAAG-OH3'
	5'-AAGGGCAGAAGCTCTCATGG-OH3'
Th	5'-GTGCACACAGTACATCCGTCA-OH3'
	5'-AGCCAACATGGGTACGTGTC-OH3'
Hdac1	5'-CGTTCTATTCGCCCAGATAAC-OH3’
	5'-AACTCAAACAAGCCATCAAAT-OH3’
Hdac4	5'-ATGTACGACGCCAAAGATGA-OH3’
	5'-CTGCTCCGTCTCTCAGCTACT-OH3’
Kat2b	5'-GGTGTCATTGAATTCCACG-OH3’
	5'-CTGGTGGGAAAACACATTCTG-OH3’
Mbd1	5'-GAGAATGTTTAAGCGAGTCGG-OH3'
	5'-ACATCACTGGGCAGTTGCAG-OH3'
Mbd3	5'-CCAGCAACAAGGTCAAGAGC-OH3’
	5'-CTGCAATGTCAAAGGCACTCA-OH3’
Mecp2	5'-TCCAGGGCCTCAGAGACAA-OH3’
	5'-CAGAATGGTGGGCTGAAGGTT-OH3’
Dnmt1	5'-CCAAGAACTTTGAAGACCCAC-OH3’
	5'-GGCTCTGACACCTGATGCTT-OH3’
Dnmt3a	5'-GGGGCGTGAAGTGCTCATGT-OH3’
	5'-GCCCCACCAAGAGATCCACAC-OH3’

miRna23	5'-CTGGGGATGGGATTTGAT-OH3’
	5'-TTGGAAATC CCTGGCAAT-OH3’
Gfap	5'-TGGAGAGAATTGAATCGC-OH3'
	5'-CCGGAGTTCTCGAACTTCCTC-OH3'
S100b	5'-ATGGAGACGCTGGACGAAGAT-OH3'
	5'-ACGAAGGCCATGAACTCCTG-OH3'
Pdgfr alpha	5'-GACGTTCAAGACCAGCGAGTT-OH3'
	5'-CAGTCTGGCGTGCGTCC-OH3'
Mbp	5'-CCTGCCCCAGAAGTCGC -OH3'
	5'-CTTGGGATGGAGGTGGTGTTC-OH3'
Plp	5'-GCAAGGTTTGTGGCTCCAAC-OH3'
	5'-CGCAGCAATAAACAGGTGGAA-OH3'
Olig2	5'-GCGGTGGCTTCAAGTCATCTT-OH3’
	5'-CGGGCTCAGTCATCTGCTTCT-OH3’
Hprt	5’-GGTGAAAAGGACCTCTCGAA-OH3’
	5’-CAAGGGCATATCCAACAACA-OH3’

Table 2: List of primers used to generate probes for whole mount in situ hybridization

Mcph1	5'-TGAGGAGCCTTTTGAACTCTC-3'
	5'-AACTGGTGCTGGTCAAGACTT-3'
Chk1	5'-GACTTTGGCTTGGCAACGGTA-3'
	5'-CCAGTTTGTCCACGTTCGAGG-3'
Vpac1	5'-CCGCCGTCTTCATCAAGGATA-3'
	5'-CTCTGCCTGCACCTCGCCATT-3'
Pax6	5'-CTGGGCAGGTATTACGAG-3'
	5'-CTGTGGGATTGGCTGGTAGAC-3'
Tbr2	5'-AGGGCAATAAGATGTACGTTC-3'
	5'-GGGCAAGGACTTAATACCATA-3'
Tbr1	5'-GATCTACACGGGCTGCGACAT-3'
	5'-TTTGATGGAGGAGGGCGTCT-3'

A. Brain perimeter

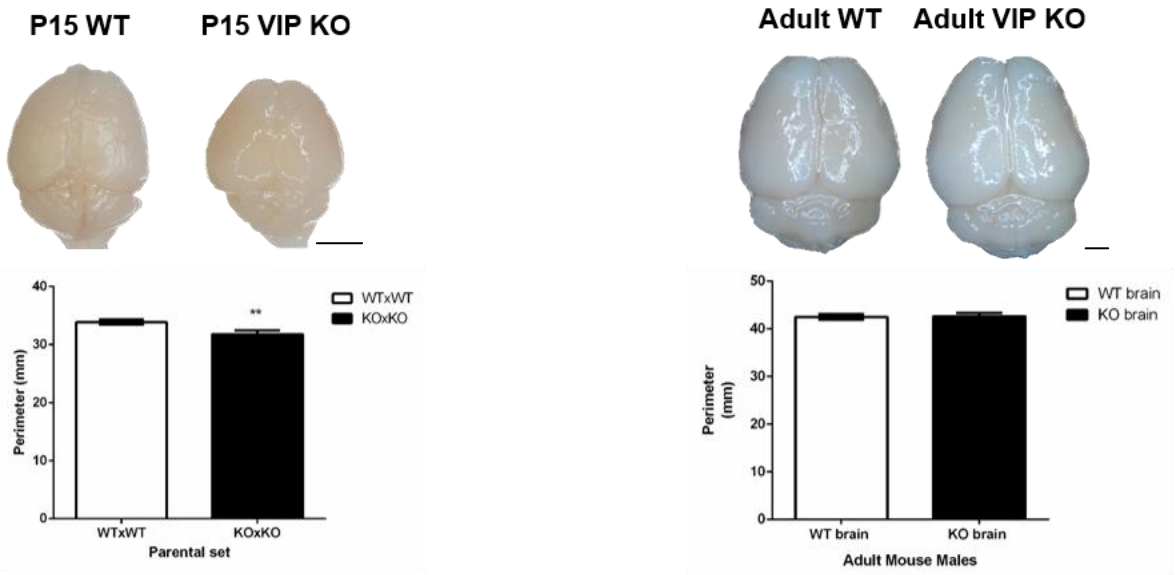

B. Cortical Surface

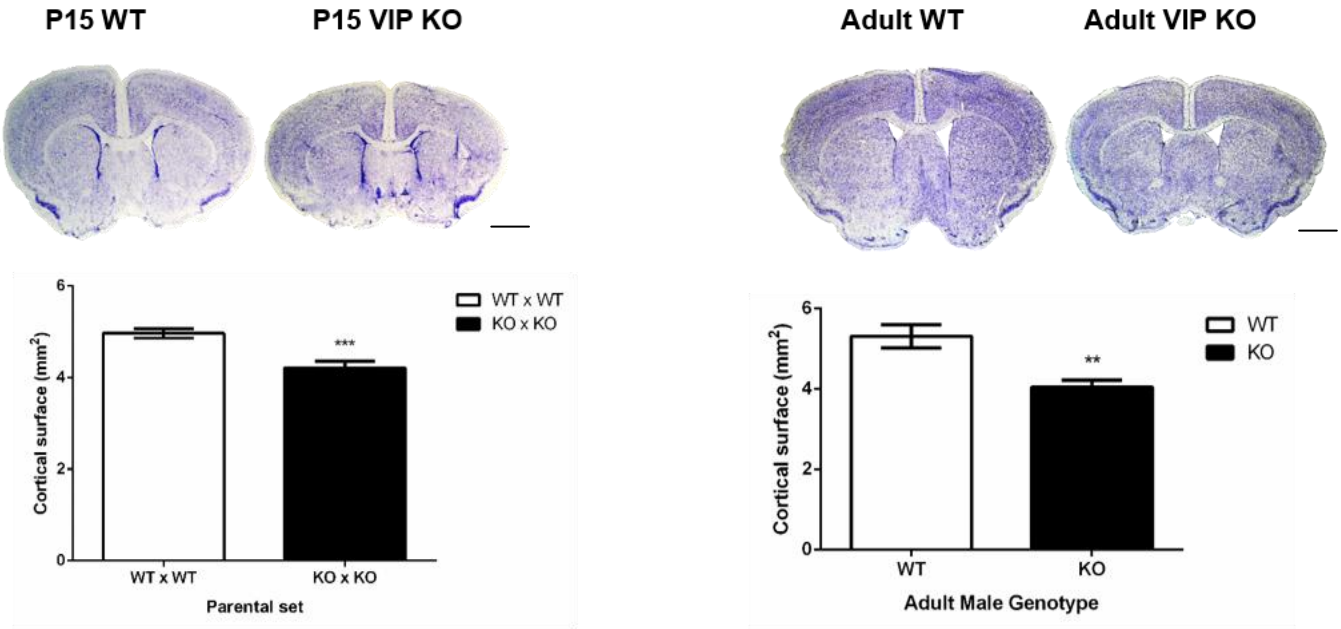

C. Cortical thickness

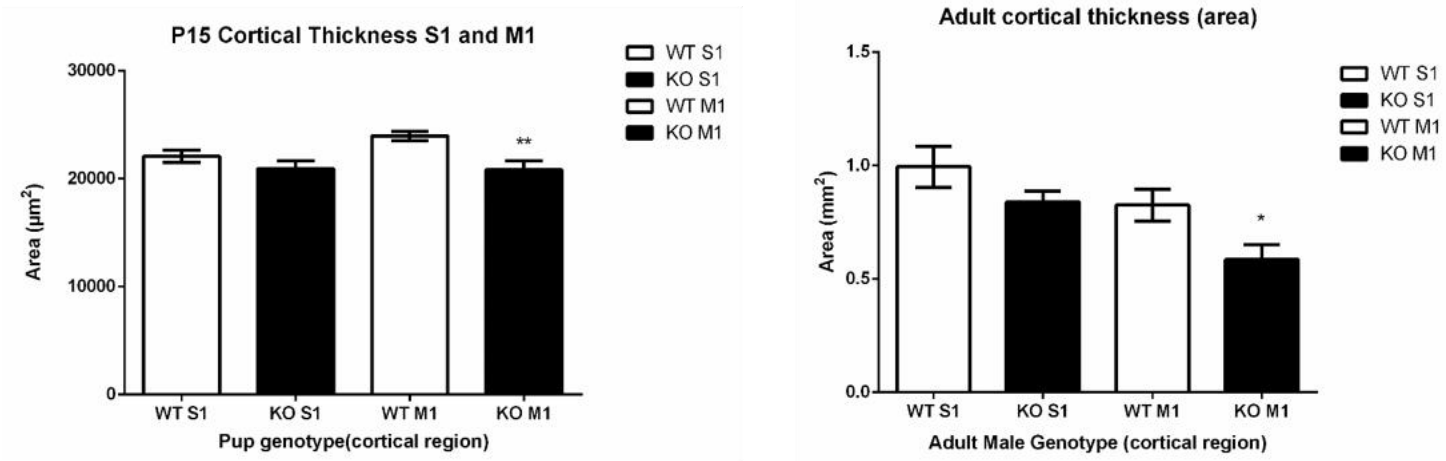

Figure 1

Cortical lamination

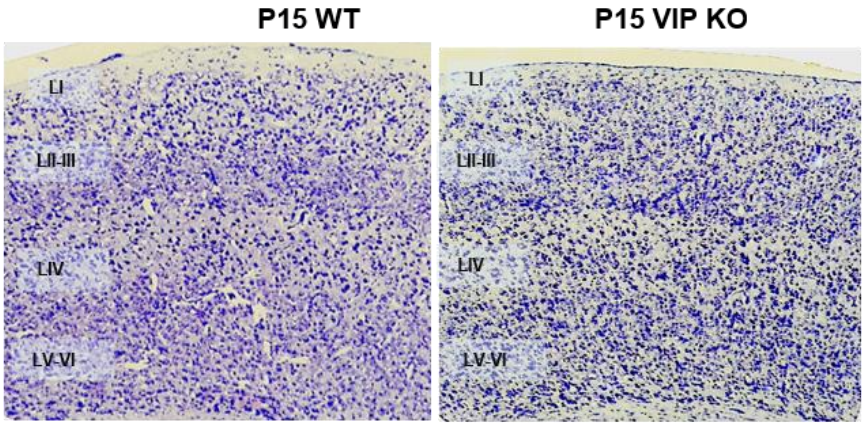

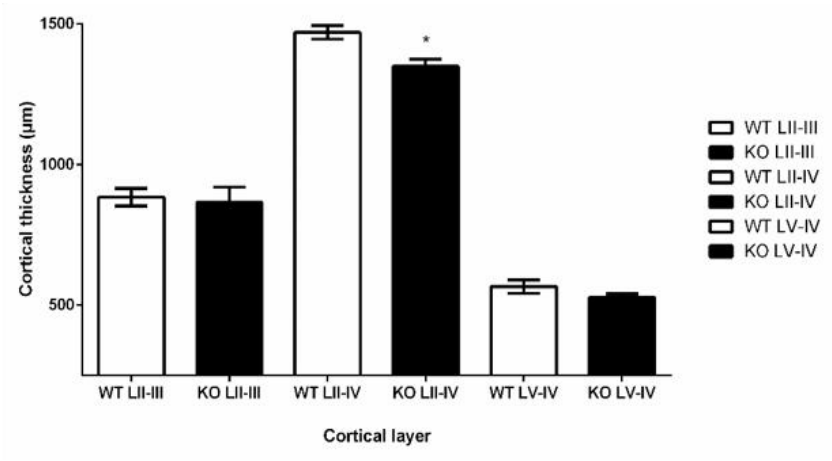

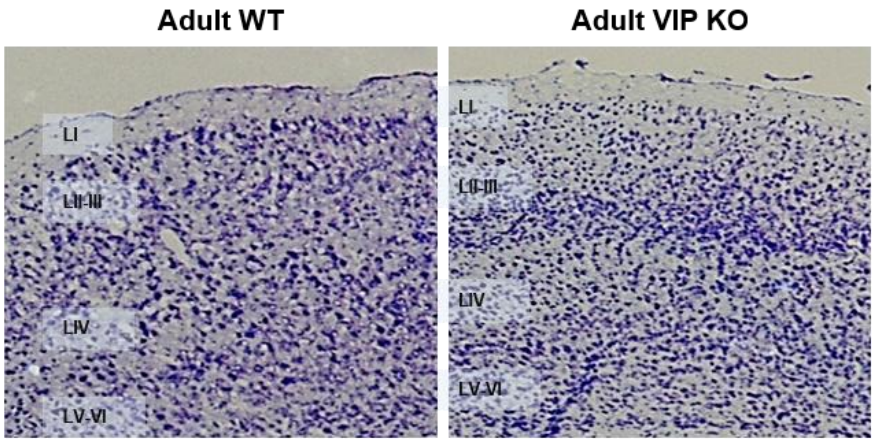

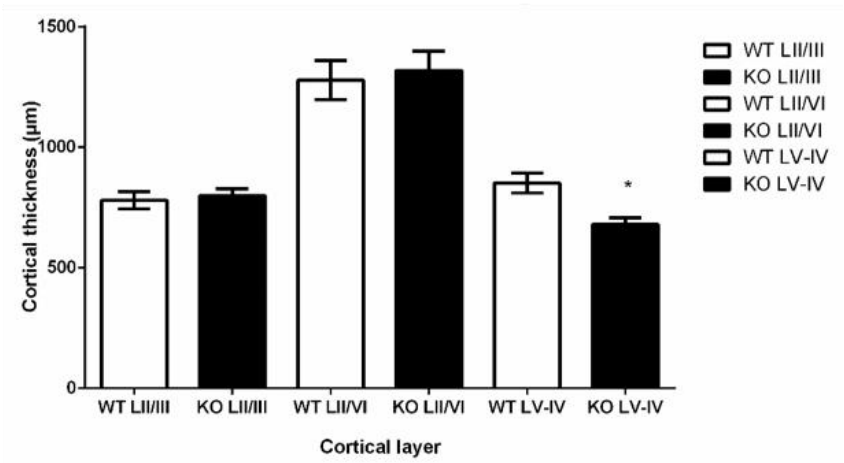

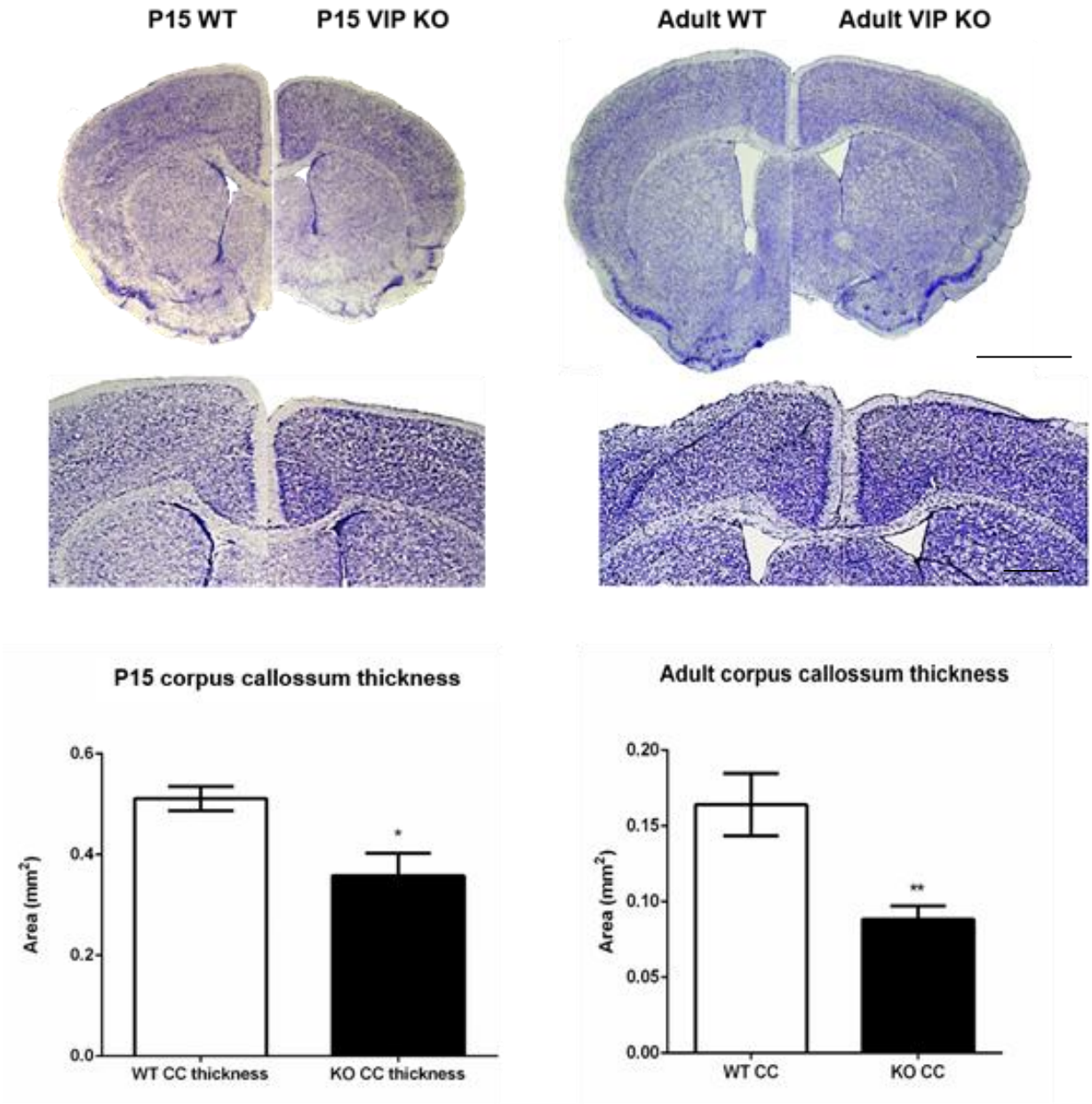
P15 WT
P15 VIP KO
Adult WT
Adult VIP KO
P15 corpus callossum thickness
Area (mm²)
0.6
0.4
0.2
0.0
*
WT CC thickness
KO CC thickness
Adult corpus callossum thickness
Area (mm²)
0.20
0.15
0.10
0.05
0.00
**
WT CC
KO CC

Figure 2

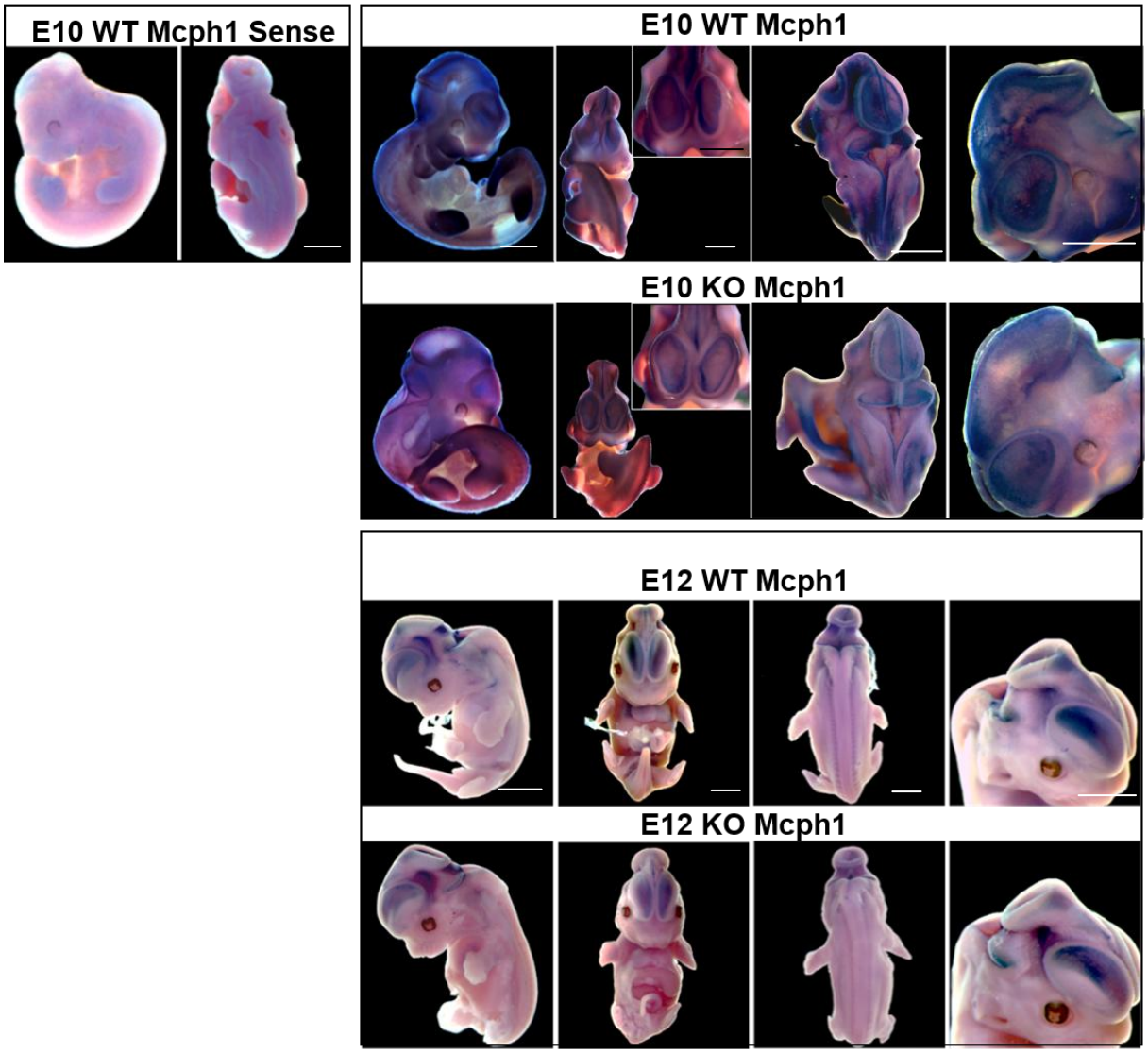
E10 WT Mcph1 Sense
E10 WT Mcph1
E10 KO Mcph1
E12 WT Mcph1
E12 KO Mcph1

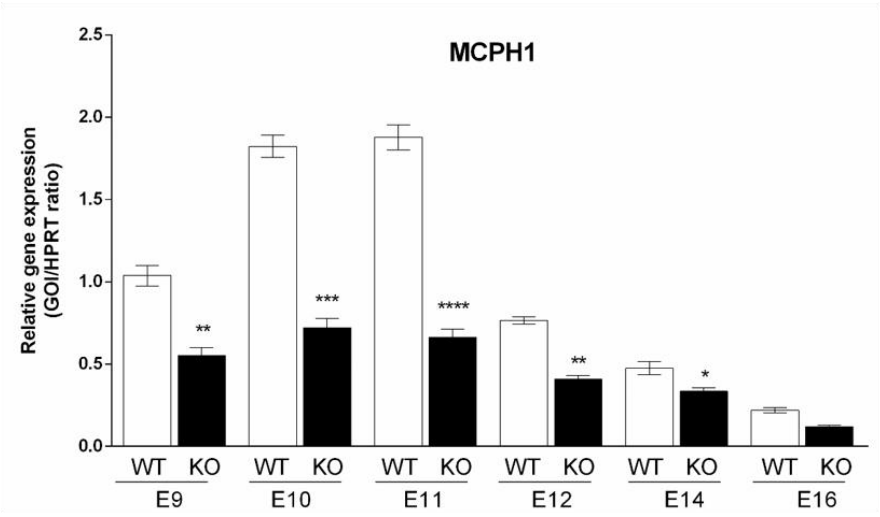
MCPH1
Relative gene expression (GOI/HPRT ratio)
2.5
2.0
1.5
1.0
0.5
0.0
**
***
****
**
*
WT KO
E9
E10
E11
E12
E14
E16

Figure 3A

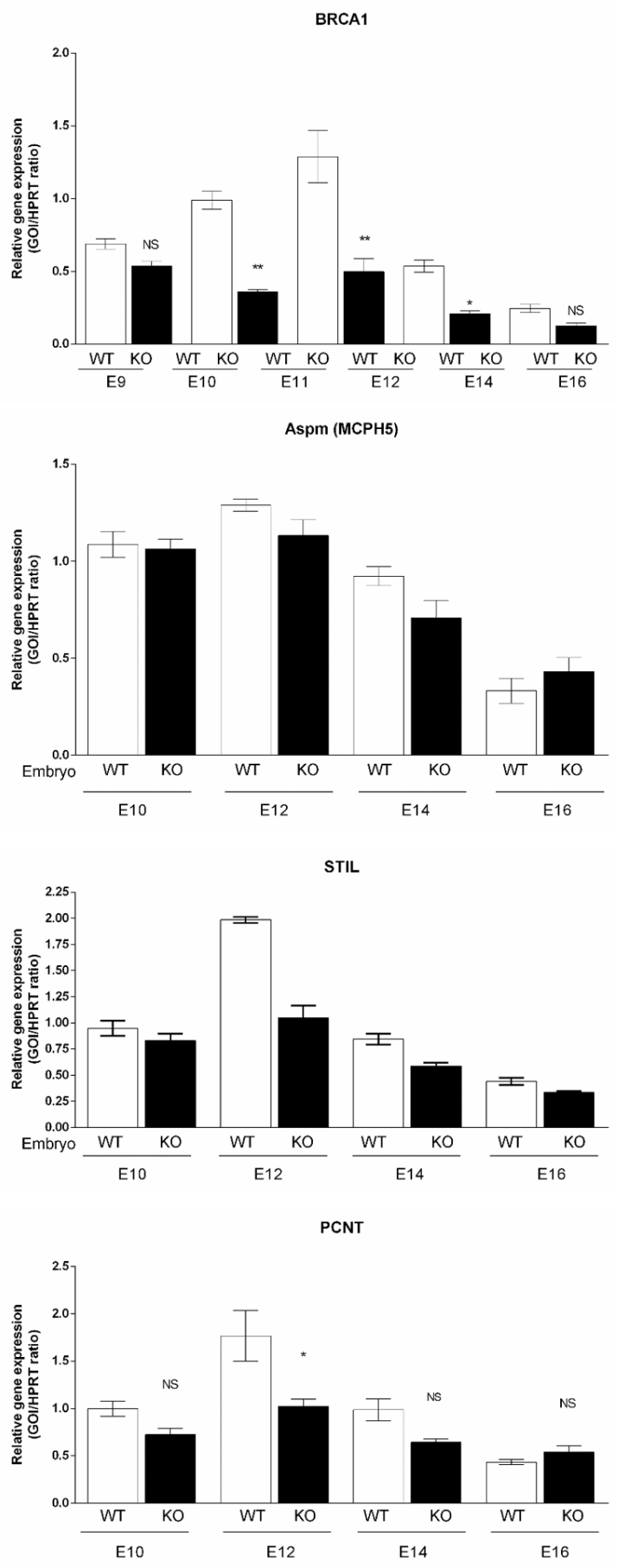
BRCA1
Relative gene expression (GOI/HPRT ratio)
2.0
1.5
1.0
0.5
0.0
NS
**
**
*
NS
WT KO WT KO WT KO WT KO WT KO WT KO
E9 E10 E11 E12 E14 E16
Aspm (MCPH5)
Relative gene expression (GOI/HPRT ratio)
1.5
1.0
0.5
0.0
Embryo
WT KO WT KO WT KO WT KO
E10 E12 E14 E16
STIL
Relative gene expression (GOI/HPRT ratio)
2.25
2.00
1.75
1.50
1.25
1.00
0.75
0.50
0.25
0.00
Embryo
WT KO WT KO WT KO WT KO
E10 E12 E14 E16
PCNT
Relative gene expression (GOI/HPRT ratio)
2.5
2.0
1.5
1.0
0.5
0.0
NS
*
NS
NS
WT KO WT KO WT KO WT KO
E10 E12 E14 E16

Figure 3B

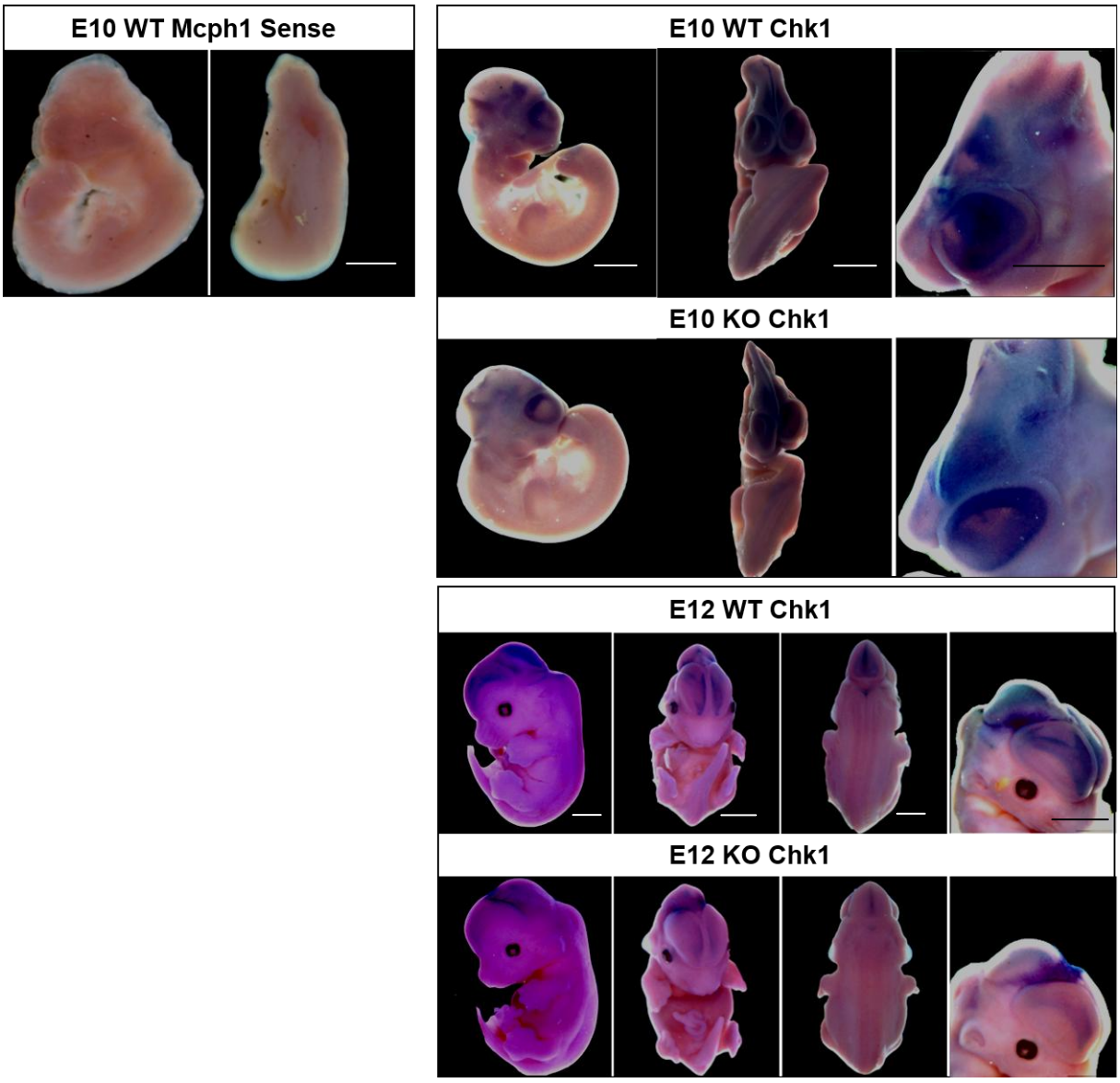
E10 WT Mcph1 Sense
E10 WT Chk1
E10 KO Chk1
E12 WT Chk1
E12 KO Chk1

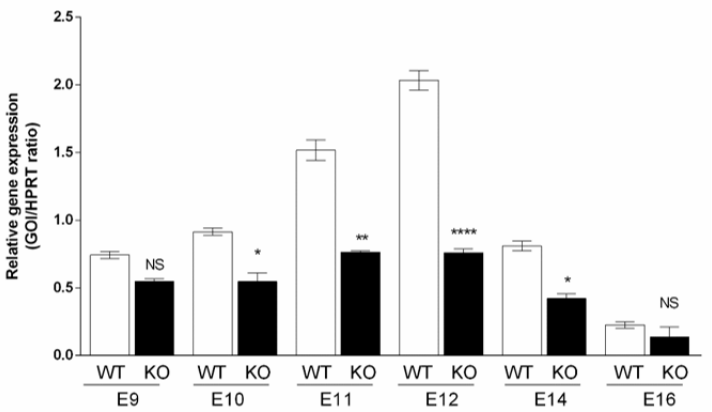
Relative gene expression
(GOI/HPRT ratio)
2.5
2.0
1.5
1.0
0.5
0.0
NS
*
**
****
*
NS
WT KO
E9
E10
E11
E12
E14
E16

Figure 4

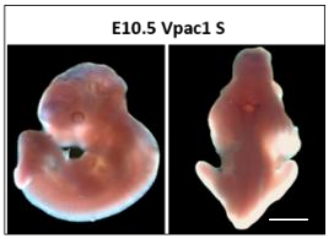
E10.5 Vpac1 S

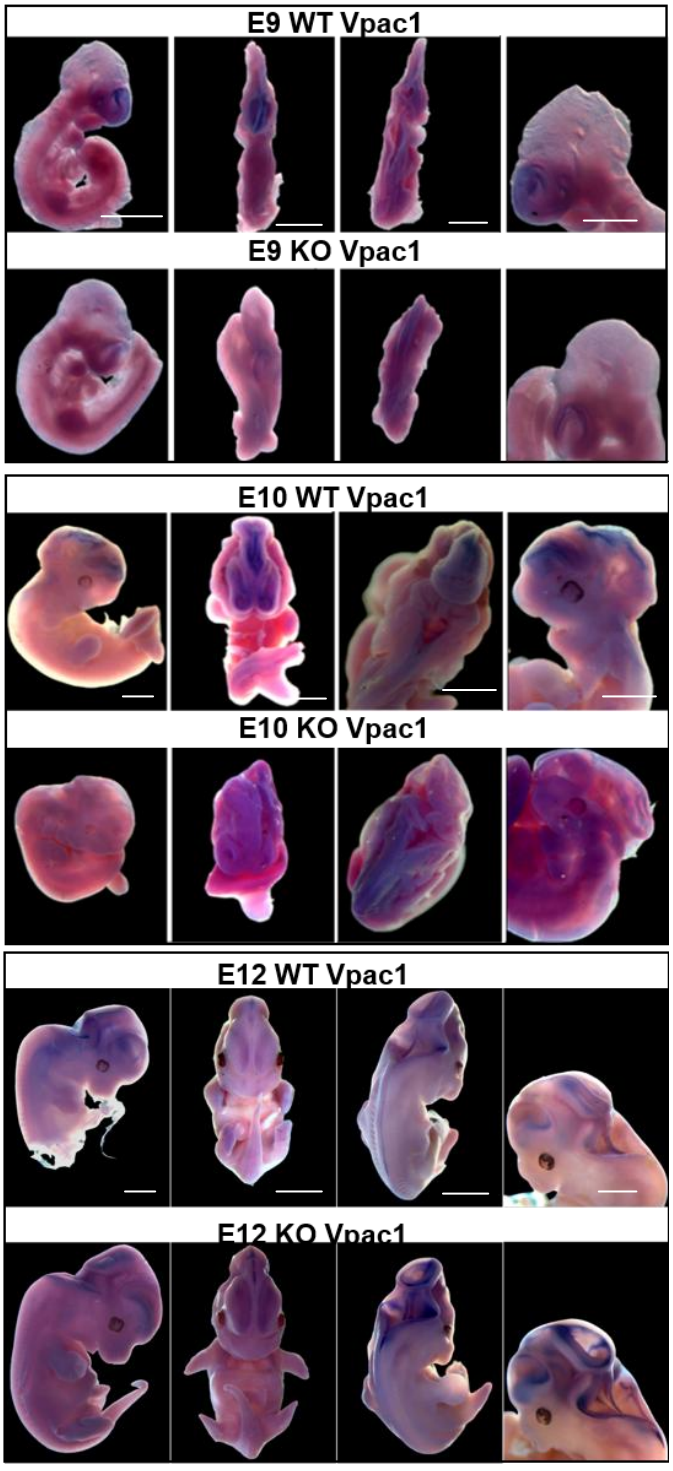
E9 WT Vpac1
E9 KO Vpac1
E10 WT Vpac1
E10 KO Vpac1
E12 WT Vpac1
E12 KO Vpac1

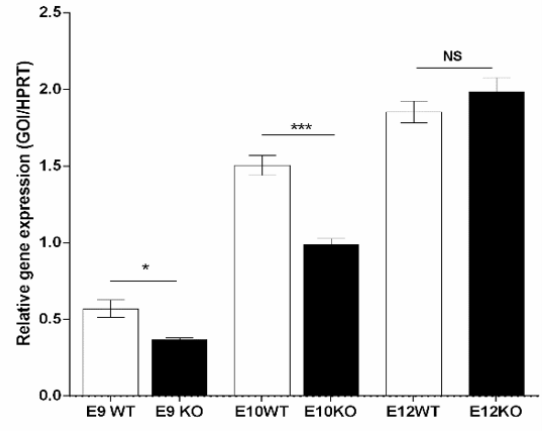
Relative gene expression (GOI/HPRT)
2.5
2.0
1.5
1.0
0.5
0.0
*
***
NS
E9 WT
E9 KO
E10WT
E10KO
E12WT
E12KO

Figure 5

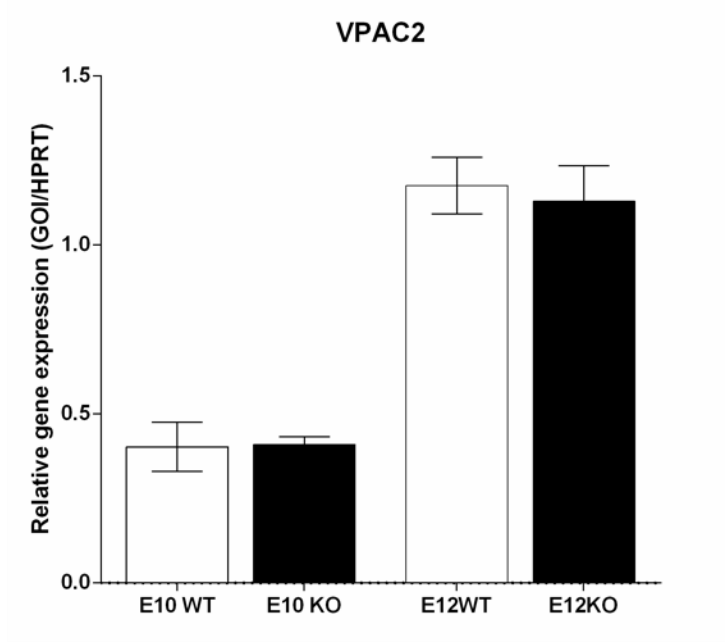
VPAC2
Relative gene expression (GOI/HPRT)
1.5
1.0
0.5
0.0
E10 WT
E10 KO
E12WT
E12KO

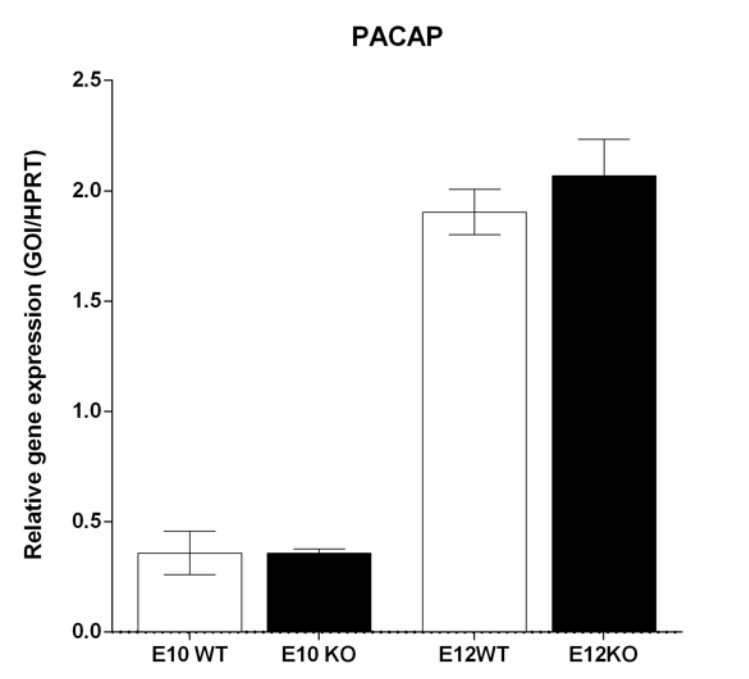
PACAP
Relative gene expression (GOI/HPRT)
2.5
2.0
1.5
1.0
0.5
0.0
E10 WT
E10 KO
E12WT
E12KO

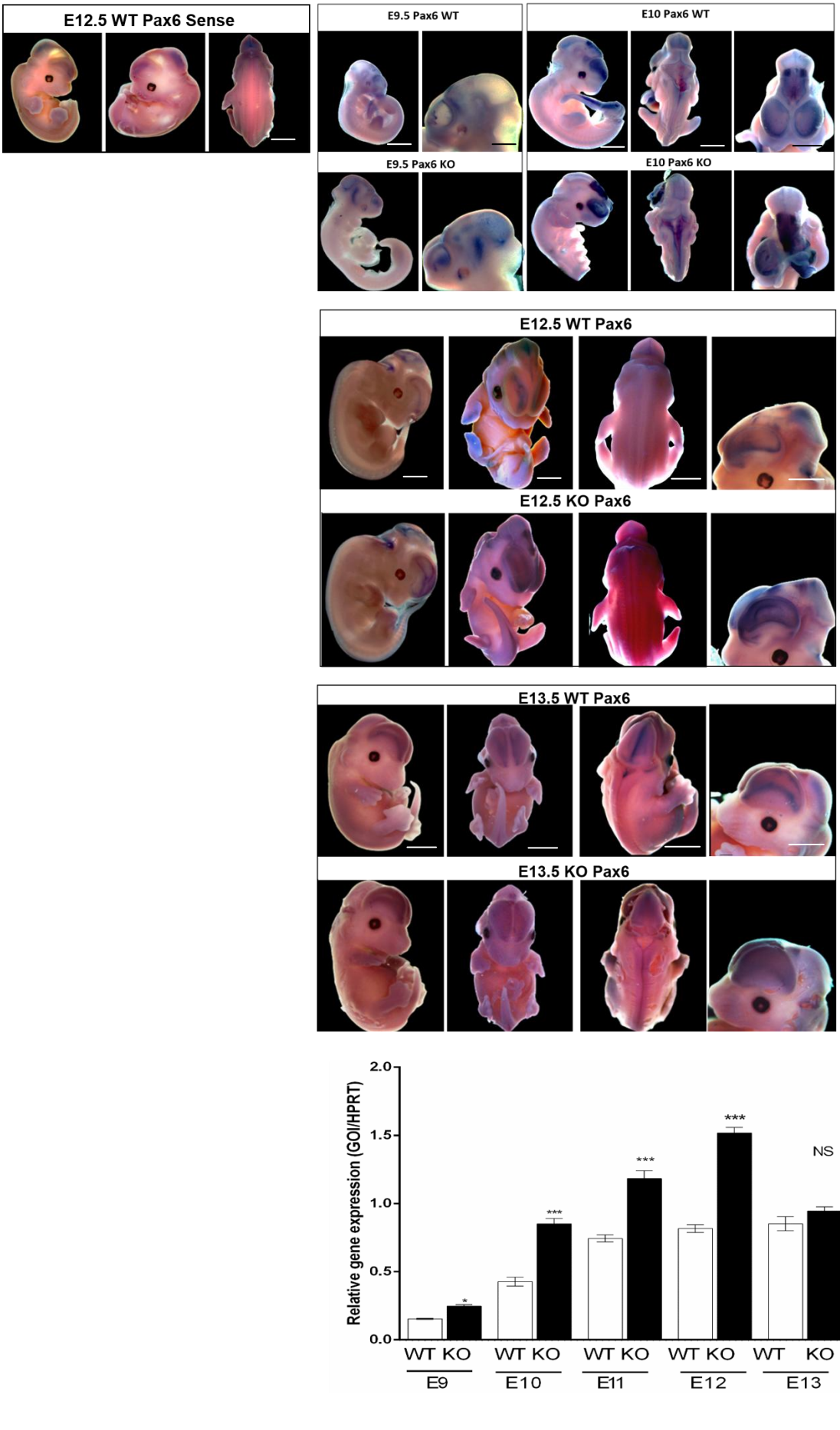
E12.5 WT Pax6 Sense
E9.5 Pax6 WT
E10 Pax6 WT
E9.5 Pax6 KO
E10 Pax6 KO
E12.5 WT Pax6
E12.5 KO Pax6
E13.5 WT Pax6
E13.5 KO Pax6
Relative gene expression (GOI/HPRT)
2.0
1.5
1.0
0.5
0.0
*
***
***
***
NS
WT KO
WT KO
WT KO
WT KO
WT KO
E9
E10
E11
E12
E13

Figure 6

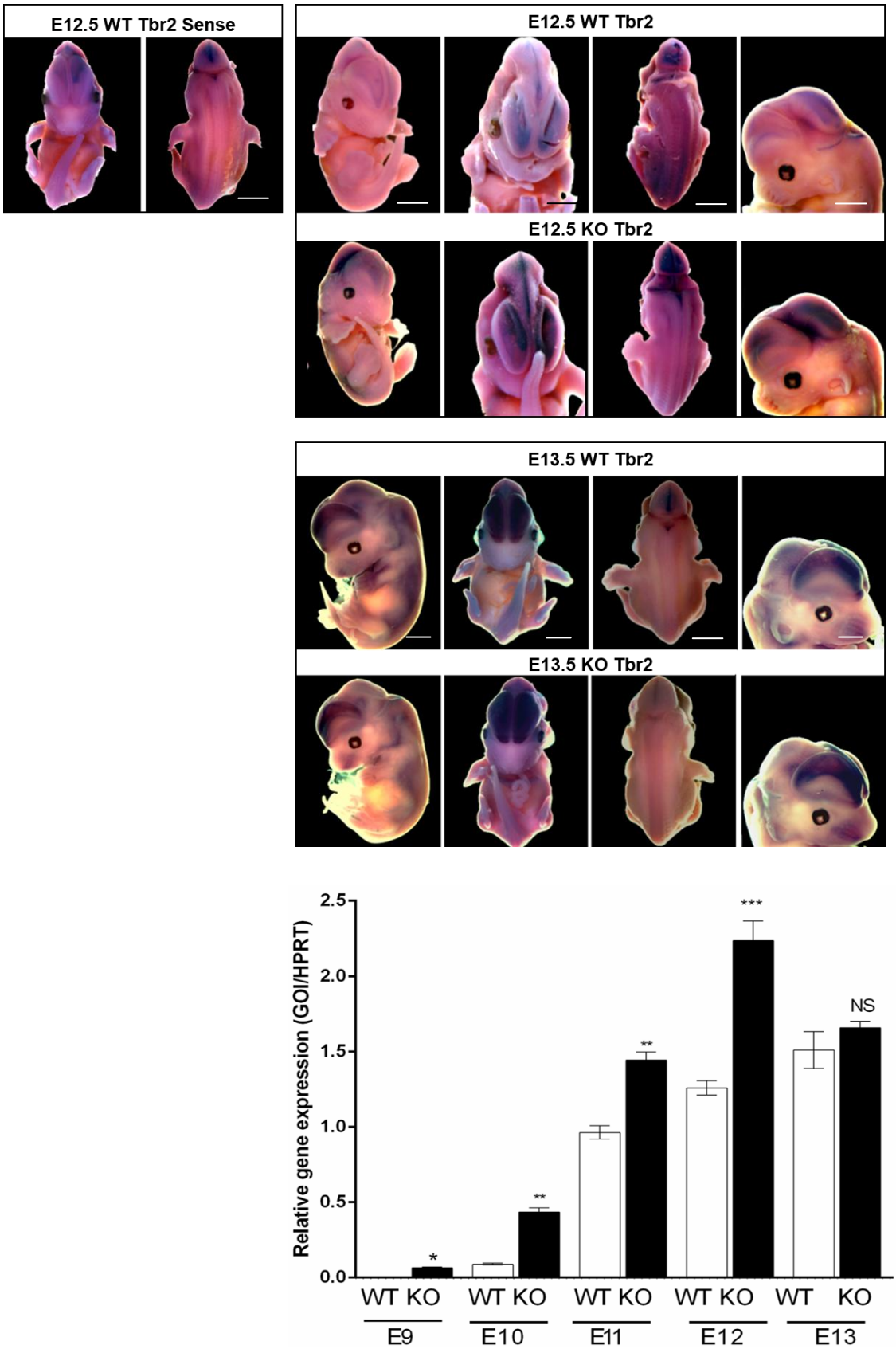
E12.5 WT Tbr2 Sense
E12.5 WT Tbr2
E12.5 KO Tbr2
E13.5 WT Tbr2
E13.5 KO Tbr2
Relative gene expression (GOI/HPRT)
2.5
2.0
1.5
1.0
0.5
0.0
*
**
**
***
NS
WT KO
WT KO
WT KO
WT KO
WT KO
E9
E10
E11
E12
E13

Figure 7

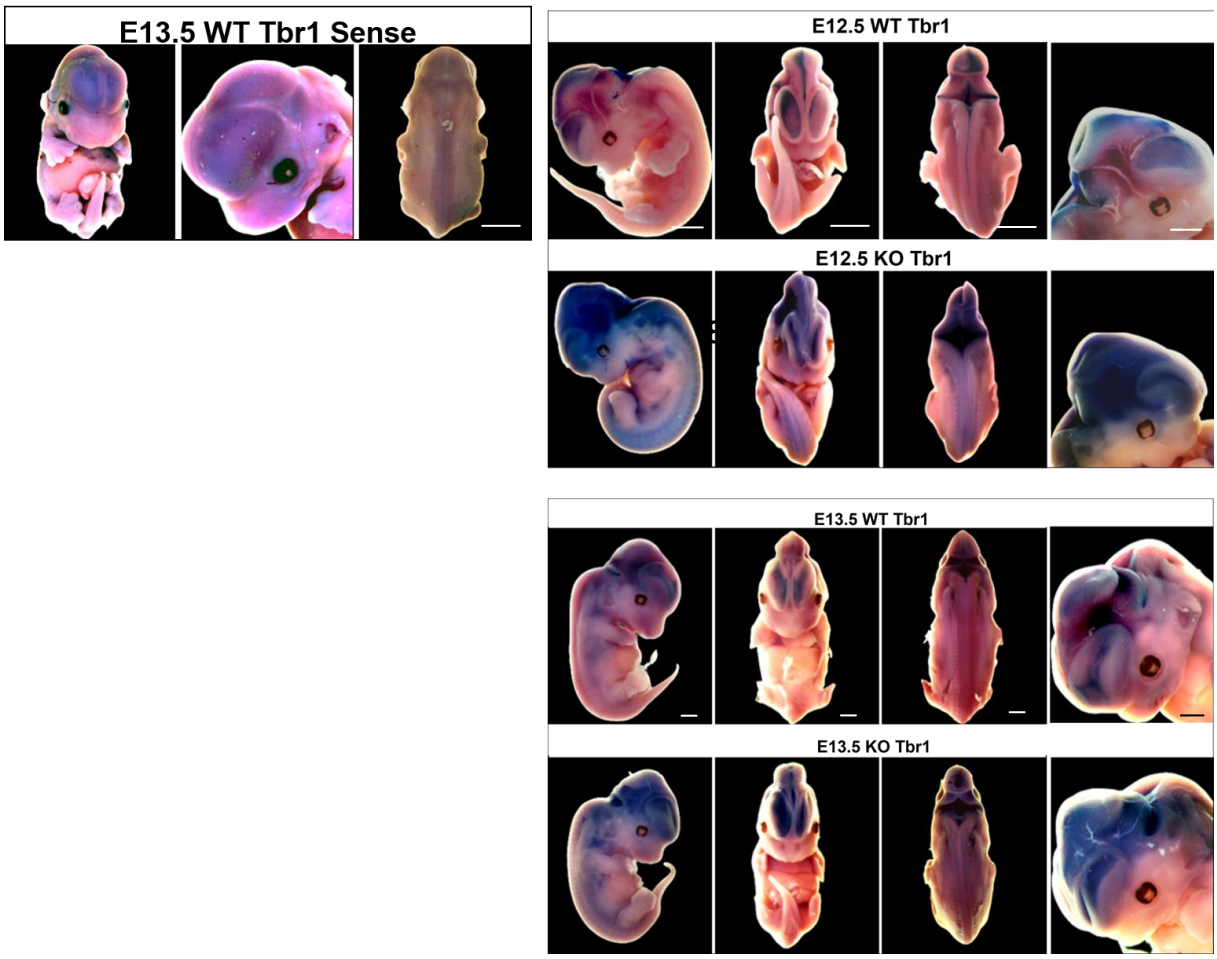
E13.5 WT Tbr1 Sense
E12.5 WT Tbr1
E12.5 KO Tbr1
E13.5 WT Tbr1
E13.5 KO Tbr1

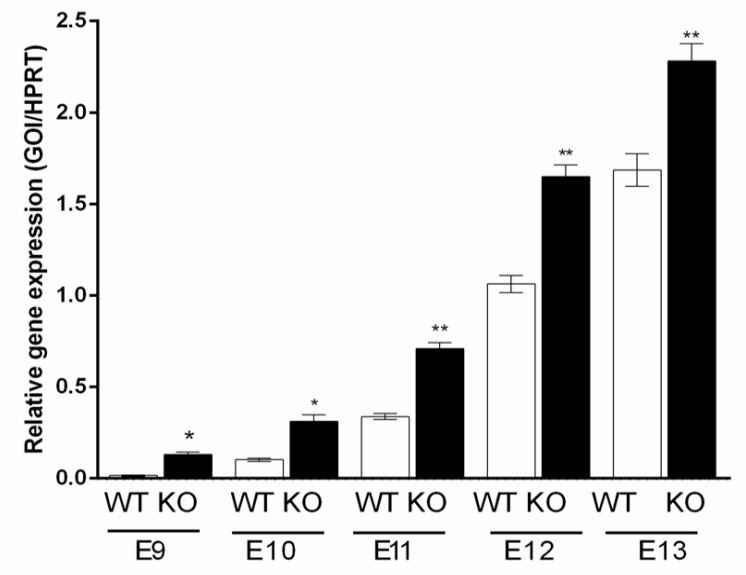
Relative gene expression (GOI/HPRT)
2.5
2.0
1.5
1.0
0.5
0.0
WT KO
WT KO
WT KO
WT KO
WT KO
E9
E10
E11
E12
E13

Figure 8

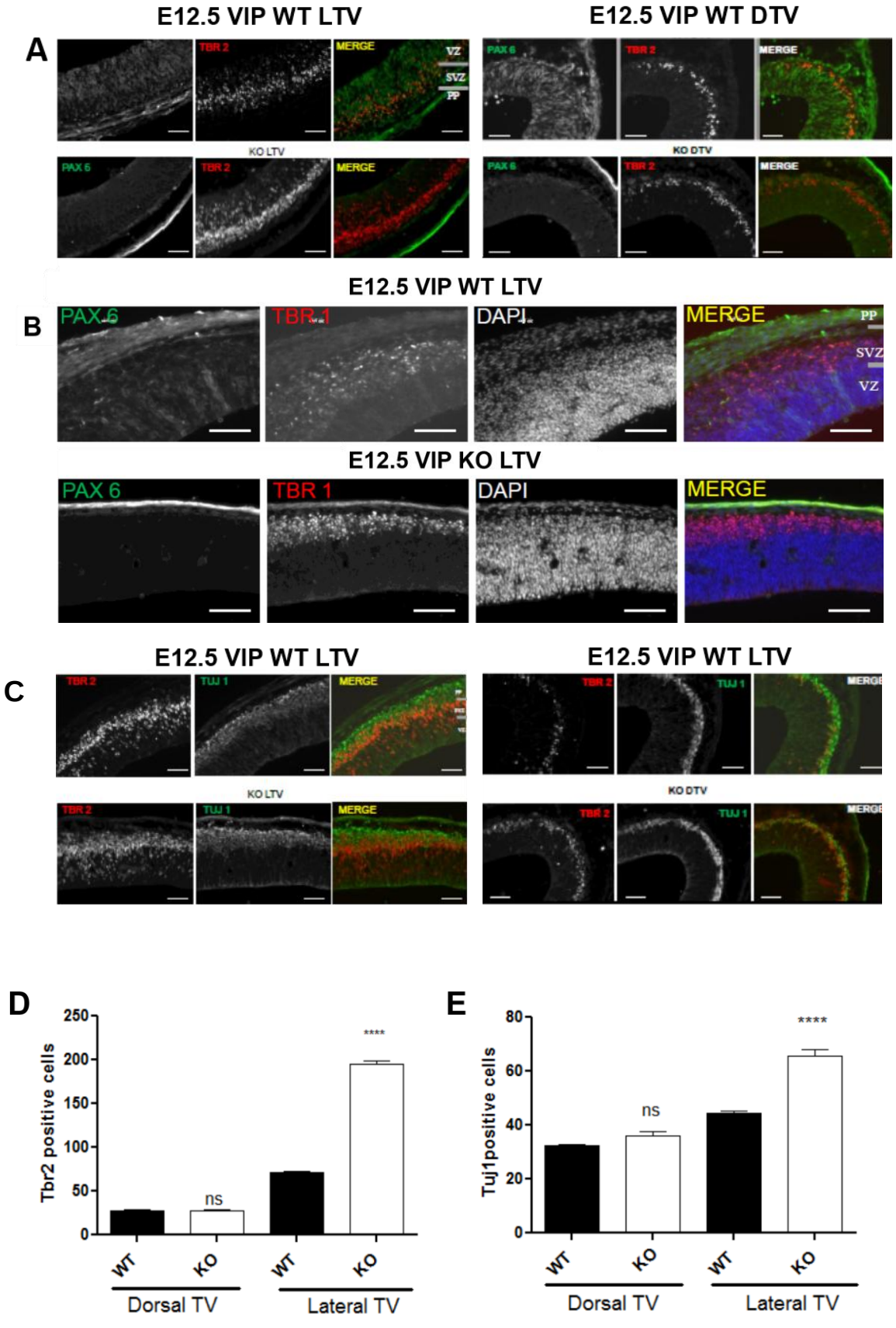
A
E12.5 VIP WT LTV
E12.5 VIP WT DTV
TBR 2
MERGE
VZ
SVZ
PP
PAX 6
KO LTV
KO DTV
B
E12.5 VIP WT LTV
PAX 6
TBR 1
DAPI
MERGE
PP
SVZ
VZ
E12.5 VIP KO LTV
C
E12.5 VIP WT LTV
E12.5 VIP WT LTV
TUJ 1
KO LTV
KO DTV
D
Tbr2 positive cells
250
200
150
100
50
0
****
ns
WT
KO
WT
KO
Dorsal TV
Lateral TV
E
Tuj1positive cells
80
60
40
20
0
****
ns
WT
KO
WT
KO
Dorsal TV
Lateral TV

Figure 9

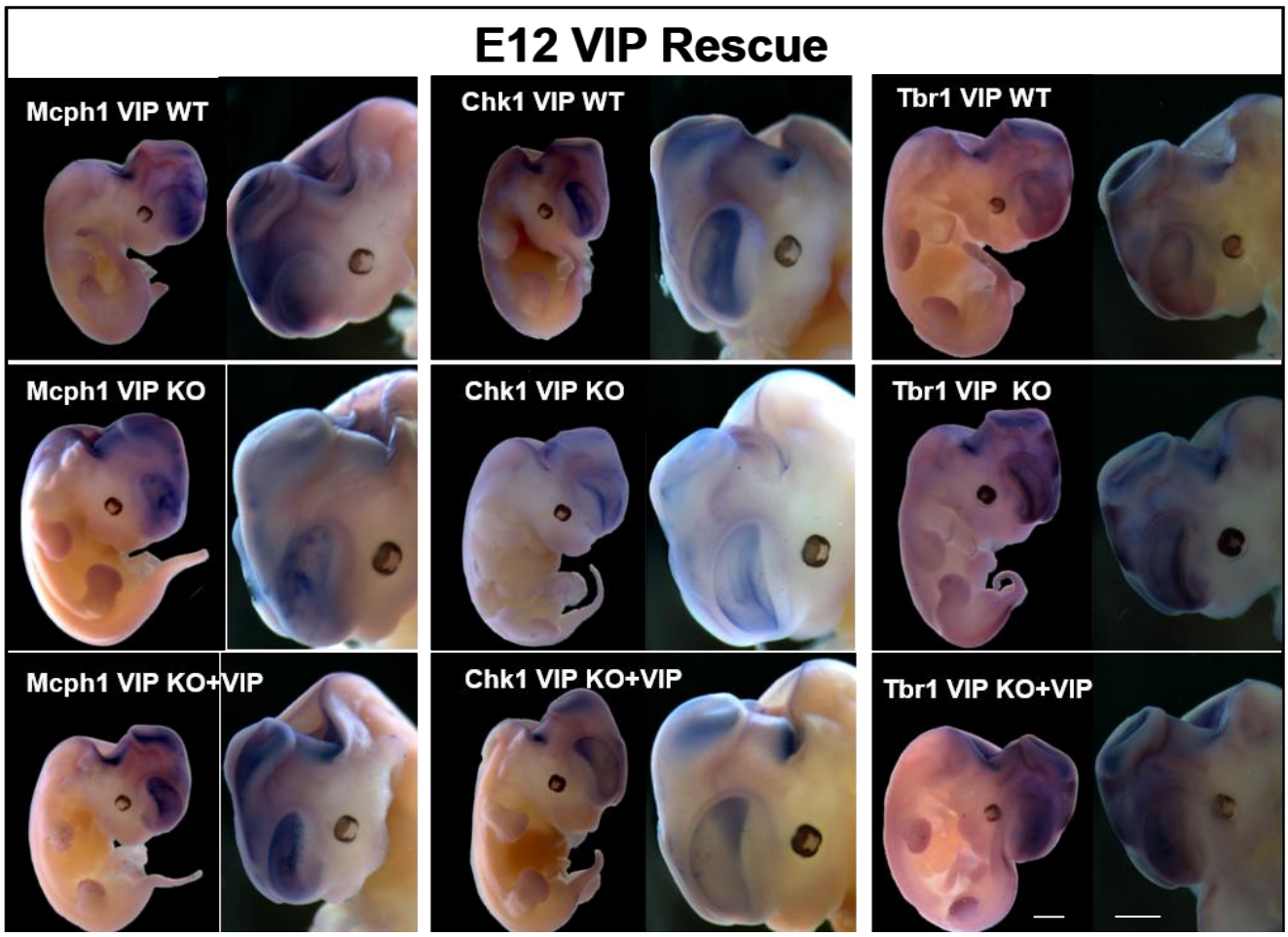
E12 VIP Rescue
Mcph1 VIP WT
Chk1 VIP WT
Tbr1 VIP WT
Mcph1 VIP KO
Chk1 VIP KO
Tbr1 VIP KO
Mcph1 VIP KO+VIP
Chk1 VIP KO+VIP
Tbr1 VIP KO+VIP

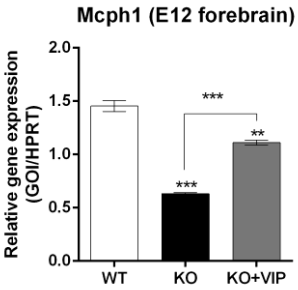
Mcph1 (E12 forebrain)
Relative gene expression (GOI/HPRT)
2.0
1.5
1.0
0.5
0.0
***
**
***
WT
KO
KO+VIP

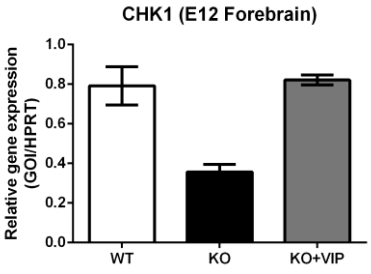
CHK1 (E12 Forebrain)
Relative gene expression (GOI/HPRT)
1.0
0.8
0.6
0.4
0.2
0.0
WT
KO
KO+VIP

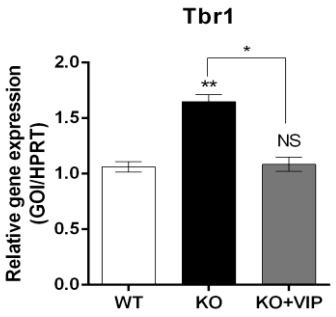
Tbr1
Relative gene expression (GOI/HPRT)
2.0
1.5
1.0
0.5
0.0
*
**
NS
WT
KO
KO+VIP

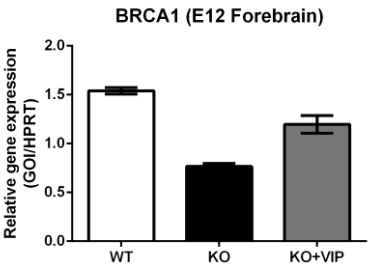
BRCA1 (E12 Forebrain)
Relative gene expression (GOI/HPRT)
2.0
1.5
1.0
0.5
0.0
WT
KO
KO+VIP

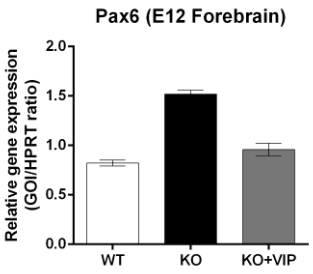
Pax6 (E12 Forebrain)
Relative gene expression (GOI/HPRT ratio)
2.0
1.5
1.0
0.5
0.0
WT
KO
KO+VIP

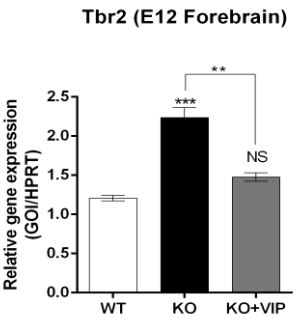
Tbr2 (E12 Forebrain)
Relative gene expression (GOI/HPRT)
2.5
2.0
1.5
1.0
0.5
0.0
**
***
NS
WT
KO
KO+VIP

Figure 10

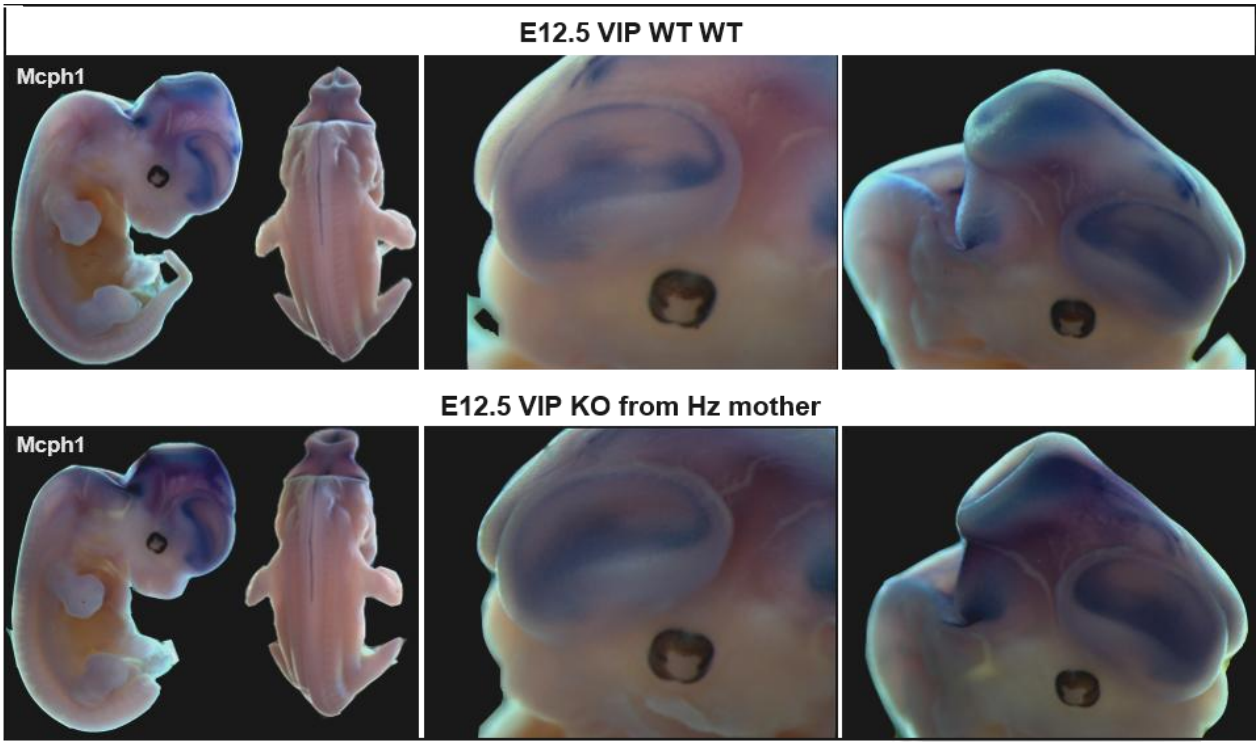
E12.5 VIP WT WT
Mcph1
E12.5 VIP KO from Hz mother
Mcph1

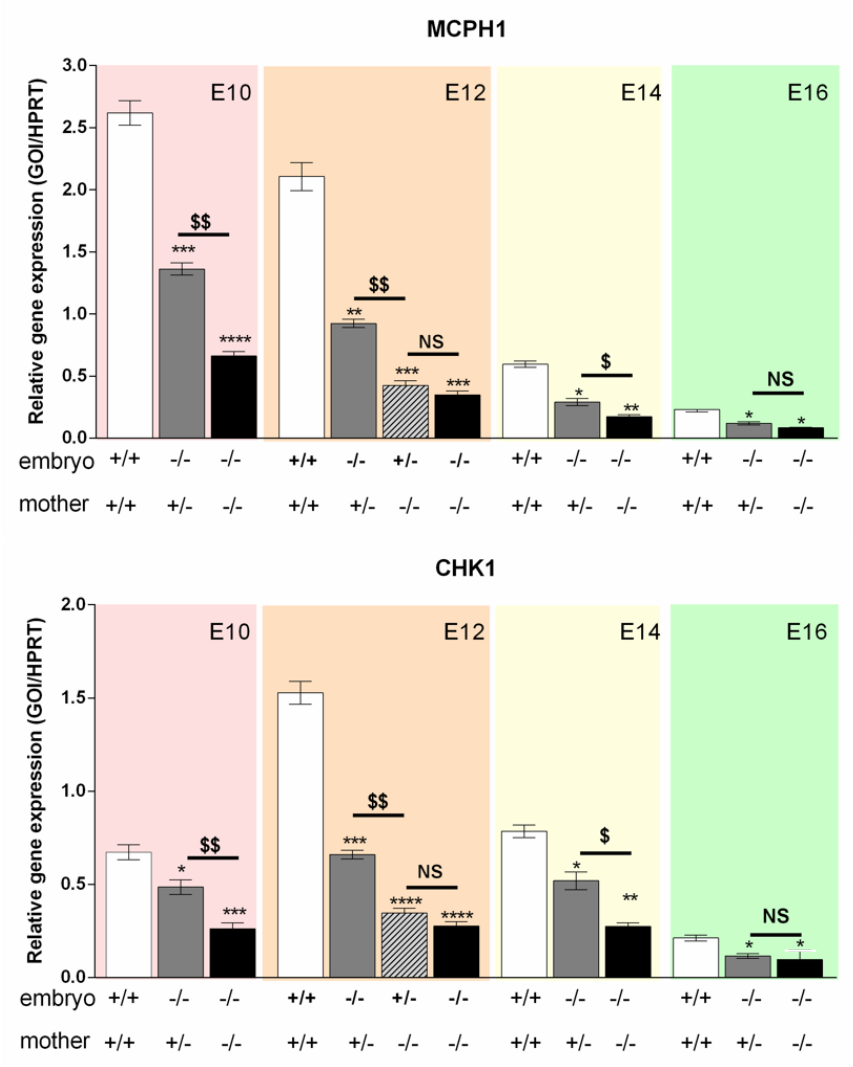
MCPH1
Relative gene expression (GOI/HPRT)
E10
E12
E14
E16
embryo +/+ -/- -/- +/+ -/- +/- -/- +/+ -/- -/- +/+ -/- -/-
mother +/+ +/- -/- +/+ +/- -/- -/- +/+ +/- -/- +/+ +/- -/-
CHK1
Relative gene expression (GOI/HPRT)
E10
E12
E14
E16
embryo +/+ -/- -/- +/+ -/- +/- -/- +/+ -/- -/- +/+ -/- -/-
mother +/+ +/- -/- +/+ +/- -/- -/- +/+ +/- -/- +/+ +/- -/-

Figure 11

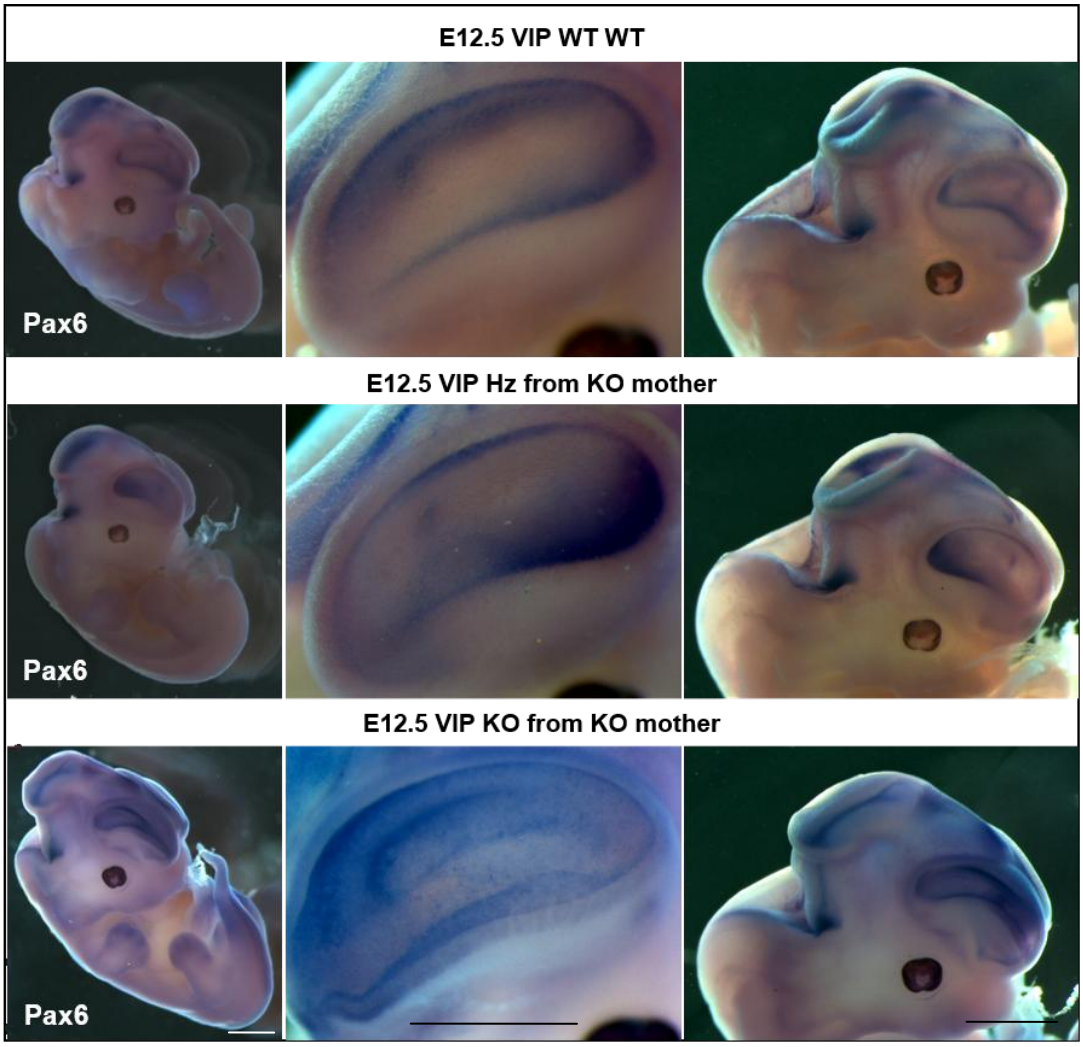
E12.5 VIP WT WT
Pax6
E12.5 VIP Hz from KO mother
Pax6
E12.5 VIP KO from KO mother
Pax6

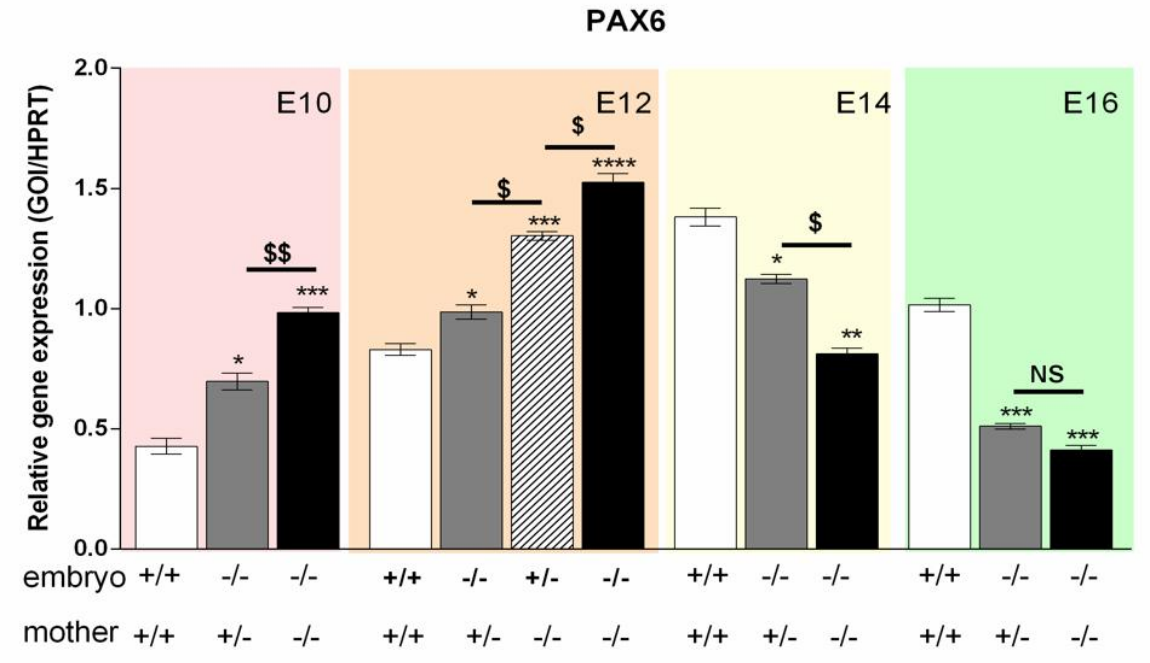
PAX6
Relative gene expression (GOI/HPRT)
2.0
1.5
1.0
0.5
0.0
E10
E12
E14
E16
$$
$
$
$
NS
*
*
*
**
***
***
***
****
embryo +/+ -/- -/- +/+ -/- +/- -/- +/+ -/- -/- +/+ -/- -/-
mother +/+ +/- -/- +/+ +/- -/- -/- +/+ +/- -/- +/+ +/- -/-

Figure 12

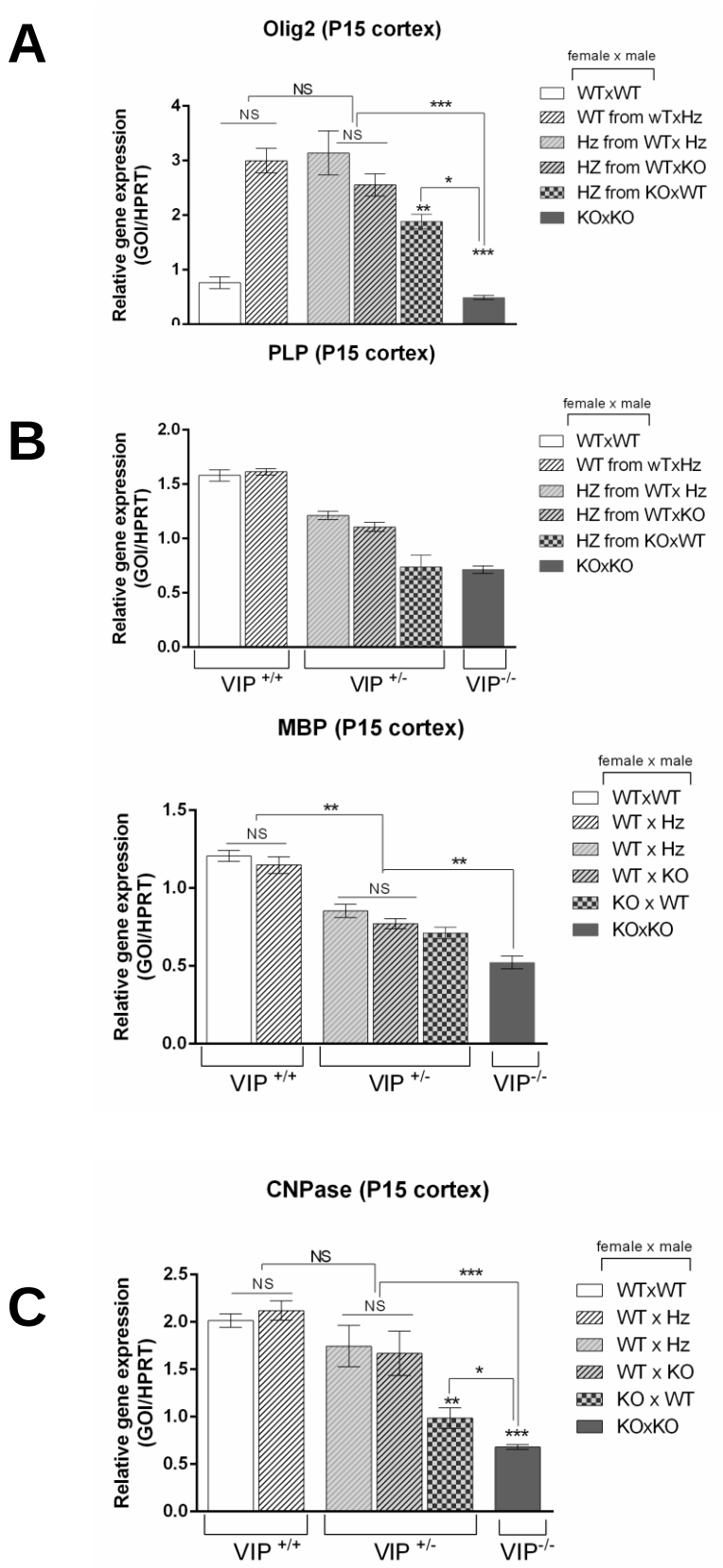
A
Olig2 (P15 cortex)
Relative gene expression (GOI/HPRT)
female x male
WTxWT
WT from wTxHz
Hz from WTx Hz
HZ from WTxKO
HZ from KOxWT
KOxKO
NS
NS
NS
***
*
**
***
B
PLP (P15 cortex)
Relative gene expression (GOI/HPRT)
female x male
WTxWT
WT from wTxHz
HZ from WTx Hz
HZ from WTxKO
HZ from KOxWT
KOxKO
VIP +/+
VIP +/-
VIP-/-
MBP (P15 cortex)
Relative gene expression (GOI/HPRT)
female x male
WTxWT
WT x Hz
WT x Hz
WT x KO
KO x WT
KOxKO
NS
**
NS
**
VIP +/+
VIP +/-
VIP-/-
C
CNPase (P15 cortex)
Relative gene expression (GOI/HPRT)
female x male
WTxWT
WT x Hz
WT x Hz
WT x KO
KO x WT
KOxKO
NS
NS
NS
***
*
**
***
VIP +/+
VIP +/-
VIP-/-

Figure 13

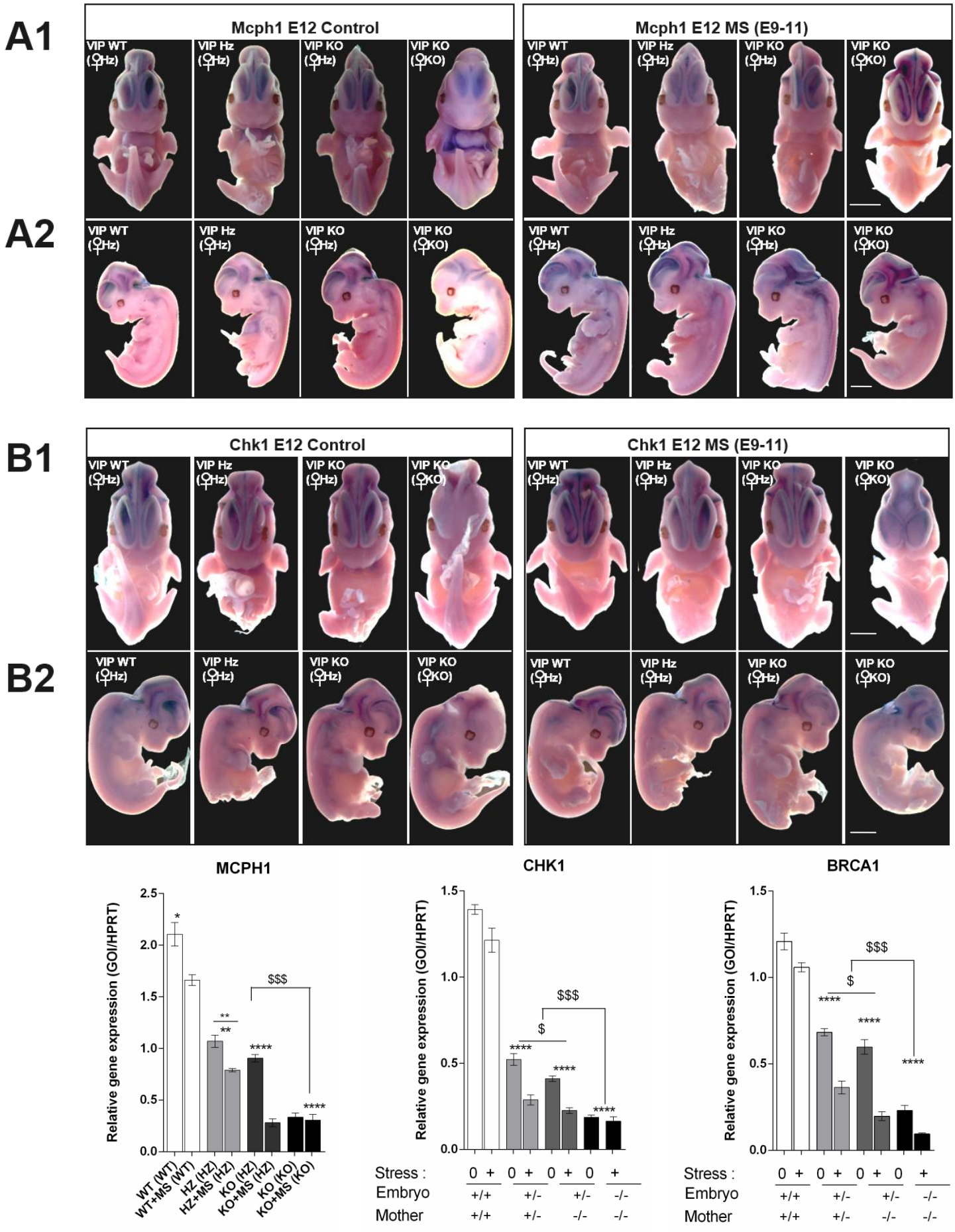
A1
A2
B1
B2
Mcph1 E12 Control
Mcph1 E12 MS (E9-11)
Chk1 E12 Control
Chk1 E12 MS (E9-11)
VIP WT (♀Hz)
VIP Hz (♀Hz)
VIP KO (♀Hz)
VIP KO (♀KO)
MCPH1
CHK1
BRCA1
Relative gene expression (GOI/HPRT)
WT (WT)
WT+MS (WT)
HZ (HZ)
HZ+MS (HZ)
KO (HZ)
KO+MS (HZ)
KO (KO)
KO+MS (KO)
Stress :
Embryo
Mother
+/+
+/-
-/-

Figure 14

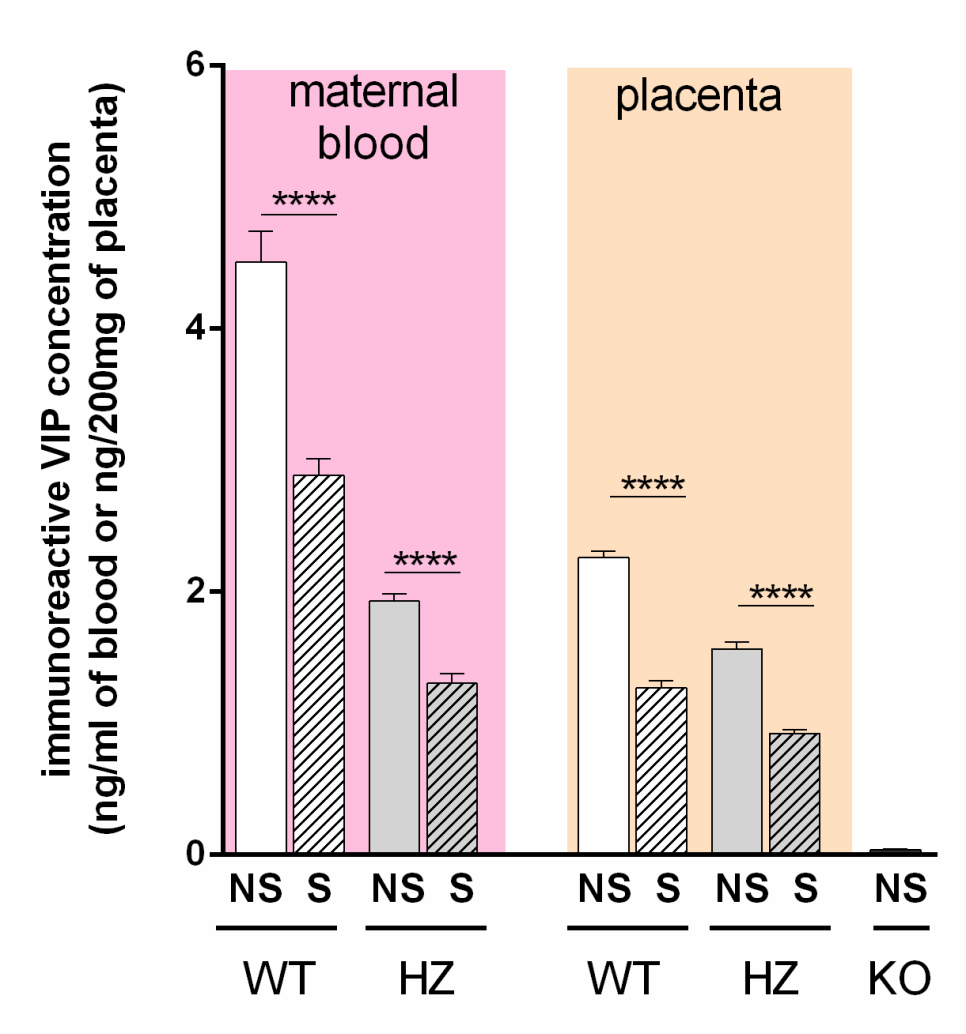
immunoreactive VIP concentration
(ng/ml of blood or ng/200mg of placenta)
6
4
2
0
maternal
blood
placenta
****
****
****
****
NS S NS S NS S NS S NS
WT HZ WT HZ KO

Figure 15

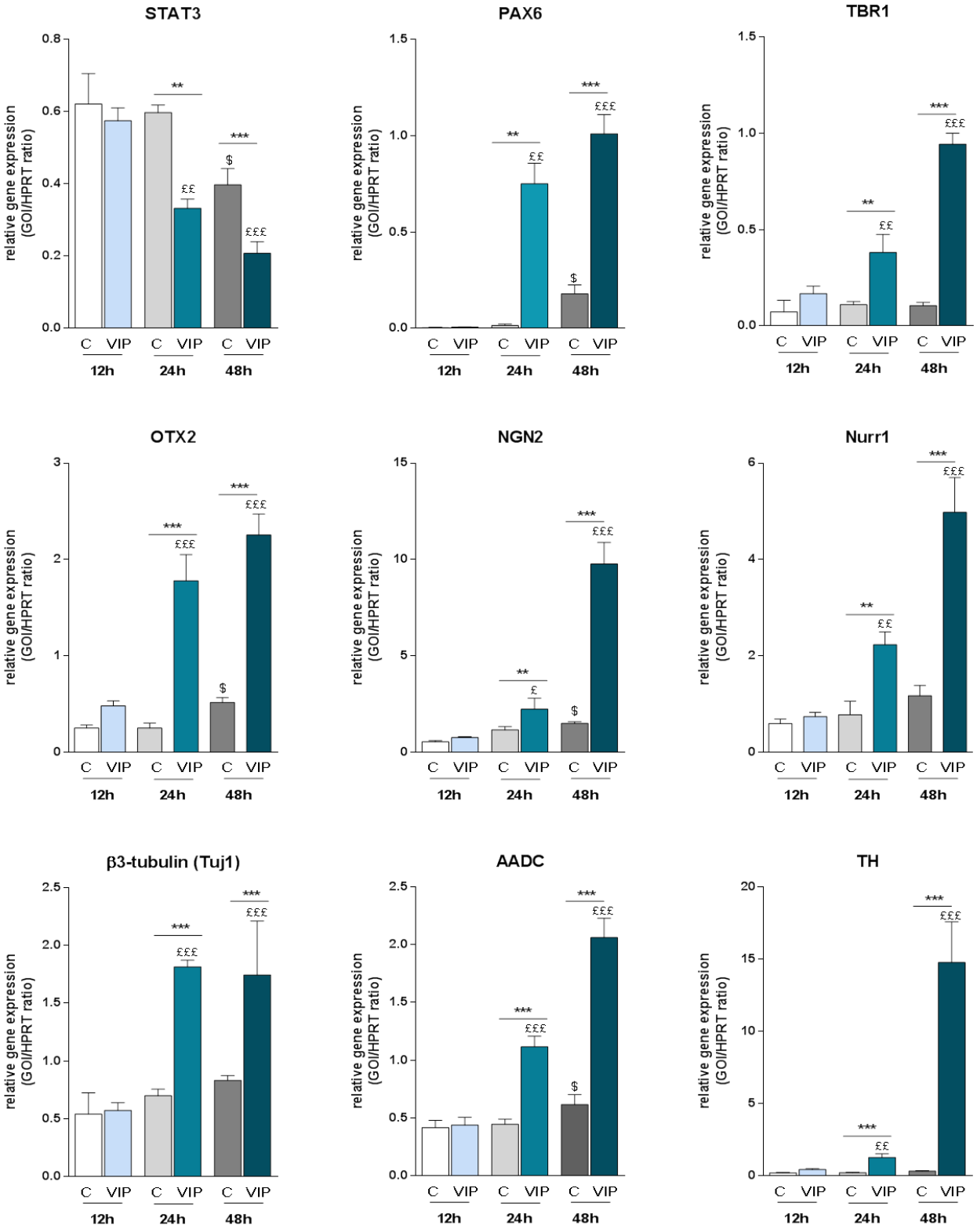
STAT3
PAX6
TBR1
OTX2
NGN2
Nurr1
β3-tubulin (Tuj1)
AADC
TH
relative gene expression (GOI/HPRT ratio)
C VIP C VIP C VIP
12h 24h 48h

Figure 16A

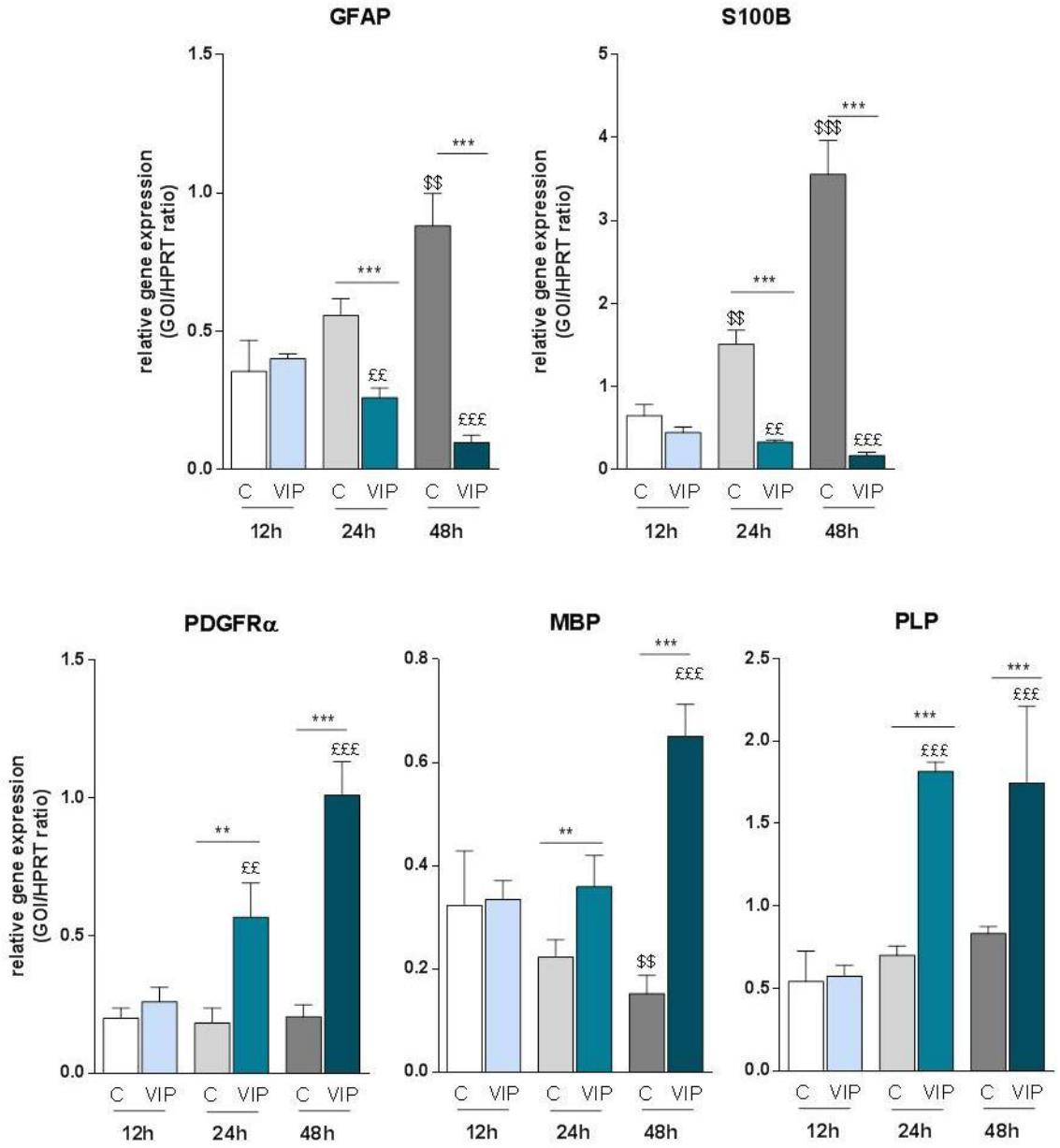
GFAP
S100B
PDGFRα
MBP
PLP
relative gene expression
(GOI/HPRT ratio)
C VIP C VIP C VIP
12h 24h 48h
***
**
$$
$$$
£
££
£££

Figure 16B

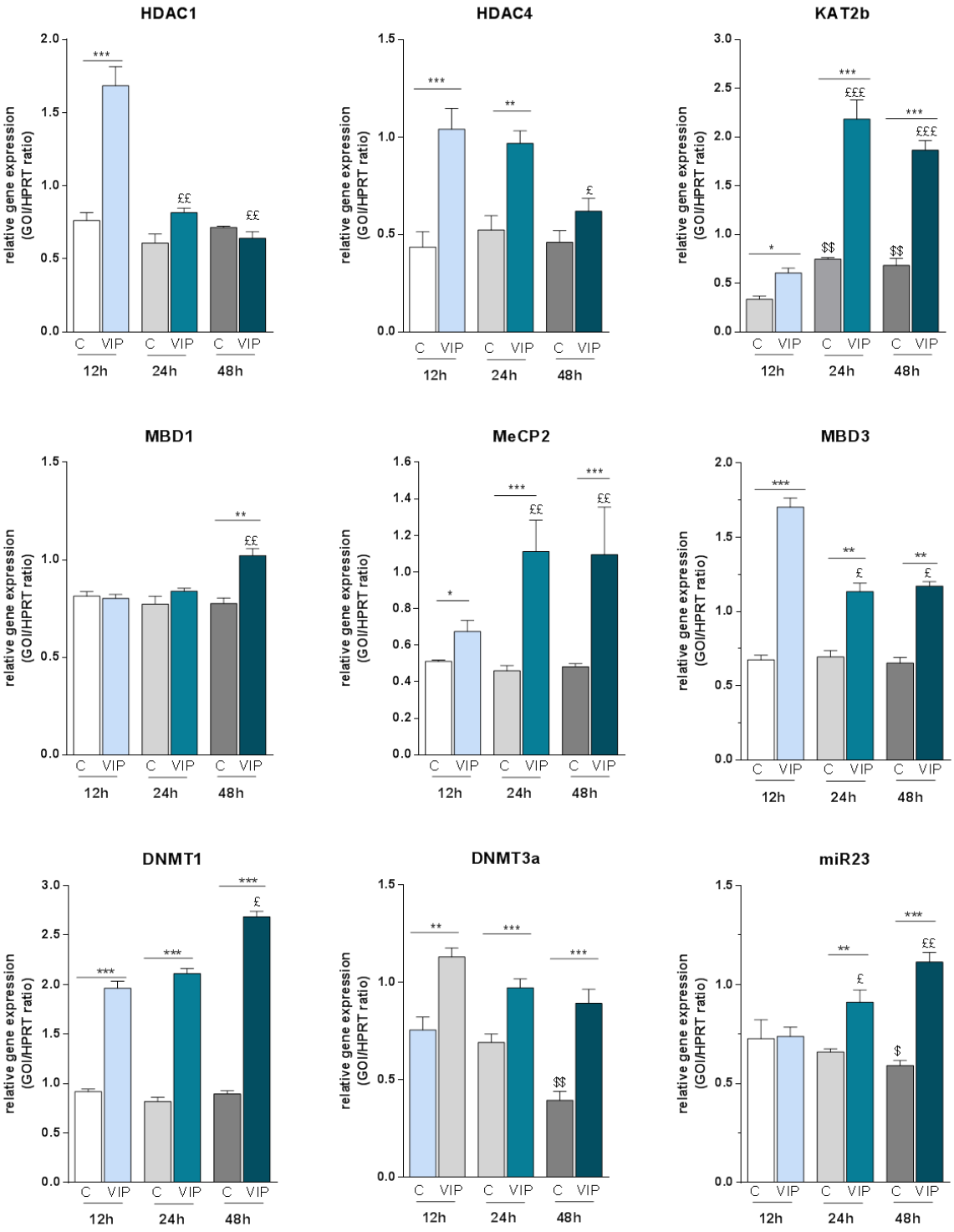
HDAC1
HDAC4
KAT2b
MBD1
MeCP2
MBD3
DNMT1
DNMT3a
miR23
relative gene expression (GOI/HPRT ratio)
C VIP
12h
24h
48h

Figure 16C

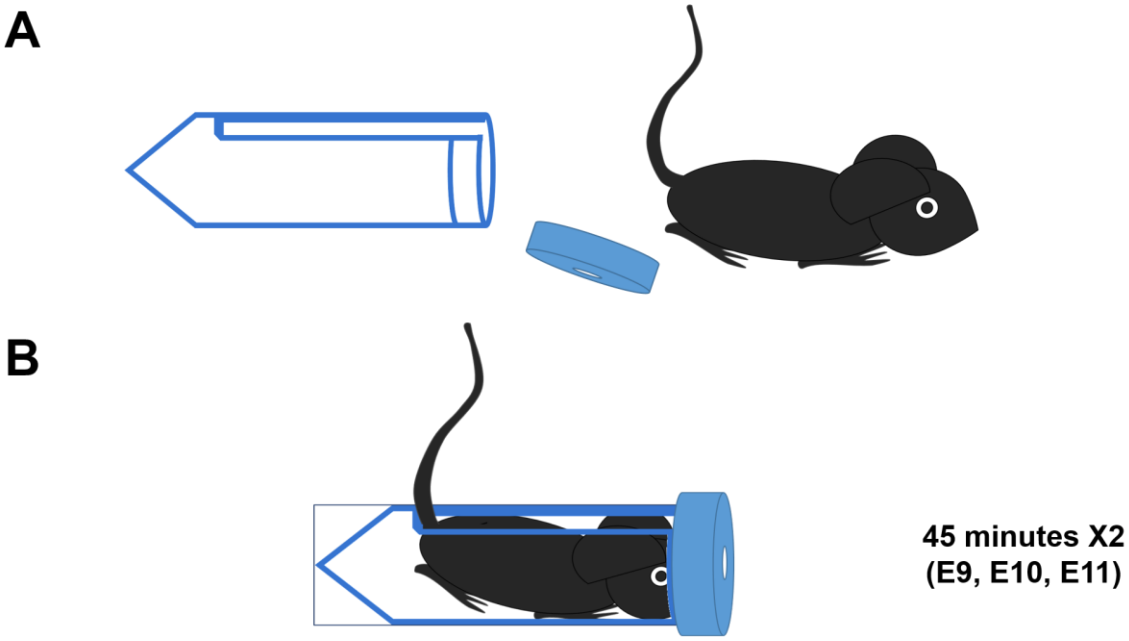

Supplementary Figure 1

Figure Legends

Figure 1: Morphometric analysis of P15 and 4 month old mice and age-matched knockout mice

A: Brain perimeter is significantly reduced in P15 VIP knockout brains, compared to age-matched wildtypes (n=5, Mann-Whitney test, p=0.0093). No significant differences observed when comparing adult brains. Scale bar : 2000 µm.

B and C: Ultrastructural analyses performed at low magnification reveal a significant reduction in cortical surface measured from the anterior cingulate cortex until the rhinal fissure of coronnaly sectioned and cresyl violet stained 14µm thick slices in P15 (n=5, Mann-Whitney test, p =0,0003) and in adult mice (n=8, Mann-Whitney test, p =0,0062) compared to wildtype (B) and a significant reduction in cortical thickness that is mainly affecting the primary motor cortex (C) at P15 (n=5, Kruskal Wallis and Dunn's multiple comparisons test, p=0,0053) and adulthood (n=5, ANOVA and Holm Sidak's multiple comparisons test, p =0,0382). Scale bar : 2000 µm.

D: Ultrastructural analyses performed at high magnification of coronally sectioned cresyl violet cortical slices (Cresyl violet stained) reveal a significant reduction of cortical lamination, specifically at Layer II-IV of P15 (n=5, ANOVA and Holm Sidak's multiple comparisons test, p=0,0016) and adult (n=4, Mann-Whitney test, p =0,0159) knockout primary somatosensory cortex . Scale bar : 200 µm.

Figure 2: Corpus callosal thickness of P15 and 4 month old mice is significantly reduced in P15 and 4 month old knockout brains

Thickness of the corpus callosum was measured at Bregma 0.98 in adults and the corresponding relative stereotaxic location in P15 brains and found to be significantly reduced both in pups (n=5, Mann-Whitney test, p =0,0317) and adults (n=5, Mann-Whitney test, p =0,0061). Scale bar: 2000 µm (top) and 500 µm (magnification).

Figure 3: *Mcph1* is the only identified microcephaly gene that is significantly downregulated in the neural tube of VIP knockout mouse embryos, along with its downstream target *Brca1* which is significantly downregulated in the developing forebrain

A (Photomicrograph): Whole mount in situ hybridization performed at E10 and E12 using PCR-generated antisense digoxigenin-labeled riboprobes spanning 688 base

pairs of the mouse Mcph1 coding sequence. Left panel: Sense probe tested on E10 embryos showed no distribution of digoxigenin labelling and verified high specificity hybridization of the Mcph1 antisense probe. Digoxigenin labeled probe was revealed with NBT/BCIP chromogenic revelation (Roche). Mcph1 labelling is reduced in the neural tubes of E10 (n=3) and E12 (n=4) knockout embryos, with the most severe reduction observed in the forebrains. Scale bars: 500 µm (E10 embryos) or 2000 µm (E12 embryos).

Lower panel: Quantitative RT-PCR was performed on RNA samples extracted from isolated wildtype and knockout forebrains. This result revealed an overall relative *Mcph1* gene expression from E9 to E16, which was significantly reduced from E9 until E16 in the forebrains of VIP knockout embryos

B: *Brca1* expression was also dowregulated in the forebrains of wildtype embryos, compared to widltypes from E9 to E14. Various other microcephaly genes were measured to evaluate whether the loss of VIP would affect their gene expression (*data not shown)*. Quantitavie RT-PCR revealed no significant differences in *Aspm (Mcph5)* expression. *Stil (Mcph7)* and the centrosomal gene *Pcnt* were both downregulated in VIP knockout forebrains at E12.

(n=6/group, ANOVA ad Bonferroni post test, $p<0.05$*, $p<0.01$**, $p<0.001$***, $p<0.0001$****).

Figure 4: *Chk1*, the downstream target for MCHP1 signaling, is downregulated throughout the neural tube in mouse embryos and specifically downrgulated in forebrains from E9 to E14

Photomicrographs: Chromogenic revelation of the *Chk*1 antisense digoxigenin-labeled riboprobes spanning 688 base pairs shows the localization of *Chk1* gene expression in E10 (n=2) and E12 (n=4) embryos. Left panel: The sense riboprobe verifies the high specificity hybridization of the *Chk1* antisense probe due to a lack of digoxigenin labelling.

Chk1 is downregulated througout the telencephalic vesicles of E10 knockout embryos (n=2). At E12, *Chk1* expression is dowregulated throught the fore- and midbrain of knockout embryos. Scale bars: 500 µm (E10 embryos) or 2000 µm (E12 embryos).

Lower panel: *Chk1* expression is downregulated specifically in the forebrains of knockout embryos from E9 to E14 as shown with quatitative RT-PCR (n=6/group, ANOVA ad Bonferroni post test, p<0.05*, p<0.01**, p<0.0001****).

Figure 5: *Vpac1* is expressed solely in the developing mouse embryo from E9 to E12 and is downregulated in the absence of VIP, whereas *Vpac2* and *Pacap* gene expression remain unchanged

A (Photomicrographs): *Vpac1* riboprobe spans 629 base pairs and is hybridizes with high specificity. The sense riboprobe labeling is not visible in E10 embryos (Left panel). Right panel: *Vpac1* labeling is initially restricted to the early forebrain at E9 (n=2), then localized throughout the neural tube at E10 (n=3) and E12 (n=4). This is grossly reduced at E9 and E10 in knockout embryos. Scale bars: 500 µm (E9 and E10 embryos) or 2000 µm (E12 embryos).

Lower panel: Quantitative RT-PCR confirmed the downregulation of *Vpac1* gene expression in E9 and E10 forebrains (n=6/group, ANOVA ad Bonferroni post test, p<0.05*, p<0.01**, p<0.001***). No significant differences were found in E12 forebrains.

B: *Vpac2* and *Pacap* are mainly expressed in wildtype forebrains at E10, increasing at E12, although no significant differences were observed when compared to knockouts (n=6/group, ANOVA, p<0.05).

Figure 6: *Pax6* is prematurely upregulated in VIP knockout embryos

Photomicrograph: (Left panel) The ribroprobe for *Pax6* spans 733 base pairs and was verified to hybridize with high specificity on E12 embryos exhibiting mininimal background staining. *Pax6* was localized during earlier gestational periods in knockout embryos than in wildtypes, exhibiting strong labelling in the fore- and midbrain of E9 (n=2) and E10 (n=4) embryos. *Pax6* labelling was also more pronounced along the spine and surrounding the optic vesicle of E10 knockout embryos. At E12.5, *Pax6* labelling was still more pronounced throughout the neural tube (n=4), lasting until E13 (n=2). Scale bars: 2000 µm.

Lower panel: *Pax6* gene expression was quantified with quantitative RT-PCR and found to be prematurely upregulated at E9, remaining significantly higher at E10 until E12 in knockout embryos . RNA samples were extracted from forebrains isolated from E9 to E13 wildtype and knockout embryos. There were no significant differences

between wildtype and knockouts at E13 (n=6/group, ANOVA and Bonferroni post test, p<0.05*, p<0.001***).

Figure 7: Early expression of *Tbr2* localized throughout the neural tube of E12 VIP knockout embryos

Photomicrograph: (Left panel) The *Tbr2* riboprobe (685 base pairs) hybridizes with high specificity as demonstrated by very low background labelling of the sense riboprobe. (Right panel) *Tbr2* labelling was much higher in the neural tubes of knockout E12.5 (n=5) embryos compared to wildtypes. There were no remarkable differences at E13.5 (n=2). Scale bars: 2000 µm.

Lower panel: Quantitative RT-PCR demostrated that *Tbr2* was expressed as early as E9 in knockout forebrains. The expression continued to increase and was significantly higher from E10 until E12 in the knockouts compared to wildtype forebrains. As predicted by the above-mentioned whole mount *in situ* hybridization results, there were no significant differences at E13 (n=6/group, ANOVA ad Bonferroni post test, p<0.05*, p<0.01**, p<0.001***).

Figure 8: Early expression of *Tbr1* localized throughout the neural tube of E12 VIP knockout embryos

Photomicrograph: (Left panel) The *Tbr1* probe (672 base pairs) was verified for specificity as the sense probe showed no labelling in E13.5 embryos. Right panel: *Tbr1* showed a very high amount of staining that was more pronounced, spanning the whole neural tube, including the full length of the spine, of E12.5 knockout embryos in comparison with age-matched wildtypes (n=6). This strong labelling was still very pronounced in the neural tube of knockout E13.5 embryos compared to age-matched wildtypes (n=4). Scale bars: 2000 µm.

Lower panel: Quantitative RT-PCR demostrated that *Tbr1* was expressed as early as E9 in knockout forebrains. The expression continued to increase and was significantly higher until E13 in the knockouts compared to wildtype forebrains. (n=6/group, ANOVA ad Bonferroni post test, p<0.05*, p<0.01**).

Figure 9: Loss of VIP triggers early expression of neural differentiation markers Tbr2, Tbr1 and Tuj1 in th lateral telencephalic vesicles of E12.5 knockout embryos

A: Immunofluoresecence labelling of Pax6 and Tbr2 on saggital sections through the lateral telencephalic vesicles of E12.5 brains showed an early increase of Tbr2-positive cells widely dispersed along the ventricular and subventricular zone in knockouts, whereas the ventricular zone was mainly populated by Pax6-positive cells and Tbr2-positive are only localized in the subventricular zone in wildtypes. In the dorsal telencephalic vesicles, Tbr2 staining resembles that of the wildtype (Scale bar=50 µm).

B: Immunofluorescence staining for Pax6 and Tbr1 on saggital sections through the lateral telencephalic vesicles of E12.5 brains showed an increased Tbr1 staining in the cortical plate region of knockouts which was othewise faint and restricted to the subventricular zone in wildtypes (Scale bar=50 µm).

C: Immunofluorescence staining for Tbr2 and TuJ1 on saggital sections through the lateral telencephalic vesicles of E12.5 brains demonstrated early Tbr2 expression as previously shown (A) and premature expression of TuJ1 staining at the subventricular zone (radial like process) of lateral telencephalic vesicles in knockouts, whereas Tuj1-positive cells were restricted to the preplate in wildtype sectios (Scale bar=50 µm

D and E: Cell count of Tbr2-positive cells (D) and Tuj1-positive cells (E) were significantly higher in knockout telencephalic vesicles than in wildtypes. Equal cell counts were found in wildtype and knockout dorsal telencephalic vesicles (n=7/group, ANOVA and Bonferonni post test, $p<0.0001$****).

Figure 10: VIP adminstration to pregnant knockout females, during the peak of neurogenesis (E9-11) rescues Mcph1, Chk1 and Tbr1 forebrain expression

A (Photomicrographs): Whole mount *in situ* hybridization with antisense riboprobes for *Mcph1* and *Chk1* show a downregulation of these genes in E12 embryos, which is rescued followig intra-peritoneal injections of VIP during E9, E10 and E11 to pregnant knockout females. *Mpch1* and *Chk1* labelling in knockout embryos resembles that found in age-matched wildtype embryos, specifically withing the forebrain. The antisense riboprobe for *Tbr1* also showed that *Tbr1* expression resembled that of the wildtype embryos. (n=2/group). Scale bars: 2000 µm.

A (Lower panel): VIP rescue was confirmed and quantified with RT-PCR showing that *Mcph1* and *Chk1* expression in prenatally treated embryos were significantly higher than in naïve knockout embryos. *Tbr1* expression was significantly lower in

prenatally treated embryos, compared to naïve knockout, and exhibited the same relative level of expression as wildtype embryos.

B: *Brca1, Pax6* and *Tbr2* were also assayed with quatitative RT-PCR which demonstrated that their expression in prenatally treated samples was returned to wildtype levels.

All quantifications were performed on forebrains isolated from E12 embryos. (n=6/group, ANOVA ad Bonferroni post test, $p<0.05$*, $p<0.01$**, $p<0.001$***).

Figure 11: *Mcph1* and *Chk1* gene expression are controlled by the maternal genotype of VIP

Top panel: The antisense probe for *Mcph1* (and *Chk1, data not shown)* revealed that knockout embryos from VIP-expressing females exhibit the same localization and distribution of *Mcph1* as can be observed in age-matched (E12) wildtypes. (n=2/group). Scale bars: 2000 µm.

Lower panel: Quantitative RT-PCR demonstrated that indeed *Mcph1* and *Chk1* VIP knockout embryos from heterozygous females were upregulated and significantly higher than knockout embryos obtained from knockout females (n=6/group, ANOVA ad Bonferroni post test, $p<0.05$*, $p<0.01$**, $p<0.001$***, $p<0.001$****, $p<0.05^{\$}$, $p<0.01^{\$\$}$, $p<0.001^{\$\$\$}$).

Figure 12: *Pax6* gene expression is regulated by maternal VIP

Top panel: Whole mount *in situ* hybridization with the antisense riboprobe for *Pax6* demonstrated similar labelling in heterozygous and knockout E12 embryos extracted from knockout females, which was more marked than in wildtype age-matched embryos (n=2/group). Scale bars: 2000 µm.

Lower panel: Although significantly different, relative expression of *Pax6* in heterozygous and knockout embryos (extracted from knockout females) , measured in E12 forebrains, was significantly higher than age-matched wildtypes. Conversely, knockouts from heterozygous females exhibited lower and close to wildtype levels of *Pax6* in E12 embryos (n=6/group, ANOVA and Bonferroni post test, $p<0.05$*, $p<0.01$**, $p<0.001$***, $p<0.001$****, $p<0.05^{\$}$, $p<0.01^{\$\$}$).

Figure 13: Maternal VIP regulates expression of cortical oligodendrocyte differentiation and maturation markers of P15 VIP-deficienct mice

A: *Olig2* expression was upregulated and significanty higher in VIP-deficient P15 offspring ($VIP^{+/-}$ and $VIP^{-/-}$) of VIP-deficient (Hz and KO) mothers, compared to wildtype offspring from homozygous wildtype breeding sets

B: The oligodendrocyte maturation markers, *Plp* and *Mbp* were significantly downregulated in VIP deficient offspring ($VIP^{+/-}$ and $VIP^{-/-}$) of VIP-deficient (Hz and KO) mothers. Offspring of knockout mothers exhibited the lowest expression for cortical *Plp* and *Mbp* whereas wildtype offspring of wildtype females exhibited significantly higher levels.

C: *Cnpase* was significantly downregulated in all VIP deficient ($VIP^{+/-}$ and $VIP^{-/-}$) offspring, compared to wildtype offspring of wildtype mothers. Heterozygous pups obtained from wildtype mothers exhibited no significant difference in *Cnpase* expression, but were significantly more upregulated compared to heterozyous pups of knockout females. Knockout pups from knockout mothers exhibited the lowest expression of *Cnpase.*

All the above results were obtained with quantitative RT-PCR performed on RNA samples derived from the P15 cortex (n=6/group, ANOVA and Bonferroni post test, $p<0.05$*, $p<0.01$**, $p<0.001$***).

Figure 14: Maternal restraint stress downregulates *Mcph1, Brca1* and *Chk1* gene expression, and mimicks VIP knockout expression patterns at E12

A to B2 (Photomicrographs): The antisense riboprobes for *Mcph1* (A1 and A2) and *Chk1*(B1 and B2) demonstrated a marked decrease in gene expression in E12.5 embryos obtained from stressed females, with the lowest labelling observed in embryos from VIP-deficient females. VIP knockout embryos from heterozygous females exhibited very faint labelling for both *Mcph1* and *Chk1,* similarly as knockout embryos from knockout females (n=2/group). Scale bars : 2000 µm.

C: The impact of maternal restraint stress on *Mcph1*, *Brca1* and *Chk1* was quantitaviley demonstrated with quantitative RT-PCR. In forebrains isolated from E12 embryos, prenatal stress significantly downregulated *Mcph1, Brca1* and *Chk1* expression in all the groups except for the wildtypes. Maternal stress significantly downregulated gene expression in all heterozygous embryos regardless of their maternal genotype. *Mcph1, Brca1* and *Chk1* expression in knockout embryos was not significantly different compared to knockout embryos extracted from knockout

females (n=6/group, ANOVA and Bonferroni post test, p<0.05*, p<0.01**, p<0.001***, p<0.001****, p<0.05$, p<0.01$$, p<0.001$$$, p<0.0001$$$$).

Figure 16: VIP promotes differentaition and directs cell specification of neural stem cells through control of epigenetic factors

Neural stem cells isolated from E10 forebrains were treated and incubated with VIP for 12, 24 and 48 hours, afterwhich expression of various markers was measured with quantitative RT-PCR.

A: *Stat3* expression was significantly downregulated after 24 hours of VIP-treatment and decreased further when incubated for 48 hours, whereas early neural differentiation markers *Pax6* and *Tbr1* were markedly and significantly activated after 24 hours and subsequently upregulated after 48 hours. Expression of the neural identity markers, *Otx2, Ngn2, Nurr1* and *Tuj1* was also activated after 24 hours of VIP treatment and significantly upregulated after 48 hours of incubation. Dopaminergic neural lineage markers, *Aadc* and *Th,* were activated and equally expressed after 24 hours, then significantly upregulated after 48 hours of VIP treatment.

B: Untreated (C) neural stem cells expressed astroglial markers after 24 hours, which were upregulated significantly after 48 hours in culture. VIP treatment decreased expression of astroglial markers, *Gfap* and *S100b* and significantly downregulated their expression to less than basal levels after 24 hours of incubation. The expression of the oligodendrocyte progenitor differentiation marker *Pdgfrα* was significantly increased following 24 hours of VIP treatment, continuing to increase significantly after 48 hours of treatment. Expression of the markers for oligodendrocyte maturation, *Mbp* and *Plp,* were also activated after 24 hours of VIP treatment, then significantly upregulated after 48 hours of incubation with VIP.

C: *Hdac1* and *Hdac4* markers for histone deacetylation were immediately upregulated after 12 hours of VIP treatment, then transiently downregulated after 24 and 48 hours of incubation. *Kat2b* expression was activated after 12 hours of treatment then significantly upregulated to it's peak after 24 hours. *Kat2b* expression decreased after 48 hours of treatment. *Mbd1* was upregulated after a longer incubation with VIP (48 hours), whereas *Mecp2 and Mbd3* were immediately upregulated following 12 hours of VIP administration. The epigenetic markers for DNA methylation, *Dnmt1* and *Dnmt3a,* were immediately upregulated following 12 hours of incubation with VIP. Although *Dnmt1* expression significantly increased after

24 and 48 hours of VIP treatment, *Dnmt3* decreased between 24 and 48 hours. *miRna23*, the epigenetic marker for gene expression regulation, was significantly increased at 24 and 48 hours of VIP treatment.
(ANOVA and Bonferroni post test, $p<0.05$*, $p<0.01$**, $p<0.001$***, $p<0.05^{\$}$, $p<0.01^{\$\$}$, $p<0.001^{\$\$\$}$, $p<0.05^{£}$, $p<0.01^{££}$, $p<0.001^{£££}$)

Figure 15: Forced restraint induced during E9 to E11 significantly reduced VIP immunoreactivity in maternal plasma and placenta of E12 wildtype and heterozygous females

VIP concentration (immunoreactivity) as measured by enzyme immune assay in maternal blood plasma and placenta was significantly reduced in wildtype females that were subjected to forced restraint during E9 to E11. In addition, maternal plasma and placental VIP immunoreactivity were even more severely reduced in heterozygous females (ANOVA and Bonferroni post test, $p <0.0001$****)

Enzyme immune assay (EIA) protocol

Materials

- Plasma blood and placenta tissue samples
- HCL/ethanol solution
- Vasoactive intestinal peptide (VIP) (Human, rat, mouse, porcine, ovine) EIA KIT (Catalog No. EK-064-16, Phoenix Pharmaceuticals)
    - EIA assay buffer concentrate (20X, 50 mL; Catalog No. EK-BUF)
    - 96 well immunoplate (Catalog No. EK-PLATE)
    - Acetate plate sealer (Catalog No. EK-APS)
    - VIP antibody (rabbit anti-peptide IgG, human, rat, mouse porcine, ovine, 5 mL; Catalog No. EK-RAB-064-16)
    - VIP standard peptide (1µg, 1 mL; Catalog No. EK-S-064-16)
    - Biotinylated VIP (human, rat, mouse porcine, ovine, 5mL; Catalog No. EK-B-064-16)
    - Streptavidin-horseradish peroxidase (SA-HRP, 30µL; Catalog No. EK-SA-HRP)
    - VIP positive control (0.1-0.3 ng/mL, 200 µL; Catalog No. EK-PC-064-16)
    - Substrate solution (TMB, 12mL; Catalog No. EK-SS)
    - 2N HCL (Catalog No. EK-HCL)

EXPERIMENTAL GROUPS

The number of blood and placenta tissue samples distribution per group used is specified in the table below.

Experimental group	**Blood**	**Placenta**
wt x wt (+stress)	n = 3	n = 3
wt x wt (-stress)	n = 4	n = 4
ko x ko (+stress)	n = 1	n = 1
ko x ko (-stress)	n = 1	n = 1
hz x ko (+stress)	n = 4	n = 4
hz x ko (-stress)	n = 7	n = 7

Placental tissue peptide extraction

1) 16 mL of HCL:ethanol (1:7) solution was prepared.
2) 200 mg of each placenta tissue sample was re-suspended in 1 mL of the HCL:ethanol solution.
3) Each sample was homogenized using the Ultraturex instrument and incubated at room temperature for 30 minutes.
4) Each homogenate was centrifuged at 3,000 x g for 30 min at 4°C.
5) 200 µL of the supernatants were transferred into new tubes and evaporated to dryness using the Speedvac apparatus for 3 h.

ENZYME IMMUNE ASSAY

1) 1X assay buffer was prepared by diluting 50 mL 20x assay buffer concentrate in 950 mL DEPC-water.
2) The stock VIP standard peptide solution [1,000 ng/mL] was prepared by centrifuging for 10 seconds and diluting the VIP standard peptide vial in 1 mL 1X assay buffer. The solution was incubated for 10 min at room temperature. The solution was centrifuged and vortex immediately before use.
3) The stock solution was used to prepare standard VIP peptide solutions in labelled tubes 1-5. The standard VIP peptide solutions was prepared as detailed in the table below:

Table showing volumes used to prepare the standard peptide solutions

Standard #	Standard volume	1x assay buffer	Concentrations
STOCK	1000 µL	-	1,000 ng/mL
#1	25 µL	975 µL	25 ng/mL
#2	200 µL of #1	800 µL	5 ng/mL

#3	200 µL of #2	800 µL	1 ng/mL
#4	200 µL of #3	800 µL	0.2 ng/mL
#5	200 µL of #4	800 µL	0.04 ng/mL

4) The VIP antibody was rehydrated in 5 mL of 1x assay buffer and incubated for 5 minutes at room temperature before use.
5) The biotinylated VIP peptide was rehydrated in 5 mL of 1x assay buffer and incubated for 5 minutes at room temperature before use.
6) The VIP positive control was rehydrated in 200 µL of 1x assay buffer and incubated for 5 minutes at room temperature before use.
7) The placenta tissue dried extracts were reconstituted to be ready for use by adding 200 µL of 1x assay buffer. The plasma blood samples were diluted in 1x assay buffer (1:10) before use.
8) The 96-immunowell plate was filled following the guidelines specified in the following steps.
9) The wells A1 and A2 were left empty as blanks.
10) 50 µL of 1x assay buffer was added into wells B1 and B2 as total binding
11) 50 µL of prepared peptide standards from #5 to #1 were added into wells from C -1 and C – 2 to G – 1 and G -2, respectively.
12) 50 µL of rehydrated VIP positive control was added into wells H – 1 and H – 2.
13) 50 µL of prepared samples were added into their designated wells in duplicate
14) 25 µL of rehydrated VIP antibody was added into each well except the blank wells.
15) 25 µL of rehydrated biotinylated VIP solution was added into each well except the blank wells.
16) The immunoplate was sealed with acetate plate sealer and incubated for 2 hours at room temperature on orbital shaker at 350 rpm.
17) The SA-HRP solution was prepared by centrifuging 30µL SA-HRP vial at 5000 rpm for 5 seconds and diluting 12 µL into 12 mL of 1X assay buffer and vortex.
18) The acetate plate sealer was removed from the immunoplate and the contents in the wells were discarded.
19) Using a multichannel pipette, each well was washed and blot dried with 350 µL of 1x assay buffer. This step was repeated 4 times.
20) 100 µL of SA-HRP solution was added into each well.

21) The immunoplate was resealed with the acetate plate seal and incubated for 1 hour at room temperature over orbital shaker at 350 rpm.
22) The acetate plate sealer was removed from the immunoplate and the contents in the wells were discarded.
23) Using a multichannel pipette, each well was washed and blot dried with 350 µL of 1x assay buffer. This step was repeated 4 times.
24) 100 µL of TMB substrate solution was added to each well. The immunoplate was resealed with the acetate plate sealer and incubated for 20 minutes at room temperature over orbital shaker at 350 rpm in a dark chamber.
25) The acetate plate sealer was removed. 100 µL 2N HCL was added into each well to stop the reaction. The colour in each well changed from blue to yellow.
26) Immediately, the immunoplate was loaded onto a microtiter plate reader and the absorbance was read at 450 nm optical density.
27) The standard curve was plotted and used to analyse the concentration of VIP in each sample.

Figure Legends for Supplementary Figures

Supplementary Figure 1: Schematic presentation of maternal forced restraint
Pregnant female mice were subjected to forced restraint by tugging them by the tail and firmly forcing them into a closed compartment **(A)**. The closed comparted was ventilated along the length and closing of the centrifuge tube, also allowing mice limited space for free movement **(B)**. Females were restrained at E9, E10 and E11, twice a day, once in the morning and once in the early evening, for 45 minutes per session

Result 2. Publication 3 (submitted): Hyperalgesic VIP-deficient mice exhibit VIP-reversible alterations in molecular and epigenetic determinants of cold and mechanical nociception

Hyperalgesic VIP-deficient mice exhibit VIP-reversible alterations in molecular and epigenetic determinants of cold and mechanical nociception

Tando Maduna[1], Pierre-Eric Juif[1], Naga Praveena Uppari[1], Nathalie Petit Demouliere[1], Adrien Lacaud[1], James A Waschek[2], Pierrick Poisbeau[1] and Vincent Lelievre[1,]

[1] Centre National de la Recherche Scientifique and University of Strasbourg, Institut des Neurosciences Cellulaires et Intégratives (INCI), 5 rue Blaise Pascal, 67084 Strasbourg, France.

[2] Intellectual and Developmental Disabilities Research Center, The David Geffen School of Medicine, University of California, Los Angeles, Semel Institute for Neuroscience and Human Behavior, Neuroscience Research Building, Room 345, 635 Charles E. Young Drive South, Los Angeles, CA 90095-7332, United States.

Corresponding author: Pr Vincent Lelievre, CNRS UPR-3212, Institut des Neurosciences Cellulaires et Intégratives (INCI), Neurochem Blg. 5 rue Blaise Pascal, 67084 Strasbourg, France. Email lelievre@inci-cnrs.unistra.fr, Tel +33 388455966.

keywords: neuropeptide, Vasoactive Intestinal Peptide, receptor signaling, mechanical and thermal hyperalgesia, nociceptive hypersensitivity, pain, neurotrophic factors, channels, epigenetics

Abstract

The vasoactive intestinal (neuro)peptide (VIP) is involved in a variety of adult brain functions and with putative involvement in nervous system development and regeneration. Several studies have reported positive and negative effects of exogenous VIP on nociception that appear to depend on administration site. In the present work, we first investigated the role of endogenous VIP in nociception using mice deficient in this peptide. Compared to wild type and heterozygous adults, VIP null mice exhibited robust cold and tactile hyperalgesia whilst their sensitivity to heat remained unaffected, similar to human neuropathic symptoms. In anesthetized VIP null mice, in vivo electrophysiology revealed that the C-fiber activation of spinal dorsal horn neurons was triggered by mild (non-noxious) mechanical and electrical stimulations and the A-fiber responses were observed at significantly lower threshold compared to WT. We then attempted to rescue this neuropathic-like phenotype by supplying VIP to the deficient mice with a single intraperitoneal injection. This treatment was sufficient to restore normal C-fiber thresholds in 3 hours and to fully reverse the cold and mechanical pain symptoms for more than 3 days. To identify molecular determinants of the hypernociceptive phenotype, we performed cfos and phospho-CREB induction studies and carried out gene expression screening by quantitative RT-PCR on selected gene candidates classically altered under pain conditions. We showed that specific thermo- and mechano-induced receptors as well, as secreted factors involved in pathological pain states were altered in $VIP^{-/-}$ mice but could be rescued following VIP treatment acting through $VPAC_1$ receptors. Long term changes in nociception-related gene expression were associated with changes in genes that controlled epigenetic processes including chromatin remodeling, DNA methylation and specific microRNA expression. These results highlight a novel role for endogenous and exogenous VIP in the fine tuning of nociceptive sensitivity in basal conditions and the modulation of the associated pain responses. More importantly, its unexpected long-lasting analgesic properties in neuropathic pain states is sustained by epigenetic mechanisms, and warrants further evaluation in a translational context.

Introduction

Neuropeptides in the Secretin/Glucagon superfamily include the well known, structurally and functionally related polypeptides called pituitary adenylate cyclase activating polypeptide (PACAP) and vasoactive intestinal peptide (VIP). They are highly conserved in vertebrates implying crucial roles of their basic functions as neurotransmitters and secretion regulators. VIP and PACAP act at low concentrations (i.e nanomolar) through two high affinity common VIP/PACAP receptors, the $VPAC_1$ and $VPAC_2$ receptors (1).

VIP deficiency results in dysregulated endogenous circadian rhythms (2), alteration in psychological behavior and cognitive functions in newborn and adult mice (3-5), reduction in gut peristaltism (6), but also in andropause-related reduction in testosterone metabolism (7). VIP is not only expressed and secreted by neurons but also by neuroendocrine and immune cells, so it was not surprising to observe that VIP null mice also elicit modulation of immune response by enhancing resistance to viral infection (8) and to preclinical models of autoimmune neuroinflammatory diseases such as multiple sclerosis (9, 10). Based on its wide range of physiological activity, therapeutic use of VIP on human subjects has been proposed for pathologies such as asthma, erectile dysfunction and lung sarcoidosis.

The role of neuropeptides in pain pathway has been extensively studied during the last decades. Three key anatomical observations are consistent with the VIP-related modulation effect on pain (for review, 11). Histological studies have revealed that VIPergic fibers are highly concentrated in the superficial laminas of the spinal dorsal horn, which is the area of the central nervous system where the first modulation of pain-related information occurs. It has also been observed that VIP transcripts are largely present in the dorsal root ganglia within the cell bodies of small to medium diameter neurons known to participate to nociception. Furthermore VIP receptors reside in dorsal horn laminas with a moderate expression of $VPAC_1$ in lamina II and a greater density in lamina III and IV where they coexist with $VPAC_2$ subtypes.

Interestingly, studies that focused on the VIP-induced modulation of pain provided contradictory data. Indeed, under non-pathologic conditions, VIP induces naloxone-insensitive analgesia when injected in the periaqueductal grey (PAG) (12) whereas its intrathecal administration leads to pronociceptive facilitation (13, 14). Nevertheless, it is well established that under neuropathic conditions, i.e. following peripheral nerve injury, levels of peptides such as calcitonin gene-related peptide (CGRP) and substance P are decreased (14, 15) while the expression of specific neurotransmitters including VIP and PACAP are on the rise (11). Among the molecular events initiated right after the induction of neuropathy is the rapid and sustained up-regulation and/or phosphorylation of immediate early gene transcription factors c-jun, fos B and CREB (16-19) that has been suggested to be crucial for the up-regulation of VIP and thus for its contribution in neuropathy-induced pain behavior (20). Sensory neuropathy is associated with changes in calcium channels 3.2 (CaV3.2; 21), acid sensing ion channels 3 (ASIC3, 22), transient receptor potential (TRP) A1 and M8 (23)

expressions as well as with down-regulation of growth factor NT3, BDNF and GDNF (24). As a consequence, neuropathic animals display long lasting exaggerated painful responses to noxious and/or non-noxious stimuli known as hyperalgesia or allodynia, respectively. In addition, recent studies suggested that switch from acute to chronic is accompanied with dramatic epigenetic changes (for review, 25) at chromatin, genomic CpG islands, and microRNA expression levels.

Therefore, the open questions are whether or not basal VIPergic transmission or its induction of after injury directly contribute to the basal pain sensitivity and if the loss of VIP is sufficient to trigger neuropathic pain. In the present work we evaluated the pain phenotype of these VIP null mice using behavioural and electrophysiological tools and finally attempted to rescue their phenotype with a VIP treatment. We then assessed the pain-related molecular targets altered in these VIP KO mice. Although we focused on the intrinsic modulatory activities of VIP on pain and nociception, our data may provide the first evidence regarding epigenetic mechanisms by which VIP displays long-term and potent neurotrophic properties (26). This leads us to suggest that VIP possesses intrinsic analgesic properties that can be used in experimental therapy. Further, the "neuropathic-like" phenotype of VIP deficient mice may be helpful to better understand the molecular mechanisms promoting chronic pain states.

Results

VIP null mice exhibit hypersensitivity to mechanical and cold stimuli

Using standard von Frey protocol for mechanical stimuli, we observed that VIP null mice exhibited dramatic 3.2 fold reduction in mechanical nociceptive threshold (WT: 5.06 ± 0.38 g, n = 10; KO: 1.59 ± 0.12, n = 21; $p < 0.001$) as measured with the von Frey filaments (Figure 1A). Intermediate values were observed with heterozygous animals that exhibited nociceptive behaviors for mechanical stimuli around 3.68 ± 0.48 g (n = 10). These differences were not sex-specific (not shown) allowing us to combine males and females for subsequent studies. While measuring thermal hot nociception, we failed to reveal any differences in the hot nociceptive threshold between animal groups using Hargreaves test (Figure 1B) or slow temperature ramps from 30°C to 46°C (figure 1D). Interestingly, we observed that KO mice displayed a first aversive behaviour (paw withdrawal, licking or jump) at a mean temperature threshold of 3.84 ± 0.41 °C (n = 16) whereas threshold was of 0.78 ± 0.45 °C (n = 8; Figure 1C) for control animals. In addition, all null mice (n = 16) started to jump to escape the cold ramp while only 50% of the wild-type animals (n = 10) did the same. As shown for mechanical nociceptive thresholds, heterozygous animals (n = 6) had intermediate cold threshold values with an average of 2.36 ± 0.61 °C. Altogether, the present data shows that VIP deficient mice display mechanical hyperalgesia, cold allodynia but “normal” sensitivity to noxious hot stimuli than WT.

Excessive spinal nociceptive processing is observed in VIP null mice

To further demonstrate that VIP null mice are hyper-reactive to nociceptive stimuli, we performed extracellular single unit recordings of deep dorsal horn neurons that process non-noxious and noxious sensory information (i.e. wide dynamic range - WDR - neurons). As illustrated in figure 2A and 2B, a burst of action potentials (APs) is clearly seen in anesthetized WT animals when the hindpaw receptive field of the mice is stimulated using von Frey filaments of 15 g (corresponding to a noxious mechanical stimulation). In VIP null mice, this AP discharge is observed with smaller filament exerting a pressure of about 4 g (corresponding to a non-noxious mechanical stimulation). On average, the pressure threshold necessary to produce a C-type nociceptive discharge is significantly different between WT (9.3 ± 0.5 g, n = 10) and KO animals (Figure 2B; KO: 3.9 ± 0.4 g, n = 10; Student, $p < 0.001$). Similarly, we found that the mean electrical threshold to produce APs originating from A-type (fast conducting: 8.5 ± 0.6 V, n = 10) and C-type (slow conducting: 27.4 ± 1.0 V, n = 10) sensory fibers was significantly lower in VIP null mice (A-type: 1.5 ± 0.2 V, n = 10; C-type: 10.9 ± 0.5 V, n = 10; Student, $p < 0.001$ for both). To summarize the electrophysiological data, we found VIP null mice to be hypernociceptive to mechanical and electrical stimuli. This abnormal hyperexcitability, also seen in pain-related central sensitization, is in good agreement with the expression of pathological symptoms such as mechanical allodynia.

Rescue of VIP null mice by intraperitoneal VIP injection revealed the major contribution of VPAC1 receptor signaling through pCREB and fosB early gene response to normal nociceptive threshold.

Pain symptoms, expressed by VIP null mice, may be the result of a developmental impairment during neurogenesis and synaptogenesis (organizational defect) or of a functional impairment in adulthood (activational defect). To explore these hypotheses we attempted to rescue the pain phenotype of VIP null mice. We then performed a single i.p. injection of VIP or VIP analogs (at 2 µg ea.) then characterized their effects on mechanical nociceptive thresholds (WT) on hyperalgesic animals ($VIP^{-/-}$). As shown in figure 3, mechanical nociceptive threshold of WT mice remained unchanged during and after VIP injections. Mean threshold values were not different from those obtained after injection of the vehicle. In sharp contrast, VIP injection induced a robust, long-lasting analgesic effect in VIP null mice. This effect was rapid since normal (i.e. similar to control mice) nociceptive threshold could be seen 1-3h after the injection. Analgesic action was also maintained for about 3 days suggesting that VIP may have induced long-term effects. A time course study (figure 4) using in vivo electrophysiological recording revealed a complete recovery (i.e. threshold in VIP-injected null mice are no longer significantly different compared to WT mice) of electrical (C- and A-type fibers) as well as mechanical thresholds within the 2 hours following VIP treatment. Injection of $VPAC_1$ agonist in VIP-/- triggers a similar rescue of pain symptoms compared to VIP, whilst $VPAC_1$ antagonist fully abrogated the beneficial effects of VIP on mechanical threshold strongly supporting the main contribution of $VPAC_1$ receptor signalling to the phenotype (figure 5A). This may be also explained because VIP receptor expression is not affected in both DRG and spinal cord by the loss of VIP in null mice (Figure 5B).

Downstream VIP receptor signaling cascade involved phosphorylation of CREB that peaked in less than an hour after VIP injection in VIP KO spinal cord with special emphasis in the most superficial areas of the dorsal horn where $VPAC_1$ is mainly expressed (Figure 5D). Conversely, pain-induced nuclear FosB/ΔFosB immunoreactivity that is also highly present in the lamina I and II of dorsal horn of VIP KO mice was found greatly reduced 4 hours after after VIP injection (Figure 5D).

VIP-deficiency triggers dramatic but reversible changes in expression levels of a very limited number of nociception-related genes.

To further investigate the role of VIP on nociception in WT, VIP null mice and VIP rescued mice, we used quantitative RT-PCR to measure expression levels of subsets of genes (see table S2), previously identified to participate to neuropathic pain states (32). Considering the specific pain phenotype observed in our mouse line we mainly looked at ion channels with special emphasis on genes implicated in transducing mechanical and cold stimuli). To do so, RNA samples (n=5 per groups) were isolated from lumbar dorsal root ganglia (DRG) and spinal cord (SC) of wild-type, VIP-deficient and VIP-rescued animals. As expected from the in vivo experiments, we observed changes in expression of a very small subset of genes known to mediate mechanical and cold nociception such as Cav3.2, TRPM8 and ASIC3 (Figure 6A). These 3 target genes were significantly over-expressed in both DRG (2.1, 4.4 and 1.7 fold-increase for Cav3.2, TRPM8, and ASIC3, respectively) and SC (1.9, 2.5 and 1.7 respectively) of KO animals compared to control tissues. These elevations were greatly reduced 48h after a single injection of VIP in both DRG (by a 4.1, 2.8 and 2.7 fold-decrease for Cav3.2, TRPM8, and ASIC3, respectively) and SC (2.5, 1.8 and 2.0, respectively). Conversely we did not see any change in hot nociception-related transcripts including TRPV1, TRPV3 and TRPV4 (supplementary S3). No significant changes were observed for genes of the voltage-gated calcium (Cav) family including (Cav1.2, Cav2.2) or acid-sensing sodium channels (ASIC1, ASIC2) and others (see supplementary S2 and S3 for more details) suggesting that observed changes were highly dependent on the presence or the absence of VIP.

VIP is known to stimulate secretion of trophic and other factors, so in a second set of experiments, we also selected genes encoding secreted factors known to mediate changes in nociceptive threshold. We looked at change in expression levels of NGF-related genes and other neurotrophic factors as well as neuropeptides (figure 6B). Beside BDNF, CGRP, Galanin and NT3 whose expressions are controlled by VIP (supplementary S2 and S4) only CNTF (1.8- and 1.5-fold increase in DRG or SC), the GDNF-related persephin (2.8- and 2.0-fold increase in DRG and SC) and artemin (4.4- and 1.6-fold increase in DRG and SC) genes show consistent overexpression in mutants compared to wild type controls (Figure 6B). The overexpression of artemin, persephin and CNTF transcripts are also abrogated in rescue VIP samples from both DRG (2.4-, 2.5- and 1.6-

fold decrease, respectively) or SC (1.7-, 2.1- and 1.5-fold decrease, respectively). The other genes tested (listed in S2) did not show any dramatic change in expression consistent with the pain phenotype.

Epigenetic regulation contributes to long-term hyperalgesia in VIP KO mice

In the subsequent set of experiment we focused on changes in expression of genes encoding for histone acetylases/deacetylases, CpG methyltransferases, methylated DNA binding proteins and pain-related MiRs in DRG and SC RNA samples extracted from WT and VIP KO, injected or not with VIP as above described. All together we observed, that between WT and KO, many of them were subjected to complex but significant changes (figure 6C and S5).

When focusing on chromatin remodeling genes exhibiting variations that can be restored by VIP injection, only 4 subtypes of HDACs and one subtype of HAT were found relevant in our studies. In particular, we found that HDAC1 (3.1 and 1.9 fold decrease in SC and DRG, respectively) and HDAC2 (1.8 and 1.6 fold decrease in SC and DRG, respectively) were found down-regulated in KO mice compared to WT controls but restored to normal level after VIP treatment (Figure 6C and S5). Conversely, HDAC4 (Figure 6C) and HDAC5 (S5) overexpressed in KO compared to WT in both SC (by a 2.0- and 1.6 fold respectively) and DRG (1.4- and 1.6-fold respectively) returned to baseline after VIP administration. Similarly, the overexpressed histidine acetyltransferase Kat 2A in KO compared to control (1.8- and 1-6 fold in SC and DRG respectively) underwent strong repression by VIP.

As gene methylation is now considered crucial and selective for gene transcription, we further investigated DNA methyltransferases (DNMT) and found that downregulation of DNMT-1 in VIP KO compared to WT (2.5- and 1.5-fold in SC and DRG) was fully obliterated by VIP treatment (figure 6C) suggesting their involvement in control of pain-related gene expression. Conversely the methylcytosine dioxygenase Tet1 gene, known to convert methylcytosine into hydroxymethylcytosine and therefore to favour DNA demethylation, found up-regulated (by a 2.5- and 1.5-fold in SC and DRG) in KO returned to baseline after VIP treatment (Figure 6C). In line with these observations, we also evidenced expression changes in genes encoding the methylDNA binding protein MBD6 (S5). Indeed contrary to MeCP2 (Figure 6C) showing an overall 2.5-fold down-regulation in VIP KO samples that cannot be rescued by VIP treatment, MBD6 exhibited a strong induction in VIP KO (2.7- and 1.7-fold in SC and DRG, respectively) that was fully abrogated after VIP administration.

Finally we observed a specific but opposite pattern of expression of 2 pain-related microRNAs, miR7A and miR21 (figure 6C lower panel). miR7A was found increased by a 2.4 and 5.6 fold in SC or DRG samples of VIP KO treated with VIP compared to vehicle-injected ones, while miR21 expression levels in KO samples increased by 4.5- and 2.8-folds (in spinal cord and DRG, respectively) compared to their respective controls.

To further characterize the putative link between changes in pain-related genes and epigenetic modulation, we performed an analysis of the methylation state (meDIP) of the upstream regions of Cav3.2, TRPM8 and ASIC3 coding sequences. Results illustrated in figure 7B revealed that primer sets designed to selectively quantify CaV3.2, ASIC3 and TRPV8 expression generate a single band at the expected size (92, 106 and 103 bp, respectively; see table S2) in WT DNA samples immunoprecipitated with 5-methylcytosine antibody that is absent in IgG-IP negative controls (inset on 7B). In addition qPCR data analyses revealed that methylated DNA templates is greatly reduced in KO samples compared to WT strongly suggesting that these changes in methylation states may favour their increase in expression levels.

Analgesic action of Vasoactive intestinal peptide in neuropathic mice.

Based on the observation that endogenous VIP negatively modulate nociception, we then speculated that VIP may have analgesic property when injected in neuropathic animals. In WT mice suffering from chronic constriction of the sciatic nerve (cuff), mechanical hyperalgesia develops within a week and last for more than 90 days. When mechanical hyperalgesia is present, we observed that a single intraperitoneal injection of VIP was sufficient to alleviate this pain symptom for more than 3 days (figure 8A). These analgesic effects were accompanied by a significant and sustained reduction in CaV3.2, ASIC3 and TRPM8 expression compared to expression levels before injection that last at least 96 hours (Figure 8B). In a similar manner we observed a timely reduction of the GDNF family members persephin and artemin and a concomitant overexpression of CNTF.

Discussion

In an original work published in 2006, we characterized the behavioral phenotype of VIP KO mice (3). Using SHIRPA analysis, we recorded a complex set of loco-and psycho-motor behaviors. Compared to age-matched wild type controls, VIP-deficient animals exhibited exacerbated transfer arousal, transient hyperactivity in open field, but also a greatly reduced grip strength in wire manoeuvre task. We reported the phenomenon at that time as the possible result of muscular weakness and/or fatigue. In the present report we now provide a novel explanation for these phenotypes, which is VIP-deficient mice suffer from selective mechanical hyperalgesia (i.e. hyper-reactivity to noxious mechanical stimulus) and cold allodynia (i.e. hyper-reactivity to a non-noxious cold stimulus). Indeed using both mechanical von Frey testing, dynamic hot-cold plate and Hargreaves method for thermal nociception, we found that VIP null mice display a very atypical hypersensitivity to mechanical and cold temperature without alteration in noxious heat response. This phenotype is very robust in intensity as the decrease in threshold values revealed. The presence of these pain symptoms in VIP null mice is quite similar to what is found in humans suffering from neuropathic pain and in some experimental animal models of neuropathic pain.

As previously described VIP-deficient mice exhibited many phenotypes in neonates that persist in adulthood suggesting that they may originate from alteration of their neural development. Indeed, we recently showed that interfering with VIP signalling during neurogenesis results in appearance of pups with reduced cortical structures (27) and complex behavioral deficits (28-30). Therefore, genetic or pharmacological disruption of VIP actions during embryonic development is more likely to generate irreversible phenotypes. Nevertheless, we observed that pain symptoms exhibited by the VIP deficient mice originating from null mothers can be temporary rescued by intraperitoneal injection of VIP. This result can be partially explained by the fact that VIP receptor ($VPAC_1$ and $VPAC_2$) expression remained unaffected by the loss of VIP or by the rescue. In addition, the key question remains whether this cortical deficit participates to the observed hypersensitivity or the pain phenotype solely originates from spinal network deficits. There are several reports suggesting that VIP modulate nociception and pain responses but, so far, most (if not all) of these studies have been using exogenous application onto a fully functional network. In the 1980's, microinjection of VIP into the PAG produced a significant naloxone-insensitive analgesia (12). This result led to the proposal that VIP-containing neurons in PAG may constitute a non-opioidergic pain suppression system. Later on, intrathecal injection of VIP was associated with increased spinal cord neuron excitability during processing of noxious thermal hot stimuli and, to a lesser extent, to mechanical stimuli applied to the ipsilateral paw (13) or to the tail (14). VIP immunoreactive fibers are indeed widely distributed in the rat spinal cord, with some higher extend in the superficial dorsal horn, the lateral spinal nucleus and the lamina X (31). This is fully consistent with a possible modulatory role for VIP in processing pain messages although it may affect the function of several neurons within the local spinal nociceptive circuits (32). In line with this idea, administration of VIP at nanomolar concentrations caused lowering in the activation threshold of spinal neurons, facilitated C-fibers recruitment and central sensitization (33). With regards to sensory neurons, VIP transcripts are predominantly found in small to medium diameter DRG neurons that are thought (for some of them) to convey nociceptive signals to spinal cord (15, 31). It is important to note that VIP levels of expression are low in physiological condition which long suggested that its implication to set the basal nociceptive threshold was rather limited. In summary, the previous results obtained with exogenous application of VIP have cautiously interpreted since VIP receptors might modulate nociception and pain responses at different level of the pain matrix, acting through different cell populations expressing different receptor subtypes. Therefore we took the opportunity of using VIP null mice to unravel a lack of endogenous nociceptive function. We found these mice exhibit neuropathic-like pain symptoms which are fully reversed after intraperitoneal injection of VIP.

To fully benefit from this genetic model of a reversible neuropathy, we screened for VIP-sensitive genes that can be account for painsymptoms and pain control. Taking into account that VIP has been already associated with changes in gene expression and that we observed nuclear pCREB accumulation in response to VIP administration, we decided to narrow the panel of gene candidates by looking for pain-related genes whose expression will be oppositely affected by loss of VIP and VIP rescue when compared to control samples. Among the different families of genes that are known to modulate nociception or to contribute to

neuropathic pain (34), two classes of molecules have been initially monitored: secreted factors and ionic channels. Focusing on lumbar DRG and spinal cord, we found that most of the genes studied behaved in a similar way in the two tissues. For secreted factors, we found that artemin and persephin of the GDNF ligand family were the most interesting for us since their upregulated expression observed in VIP null returned to control values after application of VIP. This overexpression may participate to the overall hypersensitivity since they have been found to enhance CGRP release of C-type capsaicin-sensitive sensory neurons (35). In contrast, we noticed that BDNF, CGRP, galaninand NT3 were unaffected by VIP gene disruption but were up-regulated by VIP application. We also found four ionic channel candidates involved in either mechanical or thermal nociception whose expressions vary in the presence or absence of VIP. Mechanical hypernociception can be driven by an increased function of several voltage-gated or acid sensing ionic channels (34). In this context we tested whether voltage-gated sodium channels (NaV) could be involved in the mechanical hypersensitivity observed in VIP null mice. Only Nav1.9 transcripts were found to be affected by the loss of VIP. However, because VIP-deficient mice exhibited a strong inhibition of this channel expression that was not restored by VIP delivery, this sodium channel is unlikely to account directly for the mechanical phenotype observed. We next focused on degenerins with special emphasis on ASIC1, 2 and 3. Only ASIC3 expression was directly affected by the presence or absence or VIP, suggesting that ASIC3 can be involved in the hypersensitivity to mechanical stimuli observed in KO mice. In line with our data, ASIC3 shown to be expressed in rodent skin, in DRG and spinal cord induces, when overexpressed, very specific features such as muscle-dependent development of mechanical hyperalgesia (36). Nevertheless, its contribution to the observed pain symptoms remains highly speculative at this stage. We then looked at the voltage gated calcium channels through the analysis of Cav2.2 and Cav3.2 subtype expression. Only Cav3.2 expression was found to be upregulated in VIP deficient mice and to return to normal levels when VIP was administrated suggesting that this low-threshold voltage-gated calcium channels could participate in the mechanical hyperalgesic phenotype. This idea is quite appealing considering that silencing Cav3.2 in DRG results in pronounced increase in mechanical threshold in healthy rats (37).

Thermal nociception is under the control of many ion channels. Many of them belong to the TRP (transient receptor potential) superfamily but others such as TREK-1 do not. TRP family includes TRPV1-V4, TRPA1 and TRPM8 that differ mainly by their thermal activation thresholds. TRPV1 and TRPV2 are engaged in reaction to very hot (>42C, potentially noxious) temperature, TRPV3 and TRPV4 react to warm stimuli (27-38°C) while colder temperature are detected by TRPM8 (<28°C) and TRPA1 (<17°C) (for review see 38,39). Consistent with our behavioral data, we found no change in expression levels of heat-sensitive TRPV1-3 and TREK-1 genes but a striking change in TRPM8 and TRPA1. These two channels are non-selective cationic channels highly expressed in small diameter DRG neurons known to discriminate pharmacological agonists and low temperatures ranging from innocuous cool (26–15°C) to noxious cold (<15°C). Gene invalidation studies revealed that the pain-related functions of TRPA1 and TRPM8 still remained unclear. In the present study, we also faced difficulties in interpreting our results. At first, TRPM8 changes were quite easy to understand

since its expression was enhanced in the VIP null mice exhibiting hypernociception to cold stimulus and cold nociception returned to normal (control) values after administration of VIP. However, TRPA1 expression appears dramatically reduced in VIP null mice independently of VIP administration. Such a reduction in TRPA1 expression in allodynic VIP null mice was rather unexpected. Nevertheless, the combined TRPA1 and TRPM8 data likely suggests that noxious action of cold stimulus is due to overexpression of TRPM8 and is not compensated by the reduction in TRPA1 transcript. This idea fits quite well with previous data from McKemy group that TRPM8 but not TRPA1 is required for neural and behavioral response to cold temperature (40).

As it has been shown by many studies over the last five years, pain in general and neuropathic pain in particular relies on epigenetic modifications to become chronic (for review: 24, 41). In addition recent studies strongly suggested that downregulation of MeCP2, DNMTs and HDACs indicate an overall upregulation of gene expression in the maintenance of persistent pain (42). In line with this general ideas, we observed a similarly significant decreases of HDAC-1 and -2 (sustained by a concomitant increase in Kat2a expression), of MeCP2 mRNAs (enhanced by the concomitant overexpression of TET1) in the hyperalgesic VIP null mice. Changes in expression pattern of epigenetic modulators may affect not only gene expression but also directly impact pain states. In this context, HDAC inhibitors have demonstrated evidence of analgesic properties in both inflammatory and neuropathic pain suggesting that HDAC hyperactivity or overexpression may trigger hyperalgesia. Therefore it may also reflect why HDAC levels remained mostly unaffected by VIP treatment in our model. At DNA levels, CpG methyltansferases (DNMT) silence gene expression whilst hydroxymethyltransferases such as TET1, convert methyl into hydroxymethyl cytosines to facilitate their demethylation. Depending of the methylation states, methylated DNA binding proteins (MBD) may regulate specific gene expression and nociception as exemplified by MeCP2 known to alleviate exacerbated pain (42). However, a recent publication (43) suggested that DNMT3b is overexpressed in DRG of neuropathic rats whilst MBD4 may be upregulated in inflammatory pain conditions confirming our general impression that the whole regulation of epigenetic enzymes in pain states is still unclear but deserves further investigation. Nevertheless our observations suggesting that epigenetic modifications indeed accounted for the observed changes in pain related genes expression were further confirmed by MEDIP experiments showing that changes in Cav3.2, TRPM8 and ASIC3 expression observed in VIP KO mice compared to VIP-injected null mice or WT controls were at least in part due to epigenetic changes leading to different methylation states. Finally, numerous recent studies support the idea that chronic pain dramatically affects microRNA expression (for review 44). Although we did not perform any global microRNA array, the pain-specific miRNA-7A and -21 presumed to underline the pain symptoms were also oppositely regulated in VIP null mice after VIP treatment as predicted by Sakai et al. (45, 46) that showed that miR-7A alleviates pain symptoms while miR-21 is up-regulated in neuropathic pain.

Taken all together our data suggested that VIP acting through $VPAC_1$ receptors represses the expression of many pain-related genes implicated in the steady state of mechanical and cold nociception. Abrogating this

signaling pathway, as shown herein, by knocking down VIP gene resulted in lowering nociceptive thresholds and generating hypernociceptive animals. Therefore the opened questions remaining are (1) whether or not VIP null mice are suffering from spontaneous pain impairing their social interaction and (2) whether VIP presents analgesic properties when administrated to neuropathic mice. Although we still have no final answer to the first question, we performed VIP administration to animal model of neuropathic pain. In WT animals exhibiting chronic pain due to unilateral sciatic nerve cuff, we observed that a single IP injection of VIP was sufficient to alleviate all pain symptoms for 72h suggesting that this neuropeptide presents unexpected analgesic properties in term of potency and duration. The data when confirmed in other experimental pain models, may open new lines of research focusing on therapeutic applications. In line with these perspectives, transcutaneous electric nerve stimulation (TENS) is a known efficient alternative and non-pharmacological methods for pain management. Although the exact mechanisms of action of TENS remains to be further investigated, it is well accepted that it relies on direct actions on the autonomic system but also an indirect effect on release hormonal mediators like enkephalins and VIP (47).

Methods

Animals: C57bl6 (WT) and $VIP^{-/-}$ and $VIP^{+/-}$mice (47) were used in these experiments. The $VIP^{-/-}$ mouse model was prepared using a VIP gene disruption strategy with confirmation of targeted mutation in mice and subsequent backcrossing to the C57BL/6 strain for more than 12 generations. VIP-deficient mice originally provided by Dr. James Waschek (University of California, LA, USA) and C57bl6 (obtained from Harlan, France) were bred locally in a germ-free facility (Chronobiotron-CNRS UMS 3415). Transgenic animals born from null mothers were genotyped by PCR of tailsnip DNA. All mice were housed (12-hr light/dark cycle) in groups in the vivarium with water and food provided *ad libitum*. Age-matched $VIP^{-/-}$ and wildtype (WT) controls were collected from different litters and breeding pairs to generate the study groups. The Institutional Animal Care and Use Committee at The University of Strasbourg approved all experiments. In particular, procedures were evaluated and received agreement from the Regional Ethic committee (nociceptive testing and model: CREMEAS n° AL/01/20/12/09; in vivo electrophysiology: n° AL/01/01/02/11).

VIP and VIP analogues treatments: In the present studies, VIP (Sigma), selective VPAC1 agonist ([$Ala^{11,22,28}$]-VIP and antagonist (PG 97-269) (Phoenix pharmaceuticals, Strasbourg, France) were reconstituted in sterile water, aliquoted and stored at -80C. For rescue experiments VIP and its analogs were intraperitoneally administered to VIP deficient mice as a single dose of 2ng after final dilution in PBS using an Hamilton syringe. Controls were injected with similar volume of PBS.

Nociceptive tests: All animals were habituated to the room and to the tests at least one week before starting the experiments. Measures were always done between 10:00 AM and 4:00 PM.

Mechanical nociception: The mechanical threshold for hindpaw withdrawal was determined using von Frey hairs. Mice were placed in clear Plexiglas boxes (7 cm x 9 cm x 7 cm) on an elevated mesh screen. Calibrated von Frey filaments (Bioseb, Vitrolles, France) were applied to the plantar surface of each hindpaw in a series of ascending forces (ranging between 0.4 g and 15 g). Mechanical thresholds were defined as 3 or more withdrawals observed out of five trials. In rescue experiments, tests were performed at least 17 hours after injection of VIP or its analogs.

Thermal nociception: We first used a computer-controlled cold/hot ramps of temperatures (Bioseb, Vitrolles, France) to determine thermal nociceptive thresholds as previously described (39). Briefly, animal was placed in a Plexiglas cylinder (10-cm diameter, 25-cm height) with a drilled cover and plate temperature was set at a fixed temperature of 30°C (for hot) or 20°C (for cold). After a 15 minutes habituation period, hot and cold ramps started at a rate of 2°C/minute. The temperature corresponding to the first aversive behavior was used as the thermal nociceptive threshold and animal was immediately removed from the test. Hot nociceptive thresholds we assessed using the Hargreaves test. Mice were placed in clear Plexiglas boxes (mice: 7 cm x 9 cm x 7 cm) on a glass surface. Consequently to the habituation period (15 minutes), the infrared beam of the radiant heat source (Bioseb, Vitrolles, France) was applied to the plantar surface of the right hindpaw. The experimental cutoff to prevent damage to the skin was set at 15 seconds. Three measures of the paw withdrawal latency were taken and averaged.

Spinal cord preparation and In vivo electrophysiology: Mice (males and females from WT and KO genotypes), aging around 2.5 months, were anesthetized with isoflurane (3% then maintained at 2% during the whole procedure) pushed by O2 (flow rate 0.5 l/min) and the core temperature was maintained at 37 °C using a temperature-controlled heating blanket (Harvard Apparatus Ltd, Les Ulis, France). Animals were mounted on a stereotaxic frame (La précision cinématographique, Eaubonne, France), spinal clamps allowed to secure the vertebral column and spinal cord segments L3-L5 were exposed by laminectomy. A recording chamber was made of agar 3 % around the spinal segment and the meninges (dura and arachnoid) were removed. Extracellular recordings on single wide dynamic range neurons were carried out using stainless electrode (10 MΩ) (FHC, Bowdoin, USA) connected to an extracellular differential amplifier (DAM-80, WPI, Aston, UK) using a protocol recently described elsewhere (40). Electrical signals were then digitized (Power 1401 CED, Cambridge, UK), visualized and stored on a personal computer equipped with the Spike 2 software (CED Cambridge, UK). Electrical stimulation was applied through two thin cutaneous pin electrodes placed in the center of the receptive field and increasing intensities were applied from 1 to 99 V (duration of 1 ms) to determine threshold for each sensory fiber type based on their respective velocities (A-type: 0-50 ms; C-type: 50-800 ms after the stimulus artefact). Mechanical stimulation threshold of the peripheral receptive field to observe a excitatory response in the recorded neuron was measured using von Frey filaments (WPI, UK) of different diameter and force (i.e. 2g to 15g). At the end of the experiment, animals were killed with an overdose of isoflurane.

Quantitative RT-PCR: Lumbar spinal cords, DRG and paws were collected from WT, VIP-/- at least a week after the final behavioral testing. For VIP rescue, animals injected with VIP were sacrificed for tissue collection a week after the last injection in accordance to the timeline of elevation of nociceptive threshold. All samples (5 per group and tissue) were flash frozen in cold isopentane then stored at -80°C. Total RNA was extracted at once according to a protocol previously described in detail (41). RNA quality and concentration were assessed by spectrophotometry and Agilent technology. Total RNA (600 ng/sample) was subjected to reverse transcription using the Iscript kit according to the manufacturer instructions (Bio-Rad). PCR was set up in 96-well plates using diluted cDNA samples, highly-selective primer sets (see sequences in Table I in supplementary S2) and SyberGreen-containing PCR reagents (Bio-Rad) accurately dispensed using a robotic workstation (Freedom EVO100 Tecan, France). Gene amplification and expression was performed on a MyIQ real-time PCR machine (Bio-Rad) using a three-step procedure (15s@96C; 10s@62C; 15s@72C). Amplification efficacy and specificity, standardization and expression quantification were assessed as previously described in great details (42).

Methylated DNA immunoprecipitation assay: Wild-type and KO animals (5 per groups) were sacrificed at P40 and lumbar spinal cords (L3-l5) were dissected. Genomic DNA was extracted extemporaneally and 2 µg DNA aliquots were sheared by sonication in 200 µl buffer (Vibram Cell™ 75186, Bioblock Scientific) with 6 cycles of 5 s ON, 30 s OFF on ice at 70% power. Methylated DNA immunoprecipitation (MeDIP) was performed using Methylamp™ Methylated DNA Capture Kit (Epigentek Group, Brooklyn, NY). Sonicated fragments ranging from 200 to 1000 bp were divided into immunoprecipitated (IP) and input (Inp) portions according to manufacturer protocol. IP DNA was incubated with anti-5-methylcytosine antibody and the negative control was normal mouse IgG. The DNA fragments recovered were then used as templates for real time PCR using specific primer sets (Table I) to amplify Cav3.2, TRPM8, and ASIC3 upstream coding regions, and generate PCR fragments of different sizes ranging from 98 to 106 bp (as shown with using primer sets # 2). Cycling conditions were similar to the quantitative RT-PCR above described. The specificity of the PCR product was verified by melting curve analysis and by 2% agarose gel electrophoresis while PCR efficacy was controlled using standard curves performed on serial dilutions of sheared spinal cord inp DNA . Real time PCR was conducted three times, with samples in duplicates. Relative enrichment of the target sequences after MeDIP was estimated as the ratio of the signals in methylated (IP) DNA over total DNA (Inp).

Early response gene immunohistological studies: Three month-old KO mice I.P. injected with VIP (2µg) for 1, 4, 8, 12 and 24h (3 per group) were deeply anesthetized by intraperitoneal injection of 100ul of ketamine solution (Imalgene 100mg/ml, Merial, France) and perfused transcardially with PFA 4% using a peristaltic pump at a flow rate of 7ml/minute. Spinal cords (L3-6) were post-fixed overnight with PFA 4%, cryoprotected with 30% of sucrose and cryo-sectioned at 14µm (CM3050S, Leica Microsystems) then mounted on Superfrost+ slides (Dutscher, France). Lumbar transversal sections were washed with PBS, blocked with 5% BSA and 0.1% Triton X-100 (diluted in PBS) for one hour at room temperature and incubated overnight at

4°C at with specific polyclonal primary antibodies raised in rabbit, either anti-phospho (ser133) CREB (1:500, 06-519, Millipore) or anti-FosB/ΔFosB (1:1000, SC-48, Santa Cruz Biotechnologies) diluted in PBS containing 1% normal serum and 0.5% Triton X-100. Sections were rinsed in PBS (5 × 10 min), incubated for 1 h in a goat anti-rabbit alexa488-labelled conjugate (1:2000, A11008, Invitrogen). Counterstaining was done with a 5 minute DAPI wash (1:500, D9542, Sigma).. Sections were observed on epifluorescent microscope Imager A1 and photographed with AxioCam MR and AxioVision software (Carl Zeiss). Positive nuclei were counted from 50 sections from all groups focusing on 3 specific areas (lamina I and II, lamina III and IV and lamina X).

Neuropathy model: Neuropathic pain was induced by placing a cuff around the right common sciatic nerve of 3 month-old C57bl/6 (WT) males as previously described (Benbouzid et al. 2009). Surgery was done under ketamine (17 mg/ml) and xylazine (2.5 mg/ml) anesthesia (intraperitoneal, 4 ml/kg). The common branch of the right sciatic nerve was exposed, and a 2-mm section of split PE-20 polyethylene tubing (Harvard Apparatus, Les Ulis, France) was placed around it for the cuff group (21–23). Sham-operated mice underwent the same procedure without cuff implantation (sham group). Pain was assessed using von Frey hairs to measure mechanical threshold to observe hind-paw withdrawal. After 2 weeks when pain symptoms were stabilized, cuffed animals received one single I.P. injection of VIP (2µg) or same bolus of saline (vehicle). At the specified times, pain relief was measured by mechanical threshold assessment.

Statistical analysis: Data are all expressed as mean ± SEM and statistical analyses performed using Prism 6 software (GraphPad Prism, USA). A one- or two-way ANOVA followed by a Tukey post hoc test was used to compare the nociceptive thresholds (thermal) of the different animal groups and gene expression changes. For the electrophysiological data, differences in mechanical threshold, or of electrical threshold per fiber type, were assessed using two-tailed Student's t-tests . To compare the von Frey mechanical thresholds, non parametric Kruskal-Wallis test was used followed by Dunn's comparisons (thresholds between animal groups) or Friedman tests (repeated measures after VIP treatment) followed by Wilcoxon comparisons. For quantitative RT-PCR, two-way ANOVA was performed followed by multiple comparison analysis, while two tailed Student's test was performed to assess significance in MEDIP experiments.

Acknowledgments: This publication has been supported by the Centre National pour la Recherche Scientifique (CNRS), the University of Strasbourg and the Institut Federatif de Recherche IFR37. The authors have no conflicting financial interests.

References

1. Harmar AJ, Fahrenkrug J, Gozes I, Laburthe M, May V, Pisegna JR, Vaudry D, Vaudry H, Waschek JA, Said SI. Pharmacology and functions of receptors for vasoactive intestinal peptide and pituitary adenylate cyclase-activating polypeptide: IUPHAR review 1. *Br J Pharmacol*. 2012; 166(1):4-17.

2. Colwell CS, Michel S, Itri J, Rodriguez W, Tam J, Lelievre V, Hu Z, Liu X, Waschek JA. Disrupted circadian rhythms in VIP- and PHI-deficient mice. *Am J Physiol Regul Integr Comp Physiol*. 2003; 285(5):R939-493.

3. Girard BA, Lelievre V, Braas KM, Razinia T, Vizzard MA, Ioffe Y, El Meskini R, Ronnett GV, Waschek JA, May V. Non compensation in peptide/receptor gene expression and distinct behavioral phenotypes in VIP- and PACAP-deficient mice. *J Neurochem*. 2006; 99(2):499-513.

4. Lim MA, Stack CM, Cuasay K, Stone MM, McFarlane HG, Waschek JA, Hill JM. Regardless of genotype, offspring of VIP-deficient female mice exhibit developmental delays and deficits in social behavior. *Int J Dev Neurosci*. 2008; 26(5):423-34.

5. Chaudhury D, Loh DH, Dragich JM, Hagopian A, Colwell CS. Select cognitive deficits in vasoactive intestinal peptide deficient mice. *BMC Neurosci*. 2008; 9:63.

6. Lelievre V, Favrais G, Abad C, Adle-Biassette H, Lu Y, Germano PM, Cheung-Lau G, Pisegna JR, Gressens P, Lawson G, Waschek JA. Gastrointestinal dysfunction in mice with a targeted mutation in the gene encoding vasoactive intestinal polypeptide: a model for the study of intestinal ileus and Hirschsprung's disease. *Peptides*. 2007; 28(9):1688-99.

7. Lacombe A, Lelievre V, Roselli CE, Muller JM, Waschek JA, Vilain E. Lack of vasoactive intestinal peptide reduces testosterone levels and reproductive aging in mouse testis. *J Endocrinol*. 2007; 194(1):153-60.

8. Li JM, Southerland L, Hossain MS, Giver CR, Wang Y, Darlak K, Harris W, Waschek J, Waller EK. Absence of vasoactive intestinal peptide expression in hematopoietic cells enhances Th1 polarization and antiviral immunity in mice. *J Immunol*. 2011; 187(2):1057-65.

9. Gonzalez-Rey E, Fernandez-Martin A, Chorny A, Martin J, Pozo D, Ganea D, Delgado M. Therapeutic effect of vasoactive intestinal peptide on experimental autoimmune encephalomyelitis: down-regulation of inflammatory and autoimmune responses. *Am J Pathol*. 2006; 168(4):1179-88.

10. Abad C, Tan YV, Lopez R, Nobuta H, Dong H, Phan P, Feng JM, Campagnoni AT, Waschek JA. Vasoactive intestinal peptide loss leads to impaired CNS parenchymal T-cell infiltration and resistance to experimental autoimmune encephalomyelitis. *Proc Natl Acad Sci USA*. 2010; 107(45):19555-60.

11. Dickinson T, Fleetwood-Walker SM. VIP and PACAP: very important in pain? *Trends Pharmacol Sci*. 1999; 20(8):324-9.

12. Moss MS, Basbaum AI. The peptidergic organization of the cat periaqueductal gray. II. The distribution of immunoreactive substance P and vasoactive intestinal polypeptide. *J Neurosci*. 1983; 3(7):1437-49.

13. Wiesenfeld-Hallin Z. Intrathecal vasoactive intestinal polypeptide modulates spinal reflex excitability primarily to cutaneous thermal stimuli in rats. *Neurosci Lett*. 1987; 80(3):293-7.

14. Cridland RA, Henry JL. Effects of intrathecal administration of neuropeptides on a spinal nociceptive reflex in the rat: VIP, galanin, CGRP, TRH, somatostatin and angiotensin II. *Neuropeptides*. 1988; 11(1):23-32.

15. Nahin RL, Ren K, De León M, Ruda M. Primary sensory neurons exhibit altered gene expression in a rat model of neuropathic pain. *Pain*. 1994; 58(1):95-108.

16. Kajander KC, Xu J. Quantitative evaluation of calcitonin gene-related peptide and substance P levels in rat spinal cord following peripheral nerve injury. *Neurosci Lett*. 1995; 186(2-3):184-8.

17. Herdegen T, Tölle TR, Bravo R, Zieglgänsberger W, Zimmermann M. Sequential expression of JUN B, JUN D and FOS B proteins in rat spinal neurons: cascade of transcriptional operations during nociception. *Neurosci Lett*. 1991; 129(2):221-4.

18. Kenney AM, Kocsis JD. Timing of c-jun protein induction in lumbar dorsal root ganglia after sciatic nerve transection varies with lesion distance. *Brain Res*. 1997; 751(1):90-5.

19. Miletic G, Pankratz MT, Miletic V. Increases in the phosphorylation of cyclic AMP response element binding protein (CREB) and decreases in the content of calcineurin accompany thermal hyperalgesia following chronic constriction injury in rats. *Pain*. 2002; 99(3):493-500.

20. Son SJ, Lee KM, Jeon SM, Park ES, Park KM, Cho HJ. Activation of transcription factor c-jun in dorsal root ganglia induces VIP and NPY upregulation and contributes to the pathogenesis of neuropathic pain. *Exp Neurol*. 2007; 204(1):467-72.

21. Messinger RB, Naik AK, Jagodic MM, Nelson MT, Lee WY, Choe WJ, Orestes P, Latham JR, Todorovic SM, Jevtovic-Todorovic V. In vivo silencing of the Ca(V)3.2 T-type calcium channels in sensory neurons alleviates hyperalgesia in rats with streptozocin-induced diabetic neuropathy. *Pain*. 2009; 145(1-2):184-95.

22. Omori M, Yokoyama M, Matsuoka Y, Kobayashi H, Mizobuchi S, Itano Y, Morita K, Ichikawa H. Effects of selective spinal nerve ligation on acetic acid-induced nociceptive responses and ASIC3 immunoreactivity in the rat dorsal root ganglion. *Brain Res.* 2008; 1219:26-31.

23. Frederick J, Buck ME, Matson DJ, Cortright DN. Increased TRPA1, TRPM8, and TRPV2 expression in dorsal root ganglia by nerve injury. *Biochem Biophys Res Commun*. 2007; 358(4):1058-64

24. Buchheit T, Van de Ven T, Shaw A. Epigenetics and the transition from acute to chronic pain. *Pain Med.* 2012; 13(11):1474-90.

25 Anand P. Neurotrophic factors and their receptors in human sensory neuropathies. *Prog Brain Res*. 2004; 146:477-92.

26. Passemard S, Sokolowska P, Schwendimann L, Gressens P. VIP-induced neuroprotection of the developing brain. *Curr Pharm Des*. 2011;17(10):1036-9.

27. Passemard S, El Ghouzzi V, Nasser H, Verney C, Vodjdani G, Lacaud A, Lebon S, Laburthe M, Robberecht P, Nardelli J, Mani S, Verloes A, Gressens P, Lelièvre V. VIP blockade leads to microcephaly in mice via disruption of Mcph1-Chk1 signaling. *J Clin Invest*. 2011; 121(8):3071-87.

28. Hill JM, Cuasay K, Abebe DT. Vasoactive intestinal peptide antagonist treatment during mouse embryogenesis impairs social behavior and cognitive function of adult male offspring. *Exp Neurol*. 2007; 206(1):101-13.

29. Hill JM, Hauser JM, Sheppard LM, Abebe D, Spivak-Pohis I, Kushnir M, Deitch I, Gozes I. Blockage of VIP during mouse embryogenesis modifies adult behavior and results in permanent changes in brain chemistry. *J Mol Neurosci*. 2007; 31(3):183-200.

30. Stack CM, Lim MA, Cuasay K, Stone MM, Seibert KM, Spivak-Pohis I, Crawley JN, Waschek JA, Hill JM. Deficits in social behavior and reversal learning are more prevalent in male offspring of VIP deficient female mice. *Exp Neurol*. 2008; 211(1):67-84.

31. Fuji K, Senba E, Fujii S, Nomura I, Wu JY, Ueda Y, Tohyama M. Distribution, ontogeny and projections of cholecystokinin-8, vasoactive intestinal polypeptide and gamma-aminobutyrate-containing neuron systems in the rat spinal cord: an immunohistochemical analysis. *Neuroscience*. 1985; 14(3):881-94.

32. Liu XH, Morris R. Vasoactive intestinal polypeptide produces depolarization and facilitation of C-fibre evoked synaptic responses in superficial dorsal horn neurons (laminae I-IV) of the rat lumbar spinal cord in vitro. *Neurosci Lett*. 1999; 276(1):1-4.

33. Dun NJ, Miyazaki T, Tang H, Dun EC. Pituitary adenylate cyclase activating polypeptide immunoreactivity in the rat spinal cord and medulla: implication of sensory and autonomic functions. *Neuroscience*. 1996; 73(3):677-86.

34. Delmas P. SnapShot: ion channels and pain. *Cell*. 2008; 134(2):366-366.

35. Schmutzler BS, Roy S, Hingtgen CM. Glial cell line-derived neurotrophic factor family ligands enhance capsaicin-stimulated release of calcitonin gene-related peptide from sensory neurons. *Neuroscience*. 2009; 161(1):148-56.

36. Sluka KA, Price MP, Breese NM, Stucky CL, Wemmie JA, Welsh MJ. Chronic hyperalgesia induced by repeated acid injections in muscle is abolished by the loss of ASIC3, but not ASIC1. *Pain*. 2003; 106(3):229-39.

37. Bourinet E, Alloui A, Monteil A, Barrère C, Couette B, Poirot O, Pages A, McRory J, Snutch TP, Eschalier A, Nargeot J. Silencing of the Cav3.2 T-type calcium channel gene in sensory neurons demonstrates its major role in nociception. *EMBO J*. 2005; 24(2):315-24.

38. Patapoutian A, Peier AM, Story GM, Viswanath V. ThermoTRP channels and beyond: mechanisms of temperature sensation. *Nat Rev Neurosci*. 2003; 4(7):529-39.

39. Tominaga M, Caterina MJ. Thermosensation and pain. *J Neurobiol*. 2004; 61(1):3-12.

40. Knowlton WM, Bifolck-Fisher A, Bautista DM, McKemy DD. TRPM8, but not TRPA1, is required for neural and behavioral responses to acute noxious cold temperatures and cold-mimetics in vivo. *Pain*. 2010; 150(2):340-50.

41. Denk F, McMahon SB. Chronic pain: emerging evidence for the involvement of epigenetics. *Neuron*. 2012; 73(3):435-44.

42. Tochiki KK, Cunningham J, Hunt SP, Geranton SM. The expression of spinal methyl-CpG-binding protein 2, DNA methyltransferases and histone deacetylases is modulated in persistent pain states. *Mol Pain*. 2012; 8:14.

43. Pollema-Mays SL, Centeno MV, Apkarian AV, Martina M. Expression of DNA methyltransferases in adult dorsal root ganglia is cell-type specific and up regulated in a rodent model of neuropathic pain. *Front Cell Neurosci.* 2014; 8:217.

44. Andersen HH, Duroux M, Gazerani P. MicroRNAs as modulators and biomarkers of inflammatory and neuropathic pain conditions. *Neurobiol Dis*. 2014; 71C:159-168.

45. Sakai A, Saitow F, Miyake N, Miyake K, Shimada T, Suzuki H. MiR-7a alleviates the maintenance of neuropathic pain through regulation of neuronal excitability. *Brain*. 2013;136(Pt 9):2738-50.

46. Sakai A, Suzuki H. Nerve injury-induced upregulation of miR-21 in the primary sensory neurons contributes to neuropathic pain in rats. *Biochem Biophys Res Com*. 2013; 435: 176-181

47. Koada B. Successful treatment of esophageal dysmotility and Raynaud's phenomenon in systemic sclerosis and achalasia by transcutaneous nerve stimulation. Increase in VIP plasma concentration. *Scand J Gastroenterol.* 1987; 22: 1137-1146.

47. Colwell CS, Michel S, Itri J, Rodriguez W, Tam J, Lelievre V, Hu Z, Liu X, Waschek JA. Disrupted circadian rhythms in VIP- and PHI-deficient mice. *Am J Physiol Regul Integr Comp Physiol*. 2003; 285(5):R939-49.

48. Yalcin I, Charlet A, Freund-Mercier MJ, Barrot M, Poisbeau P. Differentiating thermal allodynia and hyperalgesia using dynamic hot and cold plate in rodents. *J Pain*. 2009; 10(7):767-773.

49. Juif PE, Poisbeau P. Neurohormonal effects of oxytocin and vasopressin receptor agonists on spinal pain processing in male rats. *Pain*. 2013; 154(8):1449-56.

50. Lelievre V, Hu Z, Byun JY, Ioffe Y, Waschek JA. Fibroblast growth factor-2 converts PACAP growth action on embryonic hindbrain precursors from stimulation to inhibition. *J Neurosci Res*. 2002; 67(5):566-73.

51. Favrais G, Couvineau A, Laburthe M, Gressens P, Lelievre V. Involvement of VIP and PACAP in neonatal brain lesions generated by a combined excitotoxic/inflammatory challenge. *Peptides*. 2007; 28(9):1727-37.

52.Benbouzid M, Pallage V, Rajalu M, Waltisperger E, Doridot S, Poisbeau P, Freund-Mercier MJ, Barrot M. Sciatic nerve cuffing in mice: a model of sustained neuropathic pain *Eur J Pain*.2008; 12: 591–599

Figure legends

Figure 1: Mechanical and thermal nociception assessment in WT, VIP heterozygous (HZ) and KO mice. For the three animal groups, histograms (average ± SEM) illustrate the mean mechanical nociceptive threshold measured with the von Frey filaments (**A**), the mean latency (in seconds) to observe a paw withdrawal response after paw illumination with a radiant heat (**B**: Hargreaves test) and the temperature threshold to observe the first aversive behaviour (paw withdrawal, licking or jump) for mice submitted to a slow cold (**C**: from 20°C to 0°C) or a hot temperature ramp (**D**: 30°C to 46°C). Symbols (*** and $$) indicate statistical significance after Tukey *post hoc* test at $P < 0.001$ and $P < 0.01$, respectively.

Figure 2: Comparison of the spinal processing of sensory messages by a wide dynamic range (WDR) neuron in the dorsal spinal cord of WT and VIP null mice ($VIP^{-/-}$). **A**. Representative traces illustrating the responses of a deep dorsal horn neurons in WT and $VIP^{-/-}$ mice to a mechanical stimulation of the paw receptive field with von Frey filaments of 2g, 4g, 8g and 15g. **B**. Histogram illustrating the mean threshold for 10 recorded neurons in each animal group (white bar: WT; black bar: $VIP^{-/-}$). **C**. Representative traces showing the action potential discharge of a WDR neuron after stimulating electrically the peripheral receptive field. Note that APs are appearing with a variable delay from the stimulus artefact due to the different conduction properties of the stimulated sensory neurons. The responses of a WDR neuron recorded from WT and $VIP^{-/-}$ are exemplified for an electrical stimulation of 12V and 30V. **D**. Mean electrical threshold (±SEM) for A-type and C-type fibers in WT mice (white bars) and $VIP^{-/-}$ mice (black bars). Statistical code: Student, ***$p<0.001$.

Figure 3: Time course of mechanical nociceptive threshold in WT (open symbols, n = 6) and VIP null mice (black symbols; n = 6) before and after i.p. injection of VIP (2µg in saline, total volume 10µl). VIP has been injected immediately after measuring the threshold at 72h (arrow). Data (average ± SEM) were statistically analyzed and asterisks indicates statistical significance after Wilcoxon post hoc comparisons

Figure 4 : Time course of the spinal nociceptive processing recovery of VIP null mice following an i.p. injection of VIP. Low electrical (A) or mechanical (B) thresholds (average ± SEM) for A- (triangles) and C-type fibers (squares) recovered to baseline values of WT animals (black symbols) in less than 2.5 h after VIP treatment. In the upper part of panel B, traces are the representative responses of deep dorsal horn neurons in WT (right) and $VIP^{-/-}$ mice (4 left traces) to mechanical stimulations of the paw receptive field with von Frey filament of 6g in KO recorded 0, 2, 3 and 4 hours following VIP administration. All the other data (average ± SEM) were analyzed using Wilcoxon post hoc test. Symbols: NS: no significant differences (*i.e.* $p>0.05$) between KO-treated and WT mice.

Figure 5: VIP receptor-mediated signal transduction implicated in pain. **A**: pharmacological studies of VIP receptor mediating mechanical nociception in mice. Compared to WT (basal threshold) and KO mice (hypersensitive), KO animals injected with VIP, VPAC1 agonist or PACAP (2µg ea.) exhibited a normal phenotype whilst VIP or VPAC1 agonist (+VPAC1) analgesic action was completely blocked by VPAC1 antagonist (+AVPAC1). Data (average ± SEM) were statistically analyzed and asterisks indicate statistical significance after Wilcoxon post hoc comparisons B**:** Expression of VIP receptors (VPAC1 and VPAC2) in WT and VIP KO mice. Quantitative RT-PCR performed in Spinal cord samples showed that VIP deficiency or VIP injection had no significant effect on receptor expression. C: Representative micrographs of lumbar spinal cord section used for quantification of ΔFosb and pCREB immunostaining in three areas and the corresponding immunostaining observed in the area 1 of WT and VIP-deficient SC prior to VIP injection (insets; scale bar: 20µm). D: Quantification of positive nuclei in the three areas of lumbar spinal cords of KO animals (n= 5/group) treated with VIP (2ng) for 1 to 24h. Two-way ANOVAs showed that VIP significantly decreased ΔFosB in areas 1 and 2 but increased pCREB in less than an hour in all three areas.

Figure 6: Gene expression studies by quantitative RT-PCR in total RNA samples extracted from the dorsal root ganglion and spinal cord of control ($VIP^{+/+}$), VIP-deficient animals ($VIP^{-/-}$) supplemented (+VIP) or not (0).**A**: Expression and modulation by VIP of nociception-related ion channels **B** : Sensitivity to VIP of nociception-related neurotrophic factors expression. **C**: modulation of epigenetic genes (involved in histone

acetylation and DNA CpG methylation) and microRNAs. For all studies quantitative real-time RT-PCR was performed in duplicate on RNA samples collected from 5 animals per group. Data (average ± SEM) were analyzed using Two-way variance analyses (ANOVA) followed by multiple comparisons were done to confirm statistical significance compared to controls at $p < 0.05$ (*),$p < 0.01$ (**) or $p < 0.005$ (***). Significant differences at $p < 0.05$ ($^{\$}$), $p < 0.01$ ($^{\$\$}$) or $p < 0.005$ ($^{\$\$\$}$) between untreated or treated VIP KO are also reported on graphs.

Figure 7: DNA methylation status of the 3 pain-related channels found upregulated in VIP KO mice compared to WT. **A**: Position of methylation sites (|) and primers (→←) used to analyze chromatin immunoprecipitated fragments in upstream regions (-2000 to +1000) of the genes of interest. **B**: Quantification by qPCR of the enrichment of methylated DNA relative to input genomic DNA around the transcription start site was quantified using specific sets of primers. Genomic DNA extracted from the spinal cords of WT and VIP KO mice was sheared by sonication and immunoprecipitated with anti-5-methylcytosine antibody. Data represent the mean ± SEM (*$p < 0.05$, two-tailed t-test; n = 5/group). Inset: Representative gel picture of PCR products obtained by amplication of genomic DNA obtained after IP performed with antibody (C) or with control IgG (ig). Specific bands at the expected sizes (L: 100bp ladder) where obtained in positive (C) compared to negative (Ig) samples confirming the presence of methylated DNA after immunoprecipitation of WT DNA.

Figure 8: Analgesic action of VIP in neuropathic WT mice. **A**: Adult male C57 Bl/6 mice with unilateral cuff-implantation of the right sciatic nerve (●) while Sham animals underwent the same surgical procedure without cuff-implantation (○) . All animals were kept and monitored for a 1 week to let them recovered from surgery. The associated pain before the IP administration of single dose of VIP (2µg) was determined using the von Frey hairs at the given time points. Compared to the untreated, cuff-implanted animals that exhibited an ipsilateral mechanical hyperalgesia that persisted at least 2 months (not shown), VIP-injected animals exhibited a three day-long lasting analgesia. Data are expressed as mean ± SEM. Duncan post-hoc: *$P < 0.05$ compared to PT value (control). **B**: VIP induced similar changes gene expression for pain channels

and neurotrophic factors than those observed in KO mice after 24h and 96h of treatments. Quantitative real-time RT-PCR was performed in duplicate on RNA samples collected from 5 animals per group. Data (average ± SEM) were analyzed using Two-way variance analysis (ANOVA) were done to confirm statistical significance compared to controls (cuffed) at $p < 0.05$ (*),$p < 0.01$ (**) or $p < 0.005$ (***).

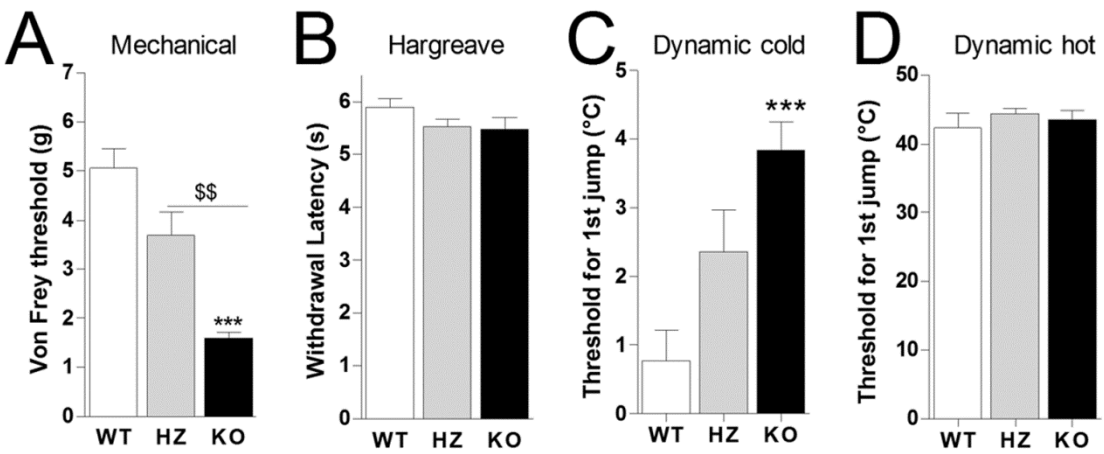

Maduna et al. Figure 1

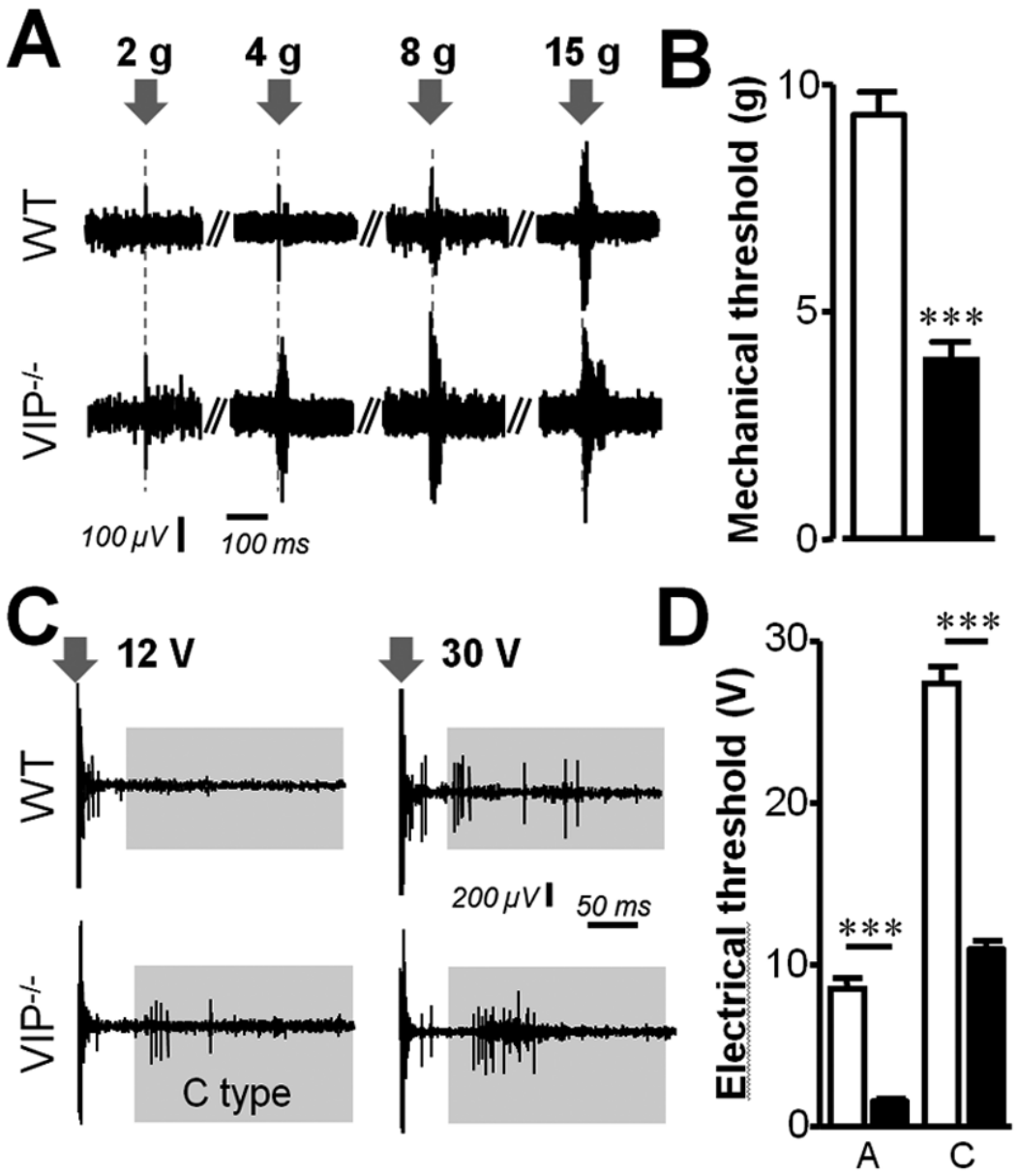

Maduna et al. Figure 2

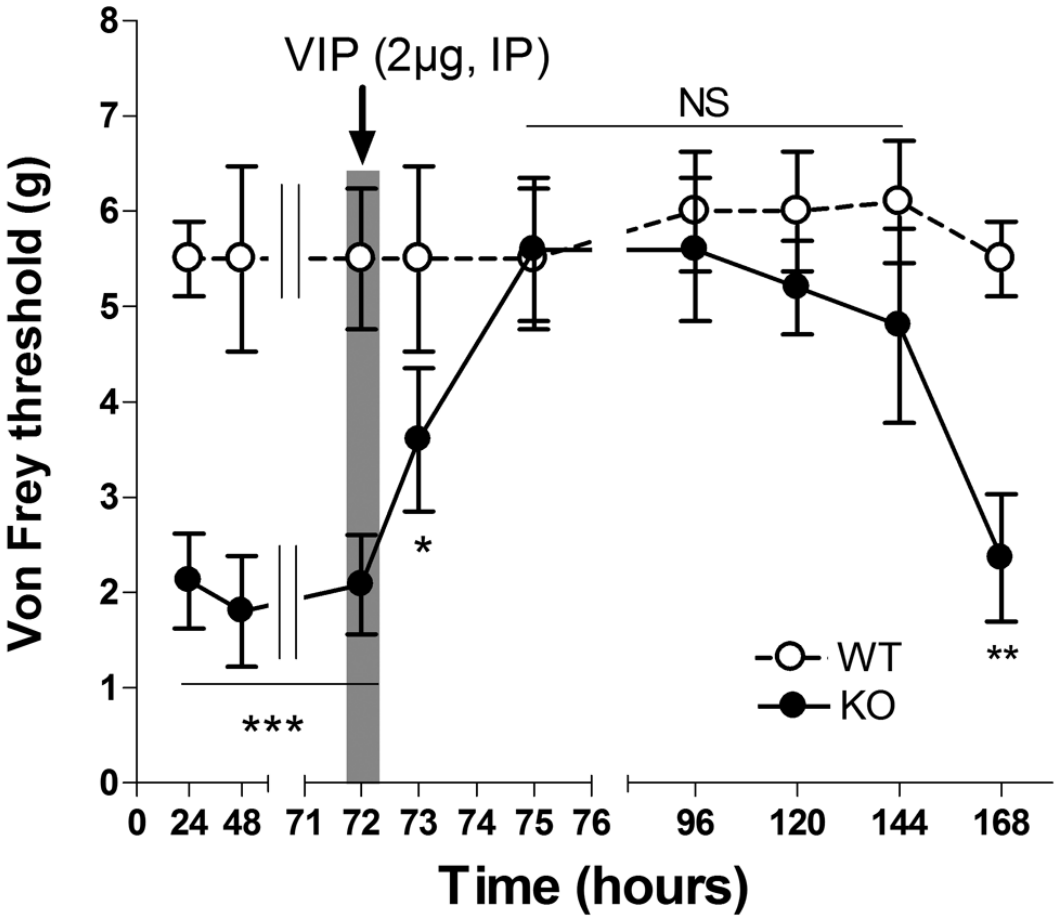

Maduna et al. Figure 3

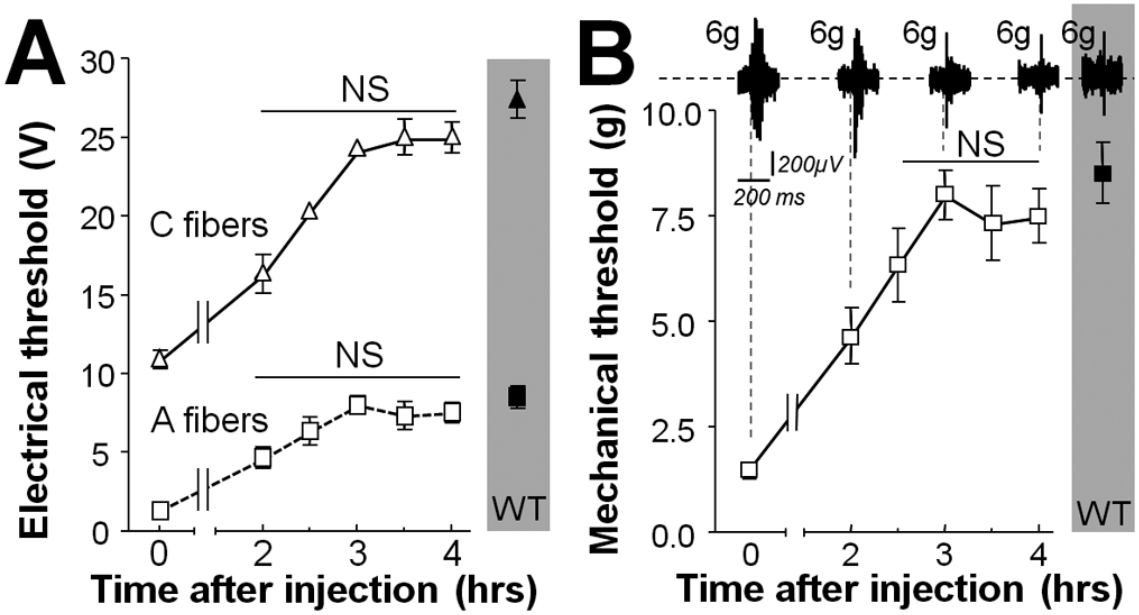

Maduna et al. Figure 4

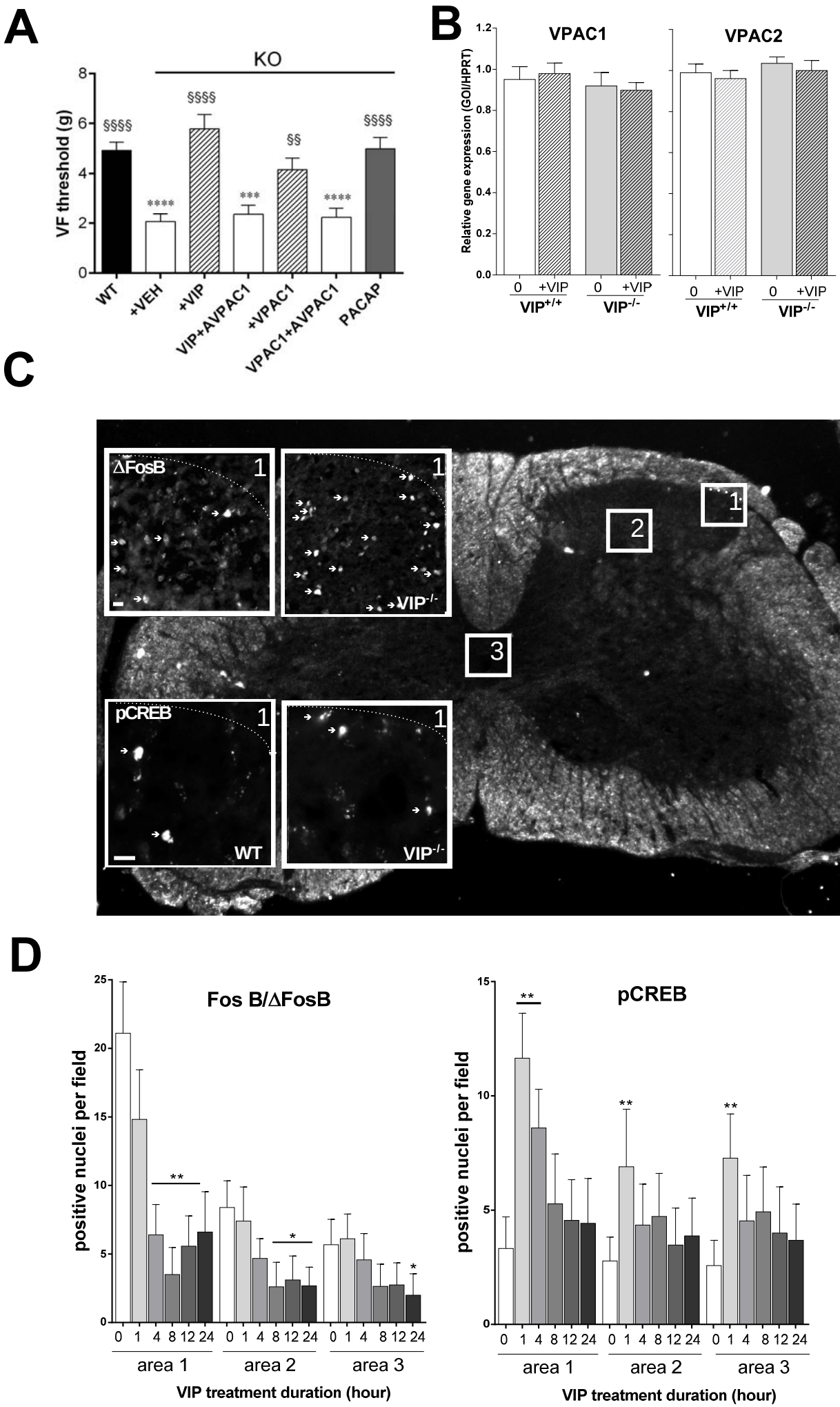

Maduna et al. figure 5

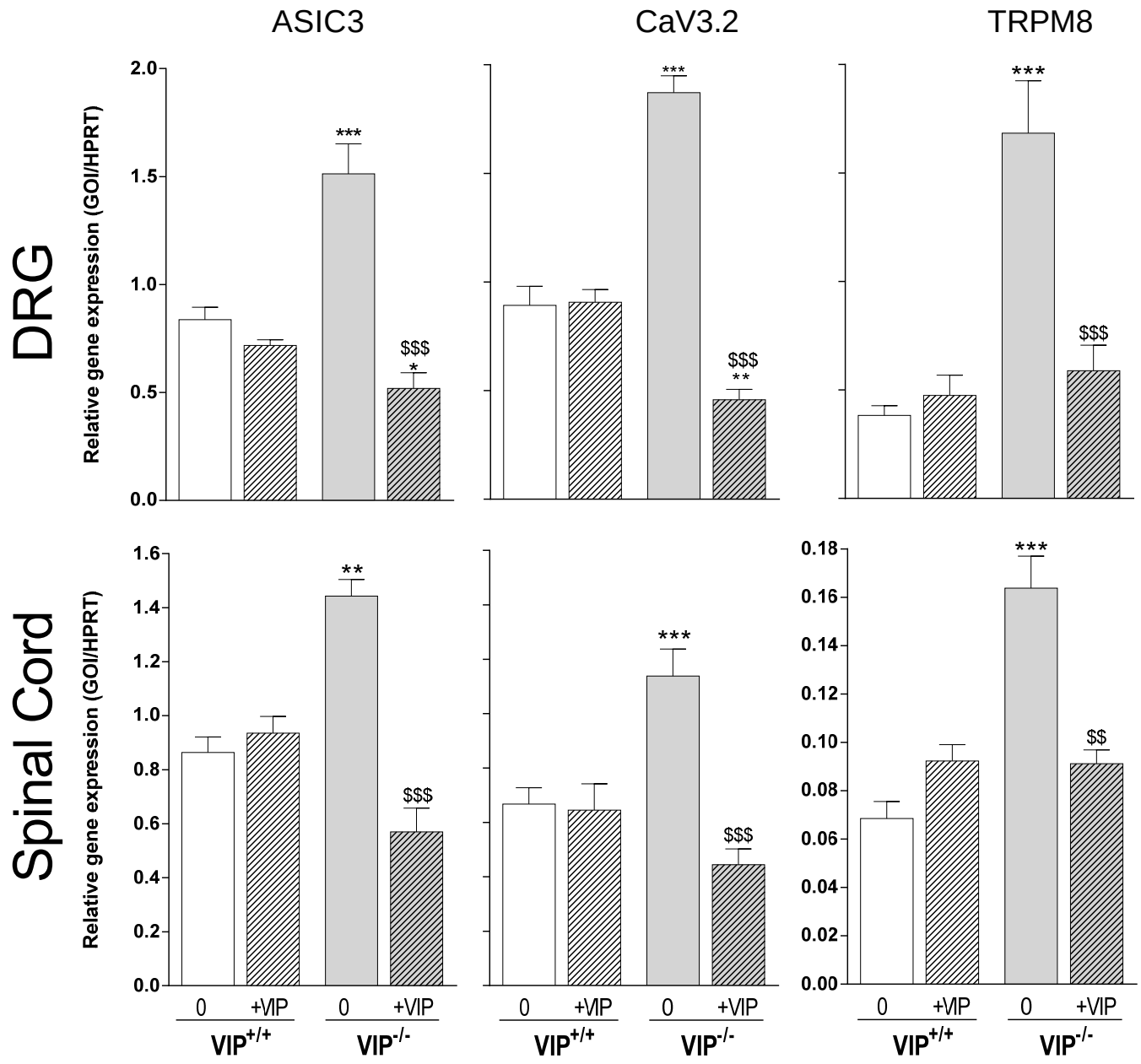

Maduna et al. figure 6A

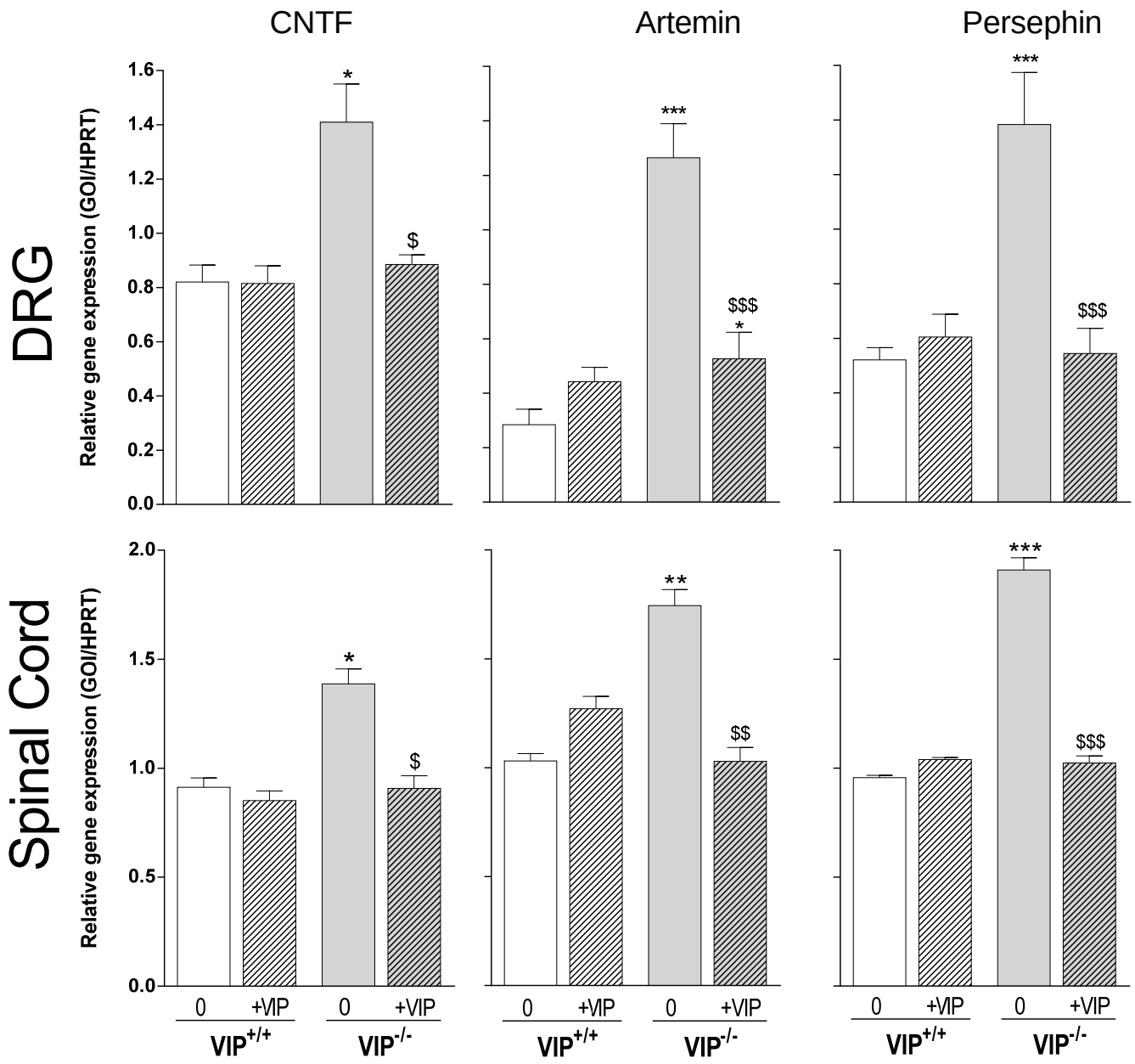

Maduna et al. figure 6B

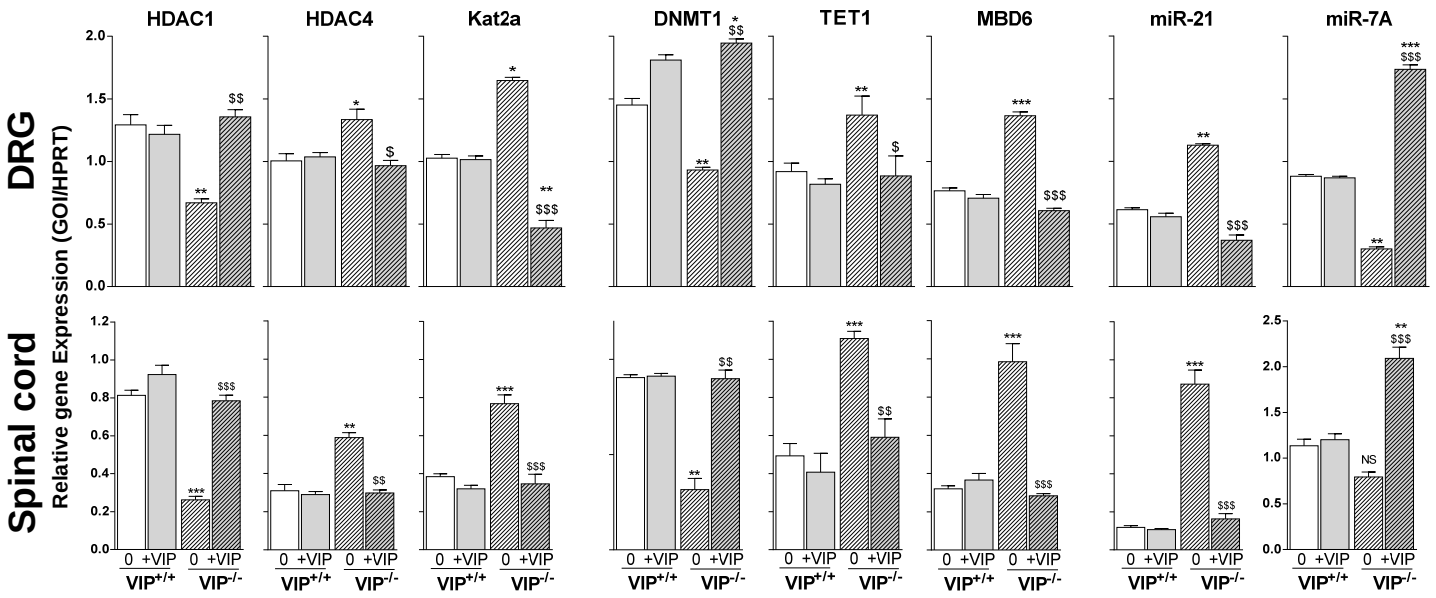

Maduna et al. Figure 6C

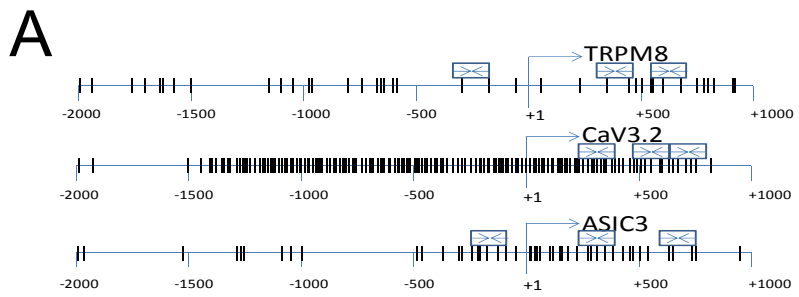

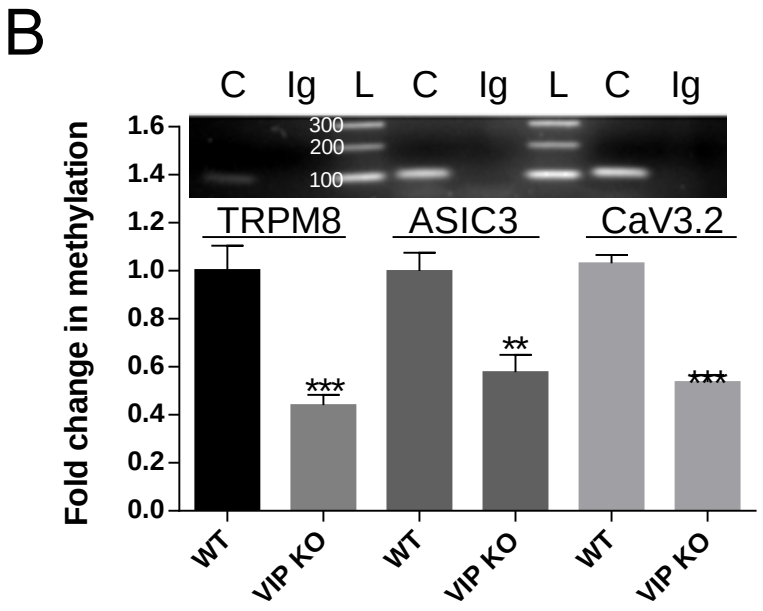

Maduna et al. figure 7

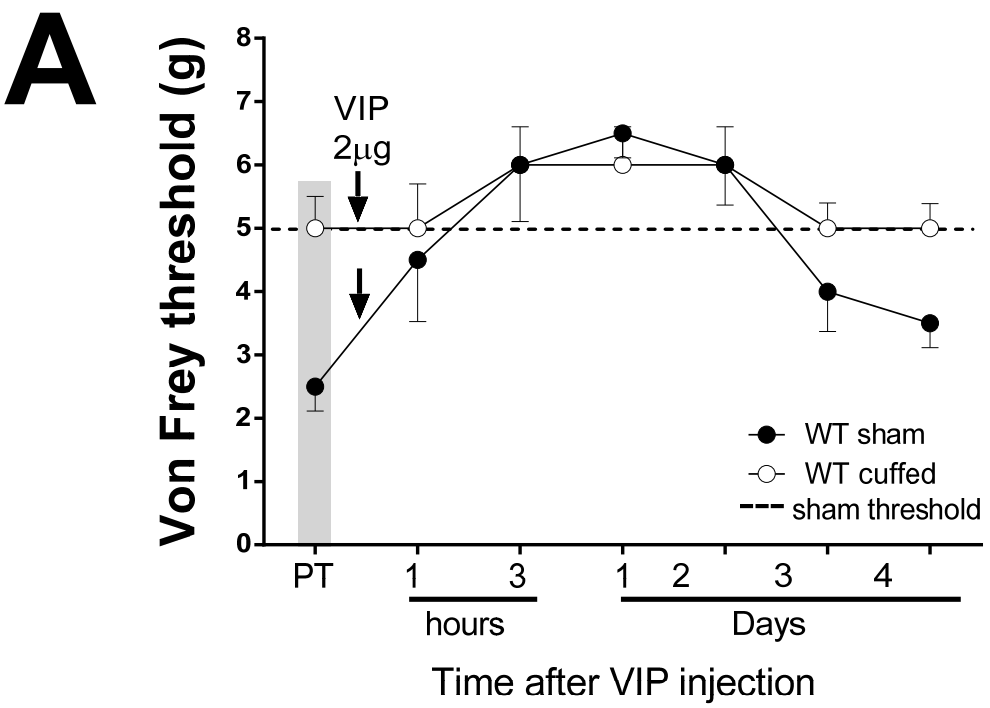

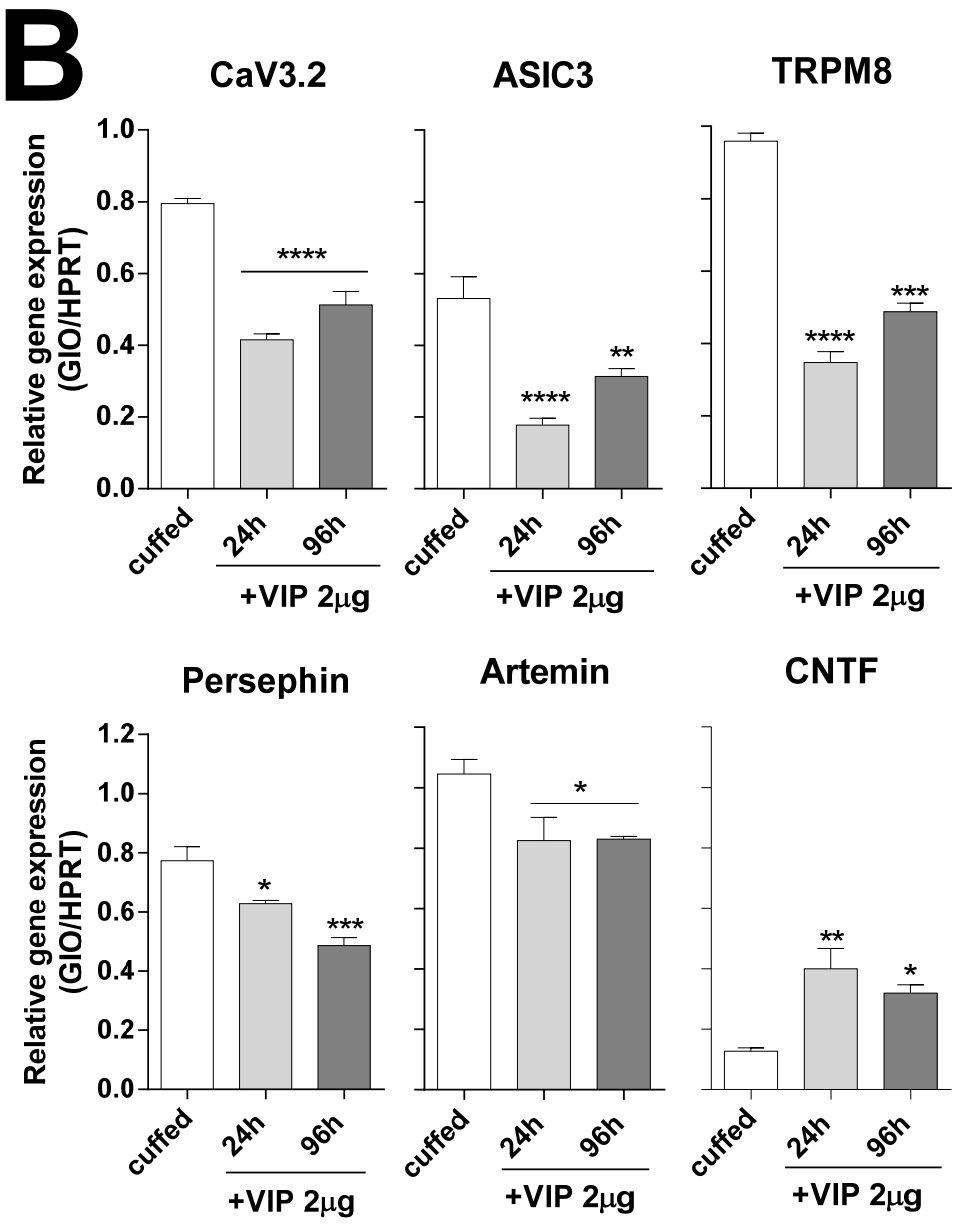

Maduna et al. figure 8

Supplementary figures

Supplementary information

S1 (Table I): information relative to the primer sets used in quantitative RT-PCR and PCR. Primers sets were designed using the similar strategy for optimal amplification at 62˚C (see methods). To do so, coding sequences of the genes of interest were retrieved from NCBI were initially blast to identify the portions of sequences that are unique in mouse. These fragments were then analyzed for secondary structure using M-fold software. Sequences (about 150-200 bp) lacking significant secondary structure were imported into oligo6 software to design highly stringent primer sets. Ultimately, these primers were blasted in cDNA databases to ensure their specificity.

S2: Expression and modulation by VIP of nociception-related ion channels in the dorsal root ganglion and spinal cord of control ($VIP^{+/+}$), VIP-deficient animals ($VIP^{-/-}$) and i.p. supplemented with a single injection of 2µg VIP (+VIP) or not (0). Quantitative real-time RT-PCR was performed in duplicate on RNA samples collected from 5 animals per group. Levels of gene expression (GOI for gene of interest) were corrected to the mRNA level of the housekeeping gene HPRT. Data (average ± SEM) were analyzed using two-way variance analysis (ANOVA) followed by multicomparison were used to confirm that gene expression increases or decreases were significantly different from controls at $p < 0.05$ (*),$p < 0.01$ (**) or $p < 0.005$ (***). Significant differences at $p < 0.05$ ($^{\$}$), $p < 0.01$ ($^{\$\$}$) or $p < 0.005$ ($^{\$\$\$}$) between untreated or treated VIP KO are also reported on graphs.

S3 : Sensitivity to VIP of nociception-related peptides expressed in spinal cord and DRG samples isolated from control ($VIP^{+/+}$), VIP-deficient animals ($VIP^{-/-}$) and i.p. supplemented with a single injection of 2µg VIP (+VIP) or not (0). Quantitative real-time RT-PCR was performed in duplicate on RNA samples collected from 5 animals per group using the similar procedure. Data (average ± SEM) were analyzed using One-way variance analysis (ANOVA) followed by Bonferroni post hoc test were done to confirm statistical significance compared to controls at $p < 0.05$ (*),$p < 0.01$ (**) or $p < 0.005$ (***). Significant differences at $p < 0.05$ ($^{\$}$), $p < 0.01$ ($^{\$\$}$) or $p < 0.005$ ($^{\$\$\$}$) between untreated or treated VIP KO are also reported on graphs.

S4 : Sensitivity to VIP of epigenetic modulators expressed in spinal cord and DRG samples isolated from control ($VIP^{+/+}$), VIP-deficient animals ($VIP^{-/-}$) supplemented (+VIP) or not (none). Quantitative real-time RT-PCR was performed in duplicate on RNA samples collected from 5 animals per group using the similar procedure. Data (average ± SEM) were analyzed using two-way variance analysis (ANOVA) followed by multicomparison were done to confirm statistical significance compared to controls at $p < 0.05$ (*),$p < 0.01$ (**) or $p < 0.005$ (***). Significant differences at $p < 0.05$ ($^{\$}$), $p < 0.01$ ($^{\$\$}$) or $p < 0.005$ ($^{\$\$\$}$) between untreated or treated VIP KO are also reported on graphs.

Gene name	Primer sequence (sense & reverse)	NBCI access	Spanning regions	Amplicon size (bp)	Gene name	Primer sequences (sense & reverse)	NBCI access	Spanning regions	Amplicon size (bp)
ACCN1 (ASIC1)	GTGGTCAAATGGGATTGTTCA CTTTGCCAAGCAGGTCTAAT	BC138530	1738-1845	108	**VPAC1**	TCACTATGTCATGTTTGCCTT GAAAGACCCTACGACGAGTT	NM011703	1195 - 1276	81
ACCN2 (ASIC2)	TGCTGTTACCATGGACTCGG GCAGTTTTCCACCAGGTAACG	BC67025	1066-1156	91	**VPAC2**	TCTACAGCAGACCAGGAAACA GTAGCCACACGCATCTATGAA	NM009511	294 - 382	88
ACCN3 (ASIC3)	GCATCTGTGGATCCCGACT GGCGACACCCTATTAAGCTAT	AY261387	856-946	91	**HDAC1**	CGTTCTATTCGCCCAGATAAC AACTCAAACAAGCCATCAAAT	NM008228	246 - 343	97
NaV1.3	CGCTTTGAAGGCATGAG AGATGAGGCACACCAGTAGCA	NM018732	4082-4166	85	**HDAC2**	TTGCCATTGCTGATGCTCG TGGGAATTTCACAATCAAGGG	NM008229	1088-1187	99
NaV1.7	TCCTGGAGTATGCTGACAAGA CAACACCAGGCATTAGTGAA	BC17247	3916-4021	106	**HDAC3**	GACAGGACTGACGAGGC CCATCATAGAACTCATTGGG	NM010411	1237-1322	85
naV1.8	ATTTTCGGTGGCTTCTTCACG TGTCCTGGCCCCCTAG	NM009134	4242-4332	91	**HDAC4**	ATGTACCACGCCAAAGATGA CTGCTCCGTCTCTCAGGTACT	NM207225	807-910	103
NaV1.9	TTCACCAATGGCTGGAACTTA GGGAAGACGTTGCTGTTCTC	NM011887	4268-4362	95	**HDAC5**	CTACATCTCCCTGCATCGCTA GCCACATTTACGTTGTACCC	NM010412	3008-3112	104
CaV2.2	ACGTCTTTGACTTTGTCACGG GGCGAAGGAAGCTTAGGT	AK134542	1009-1101	93	**HDAC6**	AATCGTGGATTGGGATGTTC CGGTGCAGGGACACGTATAAT	NM010413	2274-2360	86
CaV3.2	GATGTCATCCCTCAAACCCAT CCCTTTGAAGAGCTGCACC	NM001163691 NM021415	4518-4612	96	**HDAC7**	TCATTGTTGACTGGGATGTTC GCGATGAAGGGAAATGTAGAG	NM019572	2456-2544	88
Piezo1	GGCTACCCCACCCGTATCTTG TCCACCAGGAACGGCACTAGA	HQ215520	6298-6398	101	**HDAC8**	TTTACAGCTGGGAGCAGATAC CAGCTGCCACTGTAGGACATA	NM027382	867-972	105
Piezo2	AGTGGCAGTGTAGCATCAAGC CAGCCTCCACCTCCTCGAT	HQ215521	5449-5539	91	**HDAC9**	CCCTGCCCAATATCACTCT GTCTGAGCATCTGTGTCTCGC	NM024129	1308-1409	101
TREK1	ACATCTCCCCACGAACTGA TTCCTAGCTGATCACCAACCC	NM010607	843-950	108	**HDAC10**	CCGACTATTTGGCTGCCTTTC GAGTCAAATCCAGCCGACA	NM199198	959-1049	90
TRPV1	ATCCTCAGAGACCTGTGTCGG TATTCTTCCCATCCTCGATCA	AY445519	1720-1816	97	**HDAC11**	TTCTGTGCCTATGCAGACATC AGATCAATGATGGTGGCTC	NM144912	182-267	85
TRPV4	GCTTCCTGCTTGTGTACCTG AGTTGCTCTGGTCCTCGTCAC	NM022017	1958-2065	108	**HAT1**	ATGTTGAAGGCAAAATCAGAC TCCAAAAGGCTTGAAATTAGT	NM026115	346-449	104
TRPM8	TGTGGCCTTCTTCACGTC TGGCACTGAGTGGAAGTCCAT	NM134252	2359-2470	112	**Kat2a**	CGTGCTGCTCTGGCTCGTGGG CGAGGCGGGCGATATATT	AF254441	1524-1606	83
TRPA1	TCGACCGGAGTGTTTATCTTC TGGATTAAGGAAAGCAATGGG	NM177781	2653-2756	104	**Kat2b**	GGTGTCATTGAATTCCACG CTGGTGGGAAAACACATTCTG	NM020005	1432-1533	102
Kcna1	TATTGCCATTGTGTCGGTCAT CCGTGAAGTCCTTGTCGTC	NM010595	2581-2675	95	**DNMT1**	CCAAGAACTTTGAAGACCCAC GGCTCTGACACCTGATGCTT	NM010066	3370-3472	103
Kcna2	CTATTCCAACAGCACCATC GAAACTCAAAGGAGAACCAGA	BC138651	1105-1205	101	**DNMT2**	GAAAGGGACAGGAAACATCA ACTTGGGTGGTAAAAGGTACT	NM010067	744-846	103
BDNF	ATGGGACTCTGGAGAGCGTG AGCTCTTCGATGACGTGCTCA	NM007540	780-876	97	**DNMT3A**	GGGGCGTGAAGTGCTCATGT GCCCCACCAAGAGATCCACAC	BC007466	1858-1937	80
NGF	CACAGACATCAAGGGCAAGGA GCTCGGCACTTGGTCTCAAA	NM013609	743_838	96	**Tet1**	ACAAAAAGAAAAGGGCCCATA CTTCCCCTTCTGGCCAAACC	NM027384	4131-4230	100
PSPN	GGCAGATAAGCTCTCATTTGG AGACGGACATGGTTGTTACCC	NM008954	96-176	81	**MBD1**	GCTGGGTTGTGGCCTTA GGAGGAAGTCAGGAAGGTCGT	NM013594	1560-1648	89
NRTN	TTGCCCCGCTACGACGCCCTC TCGGGGGCGCCCTGGAGCAG	NM008738	488-543	88	**MeCP2**	TCCAGGGCCTCAGAGACAA CAGAATGGTGGGCTGAAGGTT	NM010788	235-342	108
ARTN	CCTGGTGGCCAACCCTAGC GGACATTGGGTCCAGGGAAG	NM009711	1136-1206	71	**MBD3**	CCAGCAACAAGGTCAAGAGC CTGCAATGTCAAAGGCACTCA	NM013595	1444-1545	101
NT3	AAGTCCTCAGCCATTGACATT TGTTTCACAGGAGAGTTA	BC065785	700-779	80	**MBD4**	TTTTGAAAGGAACTGCAAGTC CCACCTTCTGAACCACAGAT	NM010774	802-906	104
NT 4/5	CTCCCTCGCCACTCCTGTTCT GGGGCAGGGTGGAGGATG	NM198190	233-323	91	**MBD5**	TCTCCAGGGACACCAGAATCT AGTTCTGAAACAGACAAGCCA	NM029924	4921-4995	74
GDNF	GTGTTGCTCCACACCGCGTCT GGTCTTCAGCGGGCGCTTC	BC119031	143-215	73	**MBD6**	CAGACCCCTAGACGGACTCGT GCACAGAGGGGAGAATAGGCT	NM033072	1301-1394	93
CNTF	GCCTCTCATCCTGGACCAAT ATGTATTCCTTCCCTGCGTAG	NM016673	945-1034	90	**Sirt1**	CCAAACTTTGTTGTAACCCTG AGAGGTGTTGGTGGCAACTC	NM019812	1531-1633	102
CGRPα	AGAATAAGTTGCCTATTGTGC GGGACCATATTTGCTACCAG	AF330212	648-744	97	**Sirt2**	TCCTGCAGAAAAGAATACACG ACACGATATCAGGCTTTACCA	NM022432	695-800	105
galanin	CACATGCCATTGACAACCACA GGGCACATCAACACTTCCTA	BC044055	280-389	109	**miR-7A**	TTCTGTGTGGAAGACTAGTGA GCAGACTGTGATTTGTTGTC	LM608655	17-83	66
NPY	CGTGTGTTTGGGCATTCTGG AGCGGAGTAGTATCTGGCCA	AF273768	57-153	96	**miR-21**	CAGACAGCCCATCGACTG TTCTGTGTGGAAGACTAGTGA	NR029738	17-79	62
	MEDIP experiment								
TRPM8 Primer set 1	TATTCCCACCTGCCTATCAG GGCTCCATCAACCTACATGCT	AC087780/ NM134252	-380 to -272	108	**ASIC3 primer set 3**	ACATGCTGCCTACCTTCGTGC GGCTCTGGCGTAGAGTTGTG	NM183000	627-723	98
TRPM8 Primer set 2	TGGAGCCAAAAACTTTGCTT GTGAGAATCCACGCACCTTT	NM134252	628-720	92	**CaV3.2 Primer set 1**	AACAGCCCGTCCCATACC GATGCGGAAAACCGCTAAAT	BC138026	371-465	95
TRPM8 Primer set 3	ATAGGCGAGGTGGTGAGAGA GTGTCCCTGTTGGAGACCAT	NM134252	1021-1108	88	**CaV3.2 Primer set 2**	GTGGTTCGAGCACATTAGCA GTTCTGAACGGCACTCAACA	BC138026	632-726	94
ASIC3 Primer set 1	TTTCACCTGTCTTGGCTCCT CAGGATAGTGGTGGGGATTG	AC120353/N M183000	-172 (89) to -72 (189)	87	**CaV3.2 Primer set 3**	TGGAGGCCTTTGATGACTTC GGTGTCACCCAGGTAGCATT	BC138026	739-842	103
ASIC3 Primer set 2	TTCGCCAACAGCTGCACGATG CCGCCAGCGACAGGAGTACAG	NM183000	322-427	106					
	Housekeeping gene used in all experiments								
HPRT	TGGTGAAAAGGACCTCTCGAA TCAAGGGCATATCCAACAACA	NM013556	637 - 727	90					

Table I: information relative to the primer sets used in quantitative RT-PCR and MEDIP experiments

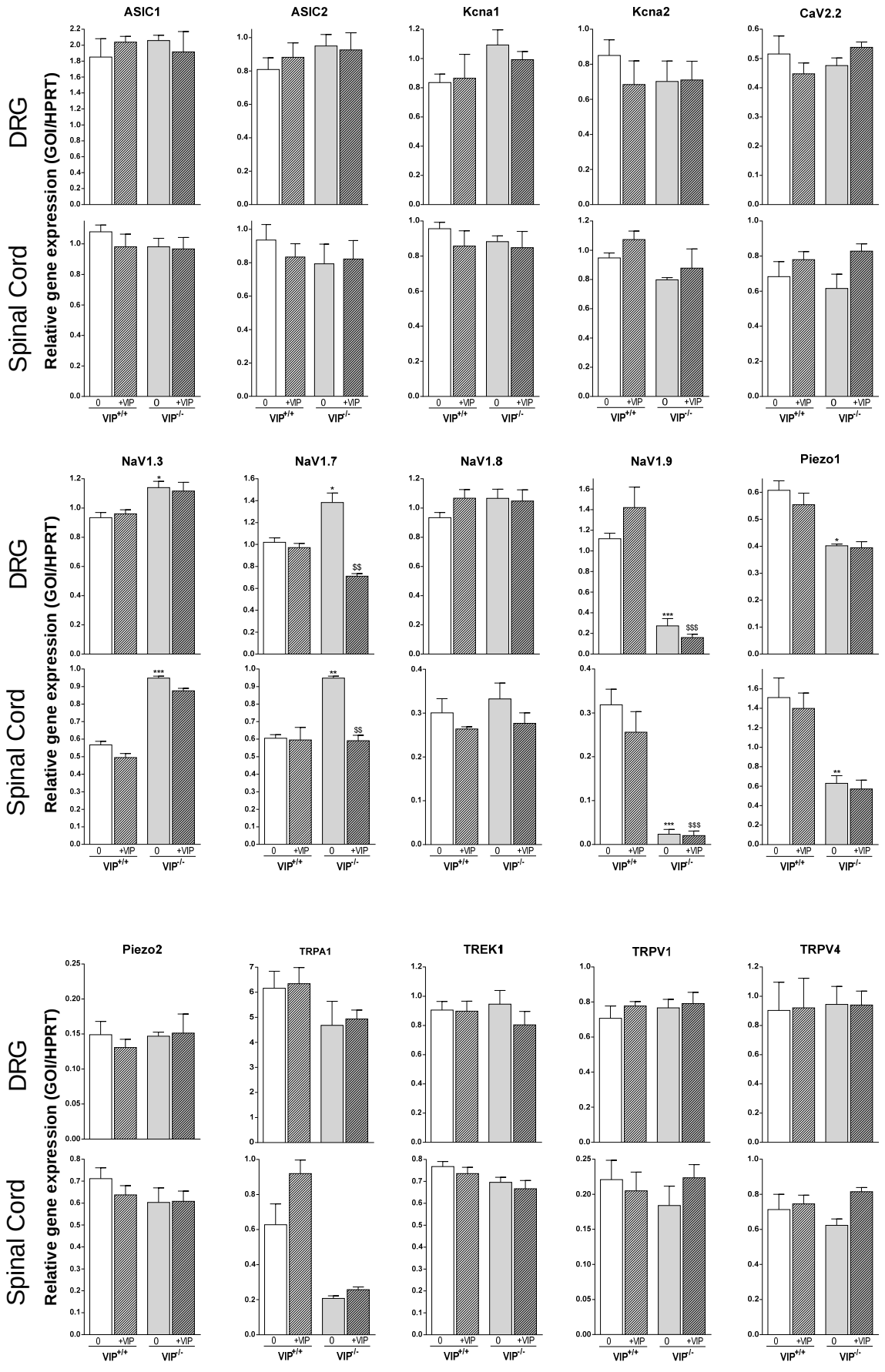

Maduna et al. S2

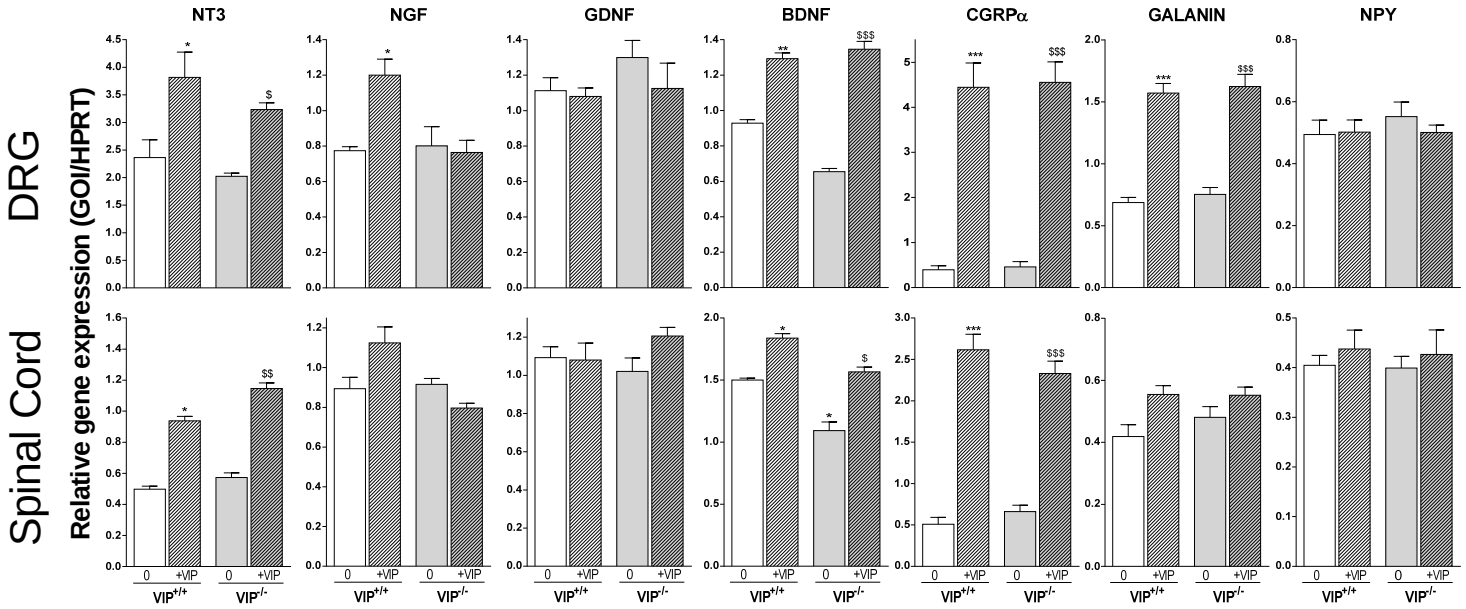

Maduna et al. S3

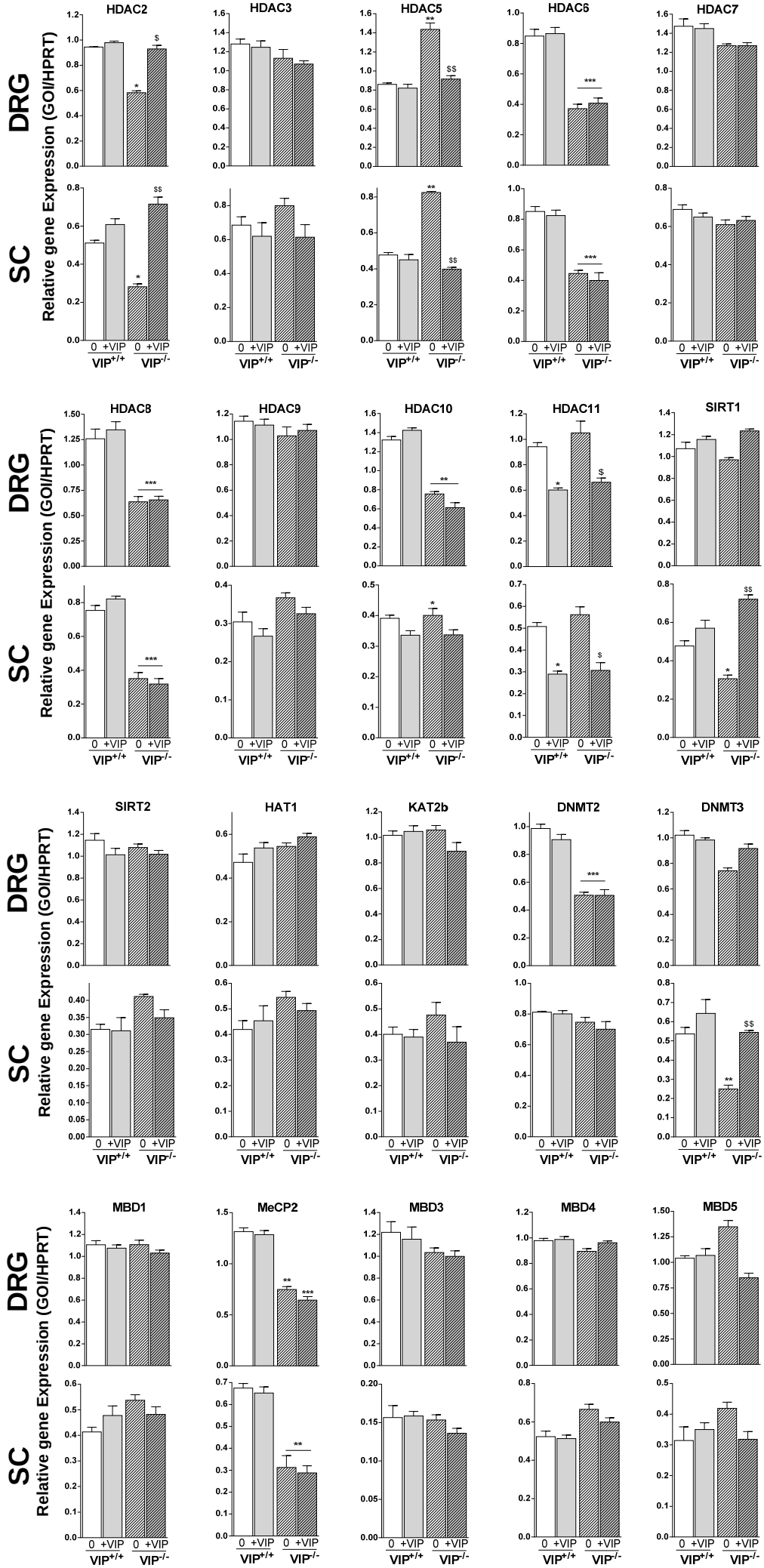

Maduna et al. S4

Results

Results will be presented in the following format:

1. Publication 2 (in preparation): Loss of VIP causes microcephaly with sustained cortical defect due to localized downregulation of Mcph1-Chk1 crosstalk and premature neuronal differentiation.

2. Publication 3 (in submission): Hyperalgesic VIP-deficient mice exhibit VIP-reversible alterations in molecular and epigenetic determinants of cold and mechanical nociception

3. VIP knockout mice exhibit spontaneous hyperactivity in the thalamus

Supplementary Results

VIP deficiency predisposes pregnant mice to mechanical but not cold allodynia

Result 3. VIP knockout mice exhibit spontaneous hyperactivity in the thalamus

As previously demonstrated (see Publication 2), VIP knockout mice are hypersensitive to mechanical and thermal (cold) pain. In addition, we also demonstrated that these mice exhibit long-term brain deficits affecting cortical regions and the corpus callosum. Therefore, we investigated whether basal sensory processing is aberrant in these mice, and whether that could provide a functional link between the neurodevelopmental deficit and heightened pain response.

Single unit recordings were performed in anesthetized mice for measurement of spontaneous activity. Initially all the cells recorded from the thalamus were pooled for statistical analysis. However, due to the high variability arising from this, the dorsal (LDDM) and the ventral (VL) thalamus were grouped separately for analysis (Figure 11, top panel). From this we found that although cells from dorsal nucleus fired at the same rate between wildtypes and knockouts, cells for the ventral nucleus showed a specific trend. In the ventral nucleus knockout cells had 3 times as much bursting activity as wildtypes though not significantly different. Interestingly, bursting cells in knockout mice fired at a significantly higher frequency than wildtypes Figure 11, lower panel). As expected, there were no significant differences in any of the parameters measured in the primary somatosensory cortex (Figure 12).

Overall Discussion

The work presented here has benefited greatly from the expansive framework offered by VIP knockout mice. This has facilitated the characterization of a genetic model from a neurodevelopmental perspective, while allowing parallel exploration of clinically relevant phenotypes. Ultimately, we could:

relate early developmental processes and their implications on adult physiology

take advantage of the exogenous availability of VIP to explore environmental influence on intrinsic biological machinery, and

explore and demonstrate the therapeutic potential of a maternally secreted factor with developmental and postnatal implications

The following sections summarize the main findings of this body of work

1. The VIP knockout mouse is a model for microcephaly

The incidence of genetic microcephaly is very low, ranging from 1 in 10000, and up to 1 in 1 000 000 depending on population and country, affecting mainly consanguineous societies (Mahmood et al. 2011). However, syndromic microcephaly is caused by environmental factors such as alcohol, drugs of abuse, infection and recently the zika virus outbreak causing neonatal microcephaly (Ghouzzi et al. 2016). We present a model that can be adapted to study the etiology of syndromic microcephalies as in these mice neurodevelopmental defects result from the downregulation of MCPH signaling instead of complete ablation or silencing of the gene. Examples of other genetic models of microcephaly include the Brca1 knockout that also induces apoptosis during early corticogenesis (Pulvers and Huttner 2009), in addition to the normal rate expected in normal housekeeping of brain development. The Mcph1 knockout causes additional morphological defects in reproductive organs in mice (Gruber et al. 2011) and defects in mushroom bodies in drosophila. Various other genetic models have been reviewed highlighting their severity (Kaindl et al.

2010), whereas we present a more viable and representative model. Table 1 presents a few similarities between human microcephaly and the VIP knockout mouse depicting how Mcph1 knockdown resembles MCPH1 loss of function found in humans.

Table 1: VIP knockout mice recapitulate human primary microcephaly

Human Microcephaly	VIP KO
Reduced occipital frontal circumference	+
Reduced cortical thickness and size	+
Reduced stature	+
Behavior	
Mental retardation	Not easy to study in mice although anxiety-like hyperactivity was reported (Girard et al, 2006)
Cognitive deficit	+
Social behavior	+ (Lim et al, 2008)
Developmental Delay	
Motor milestones	+ Stack et al, 2008

As a current perspective, we are sampling pups from 'forced restraint' females to perform morphometry and validate this model. Should the expected microcephalic phenotype persist, we would administer VIP specific time-points (before the forced restraint, comparing with during forced restraint). In addition, a major drawback in our maternal stress model is the validation of the stress itself. According to our hypothesis, VIP secretion is decreased due to stress, however, we did not measure stress in the females. Therefore, we should measure circulating cortisol levels as well as other markers for stress. We also plan to perform a cytokine array, especially from placental tissue, to get a better indication of the resident immune population surrounding the embryo and fetus.

To better relate our model to known syndromic microcephalies we propose to implement different models of stress. Of main interest, one of the main diagnostic determinants of fetal alcohol syndrome is the appearance of microcephaly in affected children (Spadoni et al. 2007), exhibiting white matter defects that specifically target the corpus callosum (Benz et al. 2009). Thus, we plan to implement prenatal alcohol exposure to generate microcephaly in pups with the following perspectives:

- to investigate whether targeted maternal administration of alcohol affects plasma VIP and placental VIP concentrations, and whether this affects the resident pro-inflammatory population and secretion in the placenta (mainly in wildtype and heterozygous females)
- to investigate whether prenatal alcohol exposure also dysregulates the VPAC1-MCPH1 crosstalk in heterozygous embryos and pups, and whether the defects observed mimic the knockout phenotype
- to investigate whether VIP knockout- induced microcephaly is also induced in heterozygous postnates obtained from prenatally 'alcoholic' females.

Our microcephaly model implicates dysregulation in VPAC1 signaling with no evidence of compensation by VPAC2. Thanks to a budding collaboration with Dr Yossan Var Tan and Dr Catalina Abad Rabat, we obtained some VPAC1 knockout pups. Preliminary results on morphometric measures taken at P15 show severe microcephaly, exhibiting significant reduction in overall brain weight, brain perimeter and cortical thickness (Figure 17, top and center panels). In addition, current evidence demonstrated a low neonatal growth and subsequent reduction in weight

gain (Figure 17, lower panel) in VPAC1 knockouts (Fabricius et al. 2011). In this study, neonatal survival was ameliorated through extended breastmilk diet as pups died at weaning. VPAC1 knockouts also suffer from gastrointestinal dysfunction (Fabricius et al. 2011). Thus, we can suggest that indeed, normal VIP and VPAC1 functioning are indeed highly implicated in microcephaly and the associated systemic perturbations that tend to accompany this disorder. As a clinical perspective, we can suggest VPAC1-targeted VIP supplementation in high-risk cases of microcephaly which can be detected as early as the 32nd week of gestation in humans (Mahmood et al. 2011) with fetal MRI which can identify morphometric abnormalities, including corpus callosum agenesis as early as 24 weeks of gestation (Sohn et al. 2007).

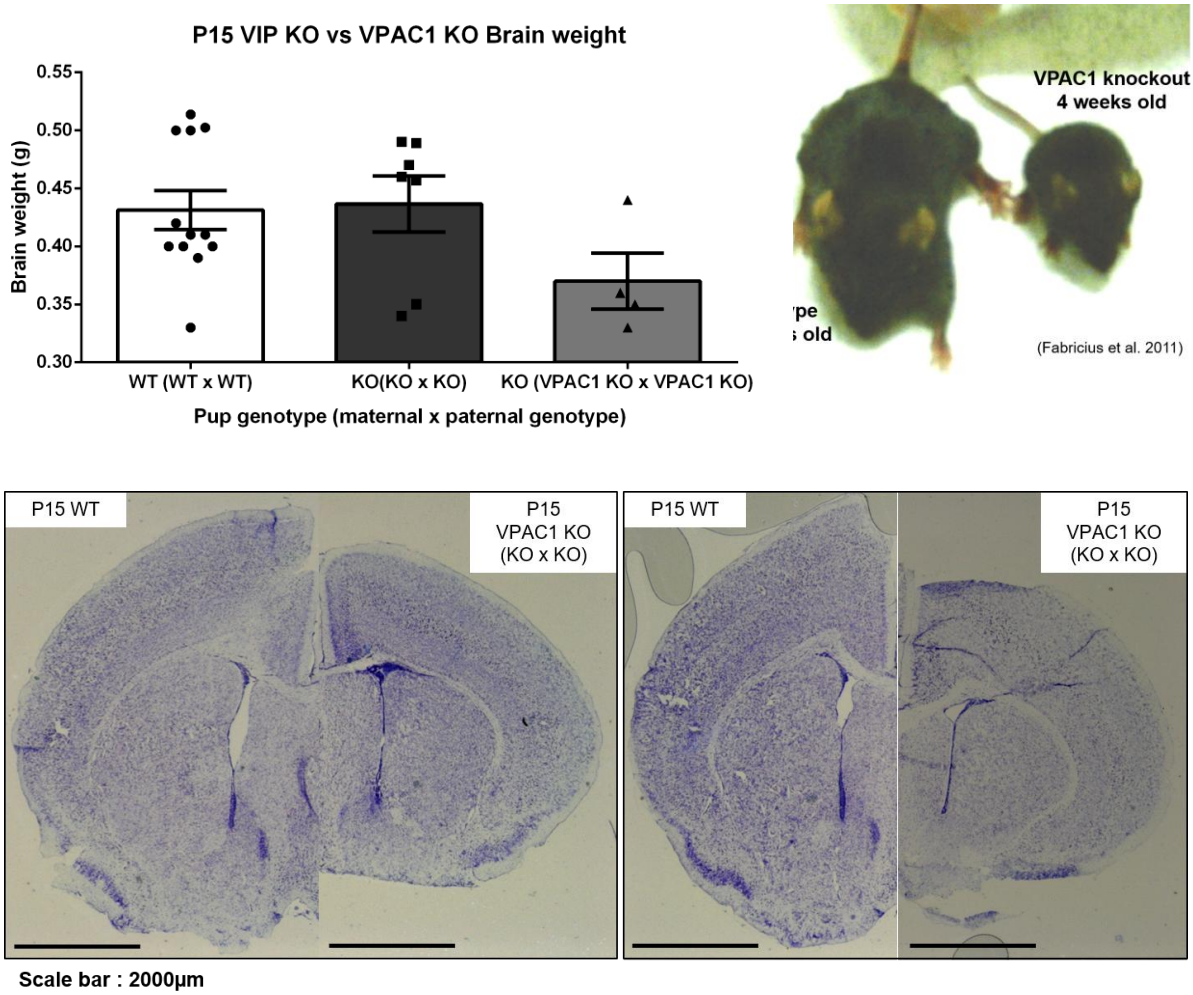

Figure 17: VPAC1 knockout mice exhibit microcephaly and severe growth impairments

Top panel: Preliminary results from cresyl violet staining suggest severe microcephaly at P15 in VPAC1 knockout mice (n =2), and show significant reduction in brain weight (center panel) compared to VIP wildtype and full knockout age-matched brains (n=4, Kruskal-Wallis, $p<0.05$)

Bottom panel: VPAC1 knockout mice have are extremely smaller than age-matched wildtypes, and fail to increase weight gain during postnatal development resulting in mortality.

As previously mentioned, BRCA1 knockouts present a more severe phenotype including an increase in apoptosis during neurogenesis. However, in this model of microcephaly, MCPH1 downregulates Brca1 expression in VIP deficiency and following forced restraint. BRCA1, breast cancer 1, is a well characterized marker for breast cancer and is also involved in DNA repair following irradiation and DNA replication (Roy et al. 2011). In addition, BRCA1 interacts with CHK1 in checkpoint regulation at the G2/M phase (Narod and Foulkes 2004; Roy et al. 2011). This is of no surprise as MCPH1 has been shown to interact BRCA1 and CHK1, which were downregulated when MCPH1 was underexpressed (Xu et al. 2004) as observed also in microcephaly patients (Lin et al. 2005). BRCA1 is also involved in chromatin remodeling (Narod and Foulkes 2004; Roy et al. 2011). Thus, we will be investigating whether there is a link between VIP-dependent BRCA1 downregulation and VIP-mediated epigenetic modifications in VIP deficiency, and whether prenatal stress exacerbates this relationship.

The finding that maternally expressed VIP acts as the intra-uterine gatekeeper exerting spatio-temporal trophic and neuroprotective effects along embryonic and fetal development presents a significant clinical potential.

As previously mentioned, pregnant women at risk of increased prenatal stress (i.e., due to stressful living conditions, such as in cases of violence, and where prenatal alcoholism and drug abuse are prevalent) could be measured for the circulating VIP levels during early stages of pregnancy for preliminary assessments, in longitudinal studies, whereby offspring would be evaluated for any possible morphological impairments including microcephaly. Should VIP levels be dysregulated as we've seen in our study, this suggest early intervention to at-risk pregnant women. Otherwise, children with microcephaly-related disorders including fetal alcohol syndrome and autism (Fombonne et al. 1999). Earlier studies have measured plasma VIP levels in children with autism, Down syndrome and cerebral palsy (Nelson 2001; Nelson et al. 2006) further suggesting a link between VIP and neurodevelopmental disorders in the clinical setup. In these cases, VIP levels were significantly higher than controls, suggesting a compensatory mechanism in affected individuals if our hypothesis that loss of VIP is the starting point in the etiology of autism and related disorders. A possible intervention, in these cases, could also be neonatal supplementation with VIP through breastmilk as VIP has been shown to be

expressed in breastmilk (Werner et al. 1985). Thus, it becomes important to identify different time-points of intervention in high risk cases. Additionally, if we suggest clinical interventions with VIP, it is important to bear in mind possible side-effects that could also negatively affect the growing embryo or fetus. VIP is administered in asthmatics due to it bronchodilatory actions (Morice et al. 1984). On the other hand, overexpression of VIP in the periphery causes diarrhea as was the case in historically termed VIPomas (Bloom et al. 1983)

2. VIP rescues allodynia with long-lasting effects, through regulation of molecular mechanisms that upregulate early gene expression related with epigenetic modifications

Pain is defined as an unpleasant sensory and emotional experience associated with actual or potential tissue damage, or described in terms of such damage.

Allodynia refers to the sensation of pain following to a stimulus that does not normally provoke pain.

Hyperalgesia is increased sensation to pain resulting from a stimulus that normally provokes pain.

(Loeser and Treede 2008)

We have shown that the neuroprotective action of VIP in treating allodynia is long-lasting. This is of high interest clinically as it presents a biological factor that does not require chronic use for treatment of pain, with no side effects characterized to date.

Preterm children undergo painful procedures at the onset of life and, in addition, present with symptoms of neurodevelopmental disability and an increased risk of behavioral problems such as Attention Deficit Hyperactivity Disorder (Parets et al. 2014). This is of no surprise as preterm birth presents a high risk of excitotoxicity and deprives offspring of maternal factors that could be essential in the final stages of brain development, i.e. synaptogenesis and oligodendrocytogenesis (Gressens 1999). In addition, preterm births are associated with long-term epigenetic modifications possibly due to DNA methylation changes as the etiology of prematurity (Parets et al. 2014). VIP emerges as one of those crucial maternal

factors that preterm children lack (Gressens 1999), which when deficient during embryonic and fetal development results in cortical defects and corpus callosum thinning. VIP-mediated neuroprotection in pain has epigenetic implications, though not yet directly demonstrated.

However, it is interesting that a model of neurodevelopmental disease is translatable to adult pathophysiology, suggesting the importance of early VIP in adult physiology and health.

In addition to the pain phenotype, VIP knockouts also exhibit hyperactivity in the ventrolateral nucleus of the thalamus. Thalamic neurons have been shown to respond to noxious and other mechanical pain stimuli (Kenshalo et al. 1980). That VIP knockout mice exhibit high frequency firing in anaesthetized preparation at basal state suggests dysfunctional spontaneous activity in this region, and thus aberrant processing from spinal to supraspinal pathways. What remains to be investigated is the development of conventionally VIPergic interneurons in VIP knockout mice, and whether they still maintain the same properties even in the absence of VIP. A question still remains as to how they play a role in sensory processing and how their absence, if at all, result in aberrant behavior as seen in VIP knockout mice.

Here we have presented a maternally secreted factor that is crucial in spatio-temporal housekeeping and maintenance of the sequence of neurogenesis, which when absent or deficient results in aberrant sensory processing and a pain phenotype in adults, mimicking what is seen in adults suffering from such neurodevelopmental disorders as cerebral palsy (Vogtle 2009).

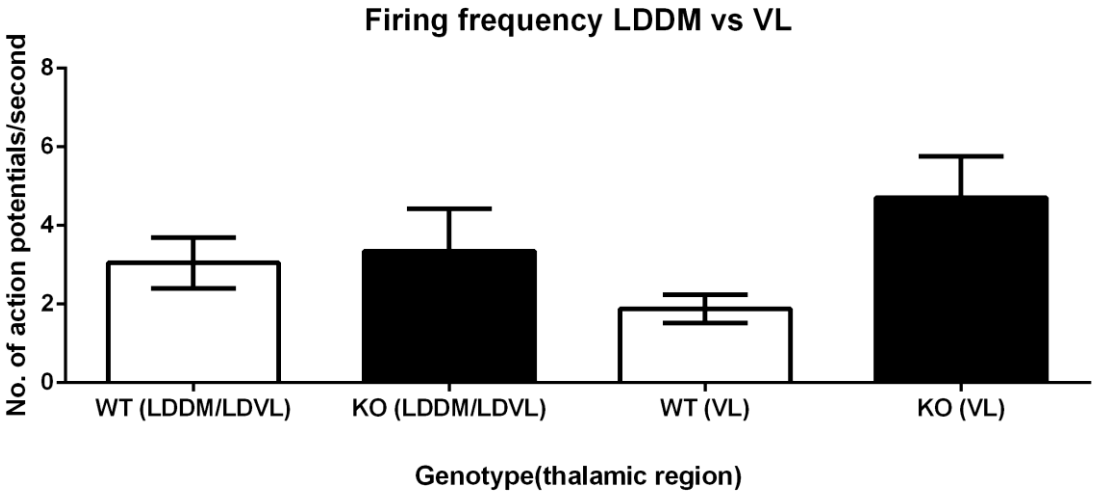
Firing frequency LDDM vs VL
No. of action potentials/second
0
2
4
6
8
WT (LDDM/LDVL)
KO (LDDM/LDVL)
WT (VL)
KO (VL)
Genotype(thalamic region)

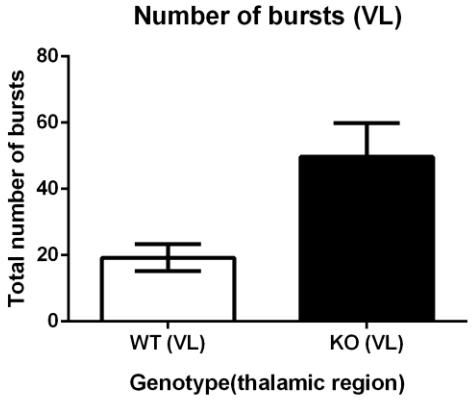
Number of bursts (VL)
Total number of bursts
0
20
40
60
80
WT (VL)
KO (VL)
Genotype(thalamic region)

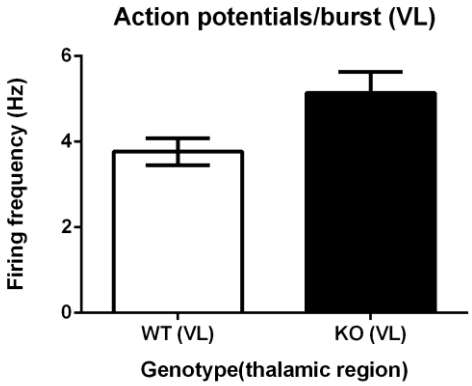
Action potentials/burst (VL)
Firing frequency (Hz)
0
2
4
6
WT (VL)
KO (VL)
Genotype(thalamic region)

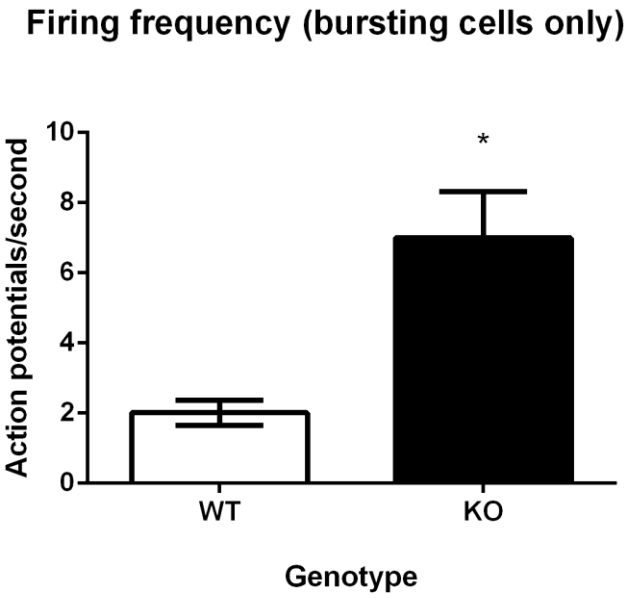
Firing frequency (bursting cells only) VL
Action potentials/second
0
2
4
6
8
10
*
WT
KO
Genotype

Figure 11

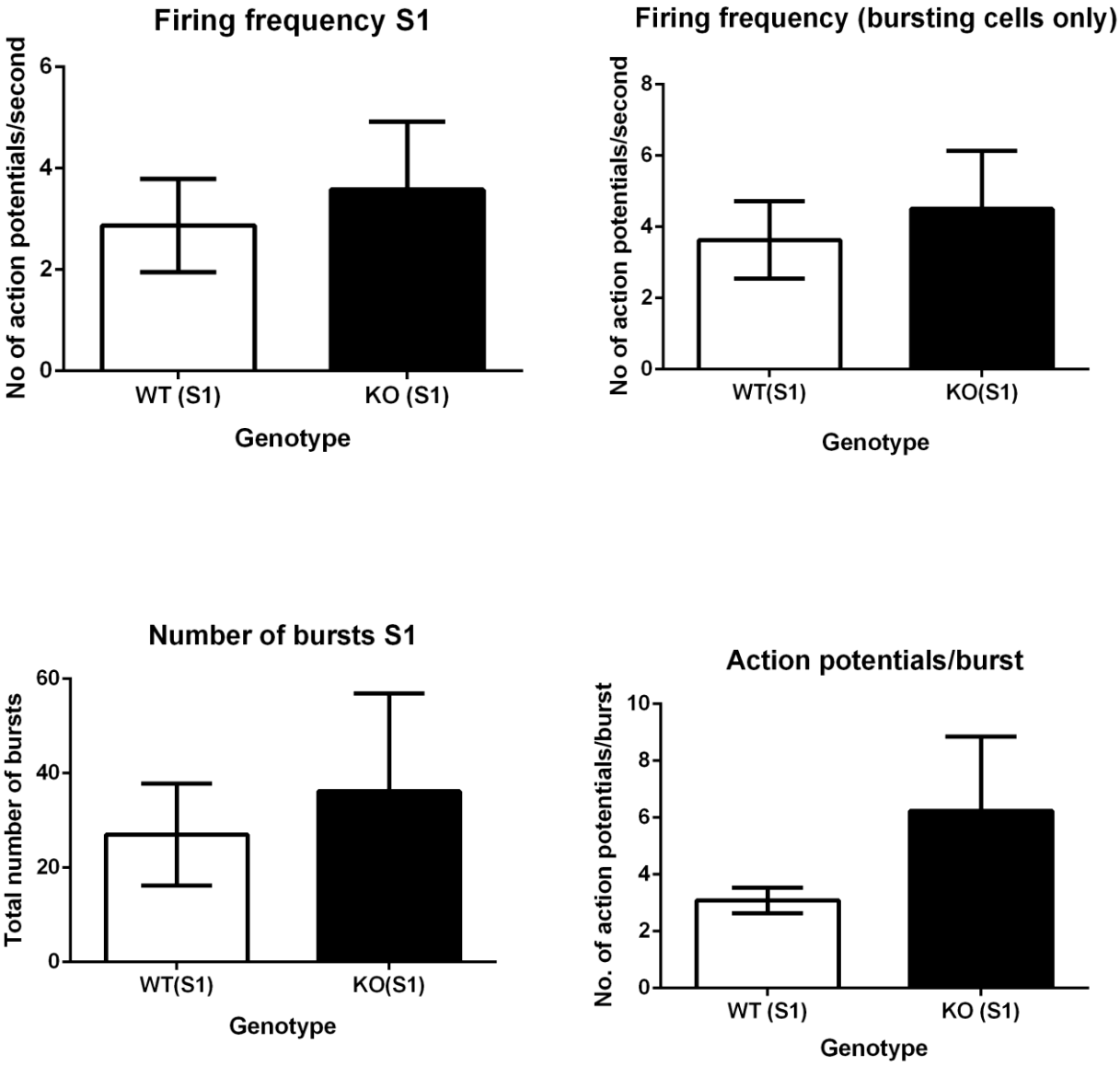
Firing frequency S1
No of action potentials/second
0
2
4
6
WT (S1)
KO (S1)
Genotype
Firing frequency (bursting cells only)
No of action potentials/second
0
2
4
6
8
WT(S1)
KO(S1)
Genotype
Number of bursts S1
Total number of bursts
0
20
40
60
WT(S1)
KO(S1)
Genotype
Action potentials/burst
No. of action potentials/burst
0
2
4
6
8
10
WT (S1)
KO (S1)
Genotype

Figure 12

Figure Legends:

Figure 11: Knockout mice exhibit significant cellular hyperactivity in the lateral thalamus

Top panel: No significant changes were observed in the dorsal thalamus (LDDM/LDVL) when VIP knockouts (n=10) were compared with wildtype (n=20) cells. Knockout cells (n=22) displayed increased firing frequency and bursting activity though these changes were not significantly different when compared to controls (n=12) (Mann-Whitney test, $p>0.05$)

Low panel: Bursting cells recorded in VIP knockouts (n=19) exhibited significantly higher firing activity in lateral thalamic cells compared to wildtypes (n=12) (Mann-Whitney test, $p<0.02$)

Figure 12: Single cell activity is not altered in the primary sensory cortex of male knockout mice

The firing frequency in the measured population of cells (n=13 in wildtype; n=8 in knockout), and firing frequency of the bursting population of cells (n=10 in wildtype, n=6 in knockout), in the primary somatosensory cortex are not statistically different between wildtype and knockout mice. There were no significant differences in bursting activity nor number of action potentials elicited within a burst when comparing wildtype and knockout mice (Mann-Whitney test, $p>0.05$).

Supplementary Results

S1. Pregnant mice are hypersensitive to mechanical pain

Adult VIP knockout males are hypersensitive to cold temperature in addition to mechanical pain, and VIP expression is upregulated in peripheral injury. In addition, circulating VIP levels are increased in pregnant females between E6, tapering back down from E12 onwards. Thus, we investigated whether VIP secretion would be affected in pregnant VIP heterozygous females, and whether this would exhibit neuroprotective actions.

The baseline Von Frey response was measured in non-pregnant females and then compared with responses from pregnant wildtype females. Pregnant females were significantly hypersensitive in the Von Frey test at E8, E9 and E12.

S2. VIP deficiency significantly heightens sensitivity to mechanical stimulation during early pregnancy

When investigating whether VIP deficiency would change the pain response reported in wildtypes, we first compared all the pregnant VIP deficient females with the non-pregnant controls. VIP deficiency lowered the threshold to mechanical sensitivity even more in these females than in wildtypes during the whole gestational period investigated (E8, E9 and E12), as shown on Table1. Pregnant heterozygous and knockout females were also significantly hypersensitive relative to pregnant wildtypes at E8. Interestingly, heterozygotes became even more sensitive by E12, compared to their initial E8 response (Supplementary Figure S2) Thus, pregnancy further exacerbates sensitivity to mechanical pain in VIP-deficient mice which were already hypersensitive compared to wildtypes.

S3. Forced restraint does not affect the threshold to mechanical pain in pregnant mice

Pregnant females were subjected to forced restraint on E9, E10 and E11, then tested for the pain threshold at E12. Pregnant wildtype females exhibited the same threshold between stressed and non-stressed females, although still significantly

lower than baseline measures (Supplementary Table 2). However, pregnant mice from the restraint group exhibit high variability in their response. In addition, these mice demonstrated a higher threshold compared pregnant VIP deficient mice though not statistically different. Forced restraint seemed to increase the threshold of mechanical pain in knockout E12 females though, also not statistically significant (Supplementary Figure S3).

S4. VIP-deficient mice are hypersensitive to descending temperature changes only during early pregnancy

Pregnant wildtype females exhibit the same threshold to cold temperature at E8, E9 and E9 as non-pregnant wildtypes females (Supplementary Figure S4A, top panel). Similar to male behaviour, VIP deficient females were more sensitive to cold temperature than wildtypes at the same gestational stage (Supplementary Figure S4A, bottom panel). However, again at E8, VIP-deficient females were more susceptible to temperature change than wildtypes. Forced restraint had no effect on cold perception in all comparisons (Supplementary Figure S4B).

Although these results suggest that VIP might be neuroprotective in mechanical and pain sensibility, the most direct evidence they provide is that the loss of VIP, whether full or partial, hypersensitizes mice to mechanical and thermal pain as we have previously shown (Publication 3). Pregnancy also lowers the threshold of mechanical and thermal pain not only in wildtypes but more severely in VIP-deficient mice. However, we have yet to demonstrate whether this is related to changes in circulating levels of VIP in pregnant females. Thus, the next step should be to compare circulating VIP levels in wildtype pregnant females and wildtype non-pregnant control females to obtain direct evidence that VIP is indeed neuroprotective in pregnant females. In addition, we have yet to demonstrate whether circulating levels of VIP are affected in heterozygous females during pregnancy and whether they are affected at all by forced restraint. In our study, forced maternal restraint did not change pain perception. This could point to a neuroprotective action of VIP as we expect it to be in higher concentrations between E8 and E12. Therefore, we suggest testing pregnant females before E8 and after E12, when we expect VIP levels to return to their baseline. We also suggest including non-pregnant females that are subjected to forced restraint, to investigate their pain responses as well as to

measure the effect of forced restraint on VIP levels, without the confounding changes in pregnancy-induced VIP expression.

Supplementary Result Figures:

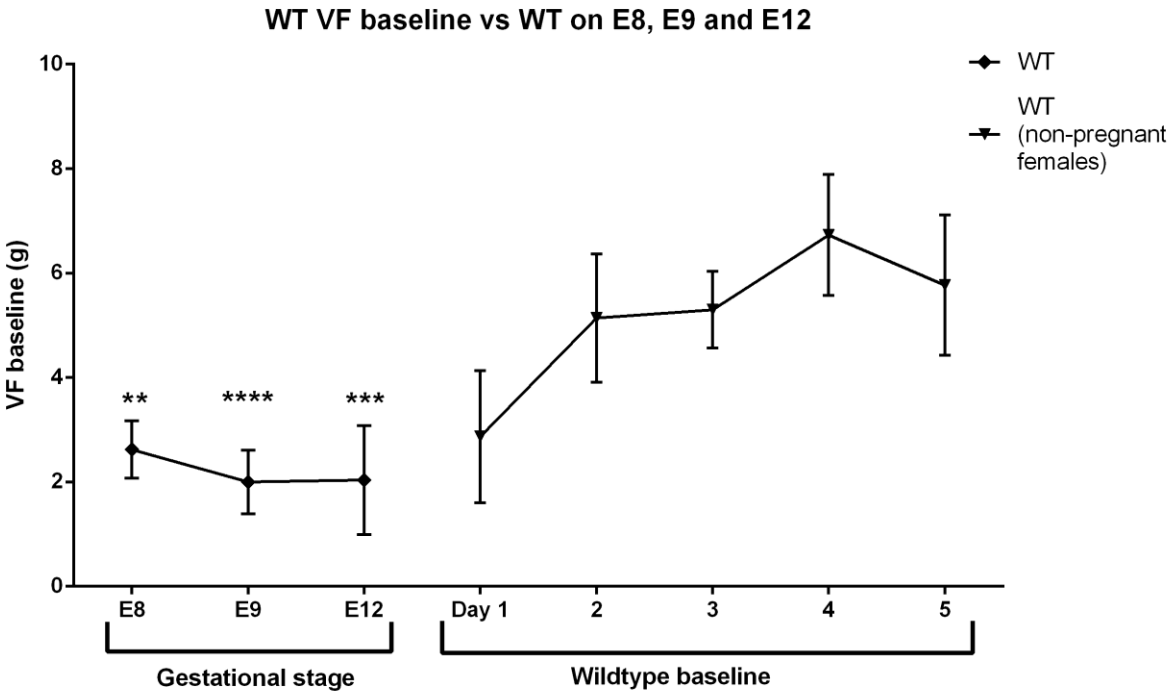

Supplementary Figure S1

Table 1: Von frey threshold of control wildtype females compared to VIP deficient females, pregnant at E8, E9 and E12

Dunn's multiple comparisons test	Significant?	Summary	Adjusted P Value
Maternal groups (gestational age)			
WT Baseline vs. Hz (E8)	Yes	**	0.0017
WT Baseline vs. Hz (E9)	Yes	****	< 0.0001
WT Baseline vs. Hz E12	Yes	****	< 0.0001
WT Baseline vs. KO (E8)	Yes	***	0.001
WT Baseline vs. KO (E9)	Yes	****	< 0.0001
WT Baseline vs. KO E12	Yes	****	< 0.0001

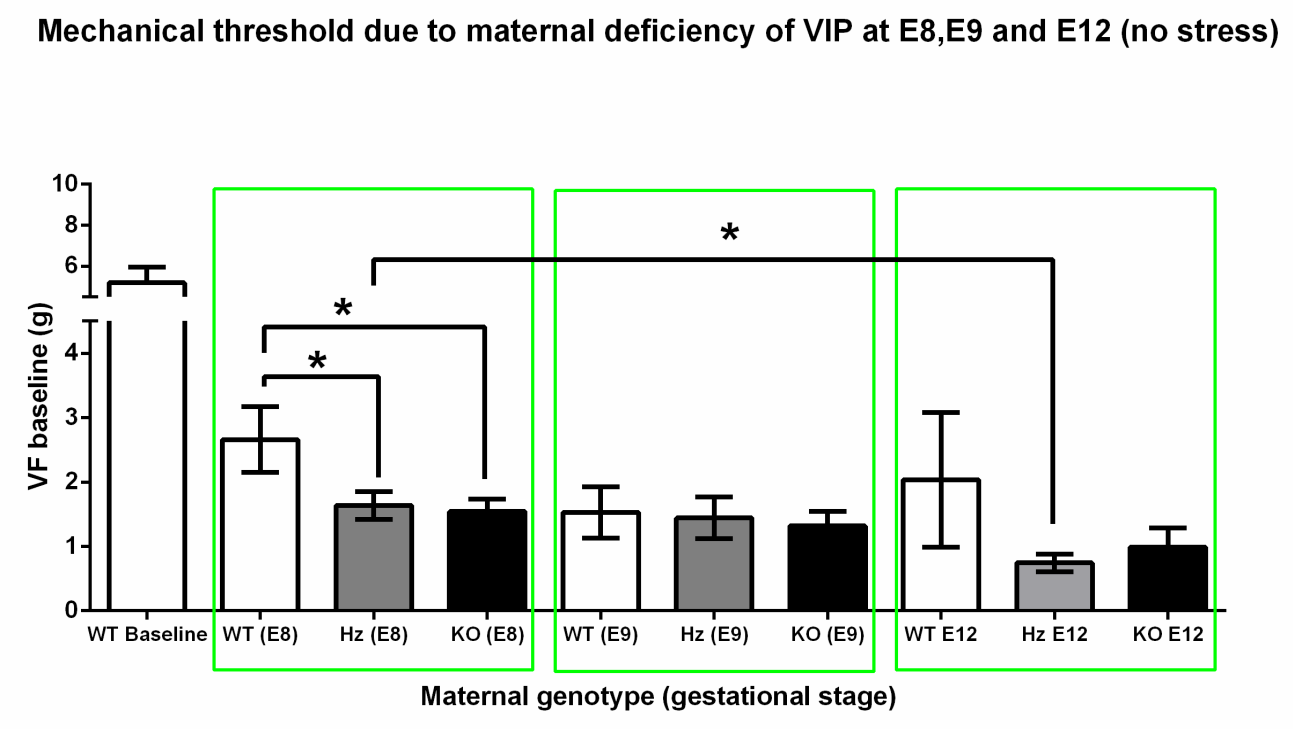

Supplementary Figure S2

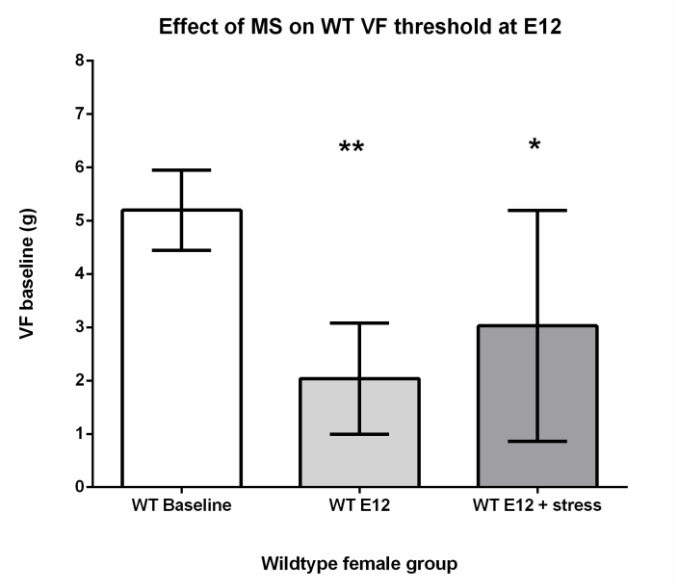

Table 2: Von frey threshold of control wildtype females compared to stressed and non-stressed VIP deficient females, pregnant at E12

Dunn's multiple comparisons test	Mean rank diff.	Significant?	Summary
WT Baseline vs. Hz E12	32.46	Yes	***
WT Baseline vs. Hz E12 + stress	32.58	Yes	****
WT Baseline vs. KO E12	32.58	Yes	****
WT Baseline vs. KO E12 + stress	21.04	Yes	*

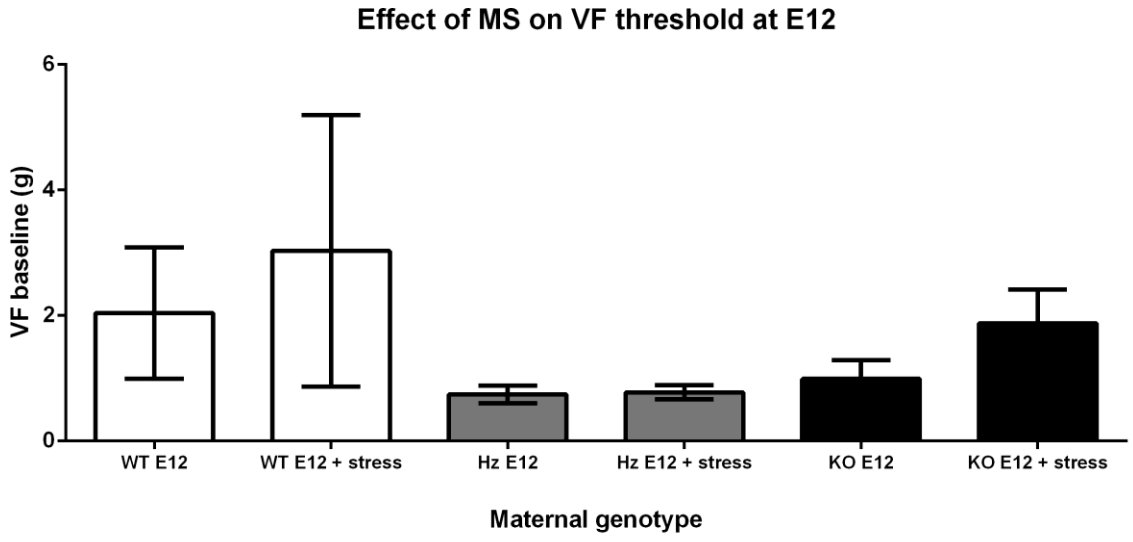

Supplementary Figure S3

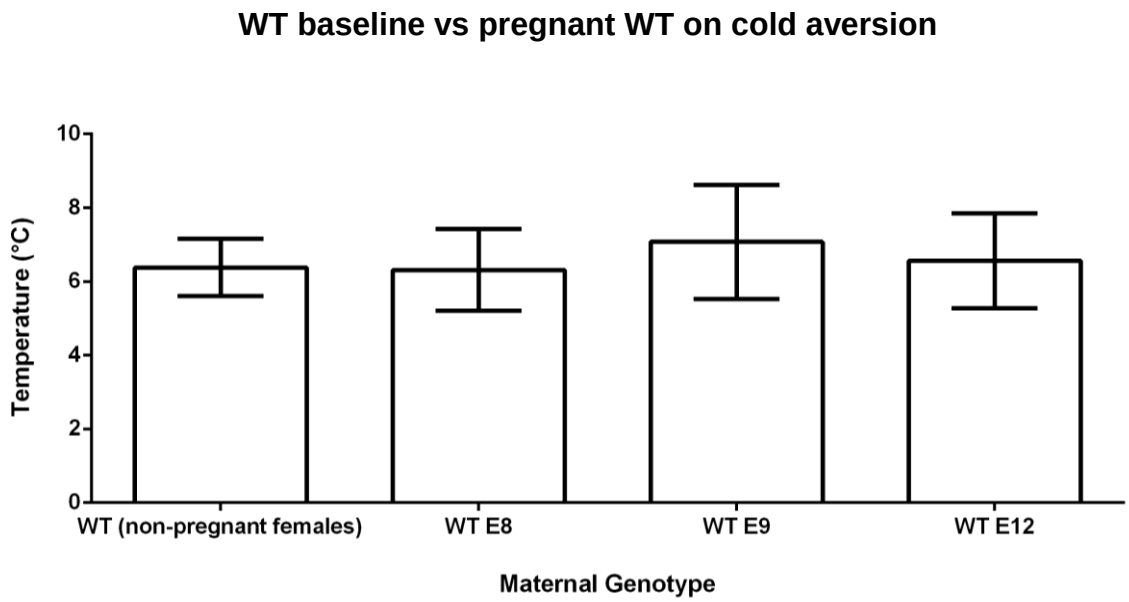

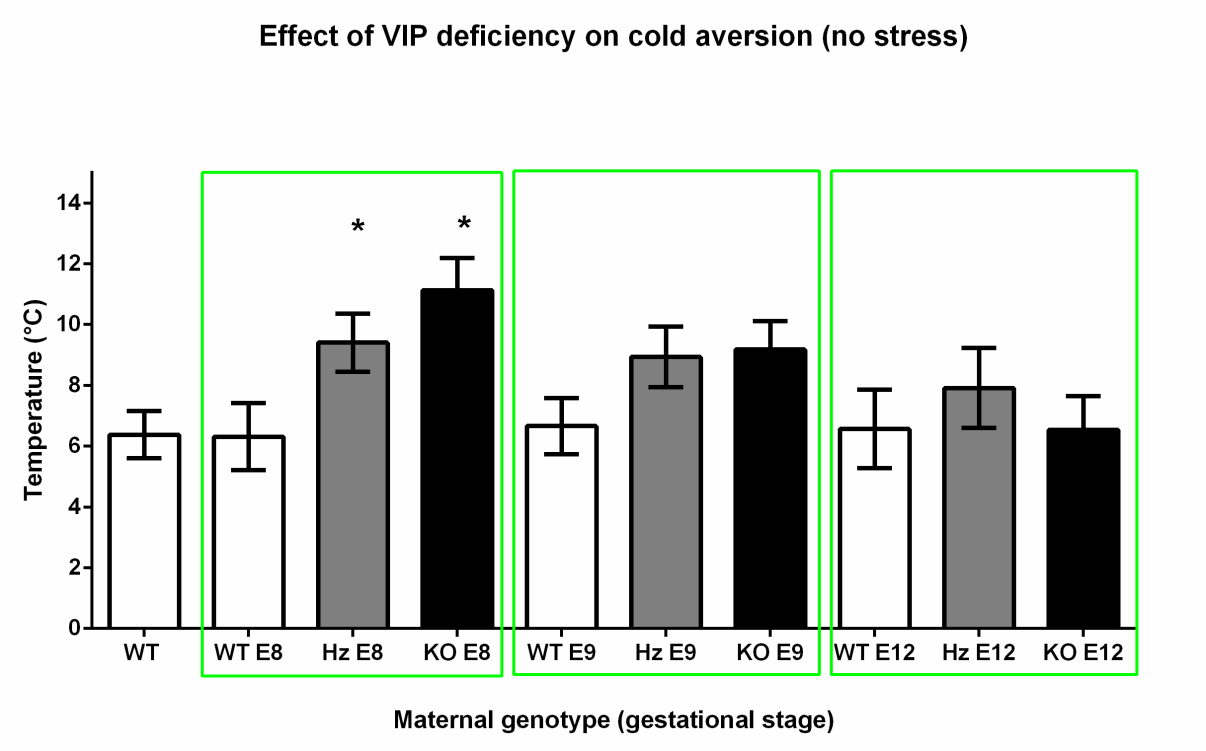

Supplementary Figure S4A

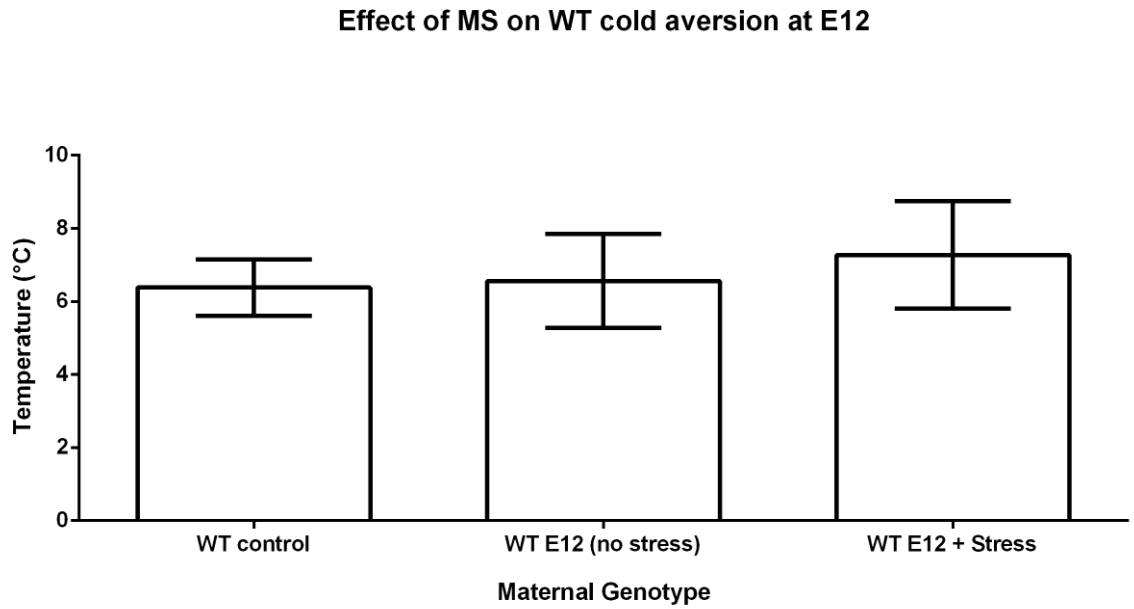

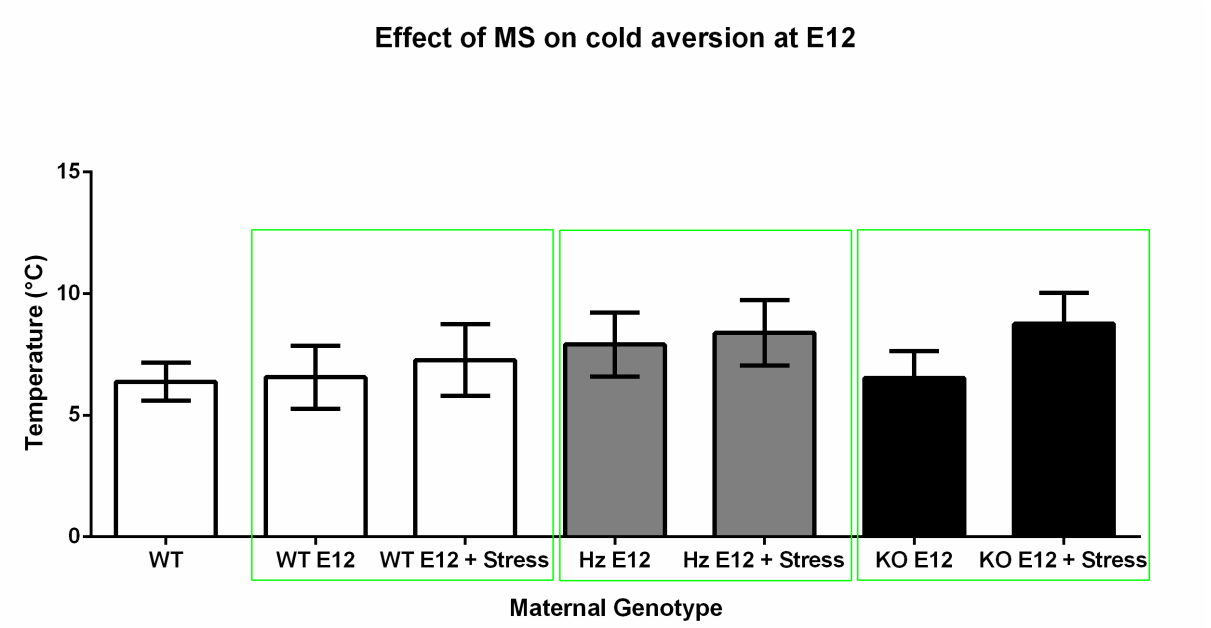

Supplementary Figure S4B

Supplementary Figure Legends:

Supplementary Figure S1: Pregnant wildtype females have a significantly lower threshold to mechanical stimulation, compared to non-pregnant wildtypes, in the Von Frey test

(Right panel): Wildtype control mice, that were not pregnant exhibited a stable baseline that lasted for 5 days, with no statistical differences in paw withdrawal between the days (Kruskal-Wallis test, $p<0.05$, $n=10$).

(Left panel): Pregnant wildtype mice ($n=15$) responded at a significantly lower stimulation at E8 ($p=0.0339$), at E9 ($p<0.0001$) and at E12 ($p=0.0007$) compared to the normal wildtype baseline

Supplementary Figure S2: Pregnant VIP deficient females are more hypersensitive to mechanical pain compared to wildtype females during early pregnancy

Top panel (Table 1): VIP heterozygous ($n=22$) and knockout females ($n=21$) all have significantly lower pain threshold when pregnant at E8, E9 and E12 compared to control mice that are not pregnant (Kruskal-Wallis test, and Dunn's multiple comparisons test), as summarized in Table 1.

Lower panel: Pregnant wildtype females are significantly less hypersensitive to mechanical stimulation, compared to heterozygous ($p<0.0399$) and knockout ($p<0.0368$) females at E8 (Mann-Whitney test).

Supplementary Figure S3: Forced restraint does not affect the pain threshold neither in pregnant wildtype nor VIP deficient mice at E12

Top panel: Wildtype mice at gestational age E12 still have a significantly lower threshold of mechanical pain, compared to control mice (Dunn's multiple comparisons test, $p<0.0035$) but exhibit equal response when compared to E12 wildtypes subjected to forced restraint (Dunn's multiple comparisons test, $p>0.05$). Restraint wildtype females were still significantly more sensitive to mechanical stimulation compared to control wildtype females (Dunn's multiple comparisons test, $p<0.0120$).

Centre panel (Table2): At E12, VIP-deficient females had a significantly lower threshold and responded with paw withdrawal to filaments as low as 1g to 2g, compared to controls (Kruskal-Wallis test, ****p<0.0001).
Lower panel: Forced restraint did not significantly change the paw withdrawal response in neither wildtype nor VIP deficient females at E12.

Supplementary Figure S4A: VIP deficient females are hypersensitive to descending temperature changes during early pregnancy, at E8

Top panel: Response to descending temperature changes is not significantly different between control and pregnant wildtype mice (Kruskal-Wallis test, p=0.6780).
Lower panel: At E8 heterozygous (Mann-Whitney test, p=0.0272) and knockout (Mann-Whitney test, p=0.0232) females exhibited hypersensitivity to descending temperature changes, compared to E8 wildtype mice. Pregnancy did not affect any other group.

Supplementary Figure S4B: Forced restraint does not affect thermal nociception in E12 wildtype and VIP deficient mice.

Top panel: Pregnant wildtype females subjected to restraint stress showed no significant difference in the threshold to descending temperature changes compared to non-restrained pregnant and non-restrained, non-pregnant females (Kruskal-Wallis test, p>0.05).
Lower panel: Forced restraint did not significant change the thermal pain response in pregnant VIP-deficient females at E12.

Bibliography

.Agoston DV, Eiden LE, Brenneman DE, Gozes I. 1991. Spontaneous electrical activity regulates vasoactive intestinal peptide expression in dissociated spinal cord cell cultures. Brain research Molecular brain research 10(3):235-240.

Alexander LD, Sander LD. 1994. Vasoactive intestinal peptide stimulates ACTH and corticosterone release after injection into the PVN. Regulatory peptides 51(3):221-227.

Anand P, Gibson SJ, McGregor GP, Blank MA, Ghatei MA, Bacarese-Hamilton AJ, Polak JM, Bloom SR. 1983. A VIP-containing system concentrated in the lumbosacral region of human spinal cord. Nature 305(5930):143-145.

Anderson P, Gonzalez-Rey E. 2010. Vasoactive intestinal peptide induces cell cycle arrest and regulatory functions in human T cells at multiple levels. Molecular and cellular biology 30(10):2537-2551.

Anton PA, Shanahan F, Sun XP, Diehl D, Kodner A, Mayer EA. 1993. VIP modulates intracellular calcium oscillations in human lymphoblasts. Immunopharmacology and immunotoxicology 15(4):429-446.

Arnold SJ, Huang GJ, Cheung AF, Era T, Nishikawa S, Bikoff EK, Molnar Z, Robertson EJ, Groszer M. 2008. The T-box transcription factor Eomes/Tbr2 regulates neurogenesis in the cortical subventricular zone. Genes & development 22(18):2479-2484.

Asami M, Pilz GA, Ninkovic J, Godinho L, Schroeder T, Huttner WB, Gotz M. 2011. The role of Pax6 in regulating the orientation and mode of cell division of progenitors in the mouse cerebral cortex. Development 138(23):5067-5078.

Barrot M. 2012. Tests and models of nociception and pain in rodents. Neuroscience 211:39-50.

Beinfeld MC, Brick PL, Howlett AC, Holt I, Pruss RM, Moskal JR, Eiden LE. 1988. The Regulation of Vasoactive Intestinal Peptide Synthesis in Neuroblastoma and Chromaffin Cellsa. Annals of the New York Academy of Sciences 527(1):68-76.

Benz J, Rasmussen C, Andrew G. 2009. Diagnosing fetal alcohol spectrum disorder: History, challenges and future directions. Paediatrics & Child Health 14(4):231-237.

Besson J, Rotsztejn W, Laburthe M, Epelbaum J, Beaudet A, Kordon C, Rosselin G. 1979. Vasoactive intestinal peptide (VIP): brain distribution, subcellular localization and effect of deafferentation of the hypothalamus in male rats. Brain Res 165(1):79-85.

Bloom SR, Christofides ND, Delamarter J, Buell G, Kawashima E, Polak JM. 1983. Diarrhoea in vipoma patients associated with cosecretion of a second active peptide (peptide histidine isoleucine) explained by single coding gene. Lancet (London, England) 2(8360):1163-1165.

Bloom SR, Yiangou Y, Polak JM. 1988. Vasoactive Intestinal Peptide Secreting Tumors. Pathophysiological and Clinical Correlations. Annals of the New York Academy of Sciences 527(1):518-527.

Bodner M, Fridkin M, Gozes I. 1985. Coding sequences for vasoactive intestinal peptide and PHM-27 peptide are located on two adjacent exons in the human genome. Proceedings of the National Academy of Sciences of the United States of America 82(11):3548-3551.

Boehm M, Yoshimoto T, Crook MF, Nallamshetty S, True A, Nabel GJ, Nabel EG. 2002. A growth factor-dependent nuclear kinase phosphorylates p27^{Kip1} and regulates cell cycle progression. The EMBO Journal 21(13):3390-3401.

Bond J, Roberts E, Mochida GH, Hampshire DJ, Scott S, Askham JM, Springell K, Mahadevan M, Crow YJ, Markham AF, Walsh CA, Woods CG. 2002. ASPM is a major determinant of cerebral cortical size. Nature genetics 32(2):316-320.

Bond J, Woods CG. 2006. Cytoskeletal genes regulating brain size. Current opinion in cell biology 18(1):95-101.

Brenneman DE, Hill JM, Glazner GW, Gozes I, Phillips TW. 1995. Interleukin-1 alpha and vasoactive interstinal peptide: Enigmatic regulation of neuronal survival. International Journal of Developmental Neuroscience 13(3–4):187-200.

Bünemann M, Hosey MM. 1999. G-protein coupled receptor kinases as modulators of G-protein signalling. The Journal of physiology 517(1):5-23.

Caughey GH, Leidig F, Viro NF, Nadel J. 1988. Substance P and vasoactive intestinal peptide degradation by mast cell tryptase and chymase. Journal of Pharmacology and Experimental Therapeutics 244(1):133-137.

Cauli B, Tong XK, Rancillac A, Serluca N, Lambolez B, Rossier J, Hamel E. 2004. Cortical GABA interneurons in neurovascular coupling: relays for subcortical vasoactive pathways. The Journal of neuroscience : the official journal of the Society for Neuroscience 24(41):8940-8949.

Chomczynski P, Sacchi N. 1987. Single-step method of RNA isolation by acid guanidinium thiocyanate-phenol-chloroform extraction. Analytical Biochemistry 162(1):156-159.

Christopoulos A, Christopoulos G, Morfis M, Udawela M, Laburthe M, Couvineau A, Kuwasako K, Tilakaratne N, Sexton PM. 2003. Novel Receptor Partners and Function of Receptor Activity-modifying Proteins. Journal of Biological Chemistry 278(5):3293-3297.

Colwell CS, Michel S, Itri J, Rodriguez W, Tam J, Lelievre V, Hu Z, Liu X, Waschek JA. 2003. Disrupted circadian rhythms in VIP- and PHI-deficient mice. American journal of physiology Regulatory, integrative and comparative physiology 285(5):R939-949.

Correia KM, Conlon RA. 2001. Whole-mount in situ hybridization to mouse embryos. Methods 23(4):335-338.

Couvineau A, Fabre C, Gaudin P, MAORET JJ, Laburthe M. 1996. Mutagenesis of N-Glycosylation Sites in the Human VIP 1 Receptora. Annals of the New York Academy of Sciences 805(1):558-562.

Couvineau A, Rouyer-Fessard C, Laburthe M. 2004. Presence of a N-terminal signal peptide in class II G protein-coupled receptors: crucial role for expression of the human VPAC1 receptor. Regulatory peptides 123(1):181-185.

Davidson A, Moody TW, Gozes I. 1996. Regulation of VIP gene expression in general. Human lung cancer cells in particular. Journal of molecular neuroscience : MN 7(2):99-110.

Dehay C, Kennedy H. 2007. Cell-cycle control and cortical development. Nat Rev Neurosci 8(6):438-450.

Dickinson T, Fleetwood-Walker SM. 1999. VIP and PACAP: very important in pain? Trends in pharmacological sciences 20(8):324-329.

Drahushuk K, Connell TD, Higgins D. 2002. Pituitary adenylate cyclase-activating polypeptide and vasoactive intestinal peptide inhibit dendritic growth in cultured sympathetic neurons. The Journal of neuroscience : the official journal of the Society for Neuroscience 22(15):6560-6569.

Du K, Nicole P, Couvineau A, Laburthe M. 1997. Aspartate 196 in the first extracellular loop of the human VIP1 receptor is essential for VIP binding and VIP-stimulated cAMP production. Biochemical and biophysical research communications 230(2):289-292.

Emson PC, Fahrenkrug J, Schaffalitzky de Muckadell OB, Jessell TM, Iversen LL. 1978. Vasoactive intestinal polypeptide (VIP): vesicular localization and potassium evoked release from rat hypothalamus. Brain Res 143(1):174-178.

Englund C, Fink A, Lau C, Pham D, Daza RA, Bulfone A, Kowalczyk T, Hevner RF. 2005. Pax6, Tbr2, and Tbr1 are expressed sequentially by radial glia, intermediate progenitor cells, and postmitotic neurons in developing neocortex. The Journal of neuroscience : the official journal of the Society for Neuroscience 25(1):247-251.

Evrard P, Marret S, Gressens P. 1997. Environmental and genetic determinants of neural migration and postmigratory survival. Acta Paediatrica 86(S422):20-26.

Fabricius D, Karacay B, Shutt D, Leverich W, Schafer B, Takle E, Thedens D, Khanna G, Raikwar S, Yang B. 2011. Characterization of intestinal and pancreatic dysfunction in VPAC1-null mutant mouse. Pancreas 40(6):861-871.

Fahrenkrug J. 1985. Evidence for common precursors but differential processing of VIP and PHM in VIP-producing tumors. Peptides 6(3):357-361.

Fahrenkrug J, Bek T, Lundberg JM, Hokfelt T. 1985. VIP and PHI in cat neurons: co-localization but variable tissue content possible due to differential processing. Regulatory peptides 12(1):21-34.

Fitzgerald M. 2005. The development of nociceptive circuits. Nat Rev Neurosci 6(7):507-520.

Fombonne E, Roge B, Claverie J, Courty S, Fremolle J. 1999. Microcephaly and macrocephaly in autism. Journal of autism and developmental disorders 29(2):113-119.

Fuji K, Senba E, Ueda Y, Tohyama M. 1983. Vasoactive intestinal polypeptide (VIP)-containing neurons in the spinal cord of the rat and their projections. Neuroscience Letters 37(1):51-55.

Furness JB. 2000. Types of neurons in the enteric nervous system. Journal of the autonomic nervous system 81(1-3):87-96.

Ghouzzi VE, Bianchi FT, Molineris I, Mounce BC, Berto GE, Rak M, Lebon S, Aubry L, Tocco C, Gai M, Chiotto AM, Sgro F, Pallavicini G, Simon-Loriere E, Passemard S, Vignuzzi M, Gressens P, Di Cunto F. 2016. ZIKA virus elicits P53 activation and genotoxic stress in human neural progenitors similar to mutations involved in severe forms of genetic microcephaly and p53. Cell death & disease 7(10):e2440.

Giachetti A, Said SI, Reynolds RC, Koniges FC. 1977. Vasoactive intestinal polypeptide in brain: localization in and release from isolated nerve terminals. Proceedings of the National Academy of Sciences of the United States of America 74(8):3424-3428.

Giladi E, Shani Y, Gozes I. 1990. The complete structure of the rat VIP gene. Brain research Molecular brain research 7(3):261-267.

Girard BA, Lelievre V, Braas KM, Razinia T, Vizzard MA, Ioffe Y, El Meskini R, Ronnett GV, Waschek JA, May V. 2006. Noncompensation in peptide/receptor gene expression and distinct behavioral phenotypes in VIP- and PACAP-deficient mice. Journal of neurochemistry 99(2):499-513.

Gottschall PE, Tatsuno I, Arimura A. 1994. Regulation of interleukin-6 (IL-6) secretion in primary cultured rat astrocytes: synergism of interleukin-1 (IL-1) and pituitary adenylate cyclase activating polypeptide (PACAP). Brain research 637(1-2):197-203.

Gottschall PE, Tatsuno I, Miyata A, Arimura A. 1990. Characterization and distribution of binding sites for the hypothalamic peptide, pituitary adenylate cyclase-activating polypeptide. Endocrinology 127(1):272-277.

Gozes I, Brenneman DE. 1989. VIP: Molecular biology and neurobiological function. Molecular neurobiology 3(4):201-236.

Gozes I, McCune SK, Jacobson L, Warren D, Moody TW, Fridkin M, Brenneman DE. 1991. An antagonist to vasoactive intestinal peptide affects cellular functions in the central nervous system. Journal of Pharmacology and Experimental Therapeutics 257(3):959-966.

Gressens P. 1999. VIP neuroprotection against excitotoxic lesions of the developing mouse brain. Annals of the New York Academy of Sciences 897:109-124.

Gressens P, Hill JM, Paindaveine B, Gozes I, Fridkin M, Brenneman DE. 1994. Severe microcephaly induced by blockade of vasoactive intestinal peptide function in the primitive neuroepithelium of the mouse. The Journal of clinical investigation 94(5):2020-2027.

Gressens P, Marret S, Martin J-L, Laquerrière A, Lombet A, Evrard P. 1998. Regulation of Neuroprotective Action of Vasoactive Intestinal Peptide in the Murine Developing Brain by Protein Kinase C and Mitogen-Activated Protein Kinase Cascades: In Vivo and In Vitro Studies. Journal of neurochemistry 70(6):2574-2584.

Gressens P, Paindaveine B, Hill JM, Brenneman DE, Evrard P. 1997. Growth Factor Properties of VIP during Early Brain Development. Annals of the New York Academy of Sciences 814(1):152-160.

Gruber R, Zhou Z, Sukchev M, Joerss T, Frappart PO, Wang ZQ. 2011. MCPH1 regulates the neuroprogenitor division mode by coupling the centrosomal cycle with mitotic entry through the Chk1-Cdc25 pathway. Nature cell biology 13(11):1325-1334.

Hahm SH, Eiden LE. 1999. Two separate cis-active elements of the vasoactive intestinal peptide gene mediate constitutive and inducible transcription by binding different sets of AP-1 proteins. The Journal of biological chemistry 274(36):25588-25593.

Hajós F, Zilles K, Gallatz K, Schleicher A, Kaplan I, Werner L. 1988. Ramification patterns of vasoactive intestinal polypeptide (VIP)-cells in the rat primary visual cortex. Anatomy and embryology 178(3):197-206.

Hamidi SA, Szema AM, Lyubsky S, Dickman KG, Degene A, Mathew SM, Waschek JA, Said SI. 2006. Clues to VIP function from knockout mice. Annals of the New York Academy of Sciences 1070:5-9.

Harmar AJ, Arimura A, Gozes I, Journot L, Laburthe M, Pisegna JR, Rawlings SR, Robberecht P, Said SI, Sreedharan SP, Wank SA, Waschek JA. 1998. International Union of Pharmacology. XVIII. Nomenclature of receptors for vasoactive intestinal peptide and pituitary adenylate cyclase-activating polypeptide. Pharmacological reviews 50(2):265-270.

Harmar AJ, Fahrenkrug J, Gozes I, Laburthe M, May V, Pisegna JR, Vaudry D, Vaudry H, Waschek JA, Said SI. 2012. Pharmacology and functions of receptors for vasoactive intestinal peptide and pituitary adenylate

cyclase-activating polypeptide: IUPHAR Review 1. British journal of pharmacology 166(1):4-17.

Heyborne KD, Cranfill RL, Carding SR, Born WK, O'Brien RL. 1992. Characterization of gamma delta T lymphocytes at the maternal-fetal interface. The Journal of Immunology 149(9):2872-2878.

Hill J, Harris A, Hilton-Clarke D. 1992. Regional distribution of guanine nucleotide-sensitive and guanine nucleotide-insensitive vasoactive intestinal peptide receptors in rat brain. Neuroscience 48(4):925-932.

Hill JM, Ades AM, McCune SK, Sahir N, Moody EM, Abebe DT, Crnic LS, Brenneman DE. 2003. Vasoactive intestinal peptide in the brain of a mouse model for Down syndrome. Experimental neurology 183(1):56-65.

Hill JM, Cuasay K, Abebe DT. 2007a. Vasoactive intestinal peptide antagonist treatment during mouse embryogenesis impairs social behavior and cognitive function of adult male offspring. Experimental neurology 206(1):101-113.

Hill JM, Gozes I, Hill JL, Fridkin M, Brenneman DE. 1991. Vasoactive intestinal peptide antagonist retards the development of neonatal behaviors in the rat. Peptides 12(1):187-192.

Hill JM, Hauser JM, Sheppard LM, Abebe D, Spivak-Pohis I, Kushnir M, Deitch I, Gozes I. 2007b. Blockage of VIP during mouse embryogenesis modifies adult behavior and results in permanent changes in brain chemistry. Journal of molecular neuroscience : MN 31(3):183-200.

Hill JM, Lee SJ, Dibbern Jr DA, Fridkin M, Gozes I, Brenneman DE. 1999. Pharmacologically distinct vasoactive intestinal peptide binding sites: CNS localization and role in embryonic growth. Neuroscience 93(2):783-791.

Hill JM, McCune SK, Alvero RJ, Glazner GW, Henins KA, Stanziale SF, Keimowitz JR, Brenneman DE. 1996. Maternal vasoactive intestinal peptide and the regulation of embryonic growth in the rodent. The Journal of clinical investigation 97(1):202-208.

Hirbec H, Perestenko O, Nishimune A, Meyer G, Nakanishi S, Henley JM, Dev KK. 2002. The PDZ Proteins PICK1, GRIP, and Syntenin Bind Multiple Glutamate Receptor Subtypes ANALYSIS OF PDZ BINDING MOTIFS. Journal of Biological Chemistry 277(18):15221-15224.

Holmgren S, Jensen J. 2001. Evolution of vertebrate neuropeptides. Brain Res Bull 55(6):723-735.

Hosseini MM, Tonekaboni SH, Papari E, Bahman I, Behjati F, Kahrizi K, Najmabadi H. 2012. A novel mutation in MCPH1 gene in an Iranian family with primary microcephaly. J Pak Med Assoc 62(11):1244-1247.

Hussain MS, Baig SM, Neumann S, Peche VS, Szczepanski S, Nurnberg G, Tariq M, Jameel M, Khan TN, Fatima A, Malik NA, Ahmad I, Altmuller J, Frommolt P, Thiele H, Hohne W, Yigit G, Wollnik B, Neubauer BA, Nurnberg P, Noegel AA. 2013. CDK6 associates with the centrosome during mitosis and is mutated in a large Pakistani family with primary microcephaly. Human molecular genetics 22(25):5199-5214.

Ishihara T, Shigemoto R, Mori K, Takahashi K, Nagata S. Functional expression and tissue distribution of a novel receptor for vasoactive intestinal polypeptide. Neuron 8(4):811-819.

Itoh N, Obata K, Yanaihara N, Okamoto H. 1983. Human preprovasoactive intestinal polypeptide contains a novel PHI-27-like peptide, PHM-27. Nature 304(5926):547-549.

Jackson AP, Eastwood H, Bell SM, Adu J, Toomes C, Carr IM, Roberts E, Hampshire DJ, Crow YJ, Mighell AJ, Karbani G, Jafri H, Rashid Y, Mueller RF, Markham AF, Woods CG. 2002. Identification of microcephalin, a protein implicated in determining the size of the human brain. American journal of human genetics 71(1):136-142.

Jang Y-C, Kao L-S, Wang F-F. 1998. Involvement of Ca 2+ Signalling in the Vasoactive Intestinal Peptide and 8-Br-cAMP Induction of c-fos mRNA Expression. Cellular signalling 10(1):27-34.

Kaindl AM, Passemard S, Kumar P, Kraemer N, Issa L, Zwirner A, Gerard B, Verloes A, Mani S, Gressens P. 2010. Many roads lead to primary autosomal recessive microcephaly. Progress in neurobiology 90(3):363-383.

Kenshalo D, Giesler G, Leonard R, Willis W. 1980. Responses of neurons in primate ventral posterior lateral nucleus to noxious stimuli. Journal of Neurophysiology 43(6):1594-1614.

Komatsu Y, Kishigami S, Mishina Y. 2014. In Situ Hybridization Methods for Mouse Whole Mounts and Tissue Sections with and Without Additional β-Galactosidase Staining. Methods in molecular biology (Clifton, NJ) 1092:1-15.

Laburthe M, Couvineau A. 1988. Molecular Analysis of Vasoactive Intestinal Peptide Receptors: A Comparison with Receptors for VIP-Related Peptides. Annals of the New York Academy of Sciences 527(1):296-313.

Laburthe M, Couvineau A. 2002. Molecular pharmacology and structure of VPAC receptors for VIP and PACAP. Regulatory peptides 108(2):165-173.

Laburthe M, Couvineau A, Marie JC. 2002. VPAC Receptors for VIP and PACAP. Receptors and Channels 8(3-4):137-153.

Laburthe M, Couvineau A, Tan V. 2007. Class II G protein-coupled receptors for VIP and PACAP: structure, models of activation and pharmacology. Peptides 28(9):1631-1639.

LaMotte CC, de Lanerolle NC. 1986. VIP terminals, axons, and neurons: Distribution throughout the length of monkey and cat spinal cord. The Journal of Comparative Neurology 249(1):133-145.

Lamperti ED, Rosen KM, Villa-Komaroff L. 1991. Characterization of the gene and messages for vasoactive intestinal polypeptide (VIP) in rat and mouse. Brain research Molecular brain research 9(3):217-231.

Langer I. 2012. Mechanisms involved in VPAC receptors activation and regulation: lessons from pharmacological and mutagenesis studies. Frontiers in endocrinology 3:129.

Langer I, Vertongen P, Perret J, Waelbroeck M, Robberecht P. 2003. Lysine 195 and aspartate 196 in the first extracellular loop of the VPAC 1 receptor are essential for high affinity binding of agonists but not of antagonists. Neuropharmacology 44(1):125-131.

Langlet C, Nachtergael I, Robberecht P, Langer I. 2006. Mutation of the phosphorylatable residue Thr429 in Glu of the human VPAC1 led to a constitutively desensitized receptor. Peptides 27(7):1865-1870.

Larsson LI, Fahrenkrug J, Schaffalitzky De Muckadell O, Sundler F, Hakanson R, Rehfeld JR. 1976. Localization of vasoactive intestinal polypeptide (VIP) to central and peripheral neurons. Proceedings of the National Academy of Sciences of the United States of America 73(9):3197-3200.

Lee S, Kruglikov I, Huang ZJ, Fishell G, Rudy B. 2013. A disinhibitory circuit mediates motor integration in the somatosensory cortex. Nature neuroscience 16(11):1662-1670.

Lelievre V, Favrais G, Abad C, Adle-Biassette H, Lu Y, Germano PM, Cheung-Lau G, Pisegna JR, Gressens P, Lawson G, Waschek JA. 2007. Gastrointestinal dysfunction in mice with a targeted mutation in the gene encoding vasoactive intestinal polypeptide: a model for the study of intestinal ileus and Hirschsprung's disease. Peptides 28(9):1688-1699.

Lelievre V, Hu Z, Byun J-Y, Ioffe Y, Waschek JA. 2002. Fibroblast growth factor-2 converts PACAP growth action on embryonic hindbrain precursors from stimulation to inhibition. Journal of Neuroscience Research 67(5):566-573.

Lelievre V, Meunier AC, Caigneaux E, Falcon J, Muller JM. 1998. Differential expression and function of PACAP and VIP receptors in four human colonic adenocarcinoma cell lines. Cellular signalling 10(1):13-26.

Lim MA, Stack CM, Cuasay K, Stone MM, McFarlane HG, Waschek JA, Hill JM. 2008. Regardless of genotype, offspring of VIP-deficient female mice exhibit developmental delays and deficits in social behavior. International journal of developmental neuroscience : the official journal of the International Society for Developmental Neuroscience 26(5):423-434.

Lin S-Y, Rai R, Li K, Xu Z-X, Elledge SJ. 2005. BRIT1/MCPH1 is a DNA damage responsive protein that regulates the Brca1–Chk1 pathway, implicating checkpoint dysfunction in microcephaly. Proceedings of the National Academy of Sciences of the United States of America 102(42):15105-15109.

Linder S, Barkhem T, Norberg A, Persson H, Schalling M, Hokfelt T, Magnusson G. 1987. Structure and expression of the gene encoding the vasoactive intestinal peptide precursor. Proceedings of the National Academy of Sciences of the United States of America 84(2):605-609.

Liu G, Dong Y, Wang Z, Cao J, Chen Y. 2014. Restraint stress alters immune parameters and induces oxidative stress in the mouse uterus during embryo implantation. Stress 17(6):494-503.

Loeser JD, Treede R-D. 2008. The Kyoto protocol of IASP Basic Pain Terminology☆. Pain 137(3):473-477.

Loren I, Emson PC, Fahrenkrug J, Bjorklund A, Alumets J, Hakanson R, Sundler F. 1979. Distribution of vasoactive intestinal polypeptide in the rat and mouse brain. Neuroscience 4(12):1953-1976.

Lutz EM, Sheward WJ, West KM, Morrow JA, Fink G, Harmar AJ. 1993. The VIP2 receptor: Molecular characterisation of a cDNA encoding a novel receptor for vasoactive intestinal peptide. FEBS Letters 334(1):3-8.

Maduna T, Lelievre V. 2016. Neuropeptides shaping the central nervous system development: Spatiotemporal actions of VIP and PACAP through complementary signaling pathways. Journal of Neuroscience Research 94(12):1472-1487.

Mahmood S, Ahmad W, Hassan MJ. 2011. Autosomal Recessive Primary Microcephaly (MCPH): clinical manifestations, genetic heterogeneity and mutation continuum. Orphanet journal of rare diseases 6:39.

Mathieu M, Tagliafierro G, Angelini C, Vallarino M. 2001. Organization of vasoactive intestinal peptide-like immunoreactive system in the brain, olfactory organ and retina of the zebrafish, Danio rerio, during development. Brain Res 888(2):235-247.

McDonald TP, Dinnis DM, Morrison CF, Harmar AJ. 1998. Desensitization of the Human Vasoactive Intestinal Peptide Receptor (hVIP2/PACAP R): Evidence for Agonist-Induced Receptor Phosphorylation and Internalizationa. Annals of the New York Academy of Sciences 865(1):64-72.

McLatchie LM, Fraser NJ, Main MJ, Wise A, Brown J, Thompson N, Solari R, Lee MG, Foord SM. 1998. RAMPs regulate the transport and ligand specificity of the calcitonin-receptor-like receptor. Nature 393(6683):333-339.

Miyata A, Jiang L, Dahl RD, Kitada C, Kubo K, Fujino M, Minamino N, Arimura A. 1990. Isolation of a neuropeptide corresponding to the N-terminal 27 residues of the pituitary adenylate cyclase activating polypeptide with 38 residues (PACAP38). Biochem Biophys Res Commun 170(2):643-648.

Miyoshi G, Hjerling-Leffler J, Karayannis T, Sousa VH, Butt SJ, Battiste J, Johnson JE, Machold RP, Fishell G. 2010. Genetic fate mapping reveals that the caudal ganglionic eminence produces a large and diverse population of superficial cortical interneurons. The Journal of neuroscience : the official journal of the Society for Neuroscience 30(5):1582-1594.

Morice AH, Unwin RJ, Sever PS. 1984. Vasoactive intestinal peptide as a bronchodilator in asthmatic subjects. Peptides 5(2):439-440.

Morrison JH, Magistretti PJ, Benoit R, Bloom FE. 1984. The distribution and morphological characteristics of the intracortical VIP-positive cell: An immunohistochemical analysis. Brain Research 292(2):269-282.

Murakami Y, Koshimura K, Yamauchi K, Nishiki M, Tanaka J, Kato Y. 2001. Roles and mechanisms of action of pituitary adenylate cyclase-activating polypeptide (PACAP) in growth hormone and prolactin secretion. Endocrine journal 48(2):123-132.

Mutt V, Said SI. 1974. Structure of the porcine vasoactive intestinal octacosapeptide. The amino-acid sequence. Use of kallikrein in its determination. European journal of biochemistry 42(2):581-589.

Narod SA, Foulkes WD. 2004. BRCA1 and BRCA2: 1994 and beyond. Nature reviews Cancer 4(9):665-676.

Nelson KB. 2001. Toward a biology of autism: Possible role of certain neuropeptides and neurotrophins. Clinical Neuroscience Research 1(4):300-306.

Nelson PG, Kuddo T, Song EY, Dambrosia JM, Kohler S, Satyanarayana G, Vandunk C, Grether JK, Nelson KB. 2006. Selected neurotrophins, neuropeptides, and cytokines: developmental trajectory and concentrations in neonatal blood of children with autism or Down syndrome. International journal of developmental neuroscience : the official journal of the International Society for Developmental Neuroscience 24(1):73-80.

Nicole P, Lins L, Rouyer-Fessard C, Drouot C, Fulcrand P, Thomas A, Couvineau A, Martinez J, Brasseur R, Laburthe M. 2000. Identification of key residues for interaction of vasoactive intestinal peptide with human VPAC1 and VPAC2 receptors and development of a highly selective VPAC1 receptor agonist. Alanine scanning and molecular modeling of the peptide. The Journal of biological chemistry 275(31):24003-24012.

Obata K-i, Itoh N, Hiroshi O, Chizuko Y, Noboru Y, Toshimitsu S. 1981. Identification and processing of biosynthetic precursors to vasoactive intestinal polypeptide in human neuroblastoma cells. FEBS Letters 136(1):123-126.

Parets SE, Bedient CE, Menon R, Smith AK. 2014. Preterm birth and its long-term effects: methylation to mechanisms. Biology (Basel) 3(3):498-513.

Passemard S, El Ghouzzi V, Nasser H, Verney C, Vodjdani G, Lacaud A, Lebon S, Laburthe M, Robberecht P, Nardelli J, Mani S, Verloes A, Gressens P,

Lelievre V. 2011. VIP blockade leads to microcephaly in mice via disruption of Mcph1-Chk1 signaling. The Journal of clinical investigation 121(8):3071-3087.

Passemard S, Titomanlio L, Elmaleh M, Afenjar A, Alessandri JL, Andria G, de Villemeur TB, Boespflug-Tanguy O, Burglen L, Del Giudice E, Guimiot F, Hyon C, Isidor B, Megarbane A, Moog U, Odent S, Hernandez K, Pouvreau N, Scala I, Schaer M, Gressens P, Gerard B, Verloes A. 2009. Expanding the clinical and neuroradiologic phenotype of primary microcephaly due to ASPM mutations. Neurology 73(12):962-969.

Pelletier G, Leclerc R, Puviani R, Polak JM. 1981. Electron immunocytochemistry in vasoactive intestinal peptide (VIP) in the rat brain. Brain Res 210(1-2):356-360.

Pincus DW, DiCicco-Bloom E, Black IB. 1994. Trophic mechanisms regulate mitotic neuronal precursors: role of vasoactive intestinal peptide (VIP). Brain research 663(1):51-60.

Pulvers JN, Huttner WB. 2009. Brca1 is required for embryonic development of the mouse cerebral cortex to normal size by preventing apoptosis of early neural progenitors. Development 136(11):1859-1868.

Purves D, Augustine GJ, Fitzpatrick D, Hall WC, LaMantia A-S, McNamara JO, Williams S. 2004. Neuroscience. Massachusetts. Publishers Sunderland.

Quinn JC, Molinek M, Martynoga BS, Zaki PA, Faedo A, Bulfone A, Hevner RF, West JD, Price DJ. 2007. Pax6 controls cerebral cortical cell number by regulating exit from the cell cycle and specifies cortical cell identity by a cell autonomous mechanism. Dev Biol 302(1):50-65.

Rossignol E. 2011. Genetics and function of neocortical GABAergic interneurons in neurodevelopmental disorders. Neural plasticity 2011:649325.

Roy R, Chun J, Powell SN. 2011. BRCA1 and BRCA2: different roles in a common pathway of genome protection. Nature reviews Cancer 12(1):68-78.

Rudy B, Fishell G, Lee S, Hjerling-Leffler J. 2011. Three groups of interneurons account for nearly 100% of neocortical GABAergic neurons. Developmental neurobiology 71(1):45-61.

Sahir N, Brenneman DE, Hill JM. 2006. Neonatal mice of the Down syndrome model, Ts65Dn, exhibit upregulated VIP measures and reduced responsiveness of cortical astrocytes to VIP stimulation. Journal of molecular neuroscience : MN 30(3):329-340.

Said SI. 1984. Isolation, localization, and characterization of gastrointestinal peptides. Clinical biochemistry 17(2):65-67.

Said SI. 1986. Vasoactive intestinal peptide. Journal of Endocrinological Investigation 9(2):191-200.

Said SI, Mutt V. 1970. Polypeptide with broad biological activity: isolation from small intestine. Science 169(3951):1217-1218.

Said SI, Mutt V. 1972. Isolation from porcine-intestinal wall of a vasoactive octacosapeptide related to secretin and to glucagon. European journal of biochemistry 28(2):199-204.

Sastry KS, Smith AJ, Karpova Y, Datta SR, Kulik G. 2006. Diverse anti-apoptotic signaling pathways activated by VIP, EGF and PI3K in prostate cancer cells converge on BAD. Journal of Biological Chemistry.

Schaeren-Wiemers N, Gerfin-Moser A. 1993. A single protocol to detect transcripts of various types and expression levels in neural tissue and cultured cells: in situ hybridization using digoxigenin-labelled cRNA probes. Histochemistry 100(6):431-440.

Servoss SJ, Lee SJ, Gibney G, Gozes I, Brenneman DE, Hill JM. 2001. IGF-I as a mediator of VIP/activity-dependent neurotrophic factor-stimulated embryonic growth. Endocrinology 142(8):3348-3353.

Sherwood NM, Krueckl SL, McRory JE. 2000. The origin and function of the pituitary adenylate cyclase-activating polypeptide (PACAP)/glucagon superfamily. Endocrine reviews 21(6):619-670.

Shetzline MA, Walker JK, Valenzano KJ, Premont RT. 2002. Vasoactive Intestinal Polypeptide Type-1 Receptor Regulation DESENSITIZATION, PHOSPHORYLATION, AND SEQUESTRATION. Journal of Biological Chemistry 277(28):25519-25526.

Shivers BD, Gorcs TJ, Gottschall PE, Arimura A. 1991. Two high affinity binding sites for pituitary adenylate cyclase-activating polypeptide have different tissue distributions. Endocrinology 128(6):3055-3065.

Sims KB, Hoffman DL, Said SI, Zimmerman EA. 1980. Vasoactive intestinal polypeptide (VIP) in mouse and rat brain: an immunocytochemical study. Brain research 186(1):165-183.

Sohn Y-S, Kim M-J, Kwon J-Y, Kim Y-H, Park Y-W. 2007. The Usefulness of Fetal MRI for Prenatal Diagnosis. Yonsei Medical Journal 48(4):671-677.

Spadoni AD, McGee CL, Fryer SL, Riley EP. 2007. Neuroimaging and fetal alcohol spectrum disorders. Neuroscience & Biobehavioral Reviews 31(2):239-245.

Spong CY, Lee SJ, McCune SK, Gibney G, Abebe DT, Alvero R, Brenneman DE, Hill JM. 1999. Maternal regulation of embryonic growth: the role of vasoactive intestinal peptide. Endocrinology 140(2):917-924.

Sreedharan SP, Robichon A, Peterson KE, Goetzl EJ. 1991. Cloning and expression of the human vasoactive intestinal peptide receptor. Proceedings of the National Academy of Sciences of the United States of America 88(11):4986-4990.

Stack CM, Lim MA, Cuasay K, Stone MM, Seibert KM, Spivak-Pohis I, Crawley JN, Waschek JA, Hill JM. 2008. Deficits in social behavior and reversal learning are more prevalent in male offspring of VIP deficient female mice. Experimental neurology 211(1):67-84.

Svoboda M, Tastenoy M, Vanrampelbergh J, Goossens J-F, Deneef P, Waelbroeck M, Robberecht P. 1994. Molecular cloning and functional characterization of a human VIP receptor from SUP-T1 lymphoblasts. Biochemical and biophysical research communications 205(3):1617-1624.

Szema AM, Dang S, Li JC. 2015. Emerging Novel Therapies for Heart Failure. Clinical Medicine Insights: Cardiology(5127-CMC-Emerging-Novel-Therapies-for-Heart-Failure.pdf):57-64.

Szema AM, Hamidi SA, Lyubsky S, Dickman KG, Mathew S, Abdel-Razek T, Chen JJ, Waschek JA, Said SI. 2006. Mice lacking the VIP gene show airway hyperresponsiveness and airway inflammation, partially reversible by VIP. American Journal of Physiology - Lung Cellular and Molecular Physiology 291(5):L880-L886.

Talbot RT, Dunn IC, Wilson PW, Sang HM, Sharp PJ. 1995. Evidence for alternative splicing of the chicken vasoactive intestinal polypeptide gene transcript. Journal of molecular endocrinology 15(1):81-91.

Tam JKV, Lee LTO, Chow BKC. 2007. PACAP-related peptide (PRP)—Molecular evolution and potential functions. Peptides 28(9):1920-1929.

Tatemoto K, Mutt V. 1980. Isolation of two novel candidate hormones using a chemical method for finding naturally occurring polypeptides. Nature 285(5764):417-418.

Thornton GK, Woods CG. 2009. Primary microcephaly: do all roads lead to Rome? Trends in genetics : TIG 25(11):501-510.

Thwaites DT, Young J, Thorndyke MC, Dimaline R. 1989. The isolation and chemical characterization of a novel vasoactive intestinal peptide-related peptide from a teleost fish, the cod, Gadus morhua. Biochimica et biophysica acta 999(2):217-220.

Tohei A. 2004. Studies on the functional relationship between thyroid, adrenal and gonadal hormones. The Journal of reproduction and development 50(1):9-20.

Tsukada T, Fink JS, Mandel G, Goodman RH. 1987. Identification of a region in the human vasoactive intestinal polypeptide gene responsible for regulation by cyclic AMP. The Journal of biological chemistry 262(18):8743-8747.

Ulrich CD, Holtmann M, Miller LJ. 1998. Secretin and vasoactive intestinal peptide receptors: members of a unique family of G protein–coupled receptors. Gastroenterology 114(2):382-397.

Van Rampelbergh J, Poloczek P, Francoys I, Delporte C, Winand J, Robberecht P, Waelbroeck M. 1997. The pituitary adenylate cyclase activating polypeptide (PACAP I) and VIP (PACAP II VIP1) receptors stimulate inositol phosphate synthesis in transfected CHO cells through interaction with different G proteins. Biochimica et biophysica acta 1357(2):249-255.

Vilardaga J-P, Deneef P, Dipaolo E, Bollen A, Waelbroeck M, Robberecht P. 1995. Properties of chimeric secretin and VIP receptor proteins indicate the importance of the N-terminal domain for ligand discrimination. Biochemical and biophysical research communications 211(3):885-891.

Vogtle LK. 2009. Pain in adults with cerebral palsy: impact and solutions. Developmental Medicine & Child Neurology 51(s4):113-121.

Waschek JA. 2013. VIP and PACAP: neuropeptide modulators of CNS inflammation, injury, and repair. Br J Pharmacol 169(3):512-523.

Waschek JA, Pruss RM, Siegel RE, Eiden LE, Bader MF, Aunis D. 1987. Regulation of enkephalin, VIP, and chromogranin biosynthesis in actively secreting chromaffin cells. Multiple strategies for multiple peptides. Annals of the New York Academy of Sciences 493:308-323.

Werner H, Koch Y, Fridkin M, Fahrenkrug J, Gozes I. 1985. High levels of vasoactive intestinal peptide in human milk. Biochemical and biophysical research communications 133(1):228-232.

Wiebold J, Stanfield P, Becker W, Hillers J. 1986. The effect of restraint stress in early pregnancy in mice. Journal of reproduction and fertility 78(1):185-192.

Wootten D, Lindmark H, Kadmiel M, Willcockson H, Caron KM, Barwell J, Drmota T, Poyner DR. 2013. Receptor activity modifying proteins (RAMPs) interact with the VPAC2 receptor and CRF1 receptors and modulate their function. Br J Pharmacol 168(4):822-834.

Wu JY, Henins KA, Gressens P, Gozes I, Fridkin M, Brenneman DE, Hill JM. 1997. Neurobehavioral Development of Neonatal Mice Following Blockade of VIP During the Early Embryonic Period. Peptides 18(8):1131-1137.

Xiao Z, Chen Z, Gunasekera AH, Sowin TJ, Rosenberg SH, Fesik S, Zhang H. 2003. Chk1 Mediates S and G2 Arrests through Cdc25A Degradation in Response to DNA-damaging Agents. Journal of Biological Chemistry 278(24):21767-21773.

Xu X, Lee J, Stern DF. 2004. Microcephalin Is a DNA Damage Response Protein Involved in Regulation of CHK1 and BRCA1. Journal of Biological Chemistry 279(33):34091-34094.

Yaksh TL, Abay EO, 2nd, Go VL. 1982. mStudies on the location and release of cholecystokinin and vasoactive intestinal peptide in rat and cat spinal cord. Brain Res 242(2):279-290.

Yalcin I, Charlet A, Freund-Mercier MJ, Barrot M, Poisbeau P. 2009. Differentiating thermal allodynia and hyperalgesia using dynamic hot and cold plate in rodents. The journal of pain : official journal of the American Pain Society 10(7):767-773.

Yamagami T, Ohsawa K, Nishizawa M, Inoue C, Gotoh E, Yanaihara N, Yamamoto H, Okamoto H. 1988. Complete nucleotide sequence of human vasoactive intestinal peptide/PHM-27 gene and its inducible promoter. Annals of the New York Academy of Sciences 527:87-102.

Yizhar O, Fenno LE, Prigge M, Schneider F, Davidson TJ, O'Shea DJ, Sohal VS, Goshen I, Finkelstein J, Paz JT. 2011. Neocortical excitation/inhibition balance in information processing and social dysfunction. Nature 477(7363):171-178.

You S, Silsby JL, Farris J, Foster DN, el Halawani ME. 1995. Tissue-specific alternative splicing of turkey preprovasoactive intestinal peptide messenger ribonucleic acid, its regulation, and correlation with prolactin secretion. Endocrinology 136(6):2602-2610.

Yung Gee H, Woo Park H, Hwan Kim K, Goo Lee M. 2009. PDZ-based adaptor proteins in epithelial anion transport and VIP receptor regulation. The Journal of Medical Investigation 56(Supplement):302-305.

Zikopoulos B, Barbas H. 2010. Changes in prefrontal axons may disrupt the network in autism. The Journal of Neuroscience 30(44):14595-14609.

Annexes

Annexe 1: Whole mount in situ hybridization protocol

MATERIALS

- **1X PBS(DEPC) ,1X PBS, 4% PFA (PBS)**

- **Methanol**

- **Proteinase K**

- **Glutaraldehyde**

- **PBT** : 0.1% Triton X100 en PBS 1X

- **Prehybridization mix (10 mL)** :
    - Formamide (50% final) 5 ml (100% initial)
    - SSC (5X final) 2.5 ml (20X initial)
    - Blocking powder (2% final) 0.2 g
    - Triton X100 (0.1% final) 10 µl
    - Chaps (0.5% final) 0.05 g
    - Yeast RNA (1mg/ml final) 0.5 ml (20 mg/ml initial)
    - EDTA (5 mM final) 100 µl (0.5 M initial)
    - Heparin (50 µg/ml final) 50 µl (10 mg/ml initial)

- **Solution 1:**
    - Formamide : 50% final
    - SSC : 5X final
    - Triton X100: 0.1% final
    - Chaps: 0.5% final

- **TBT:**
    - 50mM Tris pH 7.5
    - 150 mM NaCl
    - 0.1% Triton X100
- **TBST :** 10% Fetal bovine serum (in TBT)
- **NTMT :**
    - 100 mM NaCl
    - Tris pH 9.5 at final
    - MgCl2 at 50 mM final
    - Tween 20 at 0.1% final
    - Levamisole at 2mM final
-
- **Embryonic powder:**
    - Homogenize embryos E12.5 to E14.5 in a small volume of 1XPBS
    - Add 4 V of acetone
    - Mix and incubate on for 30 minutes
    - Centrifuge at 10 000g for 10 minutes
    - Remove the supernatant
    - Wash the pellet with 4 volumes of cold acetone and centrifuge again
    - Transfer the pellet from the tube onto a large piece of Wattmann paper and cut into a powder using a scalpel
    - Leave to dry and store at 4°C

PROCEDURE

Day1 :

- Dissect the samples
- Fix with PFA 4% in PBS, ON at 4°C

Day 2 :

- Wash with PBT 2 times 10 minutes at 4°C
- Dehydrate with 25% methanol/PBT 20 minutes
  50% methanol/PBT 20 minutes
  75% methanol/PBT 20 minutes
  100% methanol 2 times 20 minutes

Store at -20 °C

Day 3:

Rehydrate the samples:

- 75% methanol/PBT 20 minutes
- 50% methanol/PBT 20 minutes
- 25% methanol/PBT 20 minutes
- PBT 3 times 10 minutes

For E12 and E13, embryos are bleached immediately in 6% H202 (in DEPC-treated deionized water)

Procedure:

- rinse in DEPC-treated deionized water 5 minutes
- 6% H202 5-10 minutes (E12);
  20-30 minutes (E13)
- wash in DEPC-treated deionized water 5 minutes x2
- PBT 5 minutes

- **Treatment with proteinase K**

Use the proteinase K diluted at 20µg/ml in PBT for 1 minute per age of the embryo at room temperature*. Example*: 12 minutes for embryo E12.

- **Washes :**

  5 minutes in PBT x2

- **Fixation :**

  Fix in 0.2% glutaraldehyde/4%PFA in PBT 20 minutes

- **Washes**

  10 minutes in PBT x2

- **Prehybridization :**

  Prehybridize the samples overnight at 60°C

Day 4:

Hybridization overnight at 60°C

Change the prehybridization mix and replace with hybridization with, which is prehybridization mix with 1µg/ml of RNA probe labelled with digoxigenin.

*Note: In the morning, remove the samples from the 60°C bath and leave at room temperature. Add probe only in the late afternoon to make sure that hybridization occurs overnight and not the whole day!

Day 5:

Wash at 60°C with:

- 100% solution 1 5 minutes
- 70% solution 1 / 30% 2X SSC 5 minutes
- 30% solution 1 / 70% 2X SSC 5 minutes
- 2X SSC / 0.1% Chaps 2 times 30 minutes
- 0.2X SSC / 0.1% Chaps 2 times 30 minutes

At room temperature

- TBT 2 times 10 minutes

Blocking: (3 hours at room temperature)

Block the samples with 10% normal sheep serum, 2%BSA in TBT.
In the same time, prepare:

<u>Antibody solution with anti-digoxigenin</u>

- To 1 ml of TBST, add 6 mg of embryo powder
- Inactive for 30 minutes at 70°C
- Cool the tube on ice
- When the tube is cold, add 2 µL of anti-DIG-coupled with alkaline phosphatase (anti-DIG-AP).
- Centrifuge for 10 minutes at 1000 rpm
- Dilute the supernatant to 4ml with non-inactivated TBST and 2mM levamisole.
- After 3 hours of blocking, incubate the embryos with the anti-dig solution **overnight under shaking at 4°C**

Day 6

<u>Washes</u> **(Room temperature)**

- TBT/0.1% BSA — 5 times 1 hour
- TBT/0.1% BSA — OVERNIGHT à **4°C**

Day 7

<u>Washes</u> **(Room temperature)**

- TBT — 2 times 30 minutes
- NTMT — 3 times 10 minutes

<u>Revelation (</u>**without light and at room temperature)**

Put the samples in NTMT + 4.5µL of NBT + 3.5 µL of BCIP per ml
Change the medium every two hours and wait for the coloration.
(Prepare new medium every two hours)

The revelation can be stopped with PBT at 4°C

When the revelation is done, postfix the samples with formaldehyde 4% in water.

Annexe 2: Liste des communications

Présentations orales

In situ Hybridization: Seeing RNA expression at the right place. Maduna T and Lelievre V. *Neurotech Seminar Series, Strasbourg, France, Décembre 2014*

Role of VIP during neurogenesis: New insights on human microcephaly. Maduna T, Passemard S, Walia S, Lacaud A, Lelievre V. *Seminaire Interne de l'INCI (UPR3212), Strasbourg, France, Avril 2014*

WISH to localize VIP developmental role in normal corticogenesis in a mouse model of Microcephaly Maduna T, Lacaud A, Lelievre V. *1st IGBMC Annual Student Retreat, Mollkirch, France, Février 2014*

Communications affichées

VIP signaling during cortical development: Microcephalic VIP-deficient mice reveal alterations in neurogenesis program. Maduna T, Lacaud A, Lelievre V. *10th FENS Forum of Neuroscience (FENS), Copenhagen, Denmark, July 2016*

VIP regulates expression of molecular and epigenetic determinants of cold and mechanical nociception. Maduna T, Juif PE, Uppari NP, Petit Demouliere N, Lacaud A, Poisbeau P, Lelievre V. *45th annual meeting of the Society for Neuroscience, Society of Neuroscience, Chicago, IL, USA, 2015*

WISH for lessons from VIP-deficient mice during Embryonic Development. Maduna T, Lacaud A, Lelievre V.
12th International Symposium on VIP, PACAP and Related Peptides, Cappadocia, Turkey, 2015

Annexe 3: Liste des publications

Maduna T, Passemard S, Walia S, Lacaud A, Gressens P, Lelievre V. Loss of VIP causes microcephaly with sustained cortical defect due to localized downregulation of Mcph1-Chk1 crosstalk and premature neuronal differentiation. *(en préparation)*

Maduna T, Juif P-E, Uppari N P, Petit Demouliere N, Lacaud A, Poisbeau P, Lelievre V. Hyperalgesic VIP-deficient mice exhibit VIP-reversible alterations in molecular and epigenetic determinants of cold and mechanical nociception *(soumis)*

Maduna T, Lelievre V. 2016. Neuropeptides shaping the central nervous system development: Spatiotemporal actions of VIP and PACAP through complementary signaling pathways. Journal of Neuroscience Research 94(12):1472-1487.

Tando Lerato MADUNA

Vasoactive intestinal peptide (VIP) controls the development of the nervous system and its functions through VPAC1 receptor signaling: Lessons from microcephaly and hyperalgesia in VIP-deficient mice.

Résumé :

Mes études doctorales ont permis de démontrer que les souris déficientes en VIP présentent une microcéphalie ayant principalement une origine maternelle qui affecte secondairement le développement de la substance blanche. Cette production placentaire par les lymphocytes T pourrait être affectée dans des pathologies du système immunitaire. De plus, nos données indiquent qu'une déficience en VIP prédispose à l'apparition de troubles sensoriels, en particulier de la nociception. Il est donc possible que les déficits précoces de développement du cerveau murin et l'apparition de l'hypersensibilité cutanée mécanique et thermique froide soient deux facettes d'une même pathologie. Des mesures d'activité de décharge spontanée des neurones dans le thalamus sensoriel chez des mâles adultes anesthésiés ont montré que les neurones des animaux KO sont hyper-excités, ce qui suggère un traitement aberrant des informations, notamment nociceptives, ou que l'activité inhibitrice des interneurones des réseaux locaux est réduite.

Mots-clés: *Peptide vasoactif intestinal; neurogénèse, cycle cellulaire; checkpoint kinase 1; Microcephalin, différentiation neuronale; microcéphalie; moelle épinière, stress maternel; douleur*

Résumé en anglais:

The studies carried out during my PhD demonstrate that VIP-deficient mice suffer from microcephaly and as well as white matter deficits mainly due to the absence of maternal VIP during embryogenesis, Placental secretion of VIP is dependent on T lymphocytes and could be altered in pathologies of the immune system. Moreover, our data links VIP deficiency to sensory alterations, specifically, the nociceptive system. Thus, it is possible that early developmental defects and hypersensitivity to mechanical and cold stimuli are two manifestations of the same pathology.

This hypothesis was reinforced following analysis of spontaneous firing patterns of neurons in the sensory thalamus of anesthetized adult males. Neurons from VIP-KO mice are hyperactive, which suggests aberrant local processing of nociceptive input or that the inhibitory inputs from local interneuron networks is reduced.

Keywords: *Vasoactive intestinal peptide; neurogenesis, cell cycle; cortical development; checkpoint kinase 1; Microcephalin, neural differentiation; microcephaly; spinal cord, maternal stress; pain*